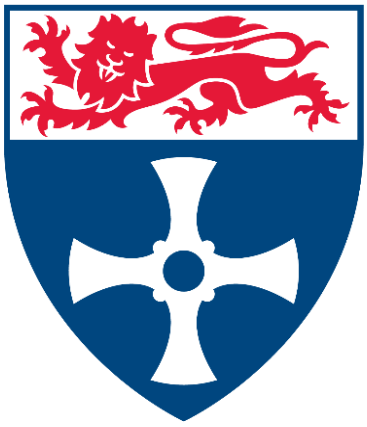

The Role of CREBBP Mutations in Lymphoid Malignancies

Zach Dixon

Thesis submitted in part requirement for the degree of Doctor of Philosophy (PhD)

Wolfson Childhood Cancer Research Centre

Northern Institute for Cancer Research

Herschel Building, Level 6

Newcastle University

Newcastle upon Tyne

NE1 7RU

November 2016

Abstract

Relapsed acute lymphoblastic leukaemia (ALL), diffuse large B-cell lymphoma (DLBCL) and follicular lymphoma (FL) comprise a group of malignancies with poor prognosis and therapeutic strategies are needed to improve outcomes. Recent studies have shown that heterozygous inactivating mutations in the histone acetyl transferase, *CREBBP*, are frequent in these malignancies, and are thought to lead to impaired transcription of glucocorticoid (GC) response genes. Given the pivotal role of GC in the treatment of lymphoid malignancies and the finding that *CREBBP* mutations often arise at relapse, it has been postulated that *CREBBP* mutations confer chemoresistance to GC therapy. To study the role of *CREBBP* haploinsufficiency in ALL, DLBCL and FL, small hairpin RNA and small interfering RNA methods were used to knock down CREBBP in a number of cell lines and primary derived samples. Models were functionally relevant, with reduced acetylation of CREBBP target residue, histone 3 lysine 18 and/or histone 3 lysine 27, but knockdown had no significant impact on activation of cAMP-dependent target genes. Impaired induction of glucocorticoid receptor targets was only seen in 1 of 4 CREBBP knockdown models of ALL, and there was no significant difference in GC-induced apoptosis or chemosensitivity to other therapeutic agents frequently used in lymphoid malignancies, including histone deacetylase inhibitors. However, CREBBP knockdown was associated with enhanced signalling of the RAS/RAF/MEK/ERK pathway in RAS pathway mutant ALL cells, and MEK inhibitor sensitivity was retained. This suggests that *CREBBP* mutation may act to enhance the activity of oncogenes and that *CREBBP*/RAS pathway mutated relapsed ALL are candidates for MEK inhibitor clinical trials.

Acknowledgements

I would like to thank my supervisor Julie Irving for giving me the opportunity to carry out this research in an excellent research environment. It has been a pleasure working under your supervision and I have been happy and felt well supported throughout, we make a great team! Many thanks to Lindsay Nicholson, who has taught me almost every scientific technique I know and helped out with just about everything throughout this project. Further thanks to Lynne Minto, Marian Case and Liz Matheson, some of the nicest people I have ever met and whose vast experience and expertise helped me a great deal. Thanks also to Rosie Jackson and Ali Alhammer, two very friendly and easy to work with people, we worked really well together and sorted out many primagraft samples! Thanks to my progression panel Christine Harrison and Luke Gaughan, who took the time to discuss my work each year and gave insightful suggestions. Further thanks to everyone who I have collaborated with during this project, from help with data processing to sharing protocols and reagents.

A huge thank you to Cancer Research UK for providing the funding that made this research possible and for supporting me throughout this project with annual meetings and training courses.

Many thanks to my fiancée Charlotte, for keeping me sane over the last 4 years, listening to me rambling on about science and supporting me in my career goals. Finally, I would like to thank my family for their constant support and encouragement throughout the years and without whom I would not have made it this far.

Contents

Chapter 3

Chapter 4

Chapter 5

Chapter 6

Appendices

References

List of Figures

List of Tables

List of Abbreviations

^{18}FDG-PET	18-fluorodeoxyglucose positron emission tomography
ABC	Activated B-cell
AcH3K18	Acetyl H3K18
AcH3K27	Acetyl H3K27
Ac-p53	Acetyl p53
Ag	Antigen
AIEOP-BFM	Italian Association of Pediatric Hematology and Oncology and Berlin Frankfurt-Münster
ALC	Absolute lymphocyte count
ALL	Acute lymphoblastic leukaemia
AMC	Absolute monocyte count
AML	Acute myeloid leukaemia
APC	Allophycocyanin
APC/C	Anaphase promoting complex/cyclosome
BCA	Bicinchoninic acid
BCP-ALL	B-cell precursor ALL
BCR	B-cell receptor
BER	Base excision repair
B-NHL	B-cell NHL
BSA	Bovine serum albumin
cAMP	Cyclic adenosine monophosphate

CCD	Charge-coupled device
cDNA	Copy DNA
CHOP	Cyclophosphamide, doxorubicin, vincristine and prednisone
CLP	Common lymphoid progenitor
CML	Chronic myeloid leukaemia
CMP	Common myeloid progenitor
CNS	Central nervous system
COG	Children's Oncology Group
COSMIC	Catalogue of somatic mutations in cancer
CPC	Common precursor clone
CREB	cAMP response element binding protein
CREBBP	CREB binding protein
CRISPR	Clustered regularly interspaced short palindromic repeats
CT	Computed tomography
C_T	Comparative threshold
CV	Control vehicle
dATP	Deoxyadenine triphosphate
DCOG	Dutch Childhood Oncology Group
dCTP	Deoxycytidine triphosphate
DDR	DNA damage repair
Dex	Dexamethasone
DFCI	Dana-Faber Cancer Institute
dGTP	Deoxyguanosine triphosphate

DHL	Double hit lymphoma
DLBCL	Diffuse large B-cell lymphoma
DNA	Deoxyribonucleic acid
dNTP	Deoxynucleotide
dTTP	Deoxythymidine triphosphate
EBV	Epstein Barr virus
EORTC CLG	European Organisation for Research and Treatment of Cancer Children's Leukemia Group
ETP	Early T-cell precursor
FACS	Fluorescence-activated cell sorting
FAM	6-carboxyfluorescein
FBS	Foetal bovine serum
FDC	Follicular dendritic cell
FISH	Fluorescent in situ hybridisation
FITC	Fluorescein isothiocyanate
FL	Follicular lymphoma
FLC	Free light chain
FLIPI	FL international prognostic index
FRET	Fluorescence resonance energy transfer
GC	Glucocorticoid
GCB	Germinal centre B-cell
GCRMA	GC robust multi-array average
GELF	Groupe d'Etude des Lymphomes Folliculaires

GEP	Gene expression profiling
GFP	Green fluorescent protein
GI_{50}	Concentration to cause 50% reduction in proliferation
GMP	Granulocyte macrophage progenitor
GO	Gene ontology
GR	Glucocorticoid receptor
GSEA	Gene set enrichment analysis
Gy	Gray (Radiation)
H3K18	Histone 3 lysine 18
H3K27	Histone 3 lysine 27
HAT	Histone acetyl transferase
HDAC	Histone deacetylase
HDACi	HDAC inhibitor
HHD	High hyperdiploid
HHV-8	Human herpes virus 8
HIV	Human immunodeficiency virus
HRP	Horseradish peroxidase
HRR	Homologous recombination repair
HSC	Haematopoietic stem cell
HSCT	Haematopoietic stem cell transplant
HTLV-1	Human T-lymphotropic virus type-1
iAMP21	Intrachromosomal amplification of chromosome 21
IBMX	3-isobutyl-1-methylxanthine

Ig	Immunoglobulin
IPA	Ingenuity pathway analysis
IPI	International prognostic index
IR	Ionising radiation
KAT	Lysine acetyl transferase
KID	Kinase inducible domain
LDH	Lactate dehydrogenase
Log2FC	Log 2 of the fold change
LPD	Lymphoproliferative disorders
LT	Long term
MAPK	Mitogen-activated protein kinase
MEKi	MEK inhibitor
MEP	Megakaryocyte erythroid progenitor
MGMT	Methyl guanine methyl transferase
MHC	Major histocompatibility complex
MITC	5-(3-methyltriazen-1-yl)imidazole-4-carboxamide
MMR	Mismatch repair
MOI	Multiplicity of infection
MPP	Multipotent progenitor
MRC-NCRI	Medical Research Council and National Cancer Research Institute
MRD	Minimal residual disease
NAD^+	Nicotinamide adenine dinucleotide
NHL	Non-Hodgkin's lymphoma

NOD-SCID	Non-obese diabetic severe combined immunodeficient
NOPHO	Nordic Society of Paediatric Oncology Haematology and Oncology
NSG	NOD-SCID IL-2R common gamma chain null
OS	Overall survival
PAR	Poly(ADP) ribose
PARP	Poly(ADP) ribose polymerase
PB	Peripheral blood
PBS	Phosphate buffered saline
PCA	Principle component analysis
PCR	Polymerase chain reaction
PDE	Phosphodiesterase
PE	Phycoerythrin
Per-CP	Peridinin-Chlorophyll-protein
p-ERK	Phosphorylated ERK
PFS	Progression free survival
PFU	Plaque forming units
PI3K	Phosphatidylinositol 3-kinase
PKA	Protein kinase A
PMBL	Primary mediastinal B-cell lymphoma
PRC2	Polycomb repressive complex 2
PVDF	Polyvinylidine difluoride
QRT-PCR	Quantitative reverse-transcriptase PCR
R-CHOP	CHOP plus Rituximab

RISC	RNA-induced silencing complex
RNA	Ribonucleic acid
RNAi	RNA interference
RPM	Revolutions per minute
RSTS	Rubinstein-Taybi Syndrome
SD	Standard deviation
SDS	Sodium dodecyl sulphate
SHM	Somatic hypermutation
shRNA	Small hairpin RNA
siRNA	Small interfering RNA
SJCRH	St Jude Children's Research Hospital
SRCAP	Snf2-Related-CBP activator protein
SSB	Single strand break
ST	Short term
TAMRA	6-carboxy-tetramethyl-rhodamine
TBE	Tris borate EDTA
TBP	TATA-box binding protein
TBS	Tris buffered saline
TBST	Tris buffered saline with Tween 20
TDG	Thymine DNA glycosylase
TFIIB	Transcription factor II B
tFL	Transformed FL
Treg	T regulatory

ULN	Upper limit of normal
WBC	White blood cell
WHO	World Health Organisation
XRT	External beam radiotherapy

Chapter 1: Introduction

Introduction

1.1Blood Cell Development

Mature blood cells are produced in the bone marrow through a hierarchical process known as haematopoiesis (Figure 1.1). Through this process a large number of specialised cell types are generated from a small number of haematopoietic stem cells (HSC) which reside in the bone marrow. Long term (LT) HSCs and short term (ST) HSCs are cells which are capable of self-renewal to maintain a pool of undifferentiated cells or differentiation over long and short term respectively. Differentiation is influenced by growth factors, cytokines and transcription factor expression, gradually changing the gene expression of cells, moving them towards a specialised phenotype. Disruption of this process can lead to uncontrolled proliferation, abnormal differentiation and apoptosis, typical features of haematological disorders such as leukaemia and lymphoma.

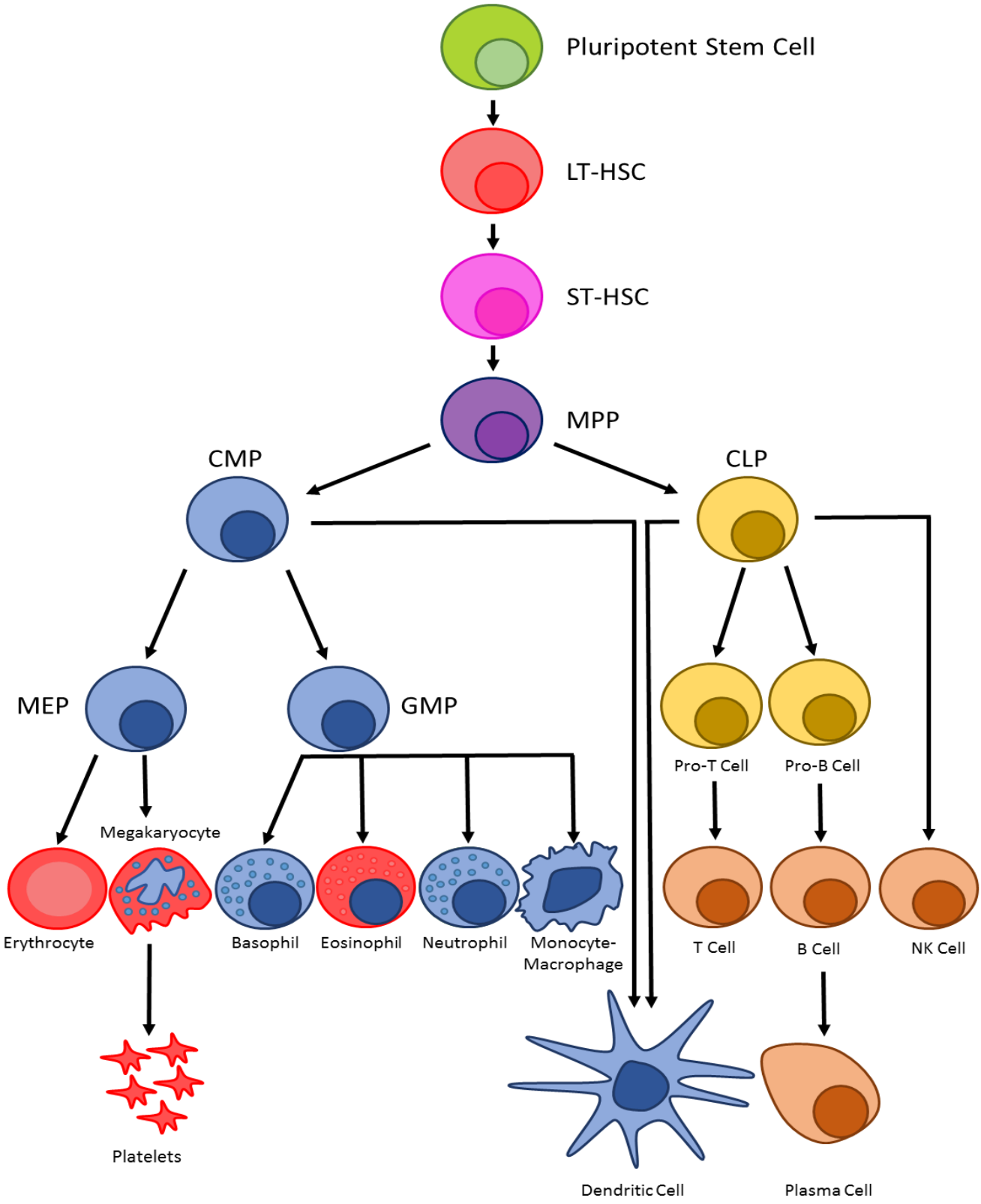

Figure 1.1 Haematopoiesis, the development of mature blood cells from stem cells. Abbreviations: LT, long term; ST, short term; MPP, multipotent progenitor; HSC, haematopoietic stem cell; CMP, common myeloid progenitor; CLP, common lymphoid progenitor; MEP, megakaryocyte erythroid progenitor; GMP, granulocyte macrophage progenitor. Adapted from (Ackermann *et al.*, 2015).

1.2 Childhood Acute Lymphoblastic Leukaemia

Acute lymphoblastic leukaemia (ALL) is a disorder of immature B and T-cells which have acquired mutations that grant them the ability to self-renew indefinitely, leading to stage-specific developmental arrest. It is the most common childhood malignancy and cause of cancer related mortality (Inaba *et al.*, 2013). The majority of leukaemias are 'pre-B', expressing the normal cell surface markers of pre-B cells.

1.2.1 Development/Aetiology

The events leading to ALL development are not well understood and only a small number can be attributed to inherited genetic defects, such as Down's syndrome (<0.5%) or the rare constitutional Robertsonion translocation between chromosomes 15 and 21 (rob(15;21)(q10;q10)c) (Pui *et al.*, 2004; Pui *et al.*, 2008; Li *et al.*, 2014). Two-infection based hypotheses exist for leukaemia development; Kinlen's 'population mixing' and Greaves' 'delayed infection', with the unifying notion that lack of exposure to common pathogens early in life, leads to a pathological development of the immune system, which may predispose the individual to haematological malignancy (Kinlen, 2004; Greaves, 2006). A proportion of ALLs have a clear prenatal origin, based on monozygotic twin studies and retrospective studies of neonatal blood spots (Guthrie Cards) in children who have gone on to develop ALL. Monozygotic twins have a high rate of concordance for ALL, this is due to the sharing of clonal progeny between twins via vascular anastomoses which develop in the monochorionic placenta (Greaves *et al.*, 2003). The *ETV6-RUNX1* (t(12;21)(p13;q22)) chromosomal translocation is found in neonates at a frequency ~100 times greater than the rate of *ETV6-RUNX1* positive childhood ALL in the population (Mori *et al.*, 2002; Greaves *et al.*, 2003). This shows that chromosomal translocations which form

pre-leukaemic clones occur *in utero,* but further genetic aberrations are needed for the development of leukaemia, such as the deletion of wild type *ETV6* (Mori *et al.*, 2002; Greaves *et al.*, 2003). Similarly, a recent study has shown that individuals who are born with a rare constitutional Robertsonion translocation between chromosomes 15 and 21 (rob(15;21)(q10;q10)c) have a vastly increased chance (~2700 fold) of developing ALL with intrachromosomal amplification of chromosome 21 (iAMP21) (Li *et al.*, 2014).

1.2.2 Clinical Features

ALL can cause a range of different symptoms, these differ depending on subtype. Many symptoms of ALL occur due to the shortage of healthy leukocytes. These include; fatigue, lethargy, fever, shortness of breath, recurrent and persistent infection, bleeding and petechiae (pinpoint-sized haemorrhages beneath the skin). Over one third of young patients present with bone pain due to expansion of the marrow by leukaemia cells

1.2.3 Disease Classification

ALL represents a diverse class of diseases which can be classified according to immunophenotyping, cytogenetics and genetic features.

1.2.3.1 Immunophenotype

This method is based on identifying cell surface expression of antigens on leukaemia cells, which reflect the stage of differentiation at which the cells became malignant. Childhood ALL can be broadly classified as precursor B-cell (85%) or T-cell (15%) (Onciu, 2009). The most important markers for sub-classifying B-lineage ALL are; CD19, CD20, CD22, CD24, and CD79a (Chiaretti *et al.*, 2014). B-cell leukaemia can be further classified into four subtypes; early pre-B cell, pre-B cell, transitional pre-B cell and mature B-cell. T-cell

markers include; CD1a, CD2, CD3 (membrane and cytoplasm), CD4, CD5, CD7 and CD8 (Chiaretti *et al.*, 2014). T-cell leukaemias are rarer than B-cell, and historically are associated with poor prognosis, however the use of more intensive chemotherapy has improved outcome substantially (Hunger *et al.*, 2012).

1.2.3.2 Cytogenetics

Chromosomal abnormalities within leukaemic blasts are important prognostic indicators and are used to classify ALL. These abnormalities include differences in number (ploidy) or structure of chromosomes. Figure 1.2 outlines the different cytogenetic subgroups seen in childhood ALL and their relative frequencies. High Hyperdiploid (>50 chromosomes), represents the most common cyotogenetic subgroup in B-cell precursor ALL (BCP-ALL), with hypodiploid (<44 chromosomes) only seen in around 1% of cases (Mullighan, 2012).

Structural abnormalities are a defining feature of ALL and can arise from chromosomal translocations, leading to the production of fusion proteins. The most common structural rearrangement in childhood ALL is *ETV6-RUNX1*, identified in around 25% of cases (Mullighan, 2012). *ETV6* is a gene involved in haematopoietic cell development, and RUNX1 is involved in embryonic haematopoiesis. Expression of this fusion protein leads to expansion of B-cell precursors, enhanced self-renewal capacity and impaired differentiation (Morrow *et al.*, 2004; Tsuzuki *et al.*, 2004; Fischer *et al.*, 2005).

Rearrangements of the *MLL* gene occur in around 6% of childhood ALL cases (Mullighan, 2012). *MLL* fusions occur with a number of different partner genes, leading to the formation of a wide range of novel chimeric proteins. These fusion proteins have been shown to interfere with transcriptional elongation, which in turn causes deregulation of

target gene expression (Mueller *et al.*, 2007; Mueller *et al.*, 2009; Lin *et al.*, 2010; Yokoyama *et al.*, 2010).

TCF3-PBX1 (t(1; 19)(q23;p13)) is the next most common chromosomal rearrangement in childhood ALL (Mullighan, 2012). *TCF3* encodes two proteins; E12 and E47, both of which are involved in the maturation of B-cells and *PBX1* is a homeobox gene expressed in most tissues except lymphocytes (Hunger, 1996). When the two are fused, a novel fusion protein is created which leads to non-physiological activation of *PBX1* in lymphocytes, which in turn leads to transactivation of a number of genes and finally transformation of the cell to a malignant phenotype (Hunger, 1996; Kamps, 1997).

BCR-ABL1 (t(9;22)), or the Philadelphia chromosome, most commonly associated with chronic myeloid leukaemia (CML), is seen in a small number of cases of childhood ALL (Mullighan, 2012). When the non-receptor tyrosine kinase ABL1, is fused to the BCR signalling protein, it becomes constitutively active, causing subsequent constitutive activation of downstream pathways such as the RAS/RAF/MEK/ERK pathway, involved in cell differentiation, survival and proliferation (Ren, 2005). More recently, another subgroup has been identified in childhood and adolescent ALL, the BCR-ABL1-like (or Ph-like) subgroup, seen in 15-20% of cases (Den Boer *et al.*, 2009; Mullighan *et al.*, 2009). BCR-ABL1-like cells have a genetic profile that is very similar to that of the BCR-ABL1 subgroup, without the *BCR-ABL1* translocation (Den Boer *et al.*, 2009; Mullighan *et al.*, 2009). BCR-ABL1-like cases of ALL have recently been shown to have a high frequency of kinase-activating alterations, with a novel ATF7IP-PDGFRB fusion shown to be sensitive to tyrosine kinase inhibitors, suggesting that a number of BCR-ALB1-like cases could be

sensitive to treatment with tyrosine kinase inhibitors (Roberts *et al.*, 2014; Ishibashi *et al.*, 2016).

The intrachromosomal amplification of chromosome 21 (iAMP21) abnormality is defined by a gain of at least 3 copies of the region of chromosome 21 containing *RUNX1*, the molecular mechanisms of which are not understood (Mullighan, 2012). iAMP21 occurs in around 2% of cases of childhood B-cell ALL and is associated with a poor outcome (Moorman *et al.*, 2007). New data suggest that outcome for these iAMP21 positive patients could be improved by using more intensive treatment (Moorman *et al.*, 2013).

1.2.3.3 Genetic Features

Mutations and deletions are also important events commonly seen in childhood ALL. RAS pathway mutations frequently occur at a rate of around 35% in diagnostic, and 25% in relapse cases (Case *et al.*, 2008; Irving *et al.*, 2014; Irving *et al.*, 2016). Furthermore, 50% of high risk (based on age at diagnosis and white blood cell count) and 70% of hypodiploid cases are RAS mutant (Zhang *et al.*, 2011; Holmfeldt *et al.*, 2013). A number of lymphoid/B-cell development related genes are also targets of somatic mutation in childhood ALL, these include; *PAX5, IKZF1 (IKAROS), TCF3, EBF1* and *IKZF2* (*AIOLOS*) (Mullighan *et al.*, 2007; Mullighan *et al.*, 2008; Mullighan *et al.*, 2009; Kuiper *et al.*, 2010; Zhang *et al.*, 2011). Alterations in *CRLF2* and the tumour suppressor gene *TP53* are also thought to be important (Russell *et al.*, 2009; Hof *et al.*, 2011; Mullighan, 2012).

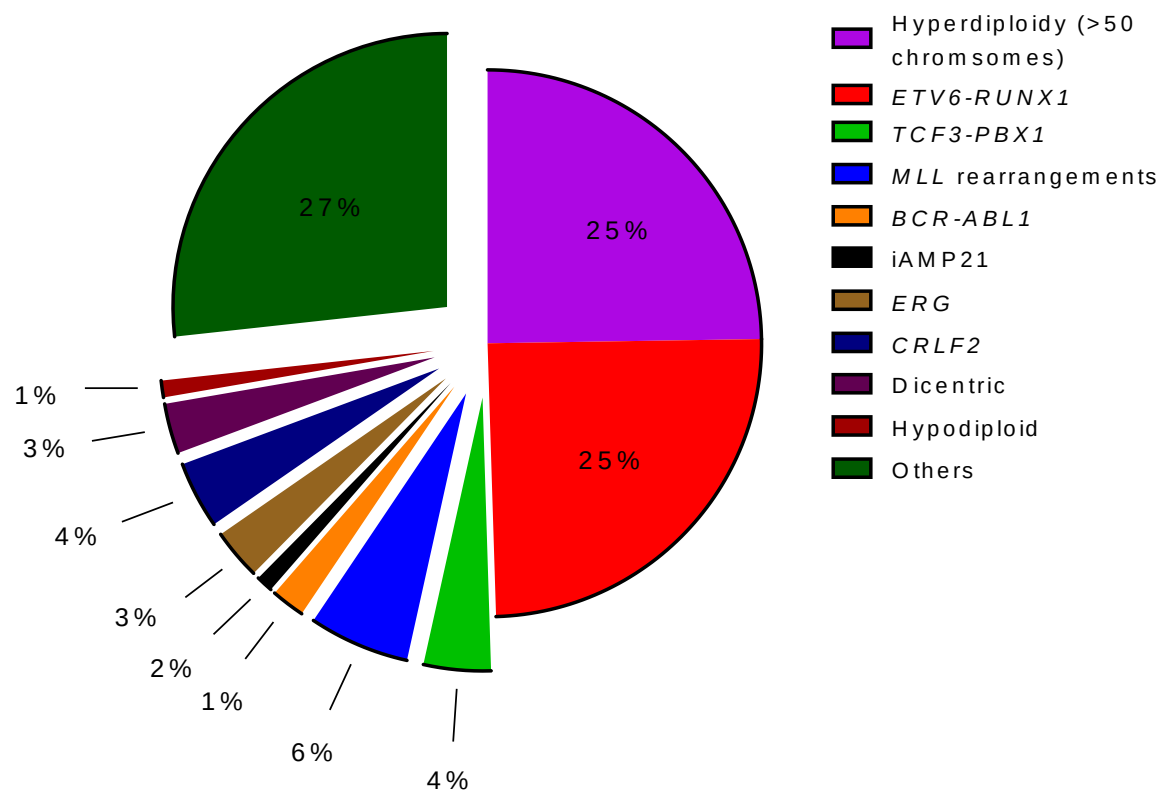

Figure 1.2 Cytogenetic subtypes seen in childhood acute lymphoblastic leukaemia (ALL) and their estimated frequencies. Adapted from (Mullighan, 2012).

1.2.4 Prognostic Factors

Clinical and disease specific features of ALL can be used as prognostic markers and allow patients to be stratified for treatment. Using this method, treatment can be tailored to the needs of the patient, those with high risk disease receiving intensified therapy, and those with lower risk disease being spared the toxicity of intensive therapy. Table 1.1 summaries the current important prognostic factors in childhood ALL.

With regards to clinical features, both age and initial white blood cell (WBC) count are predictive of outcome, with older age and/or higher WBC count representing a worse prognosis. Standard risk is defined by an age of 1 to 9.99 years and initial WBCs count of <50 000 per cubic millimetre and high risk is defined as anything greater than that stated for standard risk (Smith *et al.*, 1996). Black and Hispanic ethnic groups have a worse prognosis than White and Asian groups, likely due to the higher prevalence of *TCF3-PBX1* and *CRLF2* rearrangements respectively within these groups, but this is not used to inform treatment (Pui *et al.*, 2003; Harvey *et al.*, 2010; Hunger and Mullighan, 2015).

High hyperdiploidy, and *ETV6-RUNX1* are associated with favourable outcomes, while hypodiploid with <44 chromosomes, *MLL* rearrangement, *BCR-ABL1*, Philadelphia-like ALL, *CRLF2* rearrangement, iAMP21 and early T-cell precursor ALL are all associated with poor outcome (Nachman *et al.*, 2007; Coustan-Smith *et al.*, 2009; Arico *et al.*, 2010; Harvey *et al.*, 2010; Moorman *et al.*, 2010; Harrison *et al.*, 2014; Roberts *et al.*, 2014).

Response to treatment is an important prognostic marker, particularly with regards to glucocorticoid (GC) response. As determined by 3 individual Berlin-Frankfurt-Münster trials, one week of prednisolone monotherapy is a predictive marker of success in children

(Dordelmann *et al.*, 1999). It has been shown that leukaemic cells from high risk groups grown *in vitro* are relatively resistant to prednisolone and the largest study to date comparing diagnosis and relapse samples found that relapse cells were on average 357 fold more resistant to prednisolone than diagnosis cells (Klumper *et al.*, 1995; Pieters *et al.*, 1998). A more recent study confirms the range of GC sensitivities that are seen in ALL cells (Fischer *et al.*, 2015). Minimal residual disease (MRD), the lowest level of disease detectable in patients with complete remission, is the single most powerful prognostic factor in childhood ALL (Coustan-Smith *et al.*, 2000; Borowitz *et al.*, 2008). High sensitivity methods such as PCR of clonotypic *IGH* or *TCR* gene rearrangements that are unique to an individual patient's leukaemia, QRT-PCR identifying leukaemia-associated fusion genes such as *BCR-ABL,* or flow cytometry to identify aberrant immunophenotypic combinations, can identify as few as 1 malignant cell in 10 000 (Szczepanski, 2007; Campana, 2012; Pui *et al.*, 2015). The risk of treatment failure or death is 3-5 times higher in children with MRD ≥0.01% (MRD positive) at the end of, and at time points after, induction therapy, than in those with MRD <0.01% (MRD negative), and intensification of therapy for these patients improves their outcome (Coustan-Smith *et al.*, 2000; Borowitz *et al.*, 2008; Conter *et al.*, 2010; Schrappe *et al.*, 2011; Vora *et al.*, 2014; Pui *et al.*, 2015).

Variable	Favourable Feature	Adverse Factor	Use in Risk Stratification
Demographic and clinical features			
Age	1 to <10 years	<1 year or ≥10 years	Part of NCI risk group stratification
Sex	Female	Male	No
Race or ethnic group	White, Asian	Black, Native American, Hispanic	No
Initial WBC count	Lower (<50 000/mm^3)	Higher (≥50 000/mm^3)	Part of NCI risk group stratification
Biological or genetic features of leukaemia cells			
Immunophenotype	B-cell ALL	T-cell ALL	Often used to select therapy backbone
Cytogenetics	*ETV6-RUNX1*, hyperdiploidy, favourable chromosome trisomies	*BCR-ABL1*, *MLL* rearrangements, hypodiploidy	Often used to select treatment intensity, assign patient to HSCT, or both. Some features (e.g. *BCR-ABL1*) can be used to select targeted therapy
Genomic features	*ERG* deletions	*IKZF1* deletions or mutations; Philadelphia chromosome-like ALL with kinase gene alterations	Some research groups use *IKZF1* deletions to assign patients to more intensive therapy; kinase gene mutations may be used to assign patients to targeted therapy, but this is not yet part of routine care
Early response to treatment			
Response to 1 week of GC therapy	Good response to prednisolone (<1000 blasts/mm^3)	Poor response to prednisolone (≥1000 blasts/mm^3)	Easy measure and used by many groups; may be supplanted by MRD
Marrow blasts after 1-2 weeks of multi-agent therapy	M1 marrow (<5% blasts) by day 8 or 15	No M1 marrow (≥5% blasts) by day 8 or 15	Easy measure and used by many groups; now being supplanted by MRD
MRD quantification during or at end of induction	Reaching low (<0.01%) or undetectable MRD by specific time points	Persistence of MRD ≥0.01% at specific time points; the higher it is the worse prognosis	Most important single prognostic factor for contemporary therapy; critical for modern risk stratification
MRD at 3-4 months	Low (<0.01%), preferably undetectable	Persistence of MRD ≥0.01%	May select patients for HSCT or new therapies in first remission

Table 1.1. Important prognostic factors in childhood ALL. HSCT; haematopoietic stem cell transplant, MRD; minimal residual disease, NCI; national cancer institute. Adapted from (Hunger and Mullighan, 2015).

1.2.5 Treatment

ALL therapy is complex and comprises the use of multiple drugs over many different stages of treatment protocols. Remission induction was achieved in 80-90% of children with ALL almost 50 years ago, though almost all relapsed with central nervous system (CNS) disease, thus survival rates were only 10-20% (George *et al.*, 1968). Addition of craniospinal or cranial irradiation and intrathecal chemotherapy led to increased survival (Aur *et al.*, 1971). This was followed by the development of an intensive 8 week induction and consolidation regimen, which is now the core of most modern ALL therapies (Riehm *et al.*, 1980). Current treatment in the UK is divided into chemotherapeutic blocks; a short remission induction phase, followed by consolidation and re-intensification phases with a prolonged period of continuation therapy. A general treatment regime for childhood ALL is described in Table 1.2. Corticosteroids are of particular importance in treating ALL. Thanks to many multinational clinical trials allowing careful stratification of therapy, overall survival rates of around 90% are now being achieved (Table 1.3) (Hunger *et al.*, 2012; Vora *et al.*, 2013; Vora *et al.*, 2014). Whilst the dramatic improvements in survival achieved over the last 50 years are almost exclusively due to the successful dose stratification and scheduling, more specific, targeted therapies are beginning to be used in certain subtypes of childhood ALL. The *BCR-ABL1* fusion occurs in 3-5% of children with ALL (Ph-positive ALL) and is associated with secondary alterations such as *IKZF1* alterations (Mullighan *et al.*, 2008). Combination of the *BCR-ABL1* inhibitor imatinib, with cytotoxic chemotherapy has proved to be highly effective in Ph-positive childhood ALL, and has reduced the need for haematopoietic stem cell transplant (HSCT) in the first remission (Schultz *et al.*, 2009; Biondi *et al.*, 2012; Schultz *et al.*, 2014). Before the use of

tyrosine kinase inhibitors less than half of children with Ph-positive ALL survived (Arico *et al.*, 2010).

Phase	**Aim**	**Chemotherapeutic Agents Typically Used**
Remission Induction	Elimination of >99% blasts and restoration of normal haematopoiesis	• **Corticosteroid (E.g. dexamethasone**) • Vincristine • L-asparaginase • +/- anthracycline (high risk cases)
Consolidation/ Intensification	Reduce risk of relapse by eliminating any residual drug-resistant blasts	• Methotrexate • Mercaptopurine • Cyclophosphamide • Cytarabine (Ara-C) • Vincristine
Maintenance	Relapse prevention and elimination of residual disease	• Mercaptopurine daily • Methotrexate weekly

Table 1.2 Outline of the general regime for treatment of childhood ALL. Adapted from (Pui *et al.*, 2004)

Research Group	Trial	Reference	Region	Years	Subgroup	No. of Patients	EFS	OS
COG	Many trials	(Hunger *et al.*, 2012)	US, CA, AU, NZ	2000-2005	Overall	6994	N/A	91.3
					B-ALL	5845	N/A	92.0
					T-ALL	475	N/A	81.5
SJCRH	Total Therapy Study XV	(Pui *et al.*, 2009)	US	2000-2007	Overall	498	85.6	93.5
					B-ALL	422	86.9	94.6
					T-ALL	76	78.4	87.6
DFCI	DFCI ALL Consortium Protocol 00-01	(Vrooman *et al.*, 2013)	US, CA	2000-2004	Overall	492	80.0	91.0
					B-ALL	443	82.0	N/A
					T-ALL	49	69.0	N/A
AIEOP-BFM	AIEOP-BFM ALL 2000	(Conter *et al.*, 2010; Schrappe *et al.*, 2011)	Western Europe	2000-2006	Overall	4480	80.3	91.1
					B-ALL	4016	80.4	91.8
					T-ALL	464	75.9	80.7
MRC-NCRI	UKALL 2003	(Vora *et al.*, 2013)	UK	2003-2011	Overall	3126	87.2	91.5
					B-ALL	2731	N/A	N/A
					T-ALL	388	N/A	N/A
DCOG	DCOG Protocol ALL-9	(Veerman *et al.*, 2009)	NL	1997-2004	Overall	859	81	86
					B-ALL	701	82	N/A
					T-ALL	90	72	N/A
EORTC CLG	EORTC CLG 58591	(Domenech *et al.*, 2014)	BE, FR	1998-2008	Overall	1940	82.6	89.7
NOPHO	ALL-2000	(Schmiegelow *et al.*, 2010)	DK, FI, IS, NO, SE	2000-2007	Overall	1023	79	89
					B-ALL	906	81	91
					T-ALL	115	64	72

Table 1.3 Outcomes of modern childhood ALL trials in North America and Western Europe. Survival rates shown are at 5 years except for the AIEOP-BFM which were reported at 7 years. COG; Children's Oncology Group, SJCRH; St Jude Children's Research Hospital, DFCI; Dana-Faber Cancer Institute, AIEOP-BFM; Italian Association of Pediatric Hematology and Oncology and Berlin-Frankfurt-Münster, MRC-NCRI; Medical Research Council and National Cancer Research Institute, DCOG; Dutch Childhood Oncology Group, EORTC CLG; European Organisation for Research and Treatment of Cancer – Children's Leukemia Group, NOPHO; Nordic Society of Paediatric Oncology Haematology and Oncology. Adapted from (Hunger and Mullighan, 2015).

1.2.6 Relapse

Despite highly successful treatment, relapse occurs in 15-20% of childhood ALL cases, with 5 year survival rates between 70-25% depending on the relapse risk classification (Table 1.4) (Nguyen *et al.*, 2008; Bhojwani and Pui, 2013). This makes relapsed childhood ALL the 5th most common childhood malignancy and it is associated with a large number of childhood cancer deaths each year (Bhojwani and Pui, 2013). There are a number of relapse associated mutations, which in some cases lead to treatment resistance or an increased rate of mutation (Meyer *et al.*, 2013; Ma *et al.*, 2015). A repeated course of therapy can be used to treat relapse or allogeneic HSC transplant. In the majority of cases, relapse is established by a minor subclone which was present at diagnosis and has been selected by front-line chemotherapy (Ma *et al.*, 2015). Next generation sequencing technologies with high sequencing depth allow the identification of mutations which are present in only a small number of the cell population, i.e. subclones. To accurately identify a subclone, the presence or absence of variants must be identified and allele frequencies must be accurately assigned. The ability of this method to determine variant frequency is dependent on the depth of sequencing. A sequencing depth of 500x is required to identify variants that are present at a frequency of 5%, 1000x to determine 1% and so on (Stead *et al.*, 2013). A minimum sequencing depth of 250x is required to accurately identify and assign allelic frequencies (Stead *et al.*, 2013). Modern, ultra-deep sequencing can reach multiple thousands depth of coverage, identifying variants that occur at very low level. Allele specific PCR represents another method which can be used to identify these variants and has been used previously by our group to identify low level *KRAS* mutations (Irving *et al.*, 2014). This method is a modified application of PCR which involves the design

of primers which preferentially amplify the mutant allele over the wild type allele by exploiting the amplification efficiency of DNA polymerase in the presence of mismatched base pairs. Understanding clonal evolution and identifying minor clones which commonly establish relapse may allow better relapse prediction and targeting of low level alterations alongside standard chemotherapy at diagnosis for relapse prevention. *CREBBP* mutations are frequently found at relapse in childhood ALL and are the key focus of this thesis (Section 1.4.3) (Mullighan *et al.*, 2011; Pasqualucci *et al.*, 2011a; Inthal *et al.*, 2012; Holmfeldt *et al.*, 2013).

Risk Group	Description	5 Year Survival (%)
S1	Late extramedullary	60-70
S2	Early and very early extramedullary	60
	B-lineage late marrow	
	B-lineage combined (early or late)	
S3	B-lineage early marrow	30
S4	Very early marrow	25
	Very early combined	
	T-lineage marrow	

Table 1.4 Berlin-Frankfurt-Münster (BFM) Classification for Relapse. Adapted from (Bhojwani and Pui, 2013).

1.3 Non-Hodgkin's Lymphoma

Non-Hodgkin's lymphomas (NHLs) are cancers of the lymphatic system that are more common in old age (>65 years) and represent a heterogeneous group of lymphoid malignancies. Recurrent translocations which occur during different steps of B-cell differentiation are often the initial step in the transformation of these malignancies, but secondary genetic alterations are usually required for full malignant transformation (Nogai *et al.*, 2011).

1.3.1 Diffuse Large B-cell Lymphoma

Diffuse large B-cell lymphoma (DLBCL) is the most common form of B-cell Non-Hodgkin's lymphoma (B-NHL), accounting for 30-40% of newly diagnosed cases of B-NHL in the UK, making it the sixth most common cancer (Cancer Research UK, 2010; Campo *et al.*, 2011). It is predominantly seen later in life, with average age of onset around 70 years (Cancer Research UK, 2010).

1.3.1.1 Aetiology/Development

DLBCL is a disease of mature B-cells and the events leading to its onset are not well understood. There are however, some links between DLBCL and infection. Firstly, infection with Epstein Barr virus (EBV) has been associated with onset of DLBCL, most frequently in elderly patients (>50 years), but also in some younger patients, without evidence of immunodeficiency (Kuze *et al.*, 2000; Oyama *et al.*, 2007; Morales *et al.*, 2010). EBV is maintained as an asymptomatic, persistent infection, in around 95% of the population and is recognised as an oncogenic agent in a range of different cancers such as Burkitt's lymphoma, Hodgkin lymphoma and DLBCL as well as immunodeficiency related lymphoproliferative disorders (LPDs) (Swinnen, 1999; Kuze *et al.*, 2000; Kelly *et al.*,

2002; Thorley-Lawson and Gross, 2004; Shah and Young, 2009). EBV positive DLBCL of the elderly has been shown to have a poorer prognosis than the EBV negative disease (Nakamura *et al.*, 2008; Beltran *et al.*, 2012). Infection with human T-lymphotropic virus type-1 (HTLV-1) and human immunodeficiency virus (HIV) have also been identified as risk factors leading to the onset of DLBCL (Nakamura *et al.*, 2008; Beltran *et al.*, 2012).

1.3.1.2 Clinical Features

The first symptom of DLBCL is often swollen lymph nodes, commonly in the neck, armpit or groin and further symptoms often develop based on which parts of the body the lymphoma is developing in. For example DLBCL in the stomach can cause abdominal discomfort or pain. Other symptoms include fever, night sweats, unexplained weight loss, fatigue and loss of appetite.

1.3.1.3 Disease Classification/Genetic Features

DLBCL is a highly heterogeneous disease and shows significantly higher genomic complexity than other B-cell malignancies, with between 50 and 100 genetic lesions per case (Pasqualucci and Dalla-Favera, 2014). Despite this complexity, DLBCL can be separated into two major categories based on genetic profiling; germinal centre B-cell (GCB) and activated B-cell (ABC) (Table 1.5) (Figure 1.3) (Rosenwald *et al.*, 2002; Rosenwald *et al.*, 2003; Shaffer *et al.*, 2012). A third minor subtype has also been identified, primary mediastinal B-cell lymphoma (PMBL), which has a genetic profile that closely matches that of Hodgkin's lymphoma (Table 1.5) (Rosenwald *et al.*, 2003; Shaffer *et al.*, 2012).

DLBCL Subtype	Immunophenotype	Diagnostic Molecular Features	Frequency	Clinical Features
GCB	CD20, CD10, BCL6, GCET, LMO2, IRF4^{-}, FOXP1^{-}	Gene expression profiling	17%	Median age 61
				Nodal and extranodal
				Survival ~60% at 5 years
				Curable >50%
ABC	CD20, IRF4, FOXP1, CD10–, BCL6– GCET1–, LMO2–	Gene expression profiling	15%	Median age 66
				Nodal and extranodal
				Survival ~40% at 5 years
				Curable >30%
Primary mediastinal B-cell lymphoma	CD30, CD20, CD10–	Gene expression profiling	6%	Median age 33
				Mediastinal, thoracic > nodal
				Survival >60% at 5 years
				Curable >60%

Table 1.5. Classification of DLBCL. Adapted from (Shaffer *et al.*, 2012).

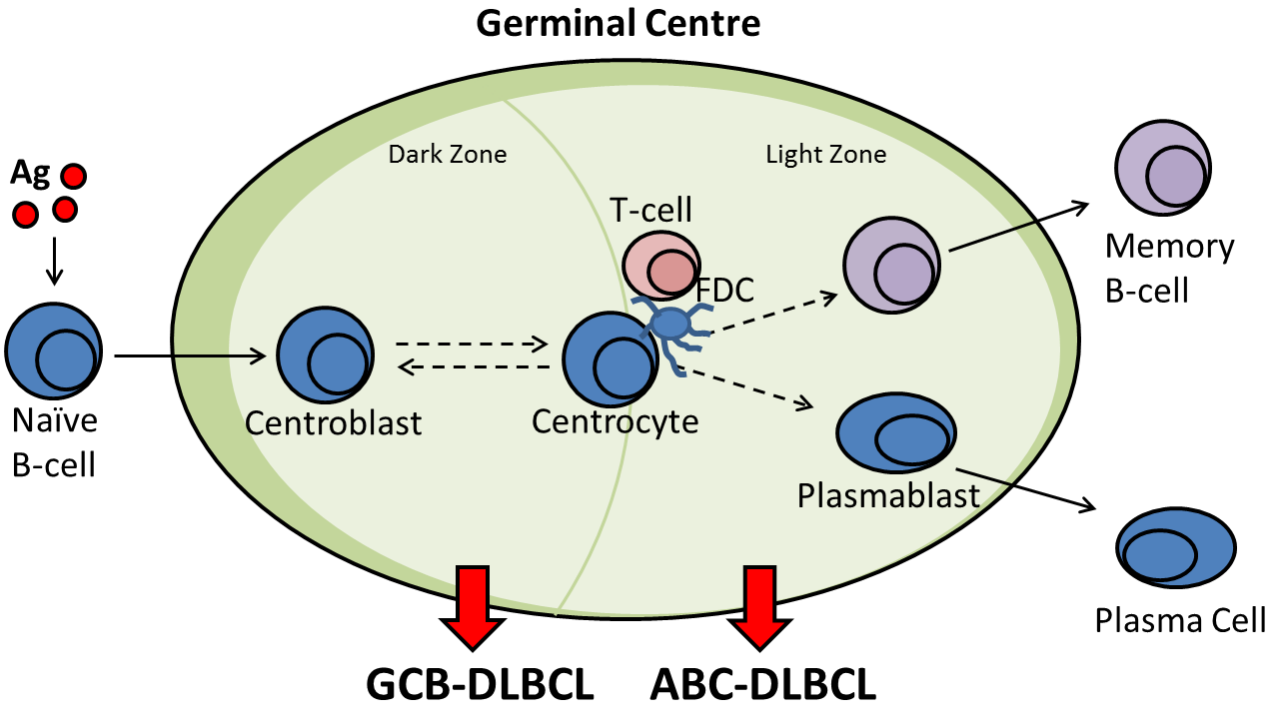

Figure 1.3. Cellular origins of diffuse large B-cell lymphoma (DLBCL). Ag; antigen, FDC; follicular dendritic cell. Adapted from (Pasqualucci and Dalla-Favera, 2014).

The gene expression profile in GCB-DLBCL resembles that of a GCB cell, with evidence of ongoing somatic hypermutation (SHM) as well as the presence of hypermutated immunoglobulin (Ig) genes (Lossos *et al.*, 2000; Shaffer *et al.*, 2012). GCB-DLBCL is categorised by the overexpression of genes involved in proliferation/apoptosis such as *BCL2*, *MYC* and the mir-17-92 cluster and other genes such as *EZH2* by either chromosomal translocation, copy number gain, or somatic mutation (Rao *et al.*, 1998; Willis and Dyer, 2000; Iqbal *et al.*, 2004; Ota *et al.*, 2004; He *et al.*, 2005; Morin *et al.*, 2010; Morin *et al.*, 2011; Schuetz *et al.*, 2012; Shaffer *et al.*, 2012; Horn *et al.*, 2013). Mutations in *GNA13* and *SGK1* are also frequently seen in this subtype along with loss of function in other genes, for instance *TNFRSF14* and *PTEN* (Morin *et al.*, 2011; Lohr *et al.*, 2012; Zhang *et al.*, 2013).

ABC-DLBCL on the other hand, resembles the transcriptional profile of an ABC, with downregulated germinal centre-specific genes, activation of BCR and NFκB pathways and no evidence of ongoing SHM (Lossos *et al.*, 2000; Davis *et al.*, 2001; Lenz *et al.*, 2007; Shaffer *et al.*, 2012). ABC-DLCB is categorised by genetic aberrations which cause the overexpression of factors leading to constitutive NFκB and B-cell receptor (BCR) activity such as; *MYD88*, *CD79A/B* and *CARD11* as well as another gene known as *SPIB*, which is involved in normal germinal centre reactions (Su *et al.*, 1997; Lenz *et al.*, 2008a; Lenz *et al.*, 2008b; Davis *et al.*, 2010; Morin *et al.*, 2011; Ngo *et al.*, 2011). Genes with frequent loss of function in ABC-DLBCL include the NFκB inhibitor *TNFAIP3*, terminal differentiation block associated *PRDM1/BLIMP1* and cell cycle checkpoint factor *CDKN2A/B* (Pasqualucci *et al.*, 2006; Lenz *et al.*, 2008b; Compagno *et al.*, 2009; Morin *et al.*, 2011).

A number of unifying genetic abnormalities are seen between both of the major subtypes of DLBCL. These include; loss of function in genes involved in histone/chromatin modifications, such as *CREBBP/EP300* and *MLL2/MLL3*, and genes involved in immune escape, for example *B2M* and *CD58,* as well as other genes, for instance *FOXO1* and *TP53* (Morin *et al.*, 2011; Pasqualucci *et al.*, 2011a; Pasqualucci *et al.*, 2011b). Gains of function in *BCL6* and *MEF2B* are also frequently seen in both subtypes (Pasqualucci *et al.*, 2003; Morin *et al.*, 2011). These alterations lead to increased activity of the *BCL6* oncogene, or acquisition of the ability to evade the immune response (Shaffer *et al.*, 2012).

1.3.1.4 Prognostic Factors

Table 1.6 shows a list of prognostic factors which are used in DLBCL (Vaidya and Witzig, 2014). The international prognostic index (IPI), established in 1993 is the most robust prognostic tool for DLBCL and is used in clinical trials (Shipp, 1993). This model uses 5 factors to predict survival, age >60, elevated serum lactate dehydrogenase (LHD), ECOG performance status ≥2, Ann Arbor state II or IV and number of involved extranodal sites ≥2 (Shipp, 1993; Vaidya and Witzig, 2014). Table 1.7 shows overall survival with and without rituximab therapy based on IPI risk group. Despite ABC-DLBCL having a much lower 5 year survival rate than the less aggressive GCB-DLBCL form of DLBCL, gene expression profiling has limited clinical utility in making treatment decisions for newly diagnosed DLBCL (Alizadeh *et al.*, 2000; Rosenwald *et al.*, 2002; Rosenwald *et al.*, 2003; Vaidya and Witzig, 2014).

Standard Prognostic Factors	1. The International Prognostic Index (IPI)
	2. Immunohistochemistry for cell of origin (e.g. Hans algorithm)
	3. Imaging with positron emission tomography (PET)/CT scan
	4. Fluorescent in situ hybridization (FISH) for MYC and BCL2 rearrangements
	5. Absolute lymphocyte and absolute monocyte count
Provisional Prognostic Factors	1. Gene expression profiling for cell of origin
	2. Serum immunoglobulin free light chains
	3. Serum 25-hydroxy vitamin D levels
	4. Serum cytokine/chemokines

Table 1.6. List of prognostic factors in DLBCL. Adapted from (Vaidya and Witzig, 2014).

Number of Risk Factors	Risk Group	5-year OS% (without rituximab)	3-year OS% (with rituximab)
0-1	Low	73	91
2	Low-intermediate	51	81
3	High-intermediate	43	65
4-5	High	26	59

Table 1.7. Treatment outcomes in diffuse large B-cell lymphoma based on IPI risk group. Risk factors: age >60 years; number of extranodal disease sites >1; serum lactate dehydrogenase (LDH) above normal ECOG performance status ≥2; Ann Arbor stage III or IV. OS; overall survival. Adapted from (Vaidya and Witzig, 2014).

Translocations involving *MYC* are present in 5-10% of DLBCL cases and are associated with one study reporting an inferior 5-year progression free survival (31% compared to 66% in cases without *MYC* translocation), however this was not confirmed in similar retrospective studies (Kramer *et al.*, 1998; Klapper *et al.*, 2008; Savage *et al.*, 2009; Barrans *et al.*, 2010). Overexpression of the anti-apoptotic protein, BCL2, occurs in 47-58% of DLBCL cases and was associated with a higher relapse rate and worse overall survival before the introduction of rituximab therapy (Hermine *et al.*, 1996; Hill *et al.*, 1996; Gascoyne *et al.*, 1997; Mounier *et al.*, 2003). Some cases of DLBCL harbour *MYC* translocation along with additional translocations involving the *BCL2* or the *BCL6* loci. These are termed double-hit lymphomas (DHL), and have a poorer prognosis than *MYC* translocation alone (Aukema *et al.*, 2011).

Absolute lymphocyte count (ALC) is a surrogate marker for host immunity. High ALC levels are associated with a good prognosis and are a prognostic marker independent of cell of origin (GCB or non-GCB) (Kim *et al.*, 2007; Oki *et al.*, 2008; Song *et al.*, 2010; Wilcox *et al.*, 2011; Porrata *et al.*, 2012). Conversely, high absolute monocyte count (AMC) is associated with a poor prognosis and a ratio of ALC/AMC has been shown to be an independent prognostic factor after adjusting for IPI (Vaidya and Witzig, 2014). Around 32% of DLBCL cases have increased immunoglobulin free light chain (FLC) (Maurer *et al.*, 2011). Immunoglobulin FLC, both polyclonal and monoclonal (polyclonal; elevations in κ and λ, monoclonal; elevations in just one of the light chains), is associated with inferior event free survival and overall survival in DLBCL (Maurer *et al.*, 2011). Low levels of circulating vitamin D and elevated pre-treatment cytokine levels have also been associated with an

inferior prognosis in DLBCL (Ennishi *et al.*, 2009; Ansell *et al.*, 2012; Bittenbring *et al.*, 2014).

18-fluorodeoxyglucose positron emission tomography (^{18}FDG-PET) with computed tomography (PET/CT) is a highly sensitive method for determining the sites of disease in DLBCL. Obtaining a FDG-PCT/CT scan at diagnosis has become the standard of care as it leads to a change in the stage of disease in between 20 and 40% of cases. Scanning in this way is also effective for the assessment of residual disease, with a positive FDG-PET/CT at the end of treatment being associated with inferior progression free survival and overall survival (Jerusalem *et al.*, 1999; Mikhaeel *et al.*, 2000; Buchmann *et al.*, 2001; Schoder *et al.*, 2001; Spaepen *et al.*, 2001; Sasaki *et al.*, 2002; Kostakoglu *et al.*, 2004; Seam *et al.*, 2007; Dupuis *et al.*, 2009).

1.3.1.5 Treatment

Cyclophosphamide, doxorubicin, vincristine and prednisone (CHOP) was identified as the best treatment for NHL in 1993, and remains the backbone of NHL today (Fisher *et al.*, 1993). The addition of the anti-CD20 monoclonal antibody rituximab (R-CHOP), led to a 15% increase in overall survival across all DLBCL cases (Coiffier *et al.*, 2002; Habermann *et al.*, 2006; Pfreundschuh *et al.*, 2006; Pfreundschuh *et al.*, 2008). Recently, a number of new agents have been trialled for use in addition to R-CHOP, such as the anti-CD22 monoclonal antibody, epratuzumab, the proteasome inhibitor, bortezomib and the immunomodulatory agent, lenalidomide (Micallef *et al.*, 2011; Nowakowski *et al.*, 2011; Ruan *et al.*, 2011; Chiappella *et al.*, 2013).

1.3.2 Follicular Lymphoma

Follicular lymphoma (FL) is the second most common form of B-NHL, making up around 20% of all new diagnoses in the UK (Cancer Research UK, 2010). FL is an initially indolent disease associated with old age, with an average age of onset around 60 years (Blood, 1997; Armitage and Weisenburger, 1998; Harris *et al.*, 1999).

1.3.2.1 Aetiology/Development

The aetiology of FL is poorly understood, but like DLBCL, risk of FL has been linked to EBV and HTLV-1 infection and also infection with human herpes virus 8 (HHV-8) (Hartage *et al.*, 2006; Ma, 2012). FL is a disease of mature B-cells, all of which share identical Ig gene rearrangements, suggesting that founding mutations occur post-VDJ recombination (Green *et al.*, 2013). FL cells express B-cell markers such as; LMO2, CD10 and BCL6 along with mature B-lineage markers, including surface Ig and CD19 (Bilalovic *et al.*, 2004).

1.3.2.2 Clinical Features

The symptoms of FL are similar to those seen in other lymphoid malignancies and include; loss of appetite and weight, fever, tiredness or fatigue and frequent infections. If FL occurs in the bone marrow it can cause low blood cell counts which can result in anaemia and low platelet counts.

1.3.2.3 Disease Classification/Genetic Features

Diagnosis of FL is based on histology, with increasing number of centroblasts indicative of increasing clinical aggressiveness. The World Health Organisation (WHO) classification adopts grading of 1-3 based on this number. FL cells express CD19, CD20, CD10, BCL6 and monoclonal Ig light chain and are negative for CD5 and CD23 (Freedman, 2014). The

genetic hallmark of FL, occurring in >90% of cases, is a t(14;18)(q32;q21) translocation, in which the oncogene *BCL2* is placed under the control of the Ig heavy-chain locus (Weiss *et al.*, 1987; Zelenetz *et al.*, 1991). There are a number of genes which have been identified as recurrently mutated in FL, these include; *CREBBP*, *MLL2*, *TNFRSF14*, *BCL2*, *HER2*, *IKZF2* and *CD40* (Pasqualucci *et al.*, 2011a; Pasqualucci *et al.*, 2011b; Lohr *et al.*, 2012; Weigert *et al.*, 2012; Green *et al.*, 2013). A recent study by Green *et al.* shed light onto the hierarchy of genetic events in FL (Figure 1.4) (Green *et al.*, 2013). *BCL2* translocation appears to be an initiating mutation, given that it is present at diagnosis and relapse but is not sufficient to cause malignant transformation alone (Ladetto *et al.*, 2003; Green *et al.*, 2013). *CREBBP* mutations on the other hand, are also seen frequently and are uniformly expressed between subpopulations (Green *et al.*, 2013). Although they are not always seen at diagnosis, they are always kept between diagnosis and relapse, suggesting they constitute driver mutations (Green *et al.*, 2013). *MLL2* and *TNFRSF14* mutations however, are variably expressed between subpopulations and can be lost between diagnosis and relapse, suggesting they are tertiary events or accelerator mutations (Green *et al.*, 2013).

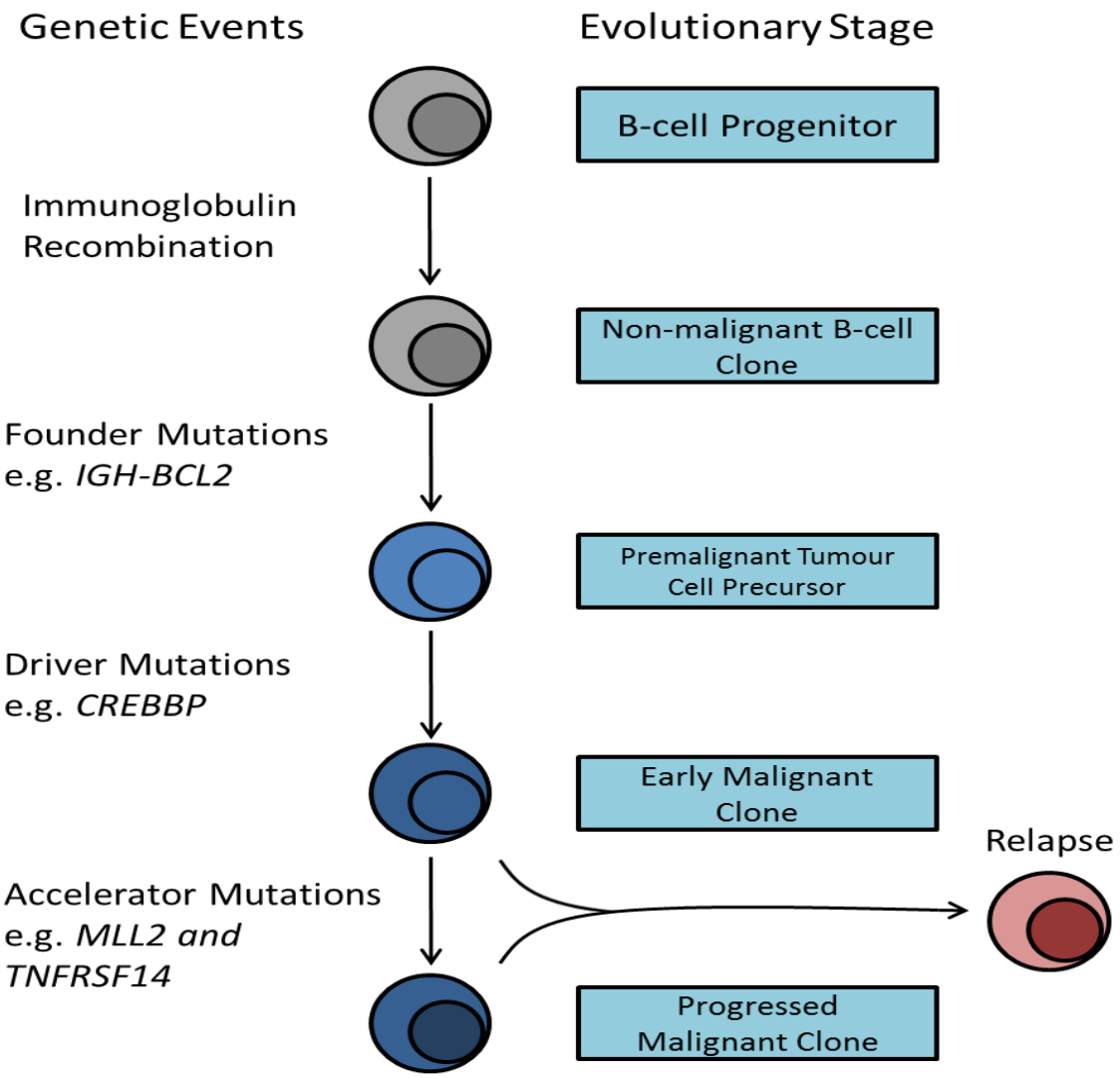

Figure 1.4. Hierarchy of somatic mutations arising in follicular lymphoma. Adapted from (Green *et al.*, 2013).

FL has a tendency to transform into the more aggressive DLBCL (Montoto and Fitzgibbon, 2011) (Section 1.3.1). Evidence suggests that between 16 and 70% of patients may undergo this transformation (Montoto and Fitzgibbon, 2011). This transformation may occur due to mutations in a common precursor clone (CPC), with mutations in genes involved in epigenetic modification and resistance to apoptosis frequently seen (Pasqualucci *et al.*, 2014). Other genetic events which are frequently observed in transformed FL (tFL) include; mutations in *TP53*, *KMT2D*, *CREBBP*, *EZH2* and *BCL2*, mutation or epigenetic silencing of *CDKN2A/p16*, *BCL6* translocations, alterations of chromosome 1p36, and altered *MYC* expression (Lo Coco *et al.*, 1993; Sander *et al.*, 1993; Pinyol *et al.*, 1998; Lossos *et al.*, 2002; Akasaka *et al.*, 2003; Martinez-Climent *et al.*, 2003; Pasqualucci *et al.*, 2014; Bouska *et al.*, 2016). Despite the frequency of these mutations, no single lesion appears to be selected for during transformation to DLBCL (Pasqualucci *et al.*, 2014).

1.3.2.4 Prognostic Factors

FL is considered an indolent disease which is usually incurable in advanced stages. Table 1.8 shows a list of prognostic models used for risk stratification in FL. The two best measures of outcome are the FL international prognostic index (FLIPI) and histological tumour grade (Relander *et al.*, 2010). FLIPI determines prognosis based on five prognostic factors; age, serum lactate dehydrogenase, haemoglobin level, tumour stage and number of nodal areas involved (Solal-Celigny *et al.*, 2004). A modified version of this named FLIPI2 has also been developed (Table 1.8) (Federico *et al.*, 2009). Loss of chromosomal material at 6q25-27 and deletions in 9p21, 6q25 and 6q26 have all been reported to be associated with inferior survival in FL (Cheung *et al.*, 2009; Schwaenen *et al.*, 2009). Transformation

to DLBCL is clinically important in FL, with an average survival of around 2 years post-transformation (Montoto and Fitzgibbon, 2011). Deletions in 1p36.22-p36-33 and 6p21-q24.3 as well as uniparental disomy of chromosome 16 are highly associated with transformation and inferior survival in FL (Viardot *et al.*, 2002; O'Shea *et al.*, 2009). Table 1.9 describes overall survival and progression free survival associated with different FLIPI classifications of FL.

Prognostic Model	Risk Factor
Follicular lymphoma international prognostic index (FLIPI)	Age >60
	Serum LDH>ULN
	Haemoglobin level <12.0g/dl
	Stage III or IV
	Number of nodal sites >4
FLIPI2	Age >60
	Bone marrow involvement
	Haemoglobin level <12.0g/dl
	Greatest diameter of the largest involved node >6cm
	Serum beta-2 microglobulin level greater than the upper limit of normal
Groupe d'Etude des Lymphomes Folliculaires (GELF) criteria for high tumour burden	Any site >7cm
	≥3 sites >3cm
	Spleen below unbilican line
	Compressive symptoms
	Pleural or peritoneal effusions – 5 000 tumour cells/mm^3
	Absolute neutrophil count <1000/mm^3
	Platelet count <100 000/mm^3

Table 1.8. Prognostic models for follicular lymphoma. LDH; lactate dehydrogenase, ULN; upper limit of normal. Adapted from (Freedman, 2014).

Risk Group	Number of Risk Factors	2 year OS%	2 year PFS%
Low risk	0-1	98	84
Intermediate risk	2	94	70
High Risk	≥3	87	42

Table 1.9. Treatment outcomes of FL based on FLIPI. OS; overall survival, PFS; progression free survival. Adapted from (Freedman, 2014).

1.3.2.5 Treatment

FL is considered 'incurable' by standard chemotherapy, though advances in understanding and treatment have improved clinical outcomes and management of the disease. Less than 10% of patients are diagnosed with early stage disease (I/II) (Friedberg *et al.*, 2012). Early stage FL is often treated with external beam radiation therapy (XRT), though recent reports showed that >50% of stage I/II patients did not require radiotherapy at a median of 6 years and 85% of patients were alive at 10 years (Wilder *et al.*, 2001; Advani *et al.*, 2004). FL is a disease predominant in older age so for those with a life expectancy of 15 years or less diagnosed with early stage FL, a wait-and-watch, or palliative approach is often the best option (Kahl and Yang, 2016).

Advanced stage FL is separated into 4 categories for treatment purposes; 1) asymptomatic, low tumour burden, 2) asymptomatic, high tumour burden, 3) symptomatic, low tumour burden and 4) symptomatic, high tumour burden. Asymptomatic, low tumour burden and symptomatic high tumour burden represent the most common groups (Kahl and Yang, 2016). Asymptomatic, low tumour burden patients are candidates for a watch and wait strategy. Treatment of symptomatic, high tumour burden FL is with R-CHOP therapy as described in section 1.3.1.5, with investigations taking place into the use of novel agents such as lenalidomide, ibrutinib, venetoclax and duvelisib (Kahl and Yang, 2016). The alkylating agent bendamustine can be used for the treatment of relapsed or refractory FL, with an overall response rate of 75% and a progression free survival of 9.3 months achieved in clinical trials (Kahl *et al.*, 2010). Fludarabine regimens, as well as radiotherapy, are also options for the treatment of relapsed or refractory FL (Kahl and Yang, 2016). A novel treatment option for relapsed FL

is the phosphatidylinositol 3-kinase (PI3K) δ inhibitor idelalisib, which showed a response rate of 27% in clinical trials (Gopal *et al.*, 2014).

1.4 CREBBP

Cyclic adenosine monophosphate (cAMP) response element binding protein (CREB), binding protein (CREBBP/CBP) is a member of the KAT3 family of histone acetyltransferases along with its paralogue EP300. It is a transcriptional co-activator and histone acetyl transferase (HAT) located on chromosome 16 at p13.3.

1.4.1 CREBBP Structure

CREBBP is a large protein, around 265kDa in size and made up of numerous discrete functional domains (Figure 1.5). The SRCAP interaction domain (amino acids 227-410) allows interaction with the Snf2-Related-CBP activator protein (SRCAP) ATPase, which is able to enhance the ability of CREBBP to activate transcription (Johnston *et al.*, 1999). The TAZ-type 1 zinc finger (amino acids 347-433) acts as a HIF1α and CITED2 interaction domain. HIF1α requires binding here to allow transcriptional activity during hypoxia (De Guzman *et al.*, 2004). CITED2, induced by HIF1α, competes for binding and allows the HIF1α response to be attenuated due to negative feedback (De Guzman *et al.*, 2004). The KIX domain (amino acids 587-666) provides an interaction site for the phosphorylated KID domain of CREB (Radhakrishnan *et al.*, 1997). Like most histone modifiers, CREBBP has a bromodomain (amino acids 1103-1175), which allows interaction with acetylated lysine residues present on the N-terminal tails of histones (Giles *et al.*, 1997; Zeng and Zhou, 2002). The largest functional domain in the CREBBP protein is the HAT domain (amino acids 1173-1849), which functions to acetylate histone and non-histone proteins leading

to a variety of cellular effects (Bannister and Kouzarides, 1996; Ogryzko *et al.*, 1996). The cysteine/histidine rich region in CREBBP (amino acids 1199-1487) contains a PHD-like zinc finger which is an important part of the enzymatic core of the HAT domain (Borrow *et al.*, 1996; Kalkhoven, 2004). The ZZ-type zine finger (amino acids 1701-1744) is linked to the TAZ-type 2 zinc finger (amino acids 1765-1846) to form an E1A binding site (Kalkhoven, 2004). This is the binding site for the transactivation domain of p53 as well as the interaction site for the adenovirus E1A oncoprotein and numerous others including the anaphase promoting complex/cyclosome (APC/C) and proteins involved in cell cycle progression and transcription (De Guzman *et al.*, 2000; Kalkhoven, 2004; Turnell *et al.*, 2005). EP300, the KAT3 family member and paralogue of CREBBP, is highly related, and shares a number of the domains described above (Bedford *et al.*, 2010).

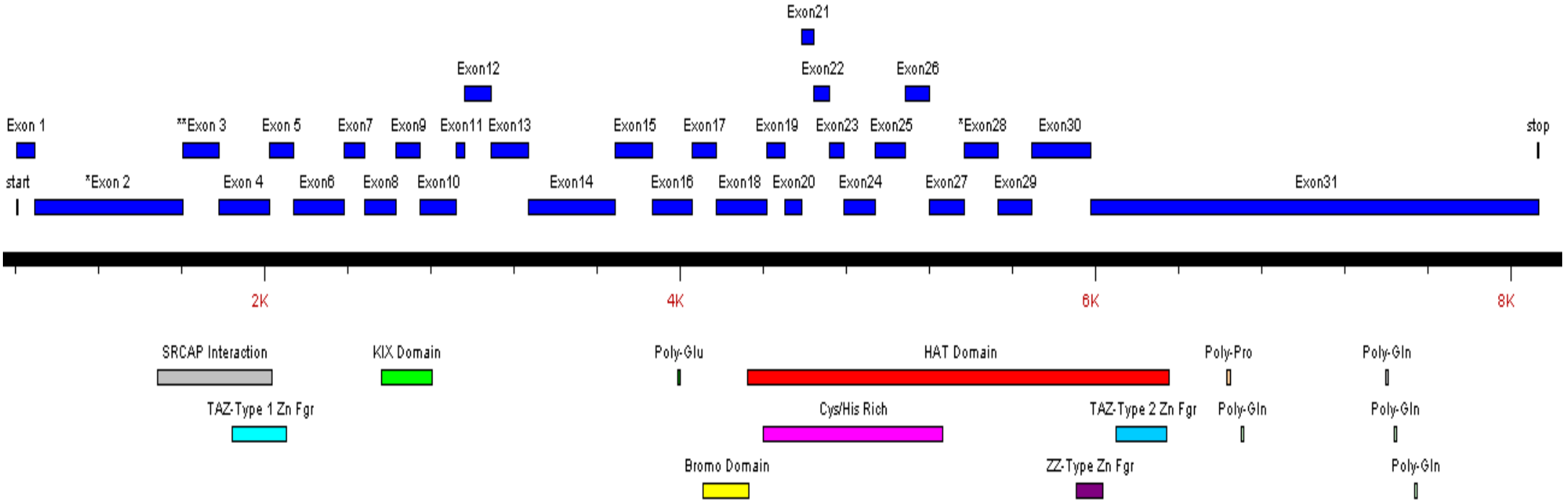

Figure 1.5. Map of *CREBBP* exons including locations of functional domains. Above nucleotide sequence (black); *CREBBP* exons (blue). Below nucleotide sequence; CREBBP functional domains. (Ensembl ID: ENST00000262367).

1.4.2 CREBBP Function

CREBBP plays a body-wide role in transcription and cell cycle control, interacting with the TATA-box binding protein (TBP) and transcription factor II B (TFIIB), both of which are involved in the formation of the RNA polymerase pre-initiation complex, as well as the E2F family of transcription factors and the APC/C (Kwok *et al.*, 1994; Yuan *et al.*, 1996; Martinez-Balbas *et al.*, 2000; Marzio *et al.*, 2000; Turnell *et al.*, 2005). Further to this CREBBP is involved in HSC function and self-renewal, acting as a signal integrator in the haematopoietic system through interaction with transcription factors such as SFPI1/PI.1 and C/EBPα (Yamamoto *et al.*, 1999; Blobel, 2000; Rebel *et al.*, 2002; Kovacs *et al.*, 2003; Iwasaki *et al.*, 2005; Zimmer *et al.*, 2011). CREBBP also acts as a co-activator for the transcription factor GATA-1, which is involved in erythroid cell maturation, coordinating the transcription of erythroid specific genes, blocking apoptosis in precursor cells and controlling the balance between cell proliferation and cell cycle arrest (Blobel *et al.*, 1998). Both CREBBP and EP300 have been shown to be concentrated at the 5' and 3' ends of genes they are associated with, suggesting that they are also involved in pre-mRNA maturation (Ramos *et al.*, 2010).

CREBBP plays a crucial role in cAMP-dependent signalling, a ubiquitous form of signal transduction. Activation of protein kinase A (PKA) by increased levels of intracellular cAMP, leads to phosphorylation of the kinase inducible domain (KID) of CREB, which in turn allows CREBBP to bind through its KIX domain, activating CREB (Chrivia *et al.*, 1993). CREB is a highly promiscuous transcription factor, with the ability to bind ~4000 different promoter start sites, so is important for the regulation of a wide range of genes throughout the body (Zhang *et al.*, 2005).

CREBBP is responsible for the acetylation of histone tails, which leads to an increase in transcriptional activation, as acetyl-lysine residues provide a binding site for chromatin remodelling factors which contain bromodomains (Loyola and Almouzni, 2004). Through bromodomain interactions, CREBBP is thought to play a role in the modulation of T regulatory (Treg) cells, more specifically, in differentiation of naïve Treg cells (Ghosh *et al.*, 2016). CREBBP and EP300 are specifically required for global levels of histone 3, lysine 18 (H3K18) and histone 3, lysine 27 (H3K27) acetylation, with knockout studies showing that acetylation of these two residues is dramatically reduced (Jin *et al.*, 2011). This CREBBP/EP300 mediated acetylation of H3K18 and H3K27 is thought to be important for nuclear receptor-dependent transcription (Jin *et al.*, 2011).

CREBBP and EP300 have a large protein interactome, known to interact with at least 400 proteins (Bedford *et al.*, 2010). Through its HAT domain CREBBP is also able to acetylate non-histone proteins, allowing modulation of their functions. Acetylation by CREBBP is vital for the activity of tumour suppressor p53, influencing its stability, DNA binding and recruitment of coactivators (Brooks and Gu, 2003; Tang *et al.*, 2008). Conversely, acetylation of the oncoprotein BCL6, leads to its inactivation by disrupting interaction with histone deacetylases (HDACs), thereby reducing its ability to repress transcription (Bereshchenko *et al.*, 2002). CREBBP also has intrinsic E4 polyubiquitin ligase activity and is involved in the rapid turnover of p53 in healthy cells (Shi *et al.*, 2009).

CREBBP plays a role in DNA damage repair through acetylation of base excision repair (BER) protein, PARP-1, which leads to enhanced activation of the anti-apoptotic NFκB pathway (Hassa *et al.*, 2005). CREBBP also interacts with direct DNA repair protein, thymine DNA

glycosylase (TDG), and homologous recombination repair (HRR) protein, BRCA1 (Pao *et al.*, 2000; Tini *et al.*, 2002; Leger *et al.*, 2014).

1.4.3 *CREBBP* Mutation

Mullighan *et al.* (2011) identified that around 18.3% of relapsed childhood ALL cases were *CREBBP* mutant (Mullighan *et al.*, 2011). These mutations were found to cause reduced acetylation of *CREBBP* target residues as well as impacting upon transcription of GC responsive and cAMP-dependent genes in *CREBBP*/*EP300* double knockout mouse embryonic fibroblast (MEF) models, engineered to express different heterozygous *CREBBP* mutations (Mullighan *et al.*, 2011). Importantly, acetylation was perturbed, but not lost in these *CREBBP* mutant models, and the intensity of this effect varied between mutations (Mullighan *et al.*, 2011). These results, coupled with the observation that *CREBBP* mutations can be seen in minor subclones at diagnosis, suggest that *CREBBP* mutation may play a role in drug resistance and thus increase the risk of relapse in childhood ALL patients (Mullighan *et al.*, 2011). *CREBBP* mutations have been shown to be significantly enriched in relapse patients in the high hyperdiploid (HHD) (51-68 chromosomes) subgroup, with around 63% of *CREBBP* mutant relapse cases occurring in this cytogenetic subgroup (Inthal *et al.*, 2012). *CREBBP* mutation as a frequent event in DLBCL and FL is becoming increasingly clear, with around 39% cases of DLBCL and 41-70% cases of FL identified as *CREBBP* mutant (Pasqualucci *et al.*, 2011a; Pasqualucci *et al.*, 2011b; Green *et al.*, 2013; Pastore *et al.*, 2015).

The precise role of *CREBBP* mutation in the pathogenesis of these diseases is yet to be understood and, given the complex role played by CREBBP in a wide range of cellular functions, there are a number of possible mechanisms which could be affected. *CREBBP* mutations in relapsed childhood ALL, DLBCL and FL are primarily heterozygous, clustering in

and around, the HAT domain. This leads to attenuation or loss of function of the mutant protein, without altering the remaining wild type allele (Figure 1.6) (Mullighan *et al.*, 2011; Pasqualucci *et al.*, 2011a; Green *et al.*, 2013). Importantly, *CREBBP* haploinsufficiency is known to be involved in the developmental condition, Rubinstein-Taybi syndrome (RSTS), which leads to an increased susceptibility to malignancies (Miller and Rubinstein, 1995; Roelfsema and Peters, 2007).

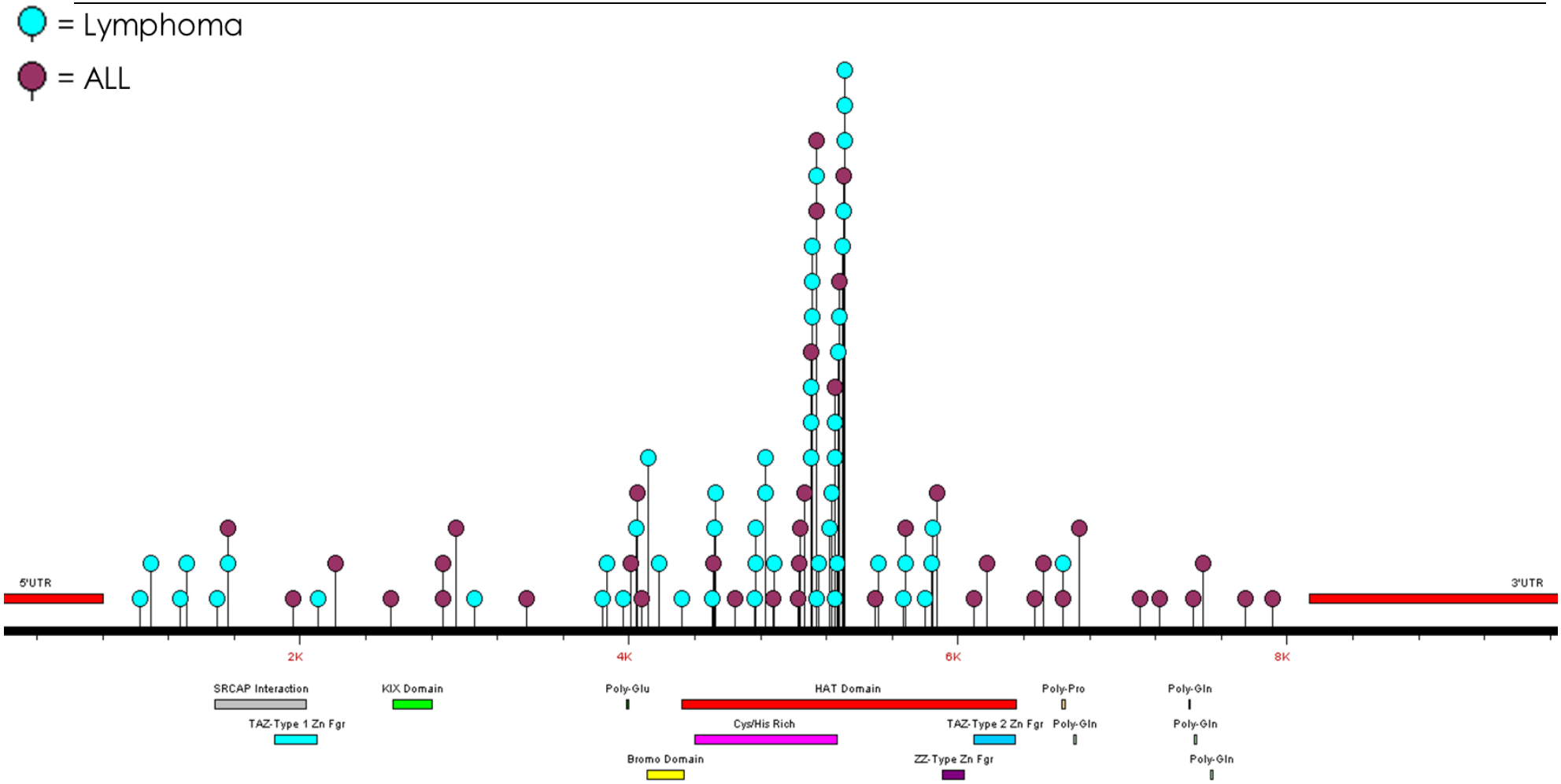

Figure 1.6. *CREBBP* mutations in acute lymphoblastic leukaemia (ALL) and lymphoma. *CREBBP* mutations documented in ALL and lymphoma (COSMIC) and their location in relation to the nucleotide sequence (black line) and functional domains. Multiple mutations at the same residue(s) are not depicted.

One potential role of *CREBBP* mutation in the pathogenesis of lymphoid malignancies is in GC sensitivity. GCs are pivotal in the treatment of childhood ALL, DLBCL and FL, specifically inducing apoptosis in developing lymphocytes (Alnemri *et al.*, 1992). CREBBP is known to interact with the GR and Mullighan *et al.* (2011) identified a link between *CREBBP* mutation and reduced expression of GC-regulated genes, with *CREBBP*-mutated T-ALL cell lines showing GC-resistance (Kino *et al.*, 1999; Mullighan *et al.*, 2011). This suggests that *CREBBP* mutation may confer resistance to GC therapy.

CREBBP plays a role in global acetylation and, with maintained expression of the wild type allele, it is likely that reduced HAT dosage plays a role in the pathogenesis of *CREBBP*-mutated disease (Mullighan *et al.*, 2011; Pasqualucci *et al.*, 2011a; Green *et al.*, 2013). Importantly, it has been reported that small changes in HAT activity can lead to significant biological consequences (Legube and Trouche, 2003). To overcome this, treatment with HDAC inhibitors (HDACi) could be used in an attempt to rebalance levels of acetylation in *CREBBP*-mutated cells. Previous studies have shown that HDACi can lead to apoptosis in *CREBBP* mutant GC-resistant ALL cells and in *CREBBP*/*EP300* mutated DLBCL may be associated with increased sensitivity to HDACi (Tsapis *et al.*, 2007; Mullighan *et al.*, 2011; Andersen *et al.*, 2012). Further to this, evidence suggests that histone acetylation deficits in RSTS cell lines can be reversed using HDACi and treatment with HDACi in *CREBBP* mutant mouse models was shown to ameliorate deficits in synaptic plasticity and cognition (Alarcon *et al.*, 2004; Korzus *et al.*, 2004; Vecsey *et al.*, 2007; Lopez-Atalaya *et al.*, 2012). Haematological malignancies in general, seem to be particularly sensitive to HDACi, and this type of therapy tends to be well tolerated in patients (Stimson *et al.*, 2009).

A further approach could be to enhance the dysfunctional cAMP/PKA pathway. It is known that lymphocytes at different stages of development are susceptible to cAMP-induced apoptosis (Daniel *et al.*, 1973; Coffino *et al.*, 1975). There is known interplay between cAMP/PKA and the GC-induced apoptotic response, with the GR being required for cAMP/PKA induced apoptosis in lymphoma cells (Rickles *et al.*, 2010). This suggests that phosphodiesterase (PDE) inhibitors (PDEi) could be beneficial in *CREBBP*-mutated lymphoid diseases. Certainly, PDEi has been shown to induce apoptosis in ALL and DLBCL cell lines and can enhance the GC-response in ALL cell lines (Ogawa *et al.*, 2002; Smith *et al.*, 2005).

A study by Pasqualucci *et al.* (2011) showed that *CREBBP* mutation leads to reduced acetylation of p53 and BCL6 *in vitro* (Pasqualucci *et al.*, 2011a). *CREBBP* mutation has also been associated with impaired BCL6 activity (Pasqualucci *et al.*, 2011a; Green *et al.*, 2013). P53 is a universally expressed tumour suppressor involved in apoptotic signalling and BCL6 is an oncogene involved in transcriptional repression able to inhibit p53, which leads to suppression of apoptosis and an environment tolerant of DNA breaks (Phan and Dalla-Favera, 2004; Basso and Dalla-Favera, 2012). As acetylation is vital for p53 function and BCL6 inactivity, this suggests that dysfunctional acetylation due to *CREBBP* mutation may lead to an imbalance between their activities, causing resistance to apoptosis and potentially induction of drug resistance.

A recent study by Zimmer *et al.* found reduced activity of BER protein, PARP-1, as well as reduced protein levels of XRCC1 and APEX1 in *CREBBP* heterozygous mice (Zimmer *et al.*, 2012). BER is a vital pathway for the repair of single strand breaks (SSBs) in DNA (Curtin, 2012). Accumulation of SSBs in a cell contributes to genetic instability, a hallmark of cancer, so heterozygous loss of *CREBBP* may lead to the acquisition of a mutator phenotype (Loeb, 2001;

Nemec *et al.*, 2010; Zimmer *et al.*, 2012). This may also provide a target for therapeutic intervention, by way of inducing synthetic lethality in *CREBBP*-mutated cells. Synthetic lethality is a process by which cell death occurs when two pathways, or genes, are defective but not when a single defect occurs alone (Curtin, 2012). Given that BER appears to be defective in *CREBBP*-mutated lymphoid diseases, inhibition of the homologous recombination repair (HRR) pathway may lead to cell death in *CREBBP*-mutated cells, allowing the survival of healthy cells with functioning BER.

Targeted therapies have had wide-spread success in a number of cancer types and are paving the way for personalised medicine for cancer therapy (Baudino, 2015). It is becoming clear that *CREBBP* mutations are a frequent event in a large number of solid tumours including; transitional cell carcinoma of the bladder, medulloblastoma, small cell lung cancer, adenoid cystic carcinoma, oesophageal squamous cell cancer, glioblastoma, squamous cell carcinoma and breast cancer (Gui *et al.*, 2011; Peifer *et al.*, 2012; Robinson *et al.*, 2012; Ho *et al.*, 2013; Gao *et al.*, 2014a; Gao *et al.*, 2014b; Han *et al.*, 2014; Huether *et al.*, 2014; Mukasa *et al.*, 2014; Song *et al.*, 2014; Jansen *et al.*, 2016; Watt *et al.*, 2016). This suggests that understanding *CREBBP* mutations and developing therapies to rebalance its activity may benefit a wide range of cancer types.

1.5 Aims and Hypotheses

The key aim of the project was to investigate routes for the therapeutic targeting of *CREBBP*-mutated lymphoid diseases.

- **Objective 1 - To investigate the molecular pathology of *CREBBP* mutations in ALL**

- Characterise a BCP-ALL cell line with stable CREBBP knockdown
- Validate data in additional BCP-ALL cell lines and primary derived samples with CREBBP knockdown
- Study the effect of stable CREBBP knockdown on cell line growth *in vivo*

- **Objective 2 – Investigate the molecular pathology of *CREBBP* mutations in lymphoma**
  - Create and characterise a DLBCL cell line with stable CREBBP knockdown

Chapter 2: Materials and Methods

Materials and Methods

2.1 General

2.1.1 Equipment

- 7500 Fast Real-Time PCR System (Applied Biosystems, Warrington, UK)
- Agarose Gel Electrophoresis Unit (BioRad, Hemel Hempstead, UK)
- Analogue Tube Roller SRT9 (Stuart Scientific, UK)
- Bead Bath (Gallenkamp/Weiss, Loughborough, UK)
- BioRad Power Pac 200 (BioRad)
- Class II microbiological safety cabinet (BIOMAT-2, Medical Air Technology Ltd., Manchester, UK)
- EPI 2500 Elektroporations-impulsgenerator
- FACSCalibur (Becton Dickinson, Oxford, UK)
- FACSCanto II (Becton Dickinson)
- FLUOStar Omega Microplate Reader (BMG Labtech, Aylesbury, UK)
- Fujifilm Luminescent Image Analyzer (LAS-3000) (Fujifilm, Billingham, UK)
- Gel Electrophoresis Tank (Pharmacia Biotech, Amersham Biosciences, UK)
- Gene Amp PCR System 2700 (Applied Biosystems)
- Gyro-Rocker STR9 (Fisher Scientific, Loughborough, UK)
- Irradiation System RS320 (Gulway Medical, UK)
- Microwave Oven (Sharp Electronics LTD., Burnley, UK)
- Mini-PROTEAN 11 Electrophoresis Cell (BioRad)
- Mini Trans-Blot Electrophoretic Transfer Cell (BioRad)

- Stirrer UC151 (Bibby Scientific Limited, Staffordshire, UK)
- Techne Dri-Block DB-3D (Bibby Scientific Limited)
- Water Bath (Grant Instruments, Cambridge, UK)
- WhirliMixer (Fisons Scientific Equipment, Leicestershire UK)

2.1.2 Centrifuges

- Eppendorf refrigerated Centrifuge 5417R (Fisher Scientific)
- Mistral 3000i Refrigerated Centrifuge (Fisher Scientific)

2.1.3 Microscopes

- Olympus transmitted light microscope (Olympus, Japan)
- Zeiss transmitted light microscope (Carl Zeiss Ltd., Welwyn Garden City, Herts., UK)

2.1.4 General Chemicals

All chemicals and reagents were purchased from either Sigma Chemical Company (Dorset, UK) or Thermo Fisher (Loughborough, UK) unless otherwise stated. Phosphate buffered saline (PBS) was prepared from tablets (Invitrogen, Paisley, UK) and autoclaved before use.

2.2 Cell Culture

2.2.1 Cell Lines

PreB 697: BCP-ALL cell line, established in 1979 from the bone marrow of a 12 year old male at relapse (Findley *et al.*, 1982).

MHH-CALL-2: BCP-ALL cell line, established in 1993 from the peripheral blood of a 15 year old Caucasian girl with ALL at diagnosis (Tomeczkowski *et al.*, 1995).

SU-DHL-4: DLBCL cell line, established in 1975 from the peritoneal effusion of a 38 year old man (Epstein and Kaplan, 1979).

2.2.2 Cell Line Maintenance

Cell lines were grown as suspension cultures. PreB 697 cells were maintained in RF10 (RPMI 1640 medium containing L-glutamine (Sigma Aldrich, Dorset, UK) supplemented with 10% foetal bovine serum (FBS) (Gibco, Rugby, UK). MHH-CALL-2 and SU-DHL-4 cells were maintained in RPMI 1640 medium containing L-glutamine (Gibco) supplemented with 20% FBS (Gibco). Tissue culture was performed in a Class II microbiological safety cabinet (Section 2.1.1) using sterilised glass and plasticware (Corning, High Wycombe, UK). Cells were grown in flasks or multi-well plates. Cell line incubation was carried out at 37°C in a humidified tissue culture incubator at 5% CO_2.

2.2.3 Mycoplasma Testing

Contamination of cell lines by mycoplasma can interfere with almost all parameters that are measured in cell culture, effects vary between cell lines and are not predictable (Drexler and Uphoff, 2002). All cell lines used in this project were routinely tested for mycoplasma infection using MycoAlert (Lonza, Basel, Switzerland). The MycoAlert assay exploits the activity of mycoplasmal enzymes to detect infection. Any viable mycoplasma are lysed and these enzymes react with MycoAlert substrate, catalysing the conversion of ADP to ATP. By measuring ATP levels in a sample before and after the addition of MycoAlert, a substrate ratio can be obtained which can effectively indicate the presence

or absence of mycoplasma infection. Cell lines were mycoplasma free throughout the project.

2.2.4 Cells Counts and Viability Assessment

Cell counting and viability assessment was carried out using trypan blue (Thermo Fisher) staining and a haemocytometer (Hawksworth, UK). Cell suspensions were mixed 1:1 (v/v) with a 0.4% solution of trypan blue in PBS and were counted using a haemocytometer with an Improved Neubauer counting chamber.

2.2.5 Cell Harvesting

Cells were harvested for RNA, DNA and protein studies when in exponential growth phase. The cell suspension was centrifuged at 1000 RPM (or 1200 RPM for primary cells) for 5 minutes at room temperature. Supernatant was removed and the pellet washed by resuspending in PBS and pelleted again by centrifugation. The wash step was carried out twice and PBS was removed before pellets were stored at -80°C until required.

2.2.6 Cryopreservation

To cryopreserve cell stocks, cells in exponential growth phase were counted and assessed for viability (Section 2.2.4). Cells were then centrifuged at 1000 RPM (or 1200 RMP for primary and primary derived cells) for 5 minutes at room temperature and resuspended in freezing mixture made up of 10% (v/v) dimethyl sulphoxide (DMSO) (Sigma Aldrich) in FBS (Gibco) at $5x10^6$-$1x10^7$/ml. Aliquots of 1ml were put into 2ml polypropylene cryotubes (Invitrogen) and placed in a polystyrene box filled with cotton wool, before being placed in a -80°C freezer. This ensured that the samples cooled at a rate of approximately 1°C per minute. After 2-14 days vials were transferred into storage in liquid nitrogen.

To recover cryopreserved cells, vials were rapidly thawed in a 37°C bead bath (Section 2.1.1), diluted 1:10 with the relevant growth media and centrifuged at 1000 RPM for 5 minutes. Freezing mixture was aspirated and the pellet resuspended in fresh growth media in a tissue culture flask.

2.2.7 Formation of Primagrafts

Principal

Cell yield from patient material is often not great enough to carry out various downstream analyses, such as gene knockdown by small interfering RNA (siRNA) (Section 2.7.2). Mice have been developed with severe immunodeficiency (Non-obese diabetic, severe combined immunodeficiency (NOD-SCID), IL-2R common gamma chain null (NSG)) which allows injection of human haematopoietic cells without rejection (Shultz *et al.*, 2005). NSG mice provide a superior platform for sustained engraftment of human hematopoietic stem cells and patient derived leukaemia (Shultz *et al.*, 2005; Shultz *et al.*, 2007; Agliano *et al.*, 2008). Importantly, engrafted cells largely retain their leukaemic profile, in terms of phenotype, chromosomal aberrations, transcriptome and MRD marker expression (Woiterski *et al.*, 2013). Leukaemia engraftment in mice can be assessed by analysing peripheral blood at frequent intervals for presence of human leukaemia by flow cytometry. Spleens taken from highly engrafted mice are enlarged and made up of a high percentage of human leukaemia cells which can be used for *ex vivo* analyses or can be re-implanted into mice to generate further material. The key drawbacks of this technique are that it is time consuming and it is difficult to predict how long each patient sample will take to engraft in the spleen as well as how deleterious each sample will be to the health

of the mouse. Further to this, peripheral blood engraftment does not always closely correlate with spleen engraftment.

Procedure

Primary patient cells (Table 2.1) were thawed (Section 2.2.6) and resuspended in RF10 at $5x10^7$/ml ($1x10^6$ in 20µl). NSG were injected intrafemorally with $1x10^6$ primary patient cells by a trained researcher with a home office licence.

Patient ID	Age at Diagnosis	CREBBP Status	Other Mutations
L779	5.5 yrs	Wild type	*NRAS* (Q61R)
L829 Relapse	3.1 yrs	Wild type (Wt 2)	*KRAS* (G13D)
L914	7.3 yrs	Wild type	*CBL/FLT3* Large del/Δ836
L885	2.2 yrs	Wild type (Wt 1)	-
G7578 NN	12 yrs	Wild type (Wt 3)	-
G7578 LN	12 yrs	Mono-allelic deletion (Del 1)	-
G1062 RN	17 yrs	Mono-allelic deletion (Del 2)	-

Table 2.1 Clinical details of patient samples used to generate primagrafts. G7578 NN, G7578 LN and G1062 RN primagraft samples were kindly donated by Paul Sinclair, and *CREBBP* status was assessed by SNP 6.0 arrays and genotyping console software (Affymetrix, High Wycombe, UK).

2.2.7.1 Monitoring peripheral blood engraftment and assessment of spleen engraftment

Around 50µl of mouse blood was taken from the tail vein, prepared for and analysed by, flow cytometry (Section 2.3.2). Once peripheral blood engraftment had reached >40%, mice were euthanised, spleens were removed and cells were resuspended in growth media to be assessed for engraftment by flow cytometry (Section 2.3.2) and other downstream analyses.

2.2.8 *In Vivo* Growth of Cell Lines

Principle

Many of the complex growth factors and cell/tissue interactions are absent in an *in vitro* growth environment, and for this reason further insight into cell growth characteristics can be gained from the use of *in vivo* models. In order to assess cell line growth within the context of a whole organism, cell lines with lentiviral gene knockdown were implanted into NSG mice, and engraftment was studied.

Procedure

PreB 697 shCBP and shNEG cells (Section 2.7.1) were implanted into NSG mice (Section 2.2.7) at 10 000 cells per mouse. Peripheral blood engraftment was monitored by tail vein bleed (Section 2.2.7). Mice were euthanised upon first signs of morbidity (weakness, loss of muscle tone, sedate behaviour etc.). Spleen and liver were weighed and a portion of the spleen was resuspended in growth medium for analysis of engraftment (Section 2.2.7). GFP positivity was used to identify lentivirally transduced cells (Section 2.3.1).

2.3 Flow Cytometry

Principle

Flow cytometry is a technique which is able to detect and enumerate specific cell types within a complex mixture. Flow cytometers are made up of three components; fluidics, optics and electronics. The fluidics system generates a stream of cells which individually and rapidly flow through an interrogation point (Henel and Schmitz, 2007). Cell attributes are then assessed by their ability to scatter laser light which intersects the cells at this

point. Standard flow cytometers have 1-2 lasers but more modern machines employ many more to detect a large number of parameters in parallel (Henel and Schmitz, 2007). Emitted light is given off in all directions and is subsequently collected by optics which direct the light into a series of filters and dichroic mirrors. Light signals are collected by photomultiplier tubes and digitised for analysis on a computer (Henel and Schmitz, 2007). The properties of cell size and granularity are determined by forward and side scatter respectively. To increase the number of parameters that can be detected by flow cytometry, antibodies conjugated to different fluorochromes are employed. Fluorochromes are molecules which absorb light of a given wavelength and emit light of a higher wavelength (Henel and Schmitz, 2007). Antibodies conjugated to different fluorochromes with similar excitation and different emission wavelengths can be used to allow analysis of several cellular properties simultaneously.

2.3.1 Assessment of Lentiviral Transduction

Between $1x10^5$ and $1x10^6$ cells were washed twice in PBS by centrifuging at 450 x g for 4 minutes and the supernatant removed. Cells were then resuspended in 350µl PBS and analysed for GFP (FITC) expression on a BD FACSCalibur (Becton Dickinson) fitted with a 488nm laser.

2.3.2 Determining Peripheral Blood and Spleen Engraftment

Around 50µl of mouse blood was taken and washed using 3ml of Dulbecco's PBS (Thermo Fisher) made up to 0.2% bovine serum albumin (BSA) and filtered (termed PBSA) and spinning for 4 minutes at 450 x g. Cells were then stained using 5µl of patient dependent (anti-CD45, anti-CD38 or anti-Korsa) FITC conjugated antibody, 5µl anti-CD10 PE conjugated antibody, 5µl anti-CD34 Per-CP conjugated antibody, 2.5µl anti-CD19 APC

conjugated antibody and 2.5µl mouse anti-CD45 PE-Cy™7 conjugated antibody and left to incubate in the dark for 15 minutes. Red cell lysis was then carried out by adding 1.2ml of ammonium chloride red cell lysis solution to the cells and mixing by inversion for 5 minutes. Two more washes were carried out before analysis by flow cytometry on a BD FACSCanto II (Becton Dickinson), fitted with 488nm and 633nm lasers. To assess spleen engraftment double the antibody volume was used and red cell lysis was omitted.

2.3.3 HLA-DR Surface Expression

Cells were harvested and washed in PBS (Section 2.2.5) before staining with a HLA-DR APC conjugated antibody (G46-6) (Becton Dickinson), isotype control (MOPC-21) (Becton Dickinson) or left unstained and incubated in the dark at room temperature for 15 minutes. Two more washes were carried out before analysis by flow cytometry on a BD FACSCanto II (Becton Dickinson), fitted with 488nm and 633nm lasers.

2.4 DNA Analysis

2.4.1 DNA Extraction

Principle

All nucleic acid extraction and purification was carried out using solid phase methods involving silica matrices, which have unique nucleic acid binding properties (Tan and Yiap, 2009). For DNA extraction samples are lysed using a protease-containing lysis buffer and binding buffers and ethanol are added to prepare the sample for binding to the silica membrane. Washing steps are carried out to remove contaminants and finally the DNA

sample is eluted using a buffer (or H_20) under low ionic strength (pH ≥7) (Tan and Yiap, 2009).

DNA was extracted from cell pellets using a QIAamp DNA Mini kit (Qiagen, Crawley, UK).

Reagents

- Qiagen protease
- Buffer AL
- Buffer AW1
- Buffer AW2
- 100% Ethanol
- Buffer AE

Procedure

Between $5x10^6$ and $1x10^7$ cells in exponential growth phase were harvested and pelleted (Section 2.2.5). Cells were resuspended in 200µl of PBS in an eppendorf containing 20µl of Qiagen protease. Two hundred microliters of buffer AL was added and mixed by pulse vortexing for 15 seconds. The sample was then incubated at 56°C for 10 minutes before the addition of 200µl of absolute ethanol and being applied to a QIAamp mini spin column. Centrifugation was carried out at 8000 rpm for 1 minute and the flow through discarded. The column was then washed with 500µl buffer AW1 at 8000 rpm for 1 minute followed by 500µl buffer AW2 at 14 000 rpm for 3 min, the flow through discarded each time. To dry the column after washing, centrifugation was carried out again at 14 000 rpm for 1 minute. Between 150 and 200µl of buffer AE was added directly to the silica membrane and left to incubate at room temperature for 1 minute before elution into a new 1.5ml

eppendorf was carried out at 8000 rpm for 1 minute. DNA purity was assessed by Nano Drop (Section 2.4.2)

2.4.2 Quantification of DNA and RNA Samples

DNA or RNA concentration was determined by assessing spectrophotometric absorbance at 260nm and 280nm, against a water blank using an ND-1000 Spectrophotometer (Nanodrop) (Nanodrop, Labtech International, UK). Purity was assessed by the ratio of 260nm and 280nm readings, with a ratio of between 1.8 and 2.0 indicative of pure RNA or DNA, with lower ratios indicating protein contamination.

2.4.3 Polymerase Chain Reaction

Principle

PCR is a well-established and widely used method for the rapid, exponential amplification of specific nucleotide sequences from a DNA target. Two oligonucleotide primers (15-30 nucleotides) must be designed to flank the target sequence to be amplified. The forward primer is designed to be complimentary to the sense strand and the reverse primer is designed to be complimentary to the antisense strand to allow amplification in both directions. Template DNA is added to a mixture of forward and reverse primers with heat stable DNA polymerase (commonly, taq polymerase), DNA precursors (dGTP, dCTP, dATP, dTTP) and $MgCl_2$. Through cycles of different temperatures, the DNA can be denatured and primers bind allowing the heat stable DNA polymerase to synthesise new DNA strands which are complimentary to the region of interest. PCR is known as a chain reaction because the newly synthesised strands act as templates for subsequent cycles in sequence. This way, the amount of newly synthesised target DNA increases exponentially with each heating cycle. An average PCR reaction consists of 30-40 cycles. After around

25 cycles the reaction mixture will contain enough copies of the target sequence (~10^5) to be visualised as a discrete band when resolved using agarose gel electrophoresis (Section 2.4.4). The heating cycles of an average PCR are as follows:

- Denaturation – 93-95°C
- Reannealing – 50-70°C (depends on the annealing temperature of the primers (T_m))
- Extension – 70-75°C

Touchdown PCR, the method used in this project, is a variation of the traditional PCR technique, designed to reduce the likelihood of primers binding to non-specific sequences. It involves starting the reaction with a higher than optimal annealing temperature and gradually approaching the desired temperature every 2 cycles. Varying $MgCl_2$ concentration and the addition of betaine are also other common methods used to optimise PCR reactions to prevent non-specific binding.

Reagents

- $MgCl_2$ (Invitrogen)
- Forward and Reverse Primers (Table 2.2) (Invitrogen)
- AmpliTaq Gold (Applied Biosystems)
- dNTPs (Applied Biosystems)
- PCR Buffer (Applied Biosystems)
- RNase free water (Gibco)

Procedure

PCR reaction mix was made up as follows; 1x PCR buffer, 100µM dNTPs, 1.5-3.5mM $MgCl_2$, 0.2µM forward and reverse primers, 1.25U AmpliTaq gold and ~50ng of DNA (Sections 2.4.1) template. Reaction volumes were between 25 and 100µl depending on the downstream application. PCR conditions were as follows; 10 minute denaturation at 95°C, touchdown protocol of 20 seconds at 94°C followed by 1 minute at the T_m of the primers +7°C (reducing towards T_m every 2 cycles) and 1 minute at 72°C for 15 cycles followed by 20 seconds at 94°C, 1 minute at T_m of primers and 1 minute at 72°C for 20 cycles with a final 7 minute extension at 72°C. All primers were purchased from Invitrogen (Table 2.2).

Target	Forward Primer	Reverse Primer	T_m	Product Size	$MgCl_2$ Conc
Exon 18	GACTGGCATTTGGATATTGGGG	TCCAAGGGACTGCATGACAG	55°C	280bp	1.5mM
Exon 21	GATTTTAAGGGGCCATCATGTC	CCCACAACCCACTCCATAAG	50°C	267bp	1.5mM
Exon 25	AGCACCTTGTCAGCAACAGC	ACACGGCTCACTGAATGACAC	56°C	247bp	2.5mM
Exon 26	AACATGTGCCTCCTTCCCAC	AAAGAGCTTGCTACGTGCCC	56°C	338bp	2.5mM
Exon 27	CCTTAAAGGCAGGGCCGATTTC	TGACAAAAGCCACCACCTTCC	56°C	264bp	2.5mM

Table 2.2. List of *CREBBP* primers used for genomic PCR, including sequence, annealing temperature and $MgCl_2$ concentration. All primers were purchased from Invitrogen.

2.4.4 Agarose Gel Electrophoresis

Principle

Agarose gel electrophoresis allows the separation of DNA by size. In this way, PCR products can be visualised in order to confirm the reaction was successful and to check product size. Agarose is a linear polymer and is used to form a porous matrix in which the DNA can be separated. The size of the pores are dependent on the concentration of agarose used. A current is passed through the agarose gel causing the DNA, which has a

negatively charged backbone at neutral pH, to migrate towards the positive anode. Smaller DNA fragments move through the matrix faster than larger ones, allowing separation. Separated DNA fragments are commonly visualised using a DNA intercalating dye such as ethidium bromine, or a modern, less toxic alternative such as gel red.

Reagents

- Electrophoresis grade agarose (Invitrogen)
- GelRed DNA Stain (10 000x) (Biotium, Cambridge Bioscience, Cambridge, UK)
- Tris borate ethylenediaminetetraacetic acid (EDTA) (TBE) Buffer (10x stock) - 1M Tris base, 1M boric acid and 20ml/litre 0.5M EDTA (pH 8.0)
- Gel Loading Buffer (6x) (Promega, Southampton, UK)
- PCR Markers 50-1000bp ladder (Promega)

Procedure

The agarose gel was formed by melting electrophoresis grade agarose in 40ml TBE (1x stock) to give a 0.4% (w/v) gel. Four microliters of 10 000 x GelRed DNA stain was then added to the molten gel mixture. The gel was poured into a casting tray with a well comb and allowed to set for at least 15 minutes. For sample loading, 10µl of PCR product was mixed with 2µl of 6x loading buffer and pipetted into a well of the agarose gel. For estimation of product size, 5µl of PCR markers were mixed with 1µl of 6x loading buffer and pipetted into a well of the agarose gel. Electrophoresis was carried out in a gel electrophoresis tank (Pharmacia Biotech) (Section 2.1.1) in TBE (1x stock) at 80V for 40-120 minutes. Gels were visualised using a BioRad Transilluminator (GelDoc) (Section 2.1.1).

2.4.5 Purification of PCR products

Principle

As described in section 2.4.1.

PCR products were purified using a QIAquick PCR purification kit (Qiagen).

Reagents

- Buffer PB1
- Buffer PE
- Buffer EB

Procedure

The PCR sample was mixed with buffer PB1 (5 volumes PB1 to 1 volume PCR sample) and vortexed briefly, ensuring that the colour of the mixture remains yellow (indicative of pH <7.5, the optimal pH for the buffers to work). Addition of 3M sodium acetate (pH 5.0) can be carried out to correct the pH if required. The sample was then added to a QIAquick column and centrifuged at 13 000 RPM for 30-60 seconds to allow DNA to bind to the column. The flow-through, collected in a collection tube, was then discarded and the spin column was washed with 750µl buffer PE by centrifugation at 13 000 RPM for 30-60 seconds. The flow-through was again discarded and the column was centrifuged once more for 60 seconds. The column was then placed into a clean 1.5ml microcentrifuge tube and 30-50µl of elution buffer (buffer EB) was added directly to the silica membrane and left to stand for 60 seconds. Elution was carried out by centrifugation at 13 000 RPM for 60 seconds into a new 1.5ml eppendorf. The concentration and purity of the DNA was checked by Nano Drop (Section 2.4.2). DNA was stored at 4°C for short term or -80°C long term.

2.4.6 Sanger Sequencing

Principle

Sequencing of DNA was carried out using the dideoxynucleotide chain termination method (Sanger *et al.*, 1977). This method is based on the selective incorporation of chain-terminating 2',3'-dideoxynucleotide triphosphates during *in vitro* DNA replication. The DNA sample to be sequenced is mixed with normal deoxynucleotides as well as dideoxynucleotides, each of which is coupled to a different fluorescent tag and DNA polymerase. The dideoxynucleotides lack a 3'OH group and so prevent any further elongation of DNA after incorporation; this results in different strand lengths. Automated DNA sequencers carry out DNA size separation by capillary electrophoresis and detection and recording of dye fluorescence, with data output in the form of a chromatogram.

Procedure

Sanger sequencing of PCR products was outsourced to Source Bioscience (Cambridge, UK). Sample requirements for this service were; 1ng/µl per 100bp to be sequenced and primers at 3.2pmol/µl. Results were received as chromatograms and analysed using FinchTV (Geospiza, Seattle, USA) and DSgene software (Accelrys, San Diego, USA).

2.4.7 Quantitative Reverse-Transcriptase Polymerase Chain Reaction

Quantitative reverse-transcriptase polymerase chain reaction (QRT-PCR) is a rapid and sensitive method used for measuring relative mRNA expression within cells. The procedure is made up of three stages:

1. Extraction of RNA from cells
2. Synthesis of copy DNA (cDNA) by reverse transcription of the RNA

3. Real-time PCR reaction using the cDNA

2.4.7.1 RNA Extraction

Principle

As described in section 2.4.1. For RNA extraction, samples are lysed and homogenised in the presence of a highly denaturing guanidine-thiocyanate-containing buffer, which leads to the immediate inactivation of RNases, keeping the RNA intact. Ethanol is added to provide the appropriate binding conditions, before applying the sample to a silica membrane. Contaminants are washed away and RNA is eluted using RNase free water (Tan and Yiap, 2009).

Total RNA was extracted using a Qiagen RNeasy Mini kit (Qiagen).

Reagents

- Buffer RLT
- Buffer RW1
- Buffer RPE
- 2-Mercaptoethanol
- 70% ethanol
- RNase free water

Procedure

Between $1x10^6$ and $1x10^7$ cells in exponential growth phase were harvested and pelleted (Section 2.2.5). Pellets were then lysed by using the appropriate volume of buffer RLT (containing 2-Mercaptoethanol) and pipetting up and down to break up the pellet. Homogenisation was carried out by passing the sample though a 20-gauge needle fitted

to a 1ml hypodermic syringe 5-10 times. An equal volume of 70% ethanol was added to the sample and mixed before transfer into an RNeasy mini spin column, placed into a 2ml collection tube and centrifuged for 15 seconds at 10 000 RPM. The flow through was discarded and the column washed by the addition of 700µl of buffer RW1 and centrifugation at 10 000 RPM for 15 seconds. The flow through was again discarded and further washing was carried out by the addition of 500µl of buffer RPE followed by centrifugation for 15 seconds at 10 000 RPM. Flow through was discarded and a further wash step with RPE buffer carried out, this time with 2 minute centrifugation at 10 000 RPM. After discarding the flow through the column was centrifuged for a further 1 minute to remove any excess ethanol. RNA was eluted by transferring the RNeasy mini spin column to a new 1.5ml collection tube, before adding 30-50µl RNase free water and centrifuging at 10 000 RPM for 1 minute. RNA concentration and purity was determined by Nano Drop (Section 2.4.2). Samples were stored at -80°C until required.

2.4.7.2 Copy DNA Synthesis

Principle

This method allows the formation of complementary copy DNA (cDNA) by a reverse transcriptase enzyme, which uses cellular mRNA as a template. This cDNA can then be used in quantitative reverse transcriptase PCR (QRT-PCR) reactions.

Synthesis of cDNA was carried out using a High-Capacity Reverse Transcription Kit (Applied Biosystems, Thermo Fisher) and the provided protocol.

Reagents

- 10x RT Buffer
- 10x RT Random Primers

- 25x dNTP Mix (100mM)
- Multiscribe™ Reverse Transcriptase (50U/µl)
- RNase Inhibitor
- RNase free water

Procedure

Each RNA sample was made up to a final concentration of 70-200µg/ml in RNase free water. The reaction buffer was prepared on ice as outlined in table 2.3.

Component	Volume/Reaction (µl)
10x RT Buffer	2.0
25X dNTP Mix (100mM)	0.8
Random Primers	2.0
MultiScribe™ Reverse Transcriptase	1.0
RNase Inhibitor	1.0
Nuclease-free H_2O	3.2

Table. 2.3 Reaction buffer used in cDNA synthesis.

The final reaction mix was made by adding 10µl of reaction buffer with 10µl of RNA (at 70-200µg/ml) in a PCR reaction tube (Applied Biosystems) and mixed by pipetting. Any tubes with bubbles were briefly centrifuged to remove them. To complete the reaction tubes were incubated in a thermal cycler (Gene Amp PCR System 2700, Applied Biosystems) at 25°C for 10 minutes, followed by 37°C for 120 minutes and 85°C for 5 seconds. cDNA was stored at 4°C for short term storage or -20°C for long term storage.

2.4.7.3 QRT-PCR

Principle

QRT-PCR relies on the measurement of PCR product after each cycle via fluorescent dyes that yield increasing fluorescent signal directly in proportion with the number of PCR product molecules. QRT-PCR provides a high degree of sensitivity and reproducibility, with accuracy within a two-fold range and a direct range of input material that covers 6 to 8 orders of magnitude.

The commercially available TaqMan® real-time PCR method was used in this project. This method allows accurate quantification of PCR product by inclusion of a fluorogenic oligonucleotide probe to components of the standard PCR product. TaqMan® probes consist of two types of fluorescent label; the reporter (6-carboxyfluorescein or FAM), attached at the 5' end and a quencher (6-carboxy-tetramethyl-rhodamine or TAMRA) attached at the 3' end.

During the PCR reaction, samples are exposed to ultra violet (UV) light after each cycle. Fluorescent output following this exposure is determined by a charge-coupled device (CCD) camera and logged by a computer. Whilst the probes are intact, the close proximity of the reporter to the quencher significantly decreases the fluorescence output. Cleavage of the probe causes a fluorescent signal to be omitted based on the fluorescence resonance energy transfer (FRET) principle (Cardullo *et al.*, 1988). If the target is present, the probe anneals downsteam and is cleaved by 5' nuclease activity of Taq polymerase during the extension phase of PCR. Importantly, this cleavage removes the probe from the target strand, allowing primer extension to continue to the end of the template strand. Reporter dye molecules are cleaved from their quencher probes with each

additional cycle, leading to an increase in the intensity of the fluorescent signal which is proportional to the amount of PCR product formed.

During amplification the fluorescence intensity is measured and an amplification plot formed. At the beginning is a linear phase (first 10-15 cycles), when the fluorescence signal has not risen above background levels, this is when the baseline fluorescence is calculated. An arbitrary threshold is chosen by the computer, it is ten times the standard deviation of the average signal of the baseline fluorescence between cycles 5 and 15. The comparative threshold (C_T) is the fractional PCR cycle number at which the reporter emission is above the threshold value.

The comparative C_T threshold method ($\Delta\Delta C_T$) can be used to quantify mRNA expression relative to the expression of an endogenous control, without the need for a standard curve (Schmittgen and Livak, 2008). The formula used for this method is as follows;

$$\Delta CT = C_T \text{ Target Gene} - C_T \text{ Reference Gene}$$

$$\Delta\Delta C_T = \Delta C_T \text{ Treated} - \Delta C_T \text{ Untreated}$$

Reagents

- 2 x TaqMan Universal PCR MasterMix (Applied Biosystems)
- Primer/probe set (Assays-on-Demand, Applied Biosystems) (Table 2.4)
- RNase free water

Procedure for assessment of basal gene expression

Total RNA was isolated from pellets of cells growing in exponential phase and cDNA synthesised (Sections 2.4.7.1 & 2.4.7.2). QRT-PCR was carried out using the relevant primer/probe sets (Table 2.4).

Procedure for assessment of cAMP-dependent targets

Cells in exponential growth phase were treated with 100µM 3-isobutyl-1-methylxanthine (IBMX) and 10µM forskolin to maximally increase intracellular cAMP levels or control vehicle (CV) (0.002% ethanol and 0.0008% DMSO). IBMX is a phosphodiesterase (PDE) inhibitor, which prevents the breakdown of cAMP within the cell. Forskolin is an adenyly cyclase agonist, causing an upregulation of cAMP production. Following 90 minutes of IBMX and forskolin treatment, cells were harvested for RNA and cDNA was subsequently synthesised (Sections 2.4.7.1 & 2.4.7.2). QRT-PCR was then carried out using the relevant primer/probe sets (Table 2.4).

Procedure for assessment of glucocorticoid receptor targets

Cells in exponential growth phase were treated with dexamethasone (17nM for cell lines or 1µM for primagrafts) to cause GR activation and transcription of downstream targets, or CV (9.0E-05% ethanol for cell lines, 0.005% ethanol for primagrafts). Following 24 hours incubation cells were harvested for RNA and cDNA was synthesised (Sections 2.4.7.1 & 2.4.7.2). QRT-PCR was then carried out using the relevant primer/probe sets (Table 2.4).

Experiment	Gene	Product Number
Assessment of *CREBBP* Knockdown	*CREBBP*	Hs00231733_m1
GR Targets	*GILZ* (*TSC22D3*)	Hs00608272_m1
	FKBP5	Hs00188025_m1
	NR3C1 (GR)	Hs00230813_m1
	ITGA9	Hs00174408_m1
cAMP Targets	*CXCR4*	Hs00607978_s1
	MKNK2	Hs00179671_m1
	DUSP10	Hs00200527_m1
	RGS16	Hs00892674_m1
	DUSP5	Hs00244839_m1
Endogenous Control	*TBP*	4310891E

Table. 2.4 List of primer/probe sets used. All primer/probe sets were purchased from Applied Biosystems.

2.4.8 Gene Expression Microarray

Principle

This method involves the synthesis and fluorescent labelling of cDNA before hybridising to a gene chip containing synthetic oligonucleotides, representing all of the expressed genes in the human genome. Sequences of 16-20 short oligonucleotides are chosen from the mRNA reference sequence of each gene, and light-directed *in situ* oligonucleotide synthesis is used to generate high-density probe arrays containing over 300 000 individual elements. *In vitro* transcription of double stranded cDNA from sample RNA is carried out, during which biotin-labelled nucleotides are incorporated into the synthesised cRNA molecules. The sample is then hybridised to a probe array and target binding is detected by staining with a fluorescent dye coupled to streptavidin. Signal intensities from probe array elements are used to calculate the mRNA abundance for each gene and

subsequently the relative gene expression. The amount of fluorescence emitted corresponds to the amount of bound nucleic acid. This process is summarised in Figure 2.1.

The data output from gene expression microarray analyses are stored as .CEL files, containing all of the raw signal intensity data from the array chip. These data must then be assessed for quality and normalised to ensure comparability across arrays. Data from samples from each condition are then assessed for differential gene expression. These data can be analysed for enrichment of gene sets by gene set enrichment analysis (GSEA) and predictions of effects on pathways can be generated using ingenuity pathway analysis (IPA) software (Qiagen).

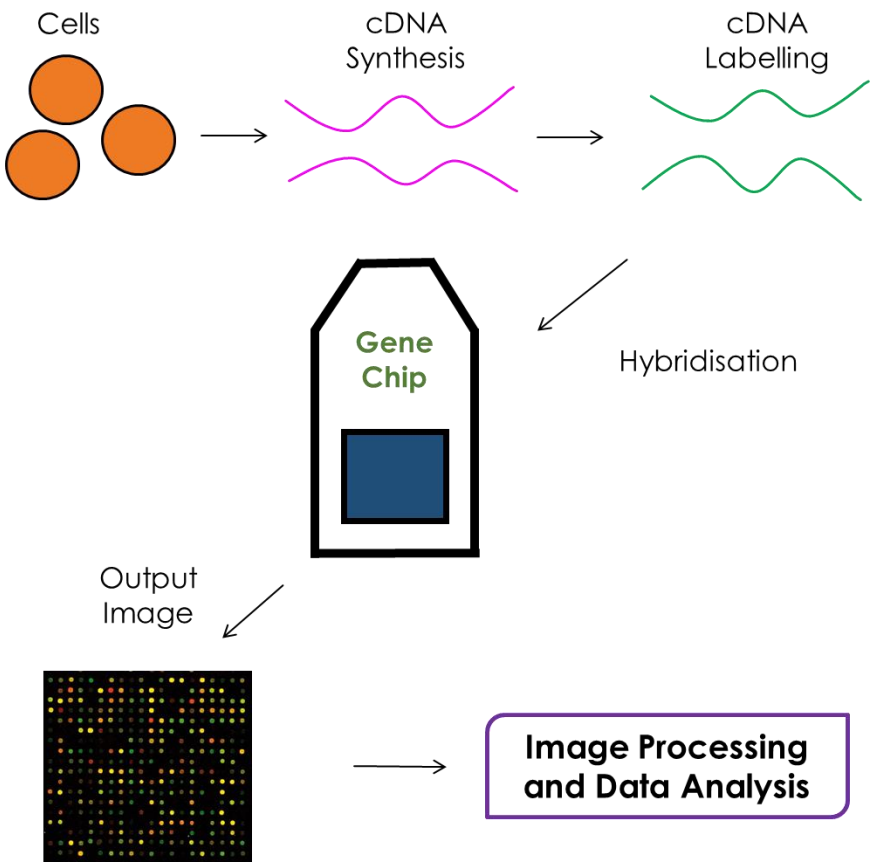

Figure 2.1. Summary of gene expression microarray analysis using high-density oligonucleotide arrays.

Procedure

Untreated cells, or cells treated with either 100µM 3-isobutyl-1-methylxanthine (IBMX) and 10µM forskolin or CV for 90 minutes were harvested in exponential growth phase, pelleted and RNA was isolated (Section 2.4.7.1). RNA samples were sent to Source Biosciences for analysis on the Affymetrix U133 Plus 2.0 platform. Raw data was then normalised and subsequently analysed for statistically significant differential gene expression.

Raw data files (.CEL) were read into 'R' software using the 'read.affy' function provided by the 'simpleaffy' R package. Expression values were obtained using GC robust multi-array average (GCRMA), which applies optical background correction to the raw data and adjusts for non-specific binding, then applies quantile normalisation to ensure that expression values across the array are comparable. Data were normalised and corrected through principle component analysis (PCA) and visual inspection of images. PCA, is a technique used to find patterns in data sets with high dimensions, reducing dimensionality by transforming the data into a new set of data (the principal components) and summarising the features. Probes with low variation or low signal across arrays were discarded. Gene symbols for probes were obtained from the 'hgu133plus2.db' R package, a database linking Affymetrix probe IDs to known annotation. Differential gene analysis was carried out using the 'limma' R software package. Linear models were fitted for each probe across the experimental groups and differences in gene expression between groups were determined using a moderated t-test. Genes were considered to be significantly differentially expressed where the p-value was <0.05 and the fold change between groups was ≥ 2.

2.4.8.1 Gene Set Enrichment Analysis

GSEA is a method of analysis for gene expression data which allows the assessment of groups of genes which share common biological functions, termed 'gene sets' (Subramanian *et al.*, 2005). These gene sets are defined based on prior biological knowledge from published data. GSEA is made up of three key elements;

1. Calculation of an enrichment score – reflects the degree to which the set is overrepresented at the extremes (top or bottom) of the list
2. Estimation of significance of enrichment score
3. Adjustment for multiple hypothesis testing

Gene ontology (GO) is used to perform enrichment analysis on gene sets, aiming to identify GO terms which are over or under represented within a data set. GO terms are a controlled vocabulary of terms for describing gene products and characteristics.

2.4.8.2 Ingenuity Pathway Analysis

IPA (Qiagen) is a web based software for analysing large 'omics' type data sets. This software takes raw data from gene expression microarray experiments and can make predictions pathways which may be altered, diseases and functions that have similar gene expression changes and upstream genes whose expression may be altered.

2.5 Protein Analysis

2.5.1 Western Blotting

Principle

This method involves the separation of proteins using a polyacrylamide gel, and visualisation of specific proteins using antibodies. There are four major stages to the process of western blotting;

1. Preparation of protein
2. Gel electrophoresis
3. Electroblotting
4. Immunodetection

2.5.1.1 Preparation of Protein Samples for Western Blotting

Principle

Before they can be separated by gel electrophoresis, cells must be lysed, proteins must be denatured into their individual polypeptide units and protein concentration determined to allow equal loading of samples. A denaturing agent containing sodium dodecyl sulphate (SDS) is used, which as well as denaturing proteins, binds polypeptides and gives them an overall negative charge, so electrophoretic separation can occur based on size. The denaturing agent also contains 2-mercaptoethanol which cleaves the intra and inter-molecular disulphide bonds, and bromophenol blue which serves as a dye front, allowing the user to visualise the sample running.

Reagents

- Cell Lysis Buffer – 50mM Tris-HC, pH 7.5, 150mM NaCl, 1% (v/v) Triton X-100, 0.5% (w/v) Na-deoxycholate, 0.1% SDS, cocktail of protease inhibitors (Roche, Welwyn Garden City, UK)
- Laemmli Buffer – 62.5mM Tris-HCL, pH 6.8, 4% SDS, 20% (v/v) glycerol, 5% 2-mercaptoethanol, 0.005% bromophenol blue
- BCA Reagent A – contains sodium carbonate, sodium bicarbonate, bicinchoninic acid and sodium tartrate in 0.1M NaOH
- BCA Reagent B – contains 4% cupric sulphate
- Albumin Standard (Invitrogen) – bovine serum albumin at 2mg/ml in 0.9% NaCl solution containing sodium azide

Procedure

Cell pellets were thawed on ice and flicked to loosen. Between 30 and 100µl cell lysis buffer was added based on cell number ($1x10^6$ cells = 40µl, $5x10^6$ = 70µl) and incubated on ice for 20 minutes with frequent vortexing. Cell debris was removed by centrifugation at 12 000 RPM for 7 minutes at 4°C. Protein containing supernatant was then removed into 1.5ml eppendorfs which had been cooled on ice. Protein concentration was determined using the bicinchoninic acid (BCA) method.

The BCA method was carried out according to the manufacturer's instructions. An aliquot of the protein sample was diluted 1:10 and plated out in quadruplicate in 10µl volumes, into a 96 well plate. Protein standards between 0.2 and 1.2mg/ml were made by diluting bovine serum albumin standard (at 2mg/ml) with dH_2O. Protein standards were also plated in quadruplicate in 10µl volumes along with dH_2O blank. A working BCA reagent

was made by mixing 50 parts BCA reagent A with 1 part BCA reagent B. To each well, 190µl of working reagent was added before being sealed and incubated at 37°C for 30 minutes. Absorbance at 562nm was measured using an Omega FLUOStar plate reader (Section 2.1.1). Data were analysed using Omega software (BMG Labtech) to generate a standard curve and unknown protein concentrations were determined based on extrapolation from this curve, taking into account the 10 fold dilution factor. Protein samples were made up to 0.5-2mg/ml using laemmli buffer and denatured by heating to 100°C for 5 minutes. Samples were stored at -20°C until required.

2.5.1.2 Polyacrylamide Gel Electrophoresis

Principle

This scientific method is based on the fact that charged molecules will migrate through a matrix upon application of an electric field. Polyacrylamide gel is used as this matrix as it is chemically inert, electrically neutral, hydrophilic and transparent. Separation of proteins in this way is based on size, with larger proteins migrating more slowly than smaller proteins. Polyacrylamide gels are formed by the polymerisation of acrylamide monomers into long chains which are then cross-linked by the reaction of N,N-methylene-bisacrylamide with free functional groups at the chain termini. The size of the pores in the polyacrylamide gel determines the rate at which proteins travel, and can be varied according to the protein size range of interest. Gels with a gradient of pore size (e.g 4-20%) are commonly used to resolve large sized proteins on the same gel as small sized proteins.

Reagents

- Electrode Buffer – 41.2nM Tris, 192mM glycine, 0.1% (w/v) SDS

- 4-20% Mini Protean TGX gels (BioRad)
- Precision Plus Dual Color protein standards (BioRad)
- Spectra Multicolour High Range Protein ladder (Thermo Fisher)

Procedure

Fifteen microliters of prepared protein sample (at 0.5-2mg/ml in laemmli buffer) was loaded per well into a BioRad mini 4-20% TGX gel. Eight to ten microliters of the relevant protein ladder for the protein of interest, was also loaded in the first well. Separation of proteins was carried out using a constant voltage of 250V for 25-60 minutes depending on the protein of interest.

2.5.1.3 Electroblotting

Principle

In order for proteins of interest to be detected by immunodetection, they must be transferred from the polyacrylamide gel to the surface of an immobilized matrix with a high capacity for protein binding e.g. polyvinylidine difluoride (PVDF) or nitrocellulose. This is carried out by sandwiching the membrane and the gel surface together, with filter paper and sponge on the outside to protect them. An electric field is then applied perpendicular to the surface of the gel, causing the proteins to move out of the gel and onto the surface of the membrane. The buffer used for transferring proteins in this way contains methanol to counteract the swelling of the gel and increase the binding affinity of the PVDF membrane for proteins.

Reagents

- Transfer Buffer – 10mM CAPS, 10% (v/v) methanol

- PVDF Membrane (BioRad)
- 3mm Filter Card (Thermo Fisher)
- Sponge (BioRad)

Procedure

Electroblotting was carried out using mini-blot equipment (BioRad) (Section 2.1.1). Filter card, sponges and PVDF membrane were briefly soaked in transfer buffer before construction of the sandwich. Before being soaked in transfer buffer, the PVDF membrane was soaked in methanol to hydrate the membrane and overcome its hydrophobicity. The electroblotting sandwich was constructed within the cassette as follows; sponge, 2 x filter card, gel, PVDF membrane, 2 x filter card, sponge. The sandwich was compressed by rolling a 5ml pipette tip over it in order to remove any bubbles. The transfer was carried out at either 25V overnight or 100V for 1 hour depending on the protein of interest. For transfers at 100V for 1 hour, an ice pack was added to the tank to prevent overheating.

2.5.1.4 Immunodetection

Principle

This process involves the detection of specific proteins by probing with mono- or polyclonal antibodies. To prevent the non-specific binding of antibodies to sites on the PVDF membrane, these sites are blocked using a buffer which contains non-fat milk powder before probing with antibodies. The antibodies themselves are also diluted in this blocking buffer. This buffer, as well as the buffer used for washing the membrane, contains Tween-20, to reduce non-specific binding of protein. Following blocking, membranes are probed with a primary antibody specific for the protein of interest. Membranes are then washed to remove any unbound primary antibody before being

probe with a secondary antibody produced in a different species of animal, raised against the immunoglobulins (Ig) of the species used to produce the primary antibody. The secondary antibody is conjugated to the horseradish peroxidase (HRP) enzyme which catalyses the oxidation of luminol (cyclic diacylhydrazide) to form acrinidium ester intermediates. These intermediates react with peroxide under slightly alkaline conditions to produce chemiluminescence with a maximal emission at 430nm. This chemiluminescence is subsequently detected by exposure of X-ray film and developing.

Reagents

- Tris-Buffered Saline (TBS) with Tween-20 (TBST) – 0.154M NaCl, 0.05M Tris, 0.5% (v/v) Tween-20
- Blocking Buffer – TBST, 5% (w/v) dried skimmed milk powder
- ECL Prime Western Blotting Detection Reagents (Amersham Biosciences)

Procedure

PVDF membranes were blocked for 30 minutes in blocking buffer following electroblotting. The membranes were then cut and probed with the relevant primary antibody at the given concentration (Table 2.5) for one hour at room temperature, in a 50ml falcon tube on a roller or overnight at 4°C on a rocking platform. Following primary antibody probing, the membrane was rinsed 3 times in TBST before a final 12 minute wash in TBST on a rocking platform. Membranes were then incubated with the relevant secondary HRP-conjugated antibody (Table 2.5) for 30 minutes at room temperature on a rocking platform. Following secondary antibody probing, the membranes were washed in TBST for 20 minutes, with TBST refreshed every 5 minutes, again on a rocking platform. Membrane bound HRP was then detected using ECL Prime western blotting detection

reagents (Amersham Biosciences) according to the manufacturer's instructions. ECL Prime reagent A was mixed 1:1 with reagent B and pipetted onto membranes and incubated at room temperature for five minutes. Membranes were then dried, wrapped in Saran Wrap (Thermo Fisher) and placed in an autoradiography cassette. For detection of chemiluminescence, membranes were exposed to X-ray film (Fuji Medical X-ray film, HA West, Gateshead, UK) for an appropriate amount of time to give visible protein bands. Where relative quantification of protein expression was required, exposed x-ray film was scanned using a Luminescent Image Analyzer (LAS-3000) (Fujifilm) and densitometry carried out using AIDA image analysis software (Raytest, Straubenhardt, Germany).

	Protein	Molecular Weight (kDa)	Catalogue Number	Species & Clonality	Supplier	Dilution Used	Dilution of Secondary Ab
Primary	CREBBP	265	sc-369	Rabbit polyclonal	Santa Cruz, Wembley, UK	1:1000	1:2000
	Acetyl Histone 3 Lysine 18	17	ab1191	Rabbit polyclonal	Abcam, Cambridge, UK	1:1000	1:2000
	Acetyl Histone 3 Lysine 27	17	ab4729	Rabbit polyclonal	Abcam	1:500	1:1000
	Acetyl p53	50	06-758	Rabbit polyclonal	Millipore, Consett, UK	1:800	1:6000
	p53	50	sc-126	Mouse monoclonal	Santa Cruz	1:8000	1:10 000
	p21	18	556430	Mouse monoclonal	Becton Dickinson	1:600	1:2000
	BCL6	75	14-9887-82	Mouse monoclonal	eBioscience, Cheshire, UK	1:10 000	1:5000
	MGMT	26	MAB16200	Mouse monoclonal	Millipore	1:1000	1:1000
	Phosphorylated ERK	42	9101	Rabbit polyclonal	Cell Signalling	1:3000	1:2000
	ERK2	42	sc-153	Rabbit polyclonal	Santa Cruz	1:3000	1:2000
	PARP1/2	116	Sc-7150	Rabbit polyclonal	Santa Cruz	1:1000	1:2000
	Alpha tubulin	50	T6074	Mouse monoclonal	Sigma-Aldrich	1:500 000	1:10 000
Secondary	Rabbit-Ig	-	P0448	Goat	Dako, Glosturp, Denmark	-	-
	Mouse Ig	-		Goat	Dako	-	-

Table 2.5 List of antibodies used with corresponding dilutions. All antibodies were diluted in blocking buffer (described previously) except anti-ERK2 which was diluted in TBST made up to 5% bovine serum albumin (w/v) and anti-p21 which was diluted in SuperBlock (Thermo Fisher) with 1% Tween-20 (v/v).

2.5.2 Irradiation of Cells

Principle

To study p53 response by western blotting, a DNA damage response must be induced. This can be achieved by sub-lethally irradiating cells.

Procedure

Cells were exposed to 5 Gray (Gy) radiation using an RS320 Irradiation System (Gulway Medical), whilst in exponential growth phase. Cell pellets were harvested (Section 2.2.5) at 0, 4 and 8 hours post-irradiation, and western blotting was carried out for p53, Ac-p53 and p21 (Section 2.5.1).

2.5.3 Histone Deacetylase Inhibition of Cells

Principle

Vorinostat (SAHA) is a pan histone deacetylase (HDAC) inhibitor. Vorinostat treatment leads to a significant increase in pan histone acetylation within cells.

Procedure

Cells growing in exponential phase were treated with 500nM vorinostat or DMSO CV for 1 hour before cell pellets were harvested (Section 2.2.5), and western blotting for AcH3K18 was carried out (Section 2.5.1).

2.5.4 Poly(ADP) Ribose Polymerase Assay

Principle

Poly(ADP) ribose polymerase (PARP) 1, is involved in DNA damage repair, acting in the base excision repair pathway. It attaches to regions of damaged DNA and catalyses the synthesis of poly(ADP) ribose (PAR) chains on itself and nuclear proteins. Synthesis of PAR

utilises nicotinamide adenine dinucleotide (NAD^+) (Morales *et al.*, 2014). Immunoblotting for the PAR product following maximum stimulation of PARP can be used to determine PARP activity.

Procedure

This procedure was carried out by Ashleigh Herriott and is outlined here (Herriott *et al.*, 2015).

2.6 Cell Growth and Drug Sensitivity

2.6.1 Growth Curves

Principle

In order to assess the effects of exongenous compounds on cell growth and apoptosis, information about the growth rate of cells under normal conditions must be gathered. This method simply involves periodically counting cells over time to establish a growth curve. Cell growth follows a characteristic pattern of lag phase, exponential phase and plateau phase.

Reagents

- Trypan blue reagent (Sigma Aldrich)

Procedure

Cells were seeded at a range of densities at time 0. Every 24 hours for 120 hours an aliquot of cells was taken and counted using trypan blue exclusion on a haemocytometer (Section 2.2.4). A growth curve of the data was plotted using GraphPad Prism software (GraphPad Software Inc., San Diego, CA, USA).

2.6.2 Drug Sensitivity

Principle

Drug sensitivity assays allow the effect of drug treatment on live cells to be measured. The alamar blue (Resazurin) (Thermo Fisher) assay was chosen for this application. In this assay, the non-fluorescent Resazurin is converted into bright red resorufin by diaphorase, a mitochondrial enzyme. The amount of fluorescence produced is proportional to the number of living cells, as dead/dying cells will be less metabolically active.

Reagents

- Alamar blue reagent (Thermo Fisher)

Procedure

Cells growing in exponential growth phase were seeded at $2x10^5$/ml (cell lines) or $4x10^6$/ml (primagraft/primary cells) and plated into 96 well plates at 100µl per well ($2x10^4$-$4x10^5$ cells per well). Drug concentrations or CV were added to each well as stated in Table 2.6. Drugs were diluted in growth media corresponding to the cells used. This dilution media was made up with CV to ensure a constant CV concentration across all drug concentrations. Outer wells were filled with media to prevent the evaporation of outer samples. Cells were incubated for 3 cell doublings (96 hours) before the addition of 20µl of alamar blue to each well. Following 4-6 hours incubation with alamar blue, fluorescence intensity was assessed using a FLUOstar Omega plate reader (Section 2.1.1) and Omega data analysis software (BMG Labtech). Absorbance readings were expressed as a percentage of CV treated cells and plotted as a survival curve using GraphPad Prism software (GraphPad Software Inc.).

The same method was used to assess sensitivity to ionising radiation (IR). Cells were subjected to a range of IR doses and plated out as described above. PreB 697 cells were exposed to between 0.292 and 6.132 Gy and SU-DHL-4 cells were exposed to between 0.876 and 8.76 Gy using an RS320 Irradiation System (Gulway Medical).

Cells	**Drug**	**Concentration Range**	**Control Vehicle (CV)**
PreB 697	Dexamethasone (Sigma-Aldrich)	0.1-100nM	0.2% ethanol
	Vorinostat (Selleckchem)	0.05-1.5µM	0.01% DMSO
	Dexamethasone and Vorinostat	0.01-1.25µM Vorinostat 17nM Dexamethasone	0.005% DMSO 0.1% ethanol
	Daunorubicin (Tocris Bioscience)	1-100nM	0.05% methanol
	Vincristine (Tocris Bioscience)	0.01-1nM	N/A (H_2O)
	Methotrexate (Sigma-Aldrich)	0.1-50nM	0.0001N NaOH
	6-thioguanine (Sigma-Aldrich)	0.1-50µM	0.02% DMSO
	BCL6 Inhibitor 79-6 (Merck Millipore)	10-1000µM	1% DMSO
	HAT Inhibitor C646 (Tocris Bioscience)	0.1-30µM	0.4% DMSO
	Temozolomide (Sigma-Aldrich)	25-257.5µM	1% DMSO
	U0126 MEK Inhibitor (Calbiochem)	0.1-50µM	1% DMSO
	Selumetinib (Sellekchem)	0.001-100µM	0.6% DMSO
MHH-CALL-2	Dexamethasone	0.1-1000nM	0.1% ethanol
	Temozolomide	50-257.5µM	1% DMSO
	U0126 MEK Inhibitor (Calbiochem)	0.1-50µM	1% DMSO
Primagraft	Dexamethasone	0.001-10µM	0.2% ethanol
SU-DHL-4	Dexamethasone	1-100µM	1% ethanol
	Vorinostat	0.25-6µM	0.05% DMSO
	Temozolomide	1-257.5µM	1% DMSO
	Vincristine	1-10nM	N/A (H_2O)
	Daunorubicin	0.0001-10µM	N/A (H_2O)

Table 2.6 List of drugs used and concentration ranges for each cell line and primagraft cells.

2.7 Gene Knockdown by RNA Interference (RNAi)

RNA interference (RNAi) is a method which allows selective repression in the expression of genes of interest.

Two forms of RNA interference (RNAi) were used in this project:

1. Small interfering RNA (siRNA)
2. Small hairpin RNA (shRNA)

Principle

Both methods of RNAi used in this project rely on the formation of a protein complex called the RNA-induced silencing complex (RISC). Multi-functional protein argonaute 2 unwinds double-stranded siRNA and the sense strand is cleaved. This leaves the antisense strand, complimentary to the target mRNA. This strand is loaded into the RISC and selectively seeks the target mRNA for degradation, exactly 10 nucleotides upstream from the first complementary nucleotide at the 5' end of the siRNA. The cleaved mRNA does not contain a poly-A tail and is degraded by exonucleases, leading to reduced gene expression. Activated RISC can move on to degrade multiple targets, accentuating gene silencing. For transient gene silencing, siRNA can be delivered to the cell directly. For stable knockdown, shRNA is used. Lentiviral transduction is used to deliver a shRNA containing vector to the cell. This vector fuses with the host DNA and so leads to the continual nuclear synthesis of this shRNA. ShRNA produced by the nucleus must undergo further processing to become siRNA and effect RNAi. The primary transcript generated from transcription is processed by the RNase enzyme Drosha and double-stranded RNA-binding protein DGCR8 into pre-mRNA. Pre-mRNA is then loaded into another complex containing the enzyme Dicer, which cleaves the double-stranded RNA into shorter

fragments (21-23 nucleotides). The process then continues as described for siRNA (Wilson and Doudna, 2013).

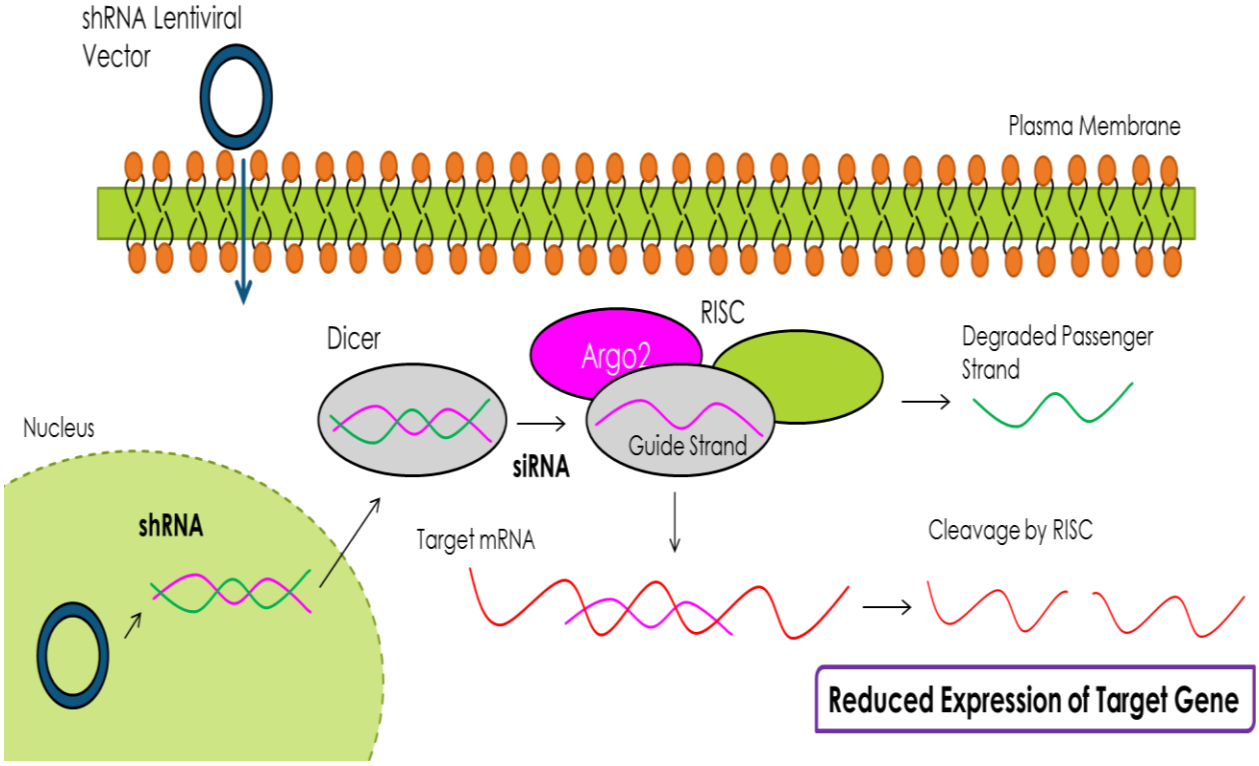

Figure 2.2. Mechanism of gene silencing using shRNA and siRNA. Adapted from (Chen *et al.*, 2008).

2.7.1 Lentiviral Transduction of Small Hairpin RNA (shRNA)

RNAi by shRNA transduction was carried out using pGIPZ Lentiviral shRNA (Thermo Fisher) allowing the formation isogenic cell lines with reduced expression of *CREBBP*, which is maintained indefinitely throughout the cell culture process. This construct contains;

- TurboGFP, allowing the visual marking of transduced cells
- Puromycin drug resistance, allowing positive selection of transduced cells
- ShRNA construct targeting *CREBBP*

Reagents

- Virus containing pGIPZ shRNA construct targeting *CREBBP* (V3LHS_358935, Thermo Fisher) and negative control shRNA (Thermo Fisher)
- Puromycin at 10mg/ml (Gibco).

Procedure

2.7.1.1 Puromycin Kill Curve

Cells were first assessed for sensitivity to puromycin by carrying out a puromycin kill curve. Cells were plated at $5x10^4$ cells per well in a 24 well plate and incubated overnight. They were then exposed to a range of puromycin (1-10µg/ml) and viability was assessed by cell counting (Section 2.2.4) for 3-6 days. The lowest concentration to kill 100% of cells within the 3-6 day time period was chosen as the concentration to use for selection of transduced cells.

2.7.1.2 Lentiviral Transduction

Twenty four hours before transduction, cells in exponential growth phase were seeded at 5×10^4 cells per well in a 24-well plate and incubated overnight. On the day of transduction growth medium was removed and virus containing a lentiviral construct targeting *CREBBP* or control construct, was added to the cells at multiplicities of infection (MOI) of between 5 and 30. MOI is the ratio of agent (i.e virus) to infection targets (i.e cells). MOI was calculated using the following formula;

MOI = plaque forming units (pfu) of virus / number of cells

4-6 hours post transduction, 1ml of growth media was added to cells followed by an overnight incubation. After 48 hours cells were assessed by flow cytometry to determine

the percentage of cells expression GFP (Section 2.3.1). Cells were then put onto puromycin selection for 3-6 days to remove any non-transduced populations. Cells were monitored routinely by flow cytometry (Section 2.3.1) until GFP expression reached >90, indicating a pure transduced population. Cells were amplified and cryopreserved (Section 2.2.6) for use in downstream applications.

2.7.2 Transfection of Small Interfering RNA (siRNA)

Principle

Knockdown of gene expression by siRNA involves the delivery of siRNA particles to a cell, leading to a reduced expression of target mRNA and thus protein expression. As the siRNA molecules delivered are subjected to the same procedures of degradation of endogenous mRNA, the knockdown achieved is transient. The application of an electrical impulse across cells membranes leads to transient pore formation, which in turn leads to greater uptake of exogenous molecules, such as RNA or DNA, into the cells (Neumann *et al.*, 1982; Sugar and Neumann, 1984). This process can be used for efficient delivery of siRNA to cells. Electroporation can be associated with a reduction in viability on a cell line basis, so whether or not cells are amenable to electroporation should be determined before attempting siRNA knockdown using this method.

Reagents

- Pooled siRNAs targeting *CREBBP* from (CBP siRNA (h)) (Santa Cruz).
- Non-targeting control siRNA pool (Control siRNA-A) (Santa Cruz).

Procedure

Cells in exponential growth phase were centrifuged at 1000 RPM for 5 minutes and resuspended at $1x10^7$/ml. Cells were then pipetted into a 4mm electroporation cuvette

(Eurogentec, Southampton, UK). For cell lines, 500µl of cells at $1x10^7$/ml were added to each cuvette ($5x10^6$ cells/cuvette) and for primagraft and primary cells 800µl of cells at $1x10^7$/ml were added ($8x10^6$ cells/cuvette). SiRNA was reconstituted using RNase free water to give a 10µM solution. Reconstituted siRNA was then added to each cuvette to a final concentration of 120-500nM. For optimisation experiments, one cuvette of cells without any siRNA added was included as a 'Mock' condition. To deliver the siRNA to cells, each cuvette was subjected to electroporation in an EPI 2500 Elektroporations-impulsgenerator (Section 2.1.1) at 350V for 10ms. Cells were subsequently incubated at room temperature for 15 minutes. Cells were then diluted 10 fold in culture medium in 6 well plates and incubated for 24 hours before use in downstream applications. Knockdown was confirmed for each discrete experiment by QRT-PCR (Section 2.4.7.3) and western blotting for CREBBP (Section 2.5).

Chapter 3 (Results 1) – Characterisation of a BCP-ALL Cell Line with Stable CREBBP Knockdown

Characterisation of a BCP-ALL Cell Line with Stable CREBBP Knockdown

3.1 Introduction

In order to assess the effect of *CREBBP* haploinsufficiency on the propensity to relapse in childhood ALL, an understanding of the molecular effects of *CREBBP* haploinsufficiency in cells must be gained. As discussed in Chapter 1, CREBBP is involved in a wide array of cellular functions, many of which could reasonably provide mechanisms for relapse establishment/development. In order to study the effect of *CREBBP* haploinsufficiency on multiple cellular processes, an isogenic model with stable CREBBP knockdown was required. To this end, a previously generated, CREBBP knockdown PreB 697 ALL cell line was studied. This enabled assessment of the effects of CREBBP knockdown on a range of cellular phenotypes in a B-ALL setting.

The aim of this chapter was to study CREBBP deficiency and its impacts on gene expression, sensitivity to ALL chemotherapeutics, tumour suppressor/oncogene balance, DNA damage repair, RAS pathway signalling and antigen presentation.

3.2 Characterisation of PreB 697 Cells with Stable CREBBP Knockdown

Previously (submitted as part of MRes dissertation), an isogenic CREBBP knockdown model was created in a BCP-ALL cell line. PreB 697 cells were selected as they had been shown to have expression of wild type *CREBBP* by PCR and western blotting. To achieve knockdown, cells were stably transfected with shRNA, targeting *CREBBP* or non-targeting

control, using a pGIPZ lentiviral vector. Following puromycin selection, CREBBP knockdown was confirmed at the protein level by western blotting. Cells with a stable knockdown in CREBBP (shCBP) showed around 40% reduction in *CREBBP* mRNA expression (p=0.005) and a much greater reduction at the protein level (Figure 3.1 A & B). These cells (shCBP) showed reduced acetylation of CREBBP target, histone 3 lysine 18 (H3K18) compared to controls (shNEG) showing that the knockdown had functional relevance (Figure 3.1 C). CREBBP knockdown was shown to have no effect on growth rate (Mean growth rate ±SD; shCBP 32.4 hours ±5.4; shNEG 30.7 hours ±4.8; p=0.7) (Figure 3.1 D), but led to a statistically significant reduction in GC induced expression of glucocorticoid receptor (GR) targets *GILZ*, *FKBP5* and *NR3C1* (p=0.009, p=0.03 and p=0.0003 respectively) (Figure 3.1 E), suggesting an impact of *CREBBP* haploinsufficiency on glucocorticoid (GC) receptor (GR) function. Despite this observation, and contrary to previous observations (Mullighan *et al.*, 2011), CREBBP knockdown was shown to have no effect on sensitivity to dexamethasone (GI_{50} values, mean ±SD; shCBP 16.6nM ±5.5 and shNEG 16.7nM ±3.1; p=0.9) or the HDACi vorinostat (GI50 values, mean ±SD; shCBP 485nM ±27.8 and shNEG 471nM ±48.75; p=0.9), alone or in combination (p=0.8) (Figure 3.1 F-H).

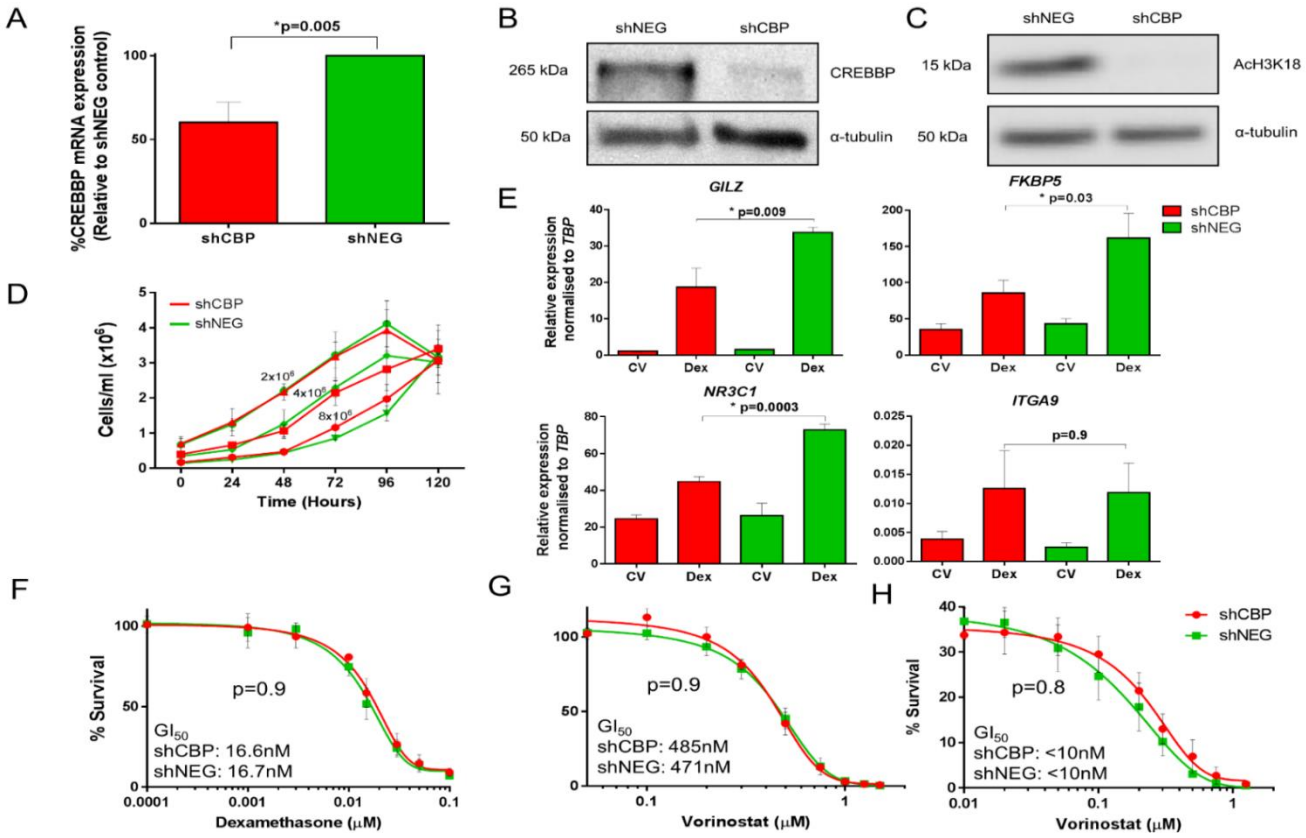

Figure 3.1. Summary of previous data outlining the creation and characterisation of a BCP-ALL cell line with stable knockdown of CREBBP. A. Cells were harvested in log growth phase and QRT-PCR was carried out for *CREBBP* expression. Expression levels were normalised to *TBP* by the $\Delta\Delta C_T$ method. Histogram shows mean expression ±SD (n=3). Whole cell lysates from PreB 697 shCBP and shNEG were assessed for **B.** CREBBP protein expression and **C.** AcH3K18 expression, by western blotting. Alpha tubulin was included as loading control. **D.** Growth rate of shCBP and shNEG cells was determined by seeding cells at 3 different starting densities and counting using trypan blue exclusion every 24 hours for 120 hours. **E.** SiCBP and control cells were treated with either control vehicle (CV) or dexamethasone (Dex) for 24 hours before determining expression of GR target genes by QRT-PCR relative to endogenous TBP expression by the ΔΔCT method. Histograms show mean expression ±SD (n=3). **F, G, H.** ShCBP and shNEG cells were treated with a range of dexamethasone or vorinostat concentrations or a combination of the two and their survival compared to CV treated cells was determined by alamar blue assay. Values plotted represent the mean % survival ±SD (n=3).

CREBBP protein expression in primagraft ALL samples with mono-allelic CREBBP deletion compared to wild type was assessed by western blotting (Section 2.5). Expression of CREBBP was reduced but not absent in samples with mono-allelic deletions, in line with previous studies (Mullighan *et al.*, 2011; Pasqualucci *et al.*, 2011) (Figure 3.2 A & B). Crucially, the protein reduction seen in PreB 697 cells with stable CREBBP knockdown is in line with what is shown in these primary derived samples (Figures 3.1 B).

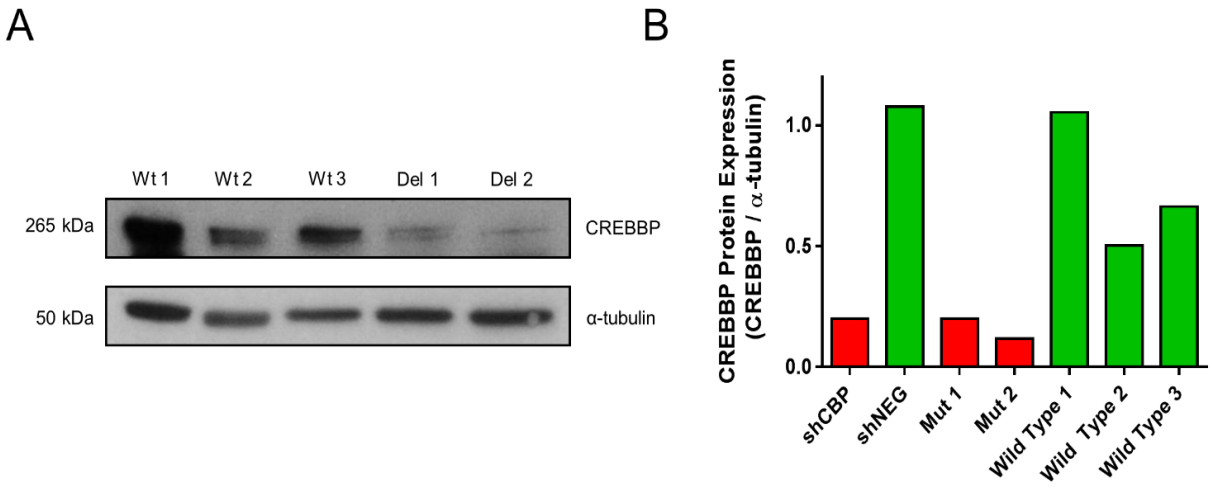

Figure 3.2. CREBBP protein expression in primagraft samples with mono-allelic CREBBP deletion. A. Whole cell lysates from primagraft ALL cells with expression of CREBBP with mono-allelic deletions (Del) or wild type (Wt) were assessed for CREBBP expression. Alpha-tubulin was included as loading control. **B.** Histogram of the relative expression of CREBBP in PreB 697 cells with and without stable CREBBP knockdown (left two bars) and primagraft samples normalised to α-tubulin after densitometric analyses.

3.3 cAMP response in PreB 697 Cells with Stable CREBBP Knockdown

As discussed in Chapter 1, CREBBP plays a key role in the cAMP-dependent signalling, acting as binding partner and co-activator of CREB (Radhakrishnan *et al.*, 1997). Given that cAMP-dependent signalling represents a major function of CREBBP, the effect of its knockdown on cAMP-dependent transcription was assessed.

Firstly, to determine relevant cAMP-dependent genes in PreB 697 cells, gene expression profiling was carried out using the Affymetrix U133 Plus 2.0 platform. RNA from PreB 697 cells transduced with non-silencing shRNA (shNEG) and treated with 3-Isobutyl-1-methylxanthine (IBMX) and forskolin for 90 minutes to induce a maximum intracellular cAMP response or CV was analysed by Source Bioscience as described in section 2.4.8. Data were analysed using R software and differentially expressed genes between IBMX and forskolin treated and control cells were compared. To select the genes which cAMP had the greatest effect on, genes which were upregulated in IBMX and forskolin treated cells were first ordered by average expression, the top 50 genes in this list were then sorted by statistical significance of differential expression and genes whose expression was reduced by IBMX & FSK treatment were removed. *CXCR4* and *MKNK2* were selected for further study as they appeared at the top of the list and were apparent with alternative probe sets, validating their significance (Table 3.1). *DUSP10* and *RGS16*, identified as cAMP-dependent in MEF cells, also appeared in this list and were also selected for further study (Mullighan *et al.*, 2011).

To assess the effect of *CREBBP* haploinsufficiency on cAMP-dependent signalling, cells were treated with IBMX and forskolin for 90 minutes to induce a maximum intracellular

cAMP response or CV (Section 2.4.7.3). Quantitative reverse transcriptase PCR (QRT-PCR) was then used to assess expression of genes identified as cAMP-dependent targets. All genes assessed were shown to be significantly upregulated by cAMP stimulation in both shCBP and shNEG cells (Fold induction; *CXCR4* ~14 fold, p values <0.007, *MKNK2* ~6 fold, p values <0.001, *DUSP10* ~3 fold, p values <0.05, *RGS16* ~5 fold, p values <0.02). CREBBP knockdown led to a small, statistically significant, reduction in basal *MKNK2* expression (p=0.005) and increase in basal *RGS16* expression (p=0.04), with no effect on basal *CXCR4* or *DUSP10* expression (p=0.7 and p=0.3 respectively) (Figure 3.3). Importantly, CREBBP knockdown had no effect on the level of cAMP induced gene expression achieved for any gene assessed (p values >0.3), suggesting that CREBBP knockdown does not impact on cAMP-dependent gene expression.

Feature	Gene	log2 Fold Change	Average Expression	P.Value
217028_at	CXCR4	3.964	10.779	7.90E-08
218205_s_at	MKNK2	2.544	10.695	2.10E-09
215111_s_at	TSC22D1	2.151	9.002	1.07E-08
209201_x_at	CXCR4	4.618	8.848	1.90E-09
202284_s_at	CDKN1A	1.260	8.406	4.63E-08
211919_s_at	CXCR4	4.697	8.163	6.30E-09
201751_at	JOSD1	1.927	8.152	4.07E-08
208622_s_at	EZR	2.343	8.117	6.80E-08
201368_at	ZFP36L2	3.152	7.895	5.70E-09
212430_at	RBM38	2.511	7.439	1.06E-07
223199_at	MKNK2	2.736	7.426	4.41E-08
227846_at	GPR176	1.734	7.424	3.33E-08

209324_s_at	RGS16	4.134	7.118	2.22E-08
201473_at	JUNB	3.488	7.076	2.00E-10
201531_at	ZFP36	2.975	6.723	3.46E-08
202499_s_at	SLC2A3	4.614	6.176	2.06E-08
205289_at	BMP2	4.636	5.992	3.50E-09
227410_at	FAM43A	4.165	5.698	5.10E-09
202815_s_at	HEXIM1	2.343	5.561	9.96E-08
41577_at	PPP1R16B	2.960	5.436	1.45E-08
203910_at	ARHGAP29	5.476	5.421	3.93E-08
207630_s_at	CREM	4.677	5.327	3.60E-09
201236_s_at	BTG2	4.681	4.624	2.68E-08
208763_s_at	TSC22D3	5.218	4.599	2.00E-10
202340_x_at	NR4A1	3.749	4.432	4.55E-08
216236_s_at	NA	3.165	4.374	6.00E-10
204491_at	PDE4D	4.680	4.244	4.00E-09
214508_x_at	CREM	5.503	4.231	3.00E-10
217875_s_at	PMEPA1	3.738	4.147	5.14E-08
209967_s_at	CREM	4.776	4.094	7.10E-09
205463_s_at	PDGFA	4.373	4.082	0.00E+00
221563_at	DUSP10	1.475	4.040	3.29E-08
216268_s_at	JAG1	2.661	4.007	2.02E-08
214873_at	LRP5L	1.481	3.837	5.43E-08
222088_s_at	NA	4.718	3.761	2.73E-08
209189_at	FOS	5.394	3.756	3.20E-08
202497_x_at	SLC2A3	4.615	3.713	1.00E-10
209305_s_at	GADD45B	3.376	3.507	7.29E-08

209099_x_at	JAG1	3.574	3.365	1.90E-09
230233_at	NA	3.181	3.292	0.00E+00
229072_at	RAB30	3.367	3.229	5.22E-08
223217_s_at	NFKBIZ	2.235	2.962	7.00E-10
223887_at	GPR132	2.057	2.896	2.59E-08
201883_s_at	B4GALT1	2.685	7.103	1.15E-07
224797_at	ARRDC3	2.521	6.437	1.15E-07
202498_s_at	SLC2A3	3.375	3.926	1.17E-07
200605_s_at	PRKAR1A	1.399	9.717	1.33E-07
223218_s_at	NFKBIZ	3.467	3.300	1.42E-07
227558_at	CBX4	3.113	9.107	1.49E-07

Table 3.1. Genes upregulated by cAMP in PreB 697 cells. List shows 50 of the genes with the highest change in expression by cAMP stimulation in PreB 697 shNEG cells ordered by statistical significance. *CXCR4* and *MKNK2* (highlighted in green) were chosen for further analysis as they appear at the top of the list and more than once. *DUSP10* and *RGS16* (highlighted in orange) were previously identified as dependent on cAMP and were also chosen for further analysis (Mullighan *et al.*, 2011). Extended gene list in appendix 1.

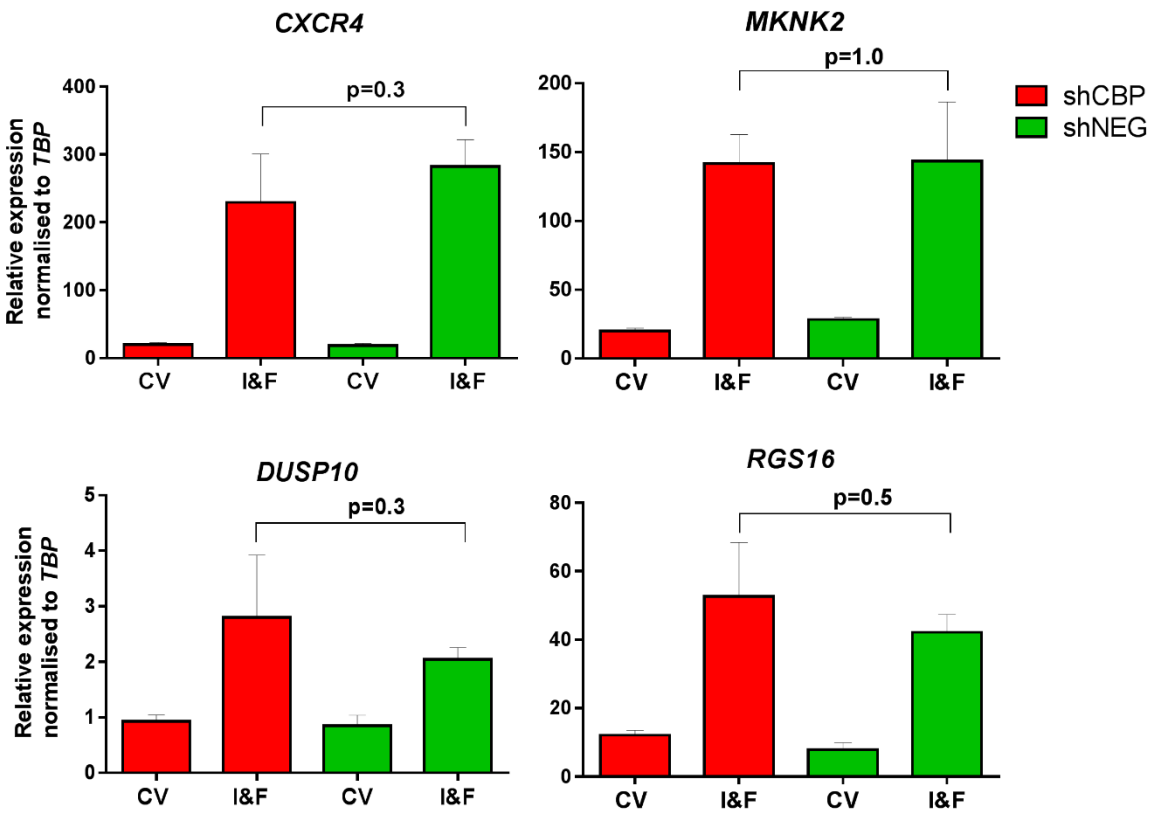

Figure 3.3. Effect of CREBBP shRNA knockdown in PreB 697 cells on cAMP-dependent gene expression. ShCBP and shNEG cells were treated with either control vehicle (CV) or IBMX and forskolin (I&F) before determining expression of cAMP-dependent genes by QRT-PCR, relative to endogenous *TBP* expression by the $\Delta\Delta C_T$ method. Histograms show mean ±SD (n=3).

3.4 Gene Expression Profiling of stable CREBBP Knockdown in PreB 697 Cells

CREBBP plays a role in body wide transcription through its interaction with TBP, TFIIB and CREB, as discussed in Chapter 1 (Kwok *et al.*, 1994; Yuan *et al.*, 1996). To determine the effect of CREBBP knockdown on total gene transcription in PreB 697 cells, the Affymetrix U133 Plus 2.0 gene expression array platform was used. RNA was collected from cells growing exponentially on 3 separate occasions before sending to Source Bioscience for Affymetrix U133 Plus 2.0 analysis (Section 2.4.8). Data were normalised (section 2.4.8) and PCA was carried out to allow visual inspection of the variation between experimental replicates (Figure 3.4). Inter-assay variation was low, with data from shCBP and shNEG cells clustering closely within their groups. ShCBP_1 and shCBP_2 clustered together more closely than shCBP_3, and the same was true for shNEG_1, shNEG_2 and shNEG_3. As expected, data from shCBP and shNEG cells clustered separately, representing the altered gene expression induced by CREBBP knockdown. Analysis of differentially expressed genes between shCBP and shNEG cells identified 28 genes which were significantly differentially expressed ($p=<0.05$, fold change ≥2) (Table 3.2). Gene set enrichment analysis was carried out and showed that no gene sets were enriched in CREBBP knockdown cell compared to control. *SSBP1*, *POLE2*, *MCM7*, *RFC2* and *MCM5* were all downregulated in shCBP cells compared to shNEG, with gene ontology (GO) analysis suggestive of DNA replication pathway perturbation (Adjusted p value $3.88x10^{-2}$) (Figure 3.4). GO analysis also identified a potential effect on the cell cycle pathway in CREBBP knockdown cells, with 7 genes in this pathway differentially expressed (Adjusted p values $<3.88x10^{-2}$) (Figure 3.5). Further to this, the data set was analysed using Ingenuity Pathway Analysis (IPA) software (Quiagen, UK). This analysis identified that, based on the

differential expression of *SCG2*, *OAT*, and *DNAJC15*, that upstream expression of *NR3C1,* the gene encoding the GR, would be altered, hinting at a link between CREBBP knockdown and GC response (p=0.04) (Table 3.2).

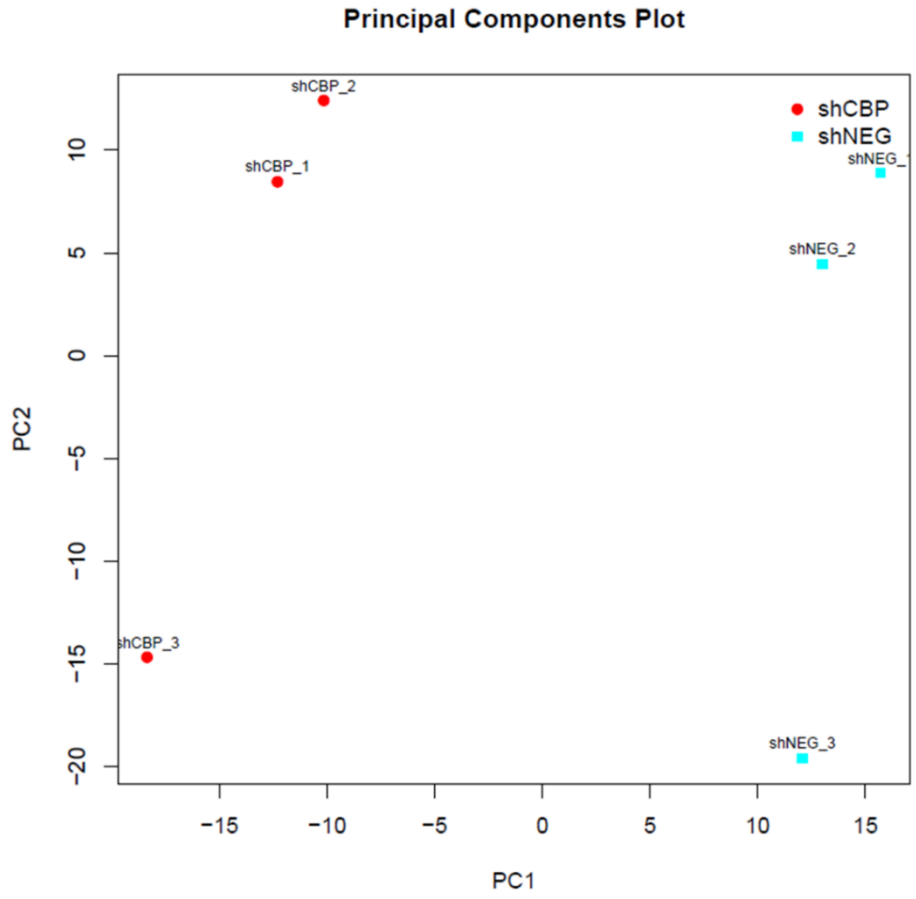

Figure 3.4. Principal component analysis of gene expression data from PreB 697 shCBP and shNEG cells. PCA scatterplot representing individual experimental replicates from PreB 697 shCBP (red) and shNEG cells (blue).

Feature	Gene	log2FC	P.Value
204035_at	SCG2	2.81E+00	3.30E-05
232327_at	THSD7B	2.64E+00	1.60E-04
201599_at	OAT	2.59E+00	1.70E-04
234987_at	SAMHD1	1.37E+00	1.60E-04
235048_at	FAM169A	1.23E+00	8.50E-05
210933_s_at	FSCN1	1.17E+00	1.10E-05
204048_s_at	PHACTR2	1.16E+00	2.60E-06
229103_at	WNT3	1.11E+00	3.00E-04
227819_at	LGR6	1.05E+00	8.20E-05
213316_at	KIAA1462	-1.01E+00	6.30E-07
209422_at	PHF20	-1.13E+00	1.20E-04
217485_x_at	PMS2P1	-1.13E+00	6.40E-05
204140_at	TPST1	-1.15E+00	2.40E-04
209970_x_at	CASP1	-1.16E+00	2.30E-05
222288_at	NA	-1.17E+00	1.80E-05
200636_s_at	PTPRF	-1.17E+00	1.60E-04
209321_s_at	ADCY3	-1.19E+00	7.00E-05
208050_s_at	CASP2	-1.28E+00	6.00E-05
223197_s_at	SMARCAD1	-1.33E+00	1.80E-05
212589_at	RRAS2	-1.38E+00	2.70E-04
203857_s_at	PDIA5	-1.50E+00	1.00E-04
228843_at	ARL10	-1.56E+00	2.20E-05
238029_s_at	SLC16A14	-1.61E+00	2.20E-04
211368_s_at	CASP1	-1.61E+00	5.80E-05
232232_s_at	SLC22A16	-1.70E+00	3.30E-05

Increased
Decreased

223204_at	FAM198B	-2.26E+00	3.10E-06
204897_at	PTGER4	-2.48E+00	1.30E-05
218435_at	DNAJC15	-2.50E+00	2.60E-06

Table 3.2. Analysis of differentially expressed genes between PreB 697 shCBP and shNEG cells. RNA samples isolated from shCBP and shNEG on three separate occasions were analysed using the Affymetrix U133 Plus 2.0 platform. Data was normalised and genes whose expression was significantly altered in shCBP compared to shNEG control were identified. Twenty eight genes in total were found to be significantly differentially expressed in shCBP cells compared to shNEG. Log2FC: log2 of the fold change.

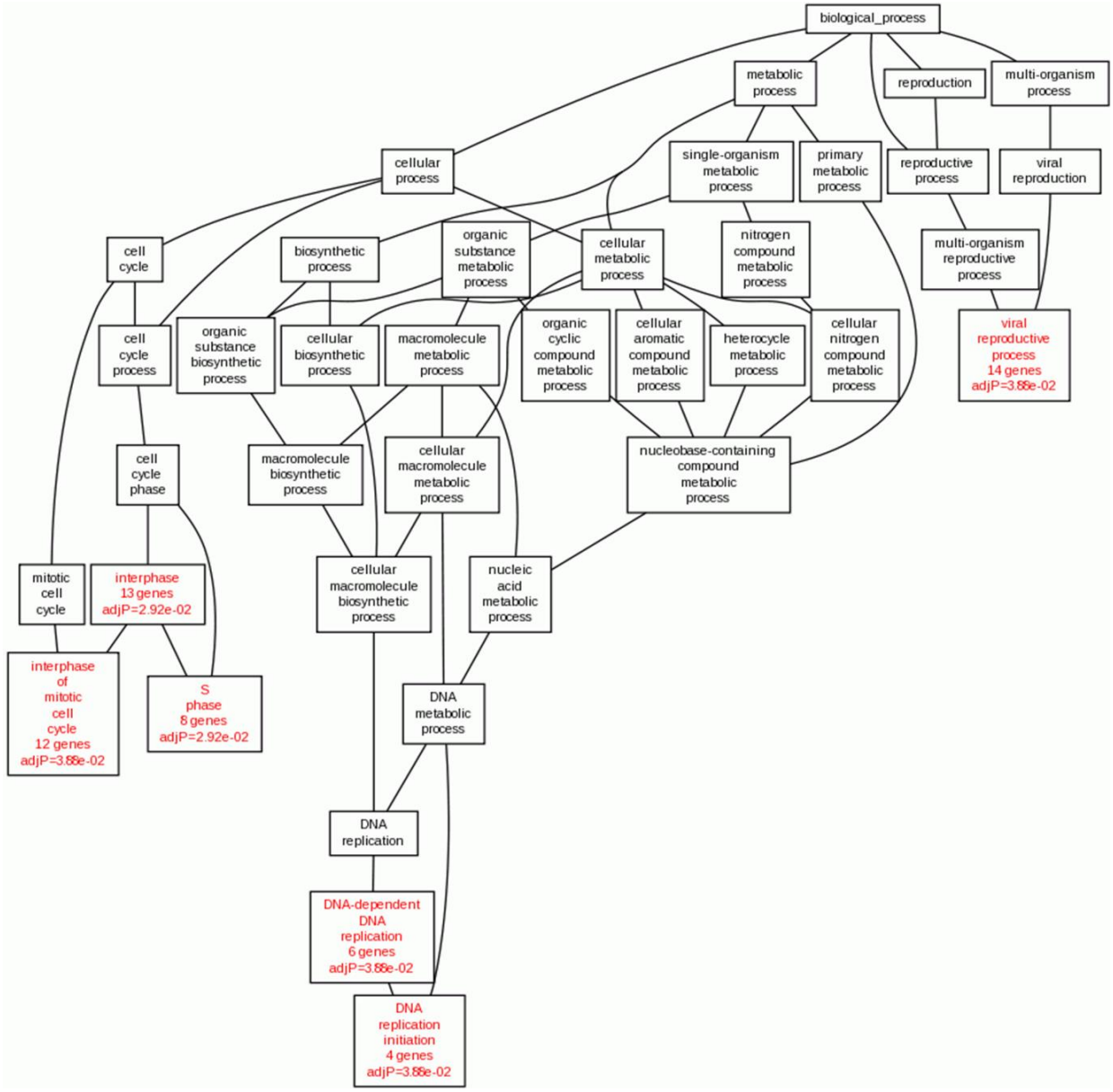

Figure 3.5. Gene Ontology (GO) pathways predicted to be affected by CREBBP Knockdown in PreB 697 cells. Pathways highlighted in red are predicted to be perturbed in cells with CREBBP knockdown.

3.5 Further Analysis of Cell Proliferation in PreB 697 Cells with Stable CREBBP Knockdown

To confirm results obtained by growth curve analysis (Section 3.3) fluorescence output readings from the control groups for each drug sensitivity experiment conducted using shCBP and shNEG cells were compared as a measure of cell proliferation over 96 hours (Section 3.3 & 3.5). The average fluorescent output for shCBP compared to shNEG cells was not significantly different (Mean fluorescent output ±SD; shCBP $1.05x10^5$ $\pm 2.45x10^4$, shNEG $1.01x10^5$ $\pm 2.21x10^4$; p=0.5) (Figure 3.6), suggesting that, despite GO term predictions (Section 3.4), CREBBP knockdown in PreB 697 cells does not influence cell proliferation over 96 hours.

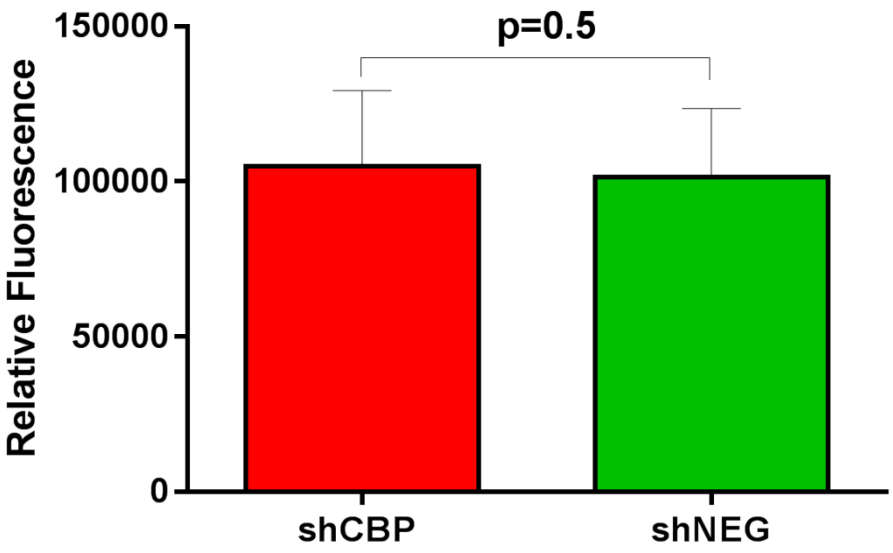

Figure 3.6. Stable CREBBP knockdown in PreB 697 cells and survival at 96 hours. The raw fluorescence output values from control treated cells from previous drug sensitivity experiments were combined and compared. Graph shows average relative fluorescence ±SD (n=15).

3.6 Chemosensitivity of PreB 697 Cells with Stable CREBBP Knockdown

Given that CREBBP knockdown in PreB 697 cells was shown to have no effect on sensitivity to dexamethasone treatment, we hypothesised that it may lead to reduced sensitivity to other ALL chemotherapeutics, thus explaining the propensity to relapse with *CREBBP* mutation in childhood ALL (Mullighan *et al.*, 2011; Inthal *et al.*, 2012). To this end, shCBP and shNEG cells were assessed for sensitivity to; daunorubicin, vincristine, methotrexate and 6-thioguanine by alamar blue drug sensitivity assay (Section 2.6.2). CREBBP knockdown in PreB 697 cells showed no significant effect on sensitivity to any of the chemotherapy agents tested compared to shNEG control (GI_{50} values, mean ±SD; daunorubicin shCBP 10.4nM ±1.5 versus shNEG 11.3nM ±0.52; p=0.4, vincristine shCBP 0.3nM ±0.02 versus shNEG 0.3nM ±0.04; p=0.07, methotrexate shCBP 9.4nM ±1.6 versus shNEG 9.8nM ±1.8; p=0.7 and 6-thioguanine shCBP 2.4µM ±0.58 versus shNEG 2.6µM ±0.32; p=0.6) (Figure 3.7 A-D).

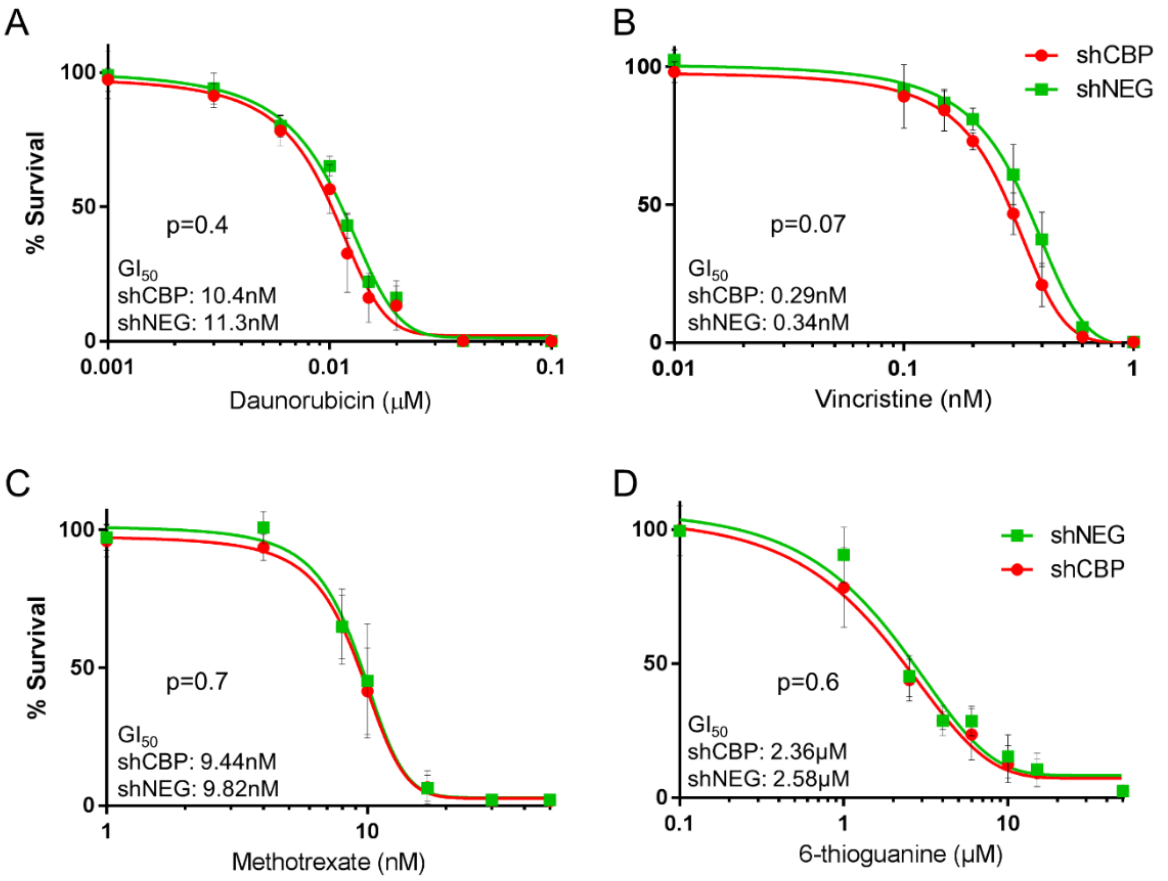

Figure 3.7. Effect of stable CREBBP knockdown in PreB 697 cells on sensitivity to common ALL chemotherapeutics. ShCBP and shNEG cells were assessed for sensitivity to common ALL chemotherapies; **A.** daunorubicin, **B.** vincristine, **C.** methotrexate, **D.** 6-thioguanine, by alamar blue drug sensitivity assay over 96 hours. Histograms show mean survival ±SD (n=3).

3.7 Expression and Activity of P53 and BCL6 in PreB 697 Cells with Stable CREBBP Knockdown

Alongside its role as a HAT, CREBBP is also able to acetylate and regulate the activity of non-histone proteins (Chapter 1). Acetylation by CREBBP is vital for the activity of tumour suppressor p53, influencing stability, DNA binding and recruitment of co-activators (Brooks and Gu, 2003; Tang *et al.*, 2008). CREBBP acetylation is also important in the inactivation of oncoprotein BCL6 by disrupting interaction with HDACs, reducing the ability to repress transcription of anti-apoptotic genes including p53 (Bereshchenko *et al.*, 2002). CREBBP is important for balancing the activity of this tumour suppressor/oncogene pair, and *CREBBP* mutation could potentially disrupt this balance, contributing to relapse in childhood ALL.

3.7.1 CREBBP knockdown and p53 Expression and Acetylation

The effect of CREBBP knockdown in PreB 697 cells, on p53 acetylation and expression of downstream target, p21, was assessed. Cells were exposed to 5 Gray (Gy) radiation, to induce DNA damage and trigger a p53 response, and harvested at 0, 4 and 8 hours post-irradiation (Section 2.5.2). Western blotting for the acetyl-p53 (CREBBP target residues; Lysine 373 and Lysine 382) (Ac-p53), p53 and p21 expression was carried out. The effect of CREBBP knockdown on acetylation of p53 in PreB 697 cells was unclear; in 2 of 4 repeats (C and D), Ac-p53 expression was unaffected, whereas the other repeats show a clear reduction of Ac-p53 levels in CREBBP knockdown cells following irradiation (A and B) (Figure 3.8). Importantly, CREBBP knockdown had no effect on p21 expression, a transcriptional target of p53 in any experiment. Taken together these data suggest that

CREBBP knockdown in PreB 697 cells may cause a small impairment of p53 acetylation, but that this is not sufficient to affect p53 activity.

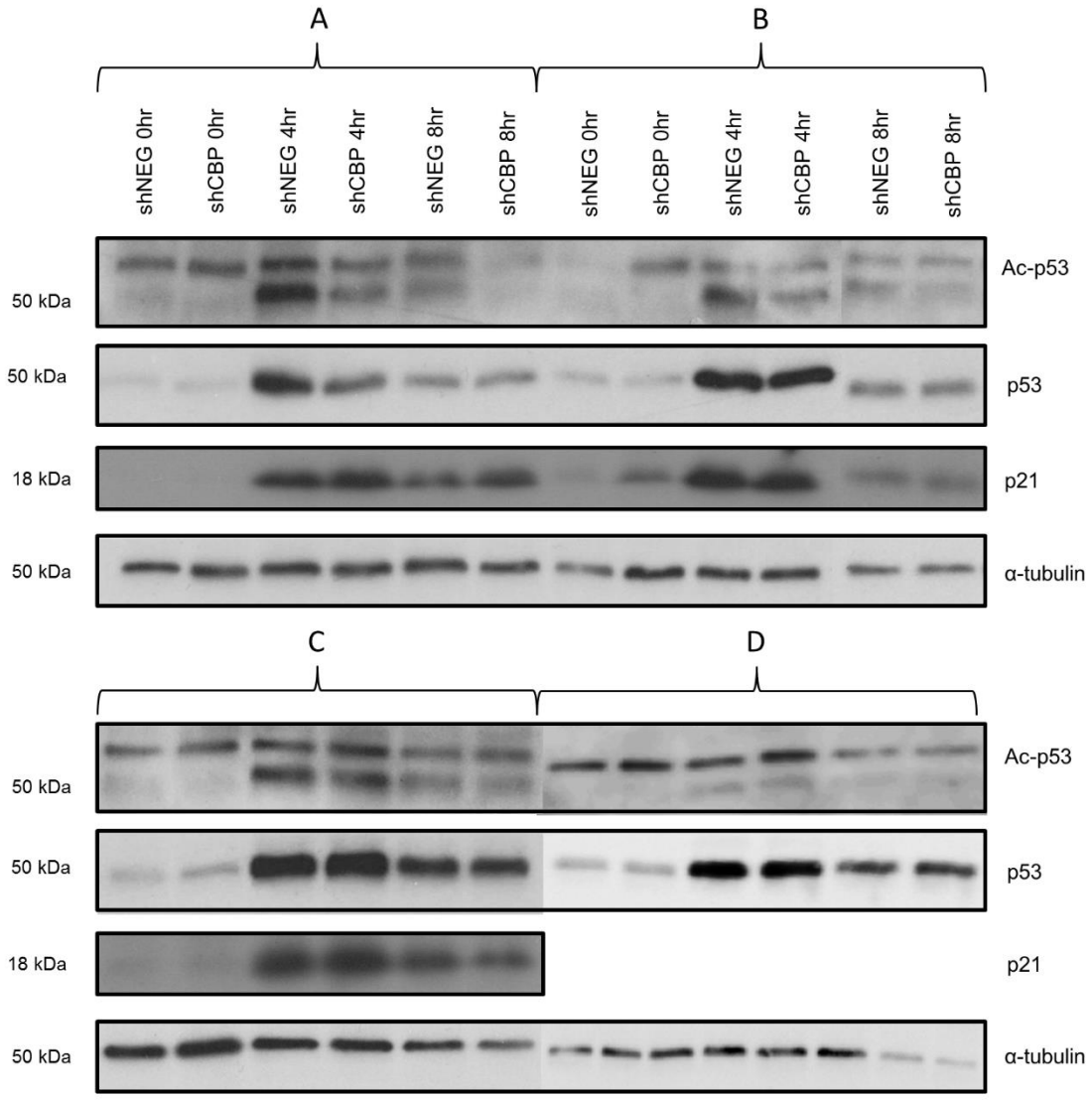

Figure 3.8. Expression of acetyl p53 (Ac-p53), p53 and p21 in PreB 697 cells with stable CREBBP knockdown. PreB 697 shCBP and shNEG cells were subjected to 5Gy radiation and whole cell lysates were harvested at 0, 4 and 8 hours on four separate occasions (A-D). Western blotting was carried out for Ac-p53, p53 and p21. Alpha tubulin was included as loading control.

3.7.2 CREBBP Knockdown and BCL6 Expression

To study the effect of CREBBP knockdown on BCL6 protein expression, western blotting was carried out using whole cell lysates from PreB 697 shCBP and shNEG cells (Section 2.5). This showed that CREBBP knockdown did not influence basal BCL6 expression in PreB 697 cells (Figure 3.9). Unfortunately, there was no commercially available antibody for acetyl-BCL6 at the time this study was carried out.

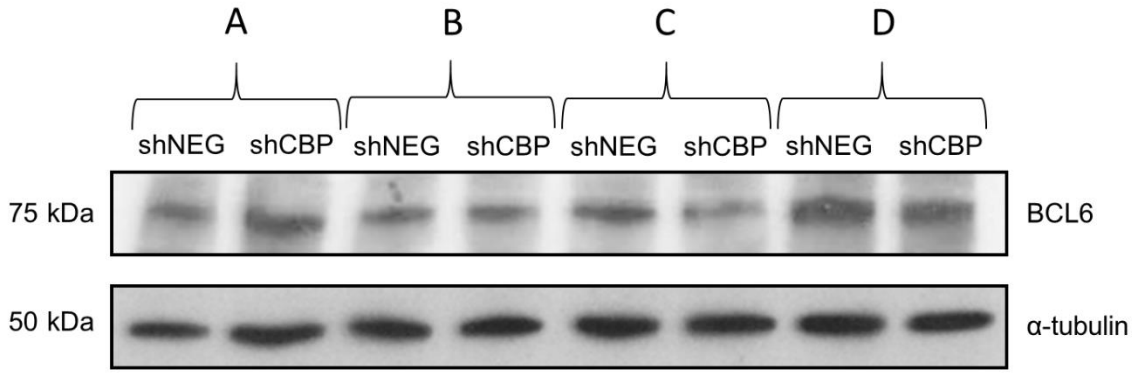

Figure 3.9. BCL6 protein expression in PreB 697 cells with stable CREBBP knockdown. Whole cell lysates were taken from PreB 697 shCBP and shNEG cells on four separate occasions (A-D) and western blotting was carried out for BCL6 expression. Alpha-tubulin was included as loading control.

To study the effect of CREBBP knockdown and *BCL6* expression at the mRNA level, gene expression microarray data (Section 3.4) was mined to determine expression of *BCL6* and a number of *BCL6* targets in PreB 697 shCBP compared to shNEG cells. *BCL6* expression was unaffected by CREBBP knockdown, and only 3 of 19 *BCL6* target genes assessed showed significant differential expression (Figure 3.10). Cells with CREBBP knockdown showed reduced expression of some *IFITM1*, *IFITM3* and *ATR* probes ($p=<0.04$, $p=0.0008$ and $p=0.02$ respectively) and increased expression of an *ID2* probe ($p=0.02$). Given that only a small number of *BCL6* targets were differentially expressed and BCL6 mRNA and protein expression were unaffected, this would suggest that CREBBP knockdown does not significantly alter BCL6 function.

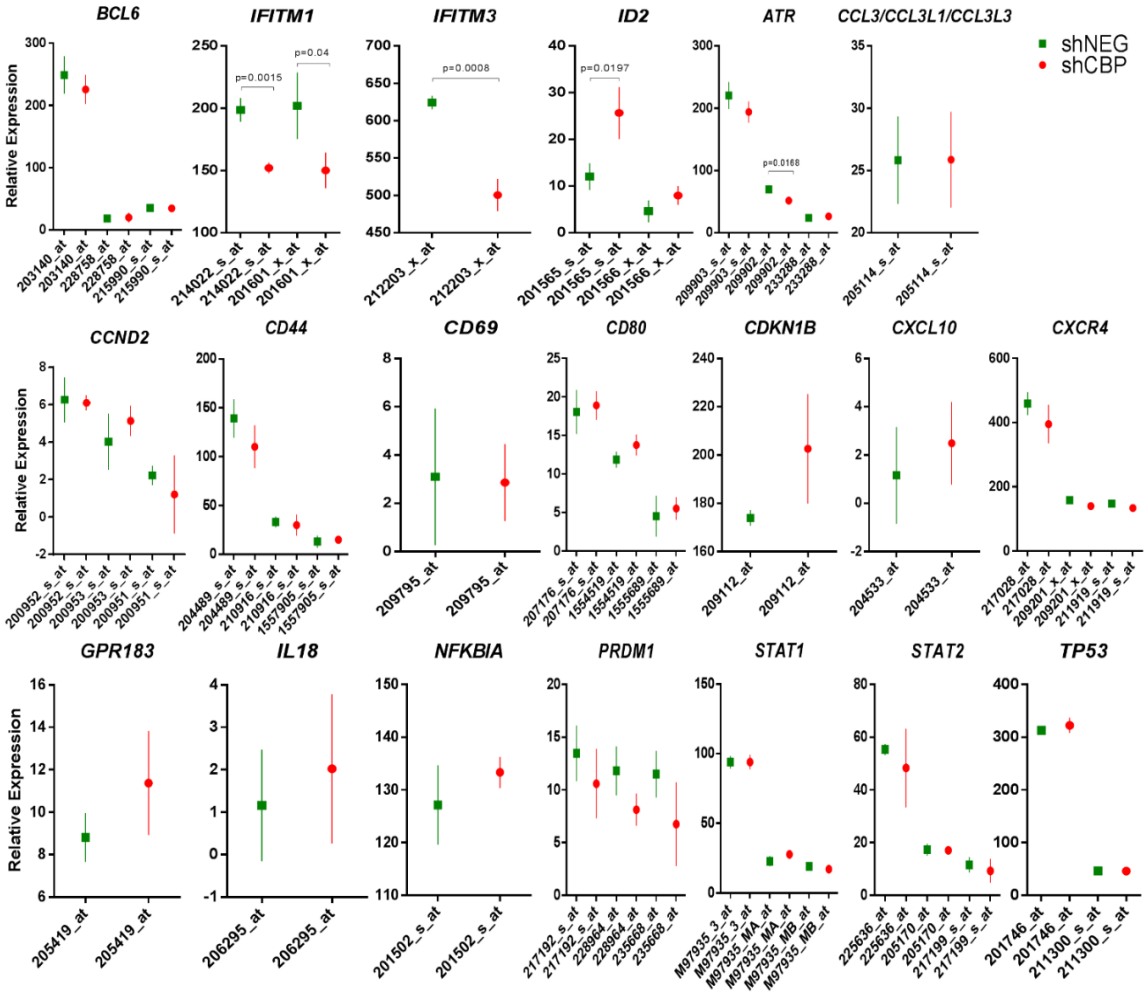

Figure 3.10. *BCL6* and *BCL6* target expression in PreB 697 cells with stable CREBBP knockdown. Gene expression microarray data from PreB 697 shCBP and shNEG cells was mined to assess the expression of *BCL6* and its targets. Graphs represent raw expression values from individual probes for each gene. Where more than 3 probes were available, the 3 with the highest relative expression values were plotted. Statistical significance was determined using the student's t test.

3.8 DNA Damage Repair in PreB 697 Cells with Stable CREBBP Knockdown

CREBBP is known to play a role in numerous DNA damage repair pathways, including; base excision repair (BER), homologous recombination repair (HRR) and direct DNA damage repair by thymine DNA glycosylase (TDG) (Chapter 1) (Pao *et al.*, 2000; Teo *et al.*, 2001; Tini *et al.*, 2002; Hassa *et al.*, 2005; Zimmer *et al.*, 2012; Leger *et al.*, 2014). Therefore, DNA damage repair mechanisms were assessed in the PreB 697 isogenic CREBBP knockdown model.

3.8.1 CREBBP Knockdown and Expression of BER Components

To assess the effects of CREBBP knockdown on BER, microarray data from PreB 697 shCBP and shNEG cells (Section 3.4) was mined for probes relating to BER components. None of the probes for the BER components analysed were found to be significantly differentially regulated in shCBP compared to shNEG cells (Figure 3.11). These data suggest that CREBBP knockdown does not impact on BER function in PreB 697 cells.

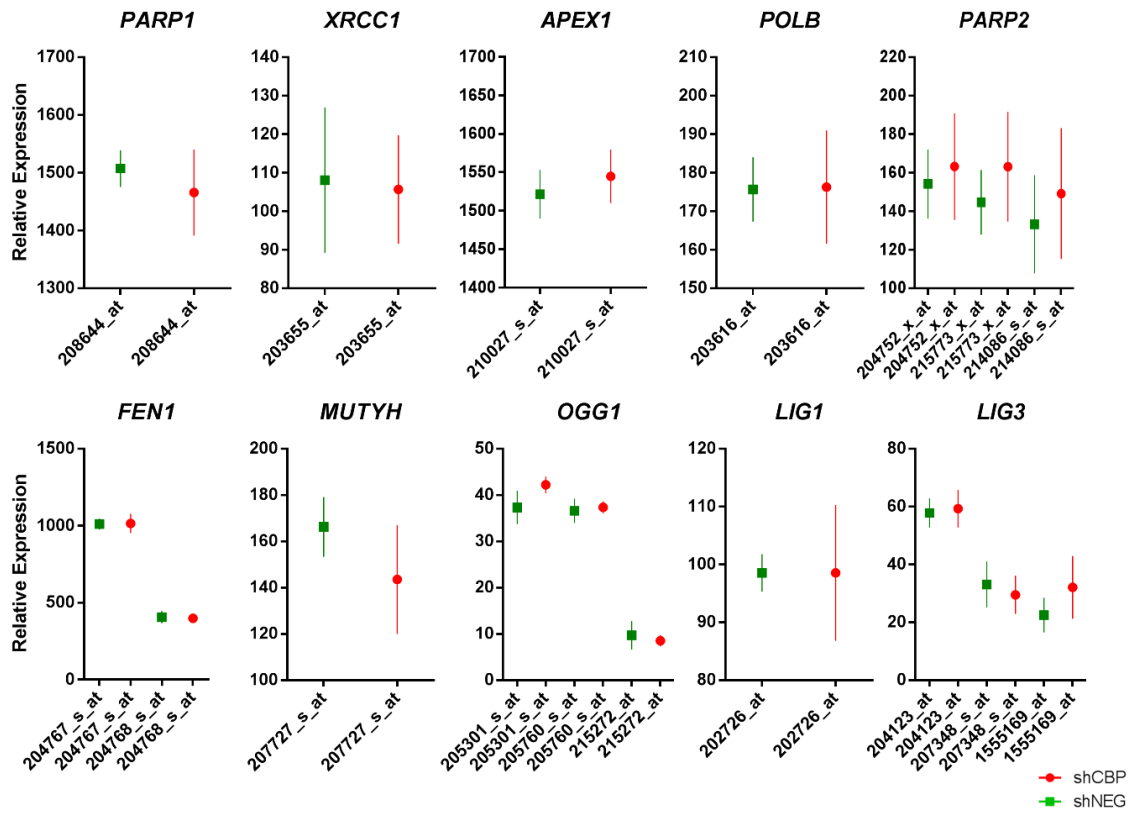

Figure 3.11. Expression of BER components in PreB 697 cells with stable CREBBP knockdown. Gene expression microarray data from shCBP and shNEG cells was mined to assess the expression of important BER components. Graphs represent raw expression values from individual probes for each gene. Where more than 3 probes were available, the 3 with the highest expression values were plotted.

3.8.2 CREBBP Knockdown and PARP Expression and Activity

CREBBP is known to acetylate BER protein, poly(ADP) ribose polymerase (PARP) 1 allowing interaction with p50 and synergistic co-activation of NF-κB by p300 (Hassa *et al.*, 2005). Firstly, western blotting for basal PARP-1 protein expression in PreB 697 shCBP and shNEG cells was carried out (Section 2.5). This showed that CREBBP knockdown had no effect on PARP-1 protein levels in PreB 697 cells (Figure 3.12). Maximally stimulated PARP activity was assessed by Ashleigh Herriott as described here (Plummer *et al.*, 2005). Whilst cells with CREBBP knockdown showed slightly higher basal PAR levels, there was no significant difference in PARP activity between shCBP and shNEG cells (Figure 3.13). This further suggests that CREBBP knockdown is not sufficient to impair BER in PreB 697 cells.

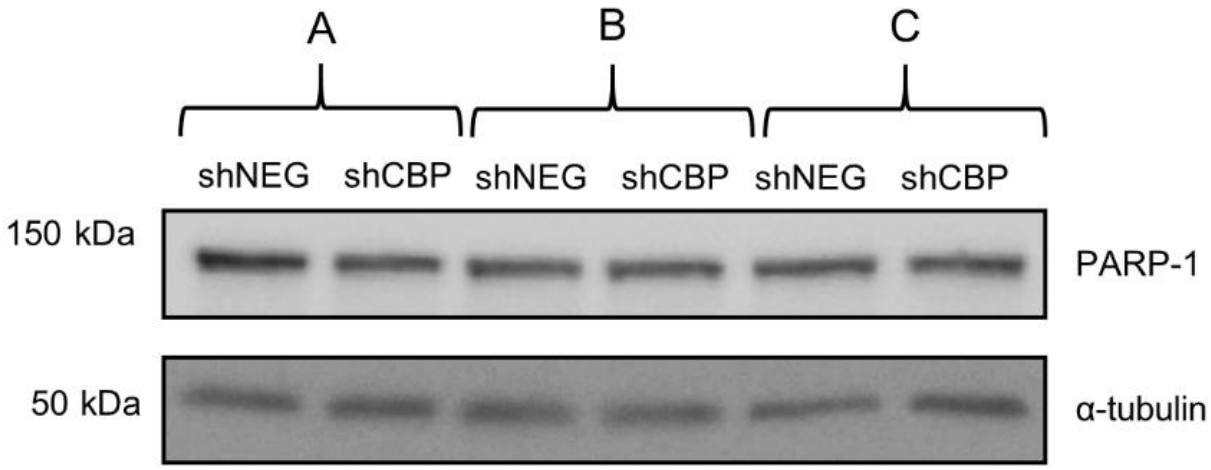

Figure 3.12. PARP-1 expression in PreB 697 cells with stable CREBBP knockdown. Whole cell lysates from PreB 697 shCBP and shNEG cells were collected on three separate occasions (A-C) and western blotting for PARP-1 expression was carried out. Alpha tubulin was included as loading control.

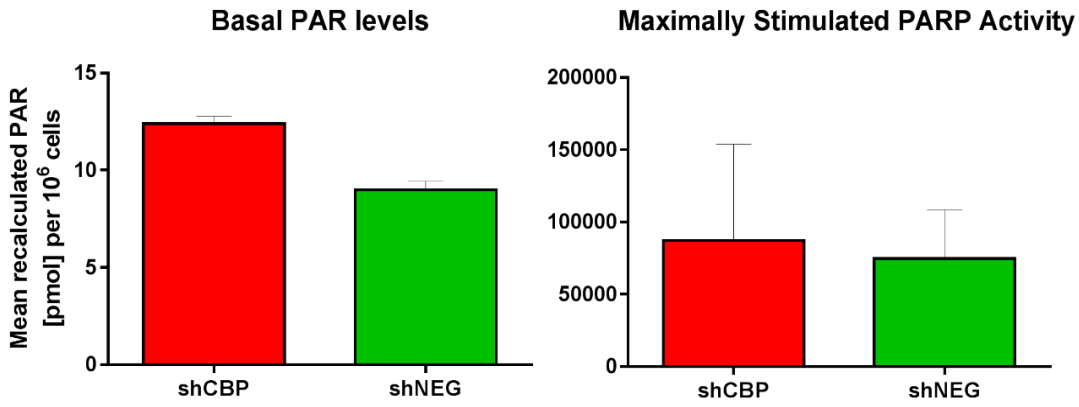

Figure 3.13. Basal PAR expression and maximally stimulated PARP activity in PreB 697 cells with stable CREBBP knockdown. Basal PAR levels and maximally stimulated PARP activity was assessed in PreB 697 shCBP and shNEG cells. Maximally stimulated PARP activity was determined based on ability to form PAR using an immunoblot assay. Graphs show mean recalculated PAR [pmol] per 10^6 cells ±SD (n=1).

3.8.3 CREBBP Knockdown and Temozolomide Sensitivity

To further assess the effect of CREBBP knockdown on DNA damage repair, PreB 697 shCBP and shNEG cells were analysed for sensitivity to the alkylating agent, temozolomide. Temozolomide rapidly undergoes pH-dependent degradation to the active intermediate 5-(3-methyltriazen-lyl)imidazole-4-carboxamide, which can add methyl adducts to N^7 guanine, O^6 guanine and N^3 adenine (Horspool *et al.*, 1990; Cheng *et al.*, 2005). Unrepaired O^6-methylguanine is a mutagenic lesion as it leads to mispairing of cytosine or thymidine, which in turn leads to G:C to A:T transitions upon DNA replication (Saffhill *et al.*, 1985). This can trigger the mismatch repair (MMR) pathway, eventually leading to double strand breaks that initiate cell cycle arrest and apoptosis (Aquilina *et al.*, 1992; Branch *et al.*, 1995; Ochs and Kaina, 2000). MGMT is a DNA repair protein that removes these alkyl groups from guanine at the O^6 position, preventing mispairing (Tubbs *et al.*, 2007). MGMT deficiency is known to cause hypersensitivity to chemotherapeutic methylating agents such as temozolomide (Glassner *et al.*, 1999).

PreB 697 shCBP and shNEG cells were treated with temozolomide or CV over 96 hours and relative cell viability was assessed using alamar blue (Section 2.6.2). CREBBP knockdown in PreB 697 cells led to a statistically significant increase in sensitivity to temozolomide compared to control (GI_{50} values, mean ±SD; shCBP 135µM ±9.15 versus shNEG 174µM ±2.31; p=0.002) (Figure 3.14). These data suggest that CREBBP knockdown cells may have deficiency in direct DNA damage repair by MGMT.

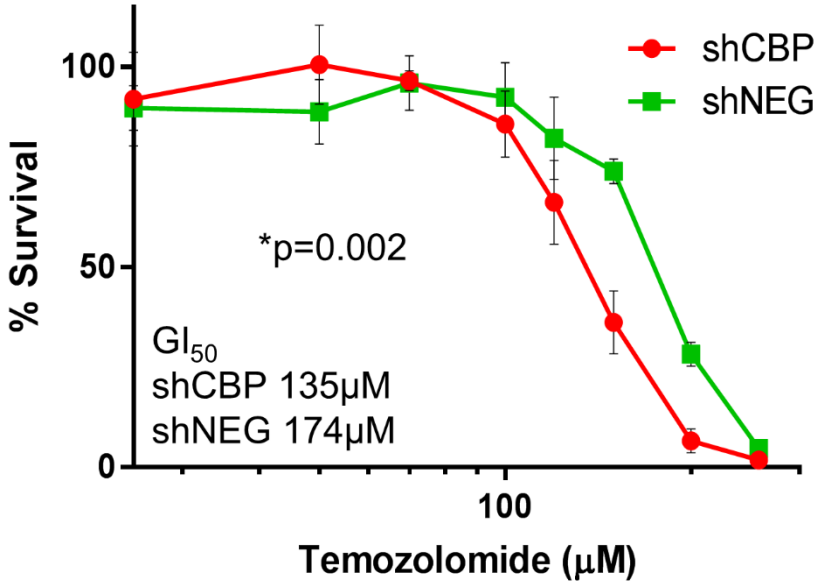

Figure 3.14. Effect of stable CREBBP knockdown in PreB 697 cells on sensitivity to temozolomide. ShCBP and shNEG cells were assessed for sensitivity to temozolomide by alamar blue drug sensitivity assay over 96 hours. Histogram shows mean survival ±SD (n=3).

3.8.4 CREBBP Knockdown and MGMT Expression

Given that PreB 697 cells with CREBBP knockdown showed an increased sensitivity to temozolomide compared to control (Section 3.8.3), MGMT protein expression was assessed by western blotting (Section 2.5). MGMT is predicted to be 25kDa on a western blot, but the antibody used showed bands at 37kDa and 20kDa as well as a band at 25kDa (Figure 3.15). This suggests that other isoforms or modified versions of MGMT could be present in the cell line, or that the antibody is prone to non-specific binding. Complications aside, western blotting for MGMT in CREBBP knockdown PreB 697 cells showed no evidence of reduced MGMT expression.

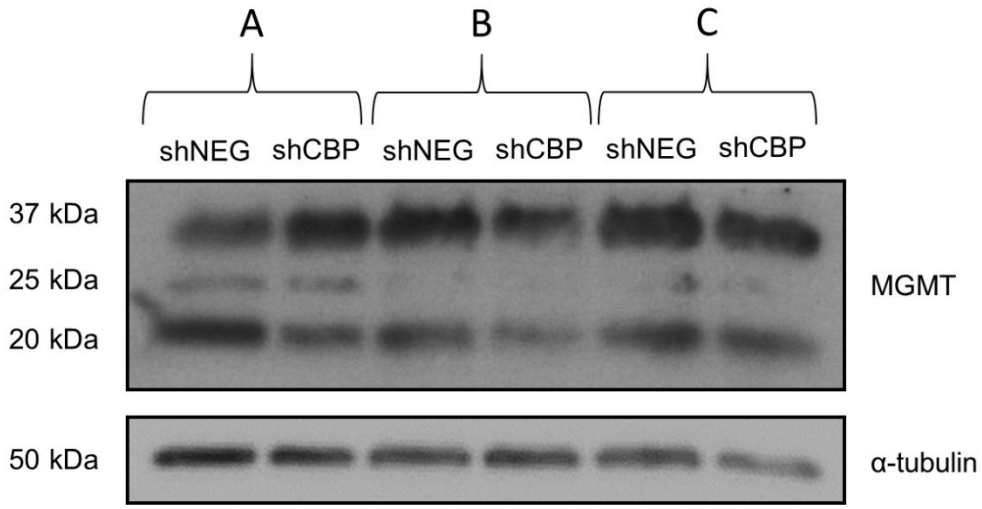

Figure 3.15. MGMT expression in PreB 697 cells with stable CREBBP Knockdown. Whole cell lysates from PreB 697 shCBP and shNEG cells were collected on three separate occasions (A-C) and western blotting for MGMT expression was carried out. Alpha tubulin was included as loading control.

3.8.5 CREBBP Knockdown and Ionising Radiation Sensitivity

BER is responsible for the repair of damage induced by ionising radiation (Curtin, 2012). Further to this, Zimmer *et al.* (2012), showed that *CREBBP* heterozygous mice were hypersensitive to gamma radiation compared to wild type controls (Zimmer *et al.*, 2012). For these reasons, the effect of CREBBP knockdown on response to ionising radiation (IR) in PreB 697 cells was assessed. Cells growing in exponential phase were dosed with 0.3-6.1 Gy radiation, and their viability assessed by alamar blue following 96 hours incubation (Section 2.6.2). CREBBP knockdown had no effect on sensitivity to IR in PreB 697 cells compared to isogenic controls (GI_{50} values, mean ±SD; shCBP 1.453Gy ±0.07 versus shNEG 1.493 ±0.27; p=0.8) (Figure 3.16), again suggesting an intact BER response.

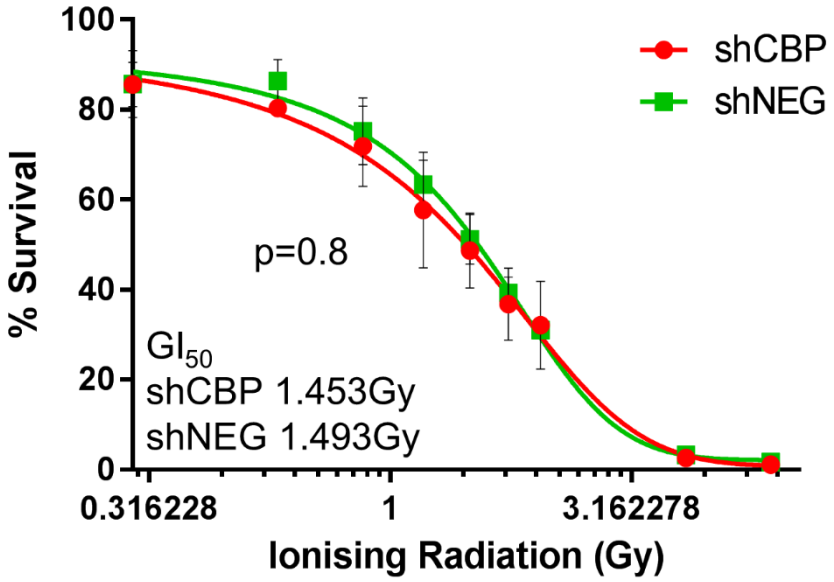

Figure 3.16. Effect of stable CREBBP knockdown in PreB 697 cells on sensitivity to ionising radiation. ShCBP and shNEG cells were assessed for sensitivity to ionising radiation by alamar blue drug sensitivity assay over 96 hours. Histogram shows mean survival ±SD (n=3).

3.9 Enhanced RAS Pathway Activation in *NRAS* Mutant PreB 697 Cells with Stable CREBBP Knockdown

As discussed in Chapter 1, genetic profiling of childhood ALL has shown that *CREBBP* mutations frequently co-occur with *RAS* pathway mutations (Malinowska-Ozdowy *et al.*, 2015; Paulsson *et al.*, 2015). Given this co-occurrence, it is possible that *CREBBP* mutations cooperate with oncogenic RAS mutations. As the PreB 697 cell line is known to harbour an *NRAS* mutation (Irving *et al.*, 2014), CREBBP knockdown in this cell line provided a model to assess the effect of the co-occurrence of these mutations on RAS pathway activation.

3.9.1 CREBBP Knockdown and p-ERK Expression

The MAPK, ERK, is phosphorylated during RAS pathway activation. For this reason, assessment of phosphorylated ERK (p-ERK) is a useful measure of RAS pathway activation. PreB 697 shCBP and shNEG cells were harvested in exponential growth phase and western blotting was carried out probing for p-ERK and basal ERK (Section 2.5). In 3 of 4 replicate experiments (B, C and D), levels of p-ERK were found to be increased in PreB 697 shCBP cells compared to shNEG controls (Figure 3.17). Basal ERK levels were found to be consistent between shCBP and shNEG cells, so changes in p-ERK expression cannot be explained by altered basal ERK expression. These data suggest that CREBBP knockdown enhances RAS pathway activation in PreB 697 cells.

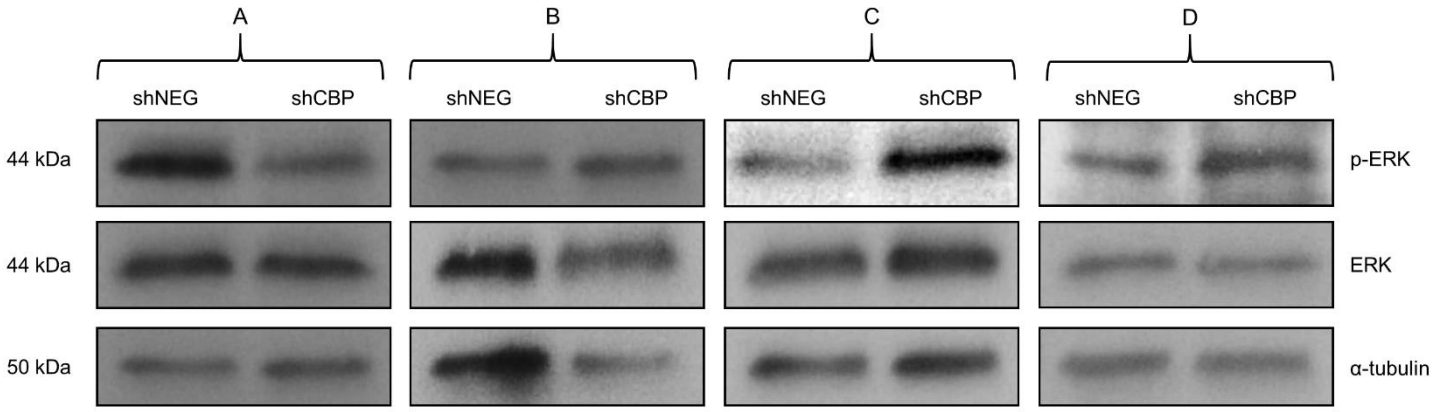

Figure 3.17. Stable CREBBP knockdown in PreB 697 cells and p-ERK expression. Whole cell lysates from PreB 697 shCBP and shNEG cells were collected on four separate occasions (A-D) and western blotting for p-ERK and ERK expression was carried out. Alpha tubulin was included as loading control.

3.9.2 CREBBP Knockdown and MEK Inhibitor Sensitivity

Given that CREBBP knockdown in RAS pathway mutant PreB 697 cells led to increased RAS pathway activation as assessed by p-ERK expression (Section 3.9.1), it was hypothesised that this may lead to altered sensitivity to MEKi. Selumetinib is a potent MEKi and recently, pre-clinical evaluation by our group showed significant differential sensitivity in RAS pathway-mutated ALL compared with wildtype cells both *in vitro* and in an orthotopic xenograft model engrafted with primary ALL cells (Irving *et al.*, 2014). PreB 697 cells with CREBBP knockdown were assessed for sensitivity to selumetinib by alamar blue drug sensitivity assay. An initial experiment (n=1) showed no difference in sensitivity to selumetinib between shCBP and shNEG cells (Figure 3.18 A). Importantly, this experiment showed that PreB 697 cells were resistant to selumetinib (GI_{50} values >100µM), suggesting that any effect of CREBBP knockdown on MEKi sensitivity may be masked by this. To overcome this, shCBP and shNEG cells were assessed for sensitivity to U0126, a selective, non-competitive inhibitor of MEK1 and MEK2, by alamar blue drug sensitivity assay (Duncia *et al.*, 1998) (Section 2.6.2). Cells with CREBBP knockdown, again had no differential response to treatment with U0126 than control cells (GI_{50} values, mean ±SD; shCBP 9.8µM ±3.5 versus shNEG 10.4µM ±1.7; p=0.8) (Figure 3.18 B). This suggests that CREBBP deficient RAS mutated ALL retain sensitivity to MEKi.

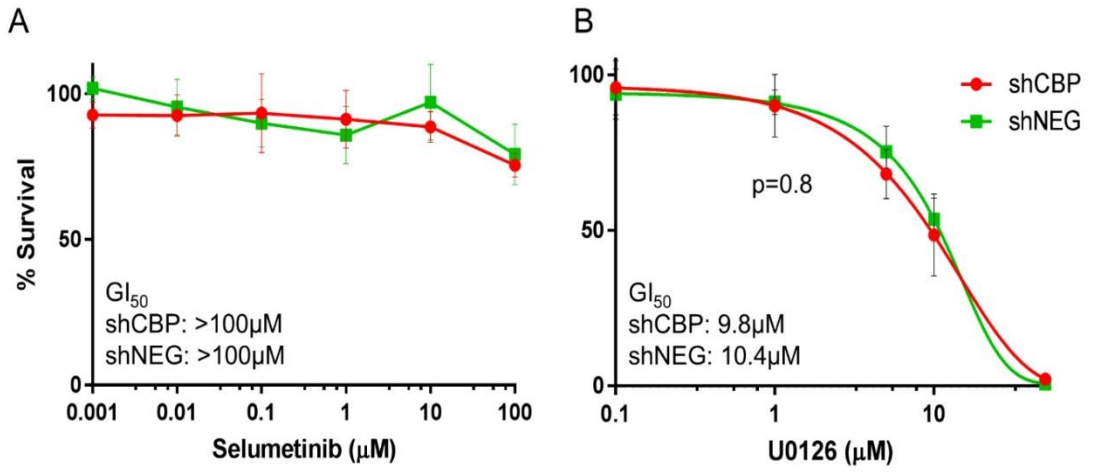

Figure 3.18. Effect of stable CREBBP knockdown in RAS mutant PreB 697 cells on sensitivity to MEK inhibition. ShCBP and shNEG cells were assessed for sensitivity to the MEKis **A.** Selumetinib and **B.** U0126 by alamar blue drug sensitivity assay over 96 hours. Histogram shows mean survival ±SD (A. n=1, B. n=3).

3.10 *In Vivo* Growth of PreB 697 Cells with Stable CREBBP Knockdown

Whilst informative, *in vitro* assays lack many factors which are present in whole organisms and so it may be that some important characteristics of CREBBP knockdown were not seen in these assays. To understand the effect of CREBBP knockdown on cells growing in a whole organism, PreB 697 shCBP and shNEG cells were grown *in vivo*. NOD SCID γ null mice were injected intrafemorally with 10 000 cells, either shCBP (n=5) or shNEG (n=6) (Section 2.2.8). Mouse numbers were determined based on previously published xenograft data, in which between 5 and 6 mice per group were sufficient to show a statistical difference in *in vivo* sensitivity to the MEKi selumetinib, given orally (Irving *et al.*, 2014). Engraftment was monitored by tail vein bleed (Section 2.2.7.1) and mice were culled when signs of ill health were seen (weakness, difficulty walking, slow movement etc.). Upon culling, spleens and livers were weighed and fixed along with femurs. Section of spleen were also put into suspension and assessed for engraftment by flow cytometry (Section 2.3.2).

Tail vein bleeds showed 0% peripheral blood engraftment at week 3 post-injection and for mice injected with shCBP (the only surviving mice at this time point) showed between 3.9 and 27.7% peripheral blood engraftment at week 6. Importantly, GFP expression of transduced cells was maintained *in vivo* (shCBP; 99.6% GFP positive, shNEG; 99.4% GFP positive), suggesting that cells retained CREBBP knockdown (or control sequence) (Figure 3.19). Time to death was significantly longer in shCBP mice, with all shNEG being culled based on health criteria, before shCBP mice (Time to death, mean ±SD; shCBP 42 days ±1.23 versus shNEG 28.17 days ±3.71; p=<0.0001) (Figure 3.20 A). Spleen weight and liver weight was also significantly higher in shCBP mice compared to shNEG (Spleen weight,

mean ±SD; shCBP 0.23g ±0.05 versus shNEG 0.13g ±0.03; p=<0.004, Liver weight, mean ±SD; shCBP 4.75g ±0.46 versus shNEG 3.66g ±0.59; p=<0.009) (Figure 3.20 B & C). There was a trend towards greater spleen engraftment in shCBP than shNEG, but this was not statistically significant (Spleen engraftment, mean ±SD; shCBP 20.88% ±9.33 versus shNEG 12.86% ±8.53; p=<0.2) (Figure 3.20 D). These data show that CREBBP knockdown leads to a markedly altered *in vivo* growth profile in PreB 697 cells.

A

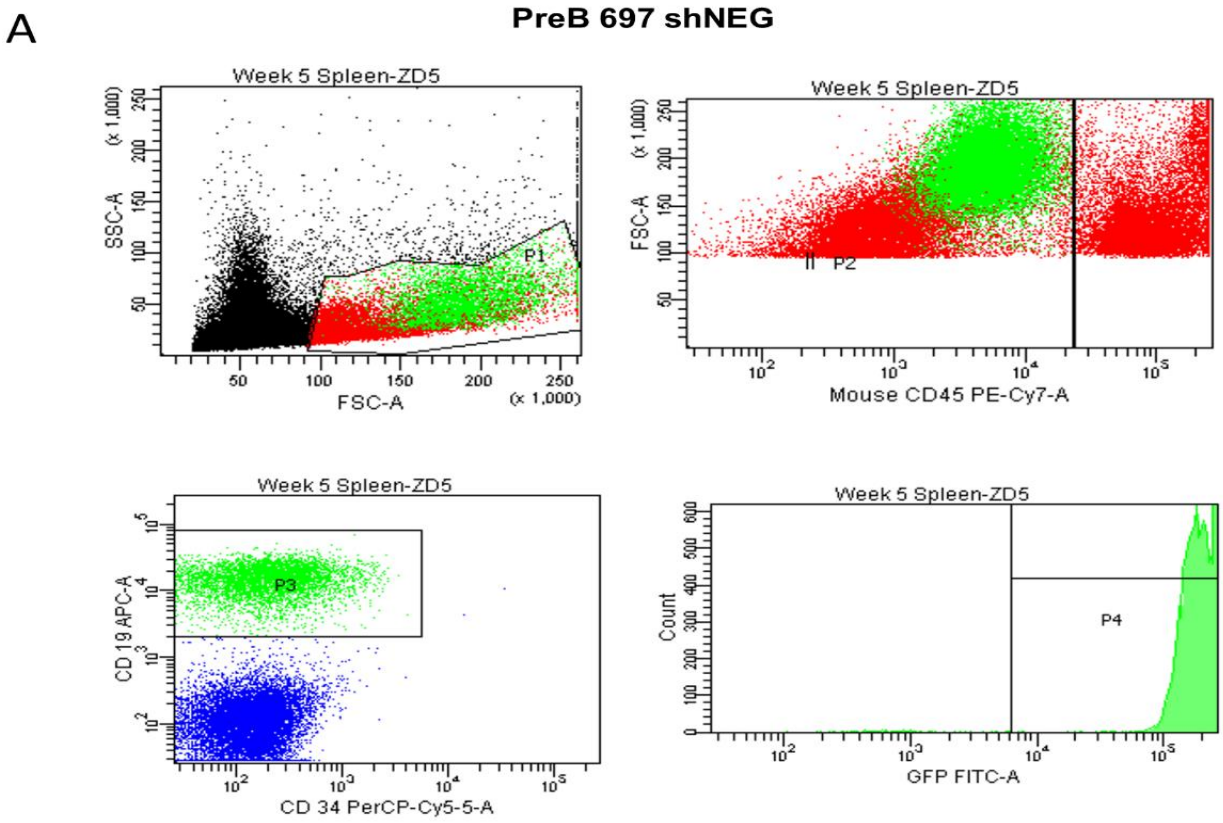
PreB 697 shNEG
Week 5 Spleen-ZD5
SSC-A
(x 1,000)
FSC-A
(x 1,000)
P1
Week 5 Spleen-ZD5
FSC-A
P2
Mouse CD45 PE-Cy7-A
Week 5 Spleen-ZD5
CD 19 APC-A
P3
CD 34 PerCP-Cy5-5-A
Week 5 Spleen-ZD5
Count
P4
GFP FITC-A

B

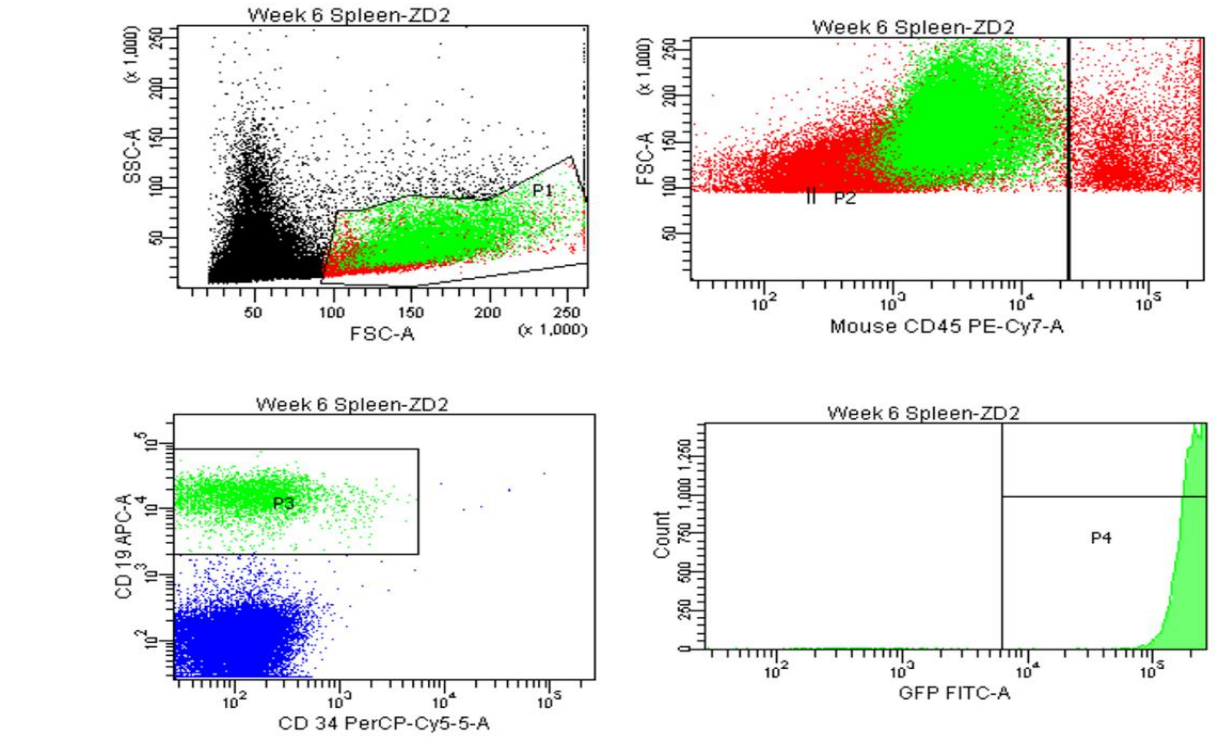
PreB 697 shCBP
Week 6 Spleen-ZD2
SSC-A
(x 1,000)
FSC-A
(x 1,000)
P1
Week 6 Spleen-ZD2
FSC-A
P2
Mouse CD45 PE-Cy7-A
Week 6 Spleen-ZD2
CD 19 APC-A
P3
CD 34 PerCP-Cy5-5-A
Week 6 Spleen-ZD2
Count
P4
GFP FITC-A

Figure 3.19. GFP expression of spleen cells from mice engrafted with PreB 697 shCBP and shNEG cells. Spleen cells from mice engrafted with PreB 697 (**A.** shNEG or **B.** shCBP) were stained with antibodies specific to human leukaemia and mouse blood cells and assessed for GFP expression. Living cells were gated based on forward and side scatter and human cells were gated based on low expression of mouse CD45 and high expression of CD19.

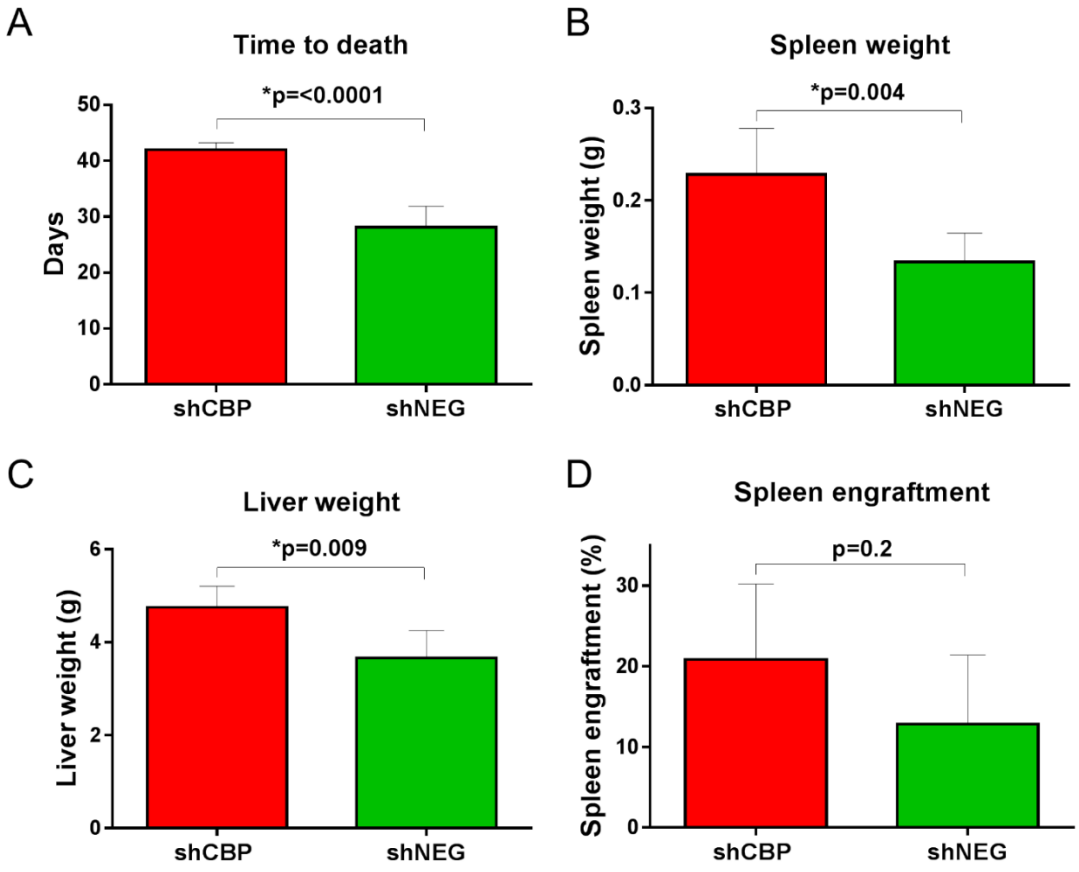

Figure 3.20. Effect of stable CREBBP knockdown in PreB 697 cells on *in vivo* growth. Immunodeficient mice were injected intrafemorally with either shCBP or shNEG and culled when signs of ill health were seen. **A.** Time to death (time from injection to culling), **B.** & **C.** spleen & liver weight and **D.** spleen engraftment. Bar charts represent mean ±SD (shCBP n=5, shNEG n=6).

3.10 Discussion

The aim of this chapter was to further characterise a BCP-ALL cell line with stable CREBBP knockdown, in order to gain understanding of how *CREBBP* haploinsufficiency contributes to relapse in childhood ALL. These studies have addressed the effects of CREBBP knockdown on gene expression, cell proliferation, drug sensitivity, oncogene/tumour suppressor activity, DNA damage repair and RAS pathway activation.

CREBBP haploinsufficiency is predicted to cause dexamethasone resistance in childhood ALL, thus explaining the associated propensity to relapse with this alteration (Mullighan *et al.*, 2011). This prediction is based on data from *CREBBP*/*EP300* double knockout MEF models engineered to express a range of *CREBBP* mutations (Mullighan *et al.*, 2011). To date, the effect of *CREBBP* haploinsufficiency on sensitivity to GC and other chemotherapeutic agents has not been assessed in an isogenic leukaemia context.

Data collected in this chapter show that CREBBP knockdown in PreB 697 cells leads to impaired expression of the GR targets; *GILZ*, *FKBP5* and *NR3C1* and IPA of GEP data in these cells predicts altered GR expression. Despite these finding, cells were no more resistant to GC than controls, suggesting that *CREBBP* haploinsufficiency may not contribute to relapse by inducing GC resistance. These data are in keeping with recent reports that patients with *CREBBP* mutations at relapse do not have a poor response to the GC, prednisone, administered during front-line treatment and that *CREBBP* mutations at relapse are not associated with intensive front line GC-containing protocols (Malinowska-Ozdowy *et al.*, 2015; Yu *et al.*, 2015). Importantly, data gathered in this chapter show that CREBBP knockdown in PreB 697 cells had no effect on sensitivity to a

panel of ALL chemotherapeutics, suggesting that CREBBP haploinsufficiency does not contribute to relapse through drug resistance. Another possibility is that important elements of biological context are being missed in the use of the PreB 697 cell line. For example, the majority of *CREBBP* mutations are found in the high hyperdiploid (HHD) and hypodiploid cytogenetic subgroups, and PreB 697 cells do not match this context (Inthal *et al.*, 2012; Holmfeldt *et al.*, 2013; Malinowska-Ozdowy *et al.*, 2015). Further to this, only a single shRNA sequence was used to knockdown CREBBP, so the data gathered may be specific to this shRNA sequence. It is also possible that the use of *in vitro* modelling of *CREBBP* haploinsufficiency ignores important microenvironmental factors that are present *in vivo*. For example, adhesion of leukaemia cells to the bone marrow stroma has been shown to contribute to chemoresistance, something which is not accounted for using *in vitro* models (Manabe *et al.*, 1992; Kumagai *et al.*, 1996; Mudry *et al.*, 2000). To overcome these limitations, studies should be carried out using additional shRNA constructs or another form of RNAi in cell lines or primary derived material with relevant cytogenetic context, or preferably *in vivo* models of *CREBBP* haploinsufficiency in ALL should be employed, where a bone marrow microenvironment is present.

CREBBP plays an important role in cAMP-dependent signalling, acting as a co-transcription factor for CREB, a transcription factor with the ability to bind ~4000 different promoter start sites, and substrate to PKA (Zhang *et al.*, 2005). Importantly there is known to be interplay between cAMP/PKA and GC-induced apoptotic response, with the GR being required for cAMP/PKA induced apoptosis in lymphoma cells (Rickles *et al.*, 2010). Data collected in this chapter identified *CXCR4* and *MKNK2* as cAMP-dependent targets in PreB 697 cells and confirmed that *RGS16* and *DUSP10*, previously identified as cAMP-

dependent in MEF cells (Mullighan *et al.*, 2011), are cAMP-dependent in PreB 697 cells. These data showed that CREBBP knockdown had no effect on the cAMP-induced expression of these genes in PreB 697 cells suggesting that remaining levels of CREBBP expression are sufficient to maintain cAMP-dependent gene expression.

CREBBP is known to play a role in many aspects of cell cycle progression and control, though whether it promotes apoptosis or cell proliferation appears to be context dependent (Kwok *et al.*, 1994; Yuan *et al.*, 1996; Goodman and Smolik, 2000; Turnell *et al.*, 2005). For example, a recent study in hepatocellular carcinoma showed that inhibiting CREBBP and its paralog EP300s, using the HAT inhibitor C646, led to reduced cell proliferation, exemplifying how CREBBP/EP300 activity can be oncogenic (Inagaki *et al.*, 2016). Further to this a recent report in lung cancer showed that CREBBP was synthetically lethal with its paralog EP300, and depletion of either, where its paralog is absent, led to apoptosis (Ogiwara *et al.*, 2015). On the contrary, CREBBP appears to act as a tumour suppressor in the context of haematopoiesis, with heterozygous loss of CREBBP in mice causing multilineage defects in haematopoietic differentiation and an increased incidence of haematological malignancies (Kung *et al.*, 2000). This shows that altered cell cycle control represents a potential mechanism by which *CREBBP* mutation could contribute to relapse in childhood ALL. Indeed, GO analysis of GEP data predicted that DNA replication and cell cycle may be altered by CREBBP knockdown in PreB 697 cells. However, previous analysis of PreB 697 cells with stable CREBBP knockdown showed no effect on the growth rate of cells and further analysis of cell proliferation based on CV treated cells from drug sensitivity experiments confirmed these previous analyses. Given that CREBBP plays a clear, but contradictory role in cell proliferation, it is possible that the use of the PreB 697

cell line model overlooks important biological context. As described previously, ALL cell have numerous interactions with bone marrow stroma and rely on these interactions for survival (Sison and Brown, 2011). For example, WNT/β-catenin signalling is involved in important in the bone marrow niche, playing a role in modulating the expression of B-cell progenitor cell cycle regulators including *E2F1*, *MYBL2* and *CDC25B* (Khan *et al.*, 2007; Malhotra and Kincade, 2009). Therefore, further study of the effects of *CREBBP* haploinsufficiency on cell cycle control in ALL may be better performed using *in vivo* models.

CREBBP mutation has been shown to impact on p53 and BCL6 acetylation impacting on their activation and inactivation respectively (Pasqualucci *et al.*, 2011). P53 is a universally expressed tumour suppressor involved in apoptotic signalling and BCL6 is an oncogene involved in transcriptional repression, which provides an environment tolerant of DNA breaks, and can inhibit p53, leading to suppression of apoptosis (Phan and Dalla-Favera, 2004; Basso and Dalla-Favera, 2012). As acetylation is vital for p53 function and BCL6 inactivity, this suggests that dysfunctional acetylation due to *CREBBP* mutation may lead to an imbalance between their activities, potentially causing resistance to apoptosis (Bereshchenko *et al.*, 2002; Tang *et al.*, 2008). In this chapter, CREBBP knockdown in PreB 697 cells showed an inconsistent effect on acetylation of p53, but importantly showed no effect on expression of an important downstream target of p53, p21 (el-Deiry *et al.*, 1994). This would suggest that CREBBP knockdown in PreB 697 cells does not impact on p53 response. Further to this, basal expression of BCL6 protein was unaffected in shCBP cells compared to shNEG and expression of *BCL6* and its targets were assessed based on GEP data showed that *BCL6* and the majority of its targets were unaffected by CREBBP

knockdown. This suggests that *CREBBP* mutation may not be sufficient to alter p53/BCL6 activity in childhood ALL.

CREBBP is known to play a role in a number of DNA damage repair processes, and abrogation of DNA damage repair through *CREBBP* mutation represents a potential mechanism for drug resistance and relapse development (Pao *et al.*, 2000; Teo *et al.*, 2001; Tini *et al.*, 2002; Hassa *et al.*, 2005; Zimmer *et al.*, 2012; Leger *et al.*, 2014). This is particularly relevant as hypermutable genotypes at relapse have been identified by whole exome sequencing in ALL (Ma *et al.*, 2015). Stable CREBBP knockdown in PreB 697 cells had no effect on expression of BER genes, PARP-1 protein expression or PARP-1 activity. CREBBP knockdown did however, led to an increased sensitivity to the alkylating agent, temozolomide. Despite this increased sensitivity to temozolomide, the expression of the direct DNA damage repair protein MGMT, responsible for the repair of damage induced by alkylating agents, was found to be normal (Tubbs *et al.*, 2007). Further to this, CREBBP knockdown was not sufficient to induce hypersensitivity to gamma radiation as is seen in *CREBBP* heterozygous mice (Zimmer *et al.*, 2012). Taken together, the data collected in this chapter do not support a role for *CREBBP* haploinsufficiency in abrogation of DNA damage repair.

CREBBP mutations frequently co-occur with RAS pathway activating mutations, including *KRAS*, *NRAS*, *PTPN11* and *FLT3* (Malinowska-Ozdowy *et al.*, 2015). PreB 697 cells harbour an *NRAS* (G12D) mutation, which leads to RAS pathway activation. Cells with CREBBP knockdown were shown to have increased expression of p-ERK, indicative of increased RAS pathway activation. This may explain the observation that time to relapse in patients with both *CREBBP* and *KRAS* mutations was shorter than in patients without or with only

one mutation (Malinowska-Ozdowy *et al.*, 2015). KRAS was shown to be directly acetylated by CREBBP (manuscript submitted), a secondary modification shown to have a negative regulatory effect on RAS activity by altering conformational stability of the Switch II domain and thus interaction with guanine nucleotide exchange factors (Yang *et al.*, 2012). This link identified between mutations *CREBBP* and enhanced oncogenic signalling is supported by a recent study in early thymocyte precursor ALL which found that inactivation of the methyltransferase, EZH2, cooperates with mutant RAS to induce hyperactive cytokine signalling, principally through STAT3, and was associated with a reduced sensitivity to JAK inhibitors.(Danis *et al.*, 2016). Despite an enhanced RAS pathway activation in CREBBP attenuated ALL cells, sensitivity to MEKi was retained, which may have important clinical implications. Our group has recently reported on the preclinical evaluation of the MEKi, selumetinib, and demonstrated significant differential sensitivity in RAS pathway-mutated ALL compared to ALL without *RAS* mutations, both *in vitro* and in an orthotopic xenograft model engrafted with primary ALL cells (Irving *et al.*, 2014) (Ryan *et al.*, 2016). Clinical trials of selumetinib for relapsed RAS pathway mutated ALL cases are underway and the data presented here suggest that patients with co-occurring *CREBBP* and RAS mutations might still be good candidates for MEKi therapy.

To overcome the limitations of using *in vitro* cell models, PreB 697 cells with stable CREBBP knockdown were injected into immunodeficient mice and their engraftment was characterised. PreB 697 shCBP and shNEG cells engrafted successfully in the spleens of mice and crucially maintained expression of GFP, suggesting that the cells maintained expression of their lentiviral constructs. Mice injected with PreB 697 cells with stable CREBBP knockdown lived longer, had bigger spleens and livers and showed a trend

towards increased spleen engraftment compared to mice injected with shNEG control cells. Data presented in this chapter show that CREBBP knockdown does not impact on cell cycle control *in vitro*, but does alter *in vivo* growth characteristics, suggesting future studies should be carried out using *in vivo* models of *CREBBP* haploinsufficiency.

CREBBP is known to be involved in the self-renewal and differentiation of HSCs, though it is not currently known whether it exerts its effects through histone remodelling functions, recruitment and/or acetylation of highly specific transcription factors or a combination of these functions (Rebel *et al.*, 2002). It is possible that *CREBBP* mutations do not work alone in the epigenetic reprogramming of cells and that other epigenetic modifiers may also be altered in *CREBBP* haploinsufficient cells. EZH2, responsible for repressive H3K27 trimethylation, is frequently mutated in DLBCL and FL and has been associated with poor prognosis in a range of cancers (Vire *et al.*, 2006; Morin *et al.*, 2011; Takawa *et al.*, 2011; Bodor *et al.*, 2013). Further to this, there is evidence to suggest that EZH2 methyltransferase activity is antagonistic to CREBBP acetyltransferase activity (Pasini *et al.*, 2010). *CREBBP* haploinsufficiency combined with an *EZH2* activating mutation, would therefore cause a shift from activating H3K27 acetylation to repressive H3K27 trimethylation leading to epigenetic reprogramming. Given the altered *in vivo* growth characteristics of PreB 697 cells with stable CREBBP knockdown, it is possible that *CREBBP* haploinsufficiency works by contributing to reprogramming the epigenetic landscape of cells to confer a cancer stem cell transcriptional profile.

In summary, these data suggest that *CREBBP* haploinsufficiency in ALL leads to increased RAS/RAF/MEK/ERK signalling in cells harbouring RAS mutation, but crucially MEKi sensitivity is retained. CREBBP attenuation in PreB 697 cells *in vitro* does not appear to contribute to drug resistance, and similarly does not impact on cell cycle control, p53/BCL6 activity or DNA damage repair. However, the *in vivo* growth characteristics of cells with CREBBP knockdown were shown to be markedly different from those *in vitro*, suggesting a potential effect on cell cycle control and a need to carry out future experiments *in vivo*.

Chapter 4 (Results 2) – CREBBP Knockdown in BCP-ALL Cell Lines and High Hyperdiploid Primagrafts

CREBBP Knockdown in BCP-ALL Cell Lines and High Hyperdiploid Primagrafts

4.1 Introduction

The effect of stable CREBBP knockdown in PreB 697 cells was extensively characterised in Chapter 3. One disadvantage of the approached used was that it was based on analysis of a single BCP-ALL cell line with a single lentiviral construct used to knock down expression of CREBBP. Another disadvantage of this model is the cytogenetic context. *CREBBP* mutations are most frequently found in relapsed HHD and hypodiploid childhood ALL, and PreB 697 cells do not represent this context (Inthal *et al.*, 2012; Holmfeldt *et al.*, 2013; Malinowska-Ozdowy *et al.*, 2015). The aim of this chapter was to validate the results described in Chapter 3, using transient CREBBP knockdown in a range of cell lines and primary derived (primagraft) samples. This would further test the hypotheses that *CREBBP* haploinsufficiency does not impact on sensitivity to ALL chemotherapeutics, and that *CREBBP* haploinsufficiency in RAS pathway mutant cells leads to increased oncogenic signalling through the RAS/RAF/MEK/ERK pathway.

4.2 Transient CREBBP Knockdown in PreB 697 Cells Using siRNA Pool Transfection

To confirm the results of CREBBP knockdown by shRNA in PreB 697 cells, transient siRNA knockdown of CREBBP was carried out. Knockdown by siRNA pool transfection was carried

out as described in section 2.7.2. As siRNA transfection is transient, knockdown was carried out before each successive downstream experiment.

4.2.1 Characterising the Effect of Transient CREBBP Knockdown in PreB 697 Cells

CREBBP knockdown was confirmed at the mRNA and/or protein level for each individual experiment. *CREBBP* mRNA expression was assessed by QRT-PCR (Section 2.4.7). As shown in PreB 697 cells with stable CREBBP knockdown, cells transfected with siRNA pool showed around 40% reduction in *CREBBP* mRNA expression (Figure 4.1). To assess the level of CREBBP protein knockdown, western blotting was carried out (Section 2.5). The reduction in CREBBP protein expression seen in transiently knocked down cells was comparable to that seen in stably knocked down cells and *CREBBP* deleted patient samples (Figure 4.2A) (Section 3.2), and was maintained for at least 96 hours (Figure 4.2B). The functional effect of CREBBP knockdown was assessed by western blotting for AcH3K18 and AcH3K27, both targets of CREBBP HAT activity (Kasper *et al.*, 2010; Henry *et al.*, 2013) (Section 2.5). CREBBP knockdown had a variable effect on AcH3K18 expression, but consistently led to reduction of AcH3K27 expression (Figure 4.3).

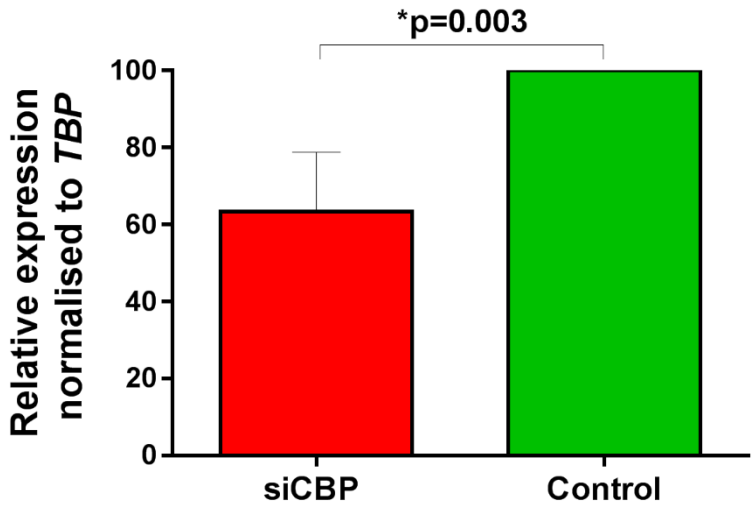

Figure. 4.1 *CREBBP* mRNA expression in PreB 697 with transient CREBBP knockdown. Cells were harvested 24 hours post-transfection and QRT-PCR was carried out for *CREBBP* expression. Expression levels were normalised to *TBP* by the $\Delta\Delta C_T$ method. Histogram represents mean ±SD of triplicate experiments.

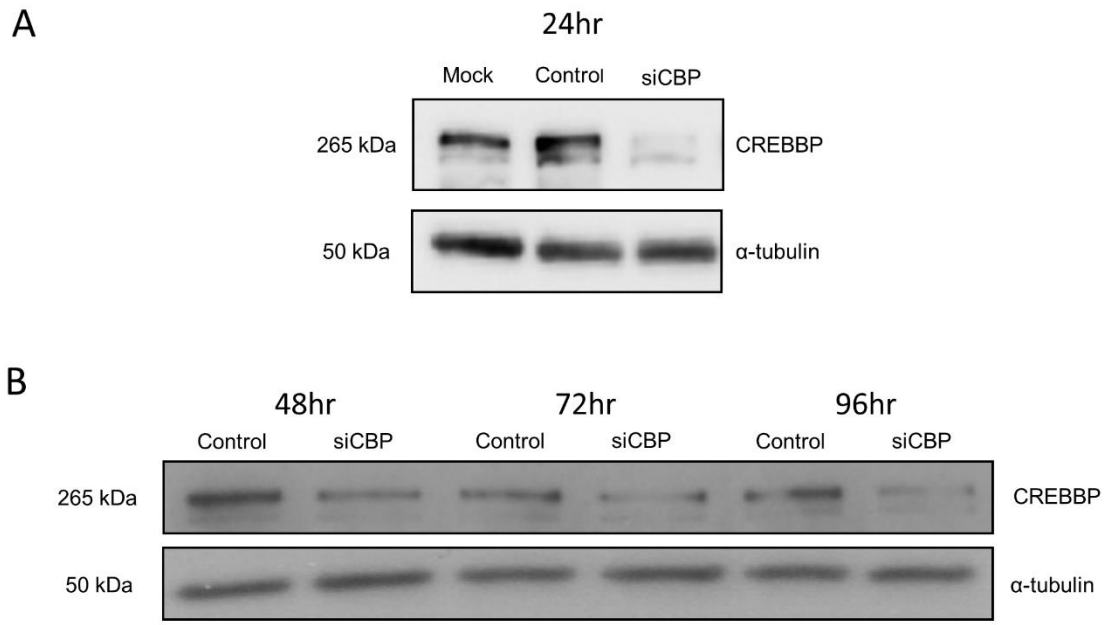

Figure 4.2 CREBBP protein expression in PreB 697 with transient CREBBP knockdown. A. PreB 697 cells were transfected with an siRNA pool targeting *CREBBP* (siCBP), control siRNA, or electroporated in absence of siRNA (Mock), and incubated for 24 hours before whole cell lysates were extracted and western blotting was carried out for CREBBP. Blot shown is representative of CREBBP knockdown following each siRNA transfection. **B.** CREBBP protein expression in whole cell lysates extracted from cells transfected with siCBP or control after 48, 72 and 96 hour incubation. Alpha tubulin was included as loading control.

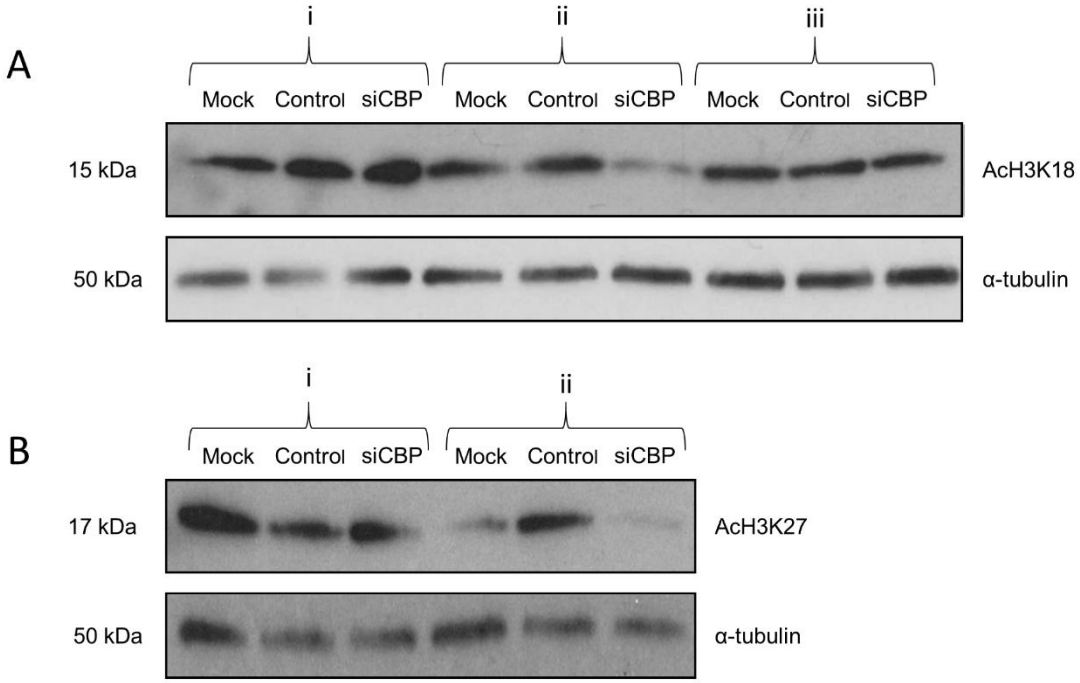

Figure 4.3 Expression of AcH3K18 and AcH3K27 in PreB 697 with transient CREBBP knockdown. PreB 697 cells were transfected with an siRNA pool targeting *CREBBP* (siCBP), control siRNA, or electroporated in absence of siRNA (Mock) on separate occasions, and incubated for 48 hours before whole cell lysates were extracted and western blotting was carried out for AcH3K18 (**A**, i-iii) or AcH3K27 (**B**, i-ii). Alpha tubulin was included as loading control.

4.2.2 cAMP response in PreB 697 Cells with Transient CREBBP Knockdown

In Chapter 3, stable CREBBP knockdown in PreB 697 cells showed no impact on cAMP-induced expression of cAMP-dependent genes (Section 3.3). To validate these results, PreB 697 cells transfected with an siRNA pool targeting *CREBBP* (siCBP) or control siRNA (control) were assessed for cAMP-dependent gene expression. Cells were treated with IBMX and forskolin to induce a maximal intracellular cAMP response, or CV and QRT-PCR was carried out using probes for the cAMP-dependent targets identified in Chapter 3 (Sections 2.4.7 and 3.3). *CXCR4* and *RGS16* were significantly induced by cAMP in both siCBP and control cells, with around 11 fold increase in *CXCR4* and 3 fold increase in *RGS16* being observed (p values <0.03 for *CXCR4* and <0.06 for *RGS16*). Whilst a trend towards increased *MKNK2* and *DUSP10* expression was seen following cAMP stimulation for siCBP and control cells, this was not statistically significant (p values >0.1 for both genes). CREBBP knockdown had no impact on the level of cAMP-stimulated expression for any gene (p values >0.4) or on unstimulated gene expression compared to control cells (p values > 0.6) (Figure 4.4).

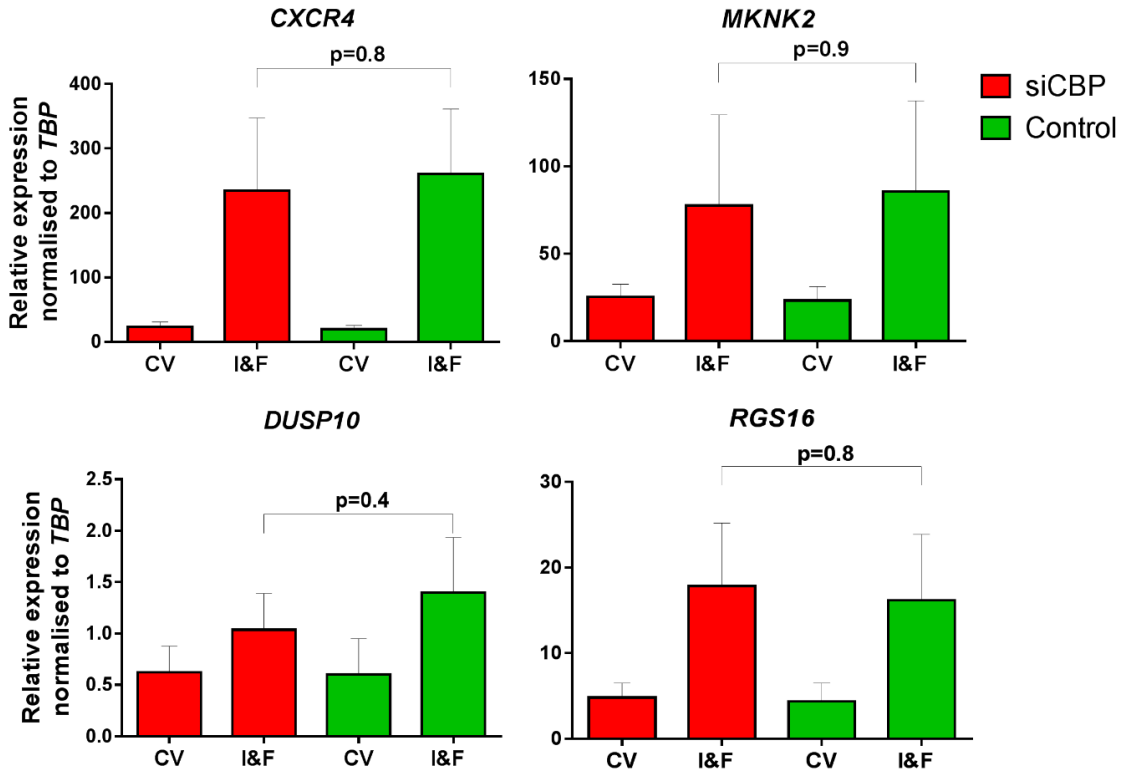

Figure 4.4. Effect of transient CREBBP knockdown in PreB 697 cells on cAMP-dependent gene expression. PreB 697 siCBP and control cells were treated with either control vehicle (CV) or IBMX and forskolin (I&F) before determining expression of cAMP-dependent genes by QRT-PCR relative to endogenous *TBP* expression by the $\Delta\Delta C_T$ method. Histograms show mean ±SD (n=3).

4.2.3 Induction of GR Transcriptional Targets in PreB 697 Cells with Transient CREBBP Knockdown

In Chapter 3, stable CREBBP knockdown in PreB 697 cells was shown to cause impaired GC-induced expression of GR targets (Section 3.2). To validate these results, PreB 697 siCBP and control cells were treated with dexamethasone for 24 hours to induce GR target expression, or CV and QRT-PCR was carried out to assess the expression of GR targets; *GILZ*, *FKBP5*, *NR3C1* and *ITGA9* (Section 2.4.7).

Unlike PreB 697 cells with stable CREBBP knockdown, *GILZ* and *FKBP5* were only significantly induced by GC exposure in siCBP cells (*GILZ* ~40 fold increase p=0.04, *FKBP5* ~6 fold increase p=0.02) with control cells showing a clear trend towards GC-induced GR targets expression that failed to reach significance (*GILZ* ~17 fold increase p=0.09, *FKBP5* ~4 fold increase p=0.06). *NR3C1* was found to be significantly induced in both siCBP and control cells, as shown in PreB 697 cells with stable CREBBP knockdown (~2 fold increase, p values <0.002). Despite a trend towards increased expression, *ITGA9* was not significantly induced by GC exposure in either siCBP or control cells (p values >0.08). Transient CREBBP knockdown led to a statistically significant reduction of basal *GILZ* and *NR3C1* expression (p=0.02 and p=0.01 respectively) but had no such effect on *FKBP5* and *ITGA9* (p=0.5 and p=0.3 respectively). CREBBP knockdown did not significantly impair the expression of genes which were shown to be significantly induced by GC in both siCBP and control transfected cells (*GILZ* p=0.6, *FKBP5* p=0.6). GC induced *NR3C1* expression was shown to be higher in siCBP cells compared to control (p=0.01), differing significantly from PreB 697 cells with stable CREBBP knockdown in which GC induced *NR3C1* expression was

significantly impaired (Section 3.2). Taken together these data suggest that transient CREBBP knockdown in PreB 697 cells does not impair transcription of GR targets.

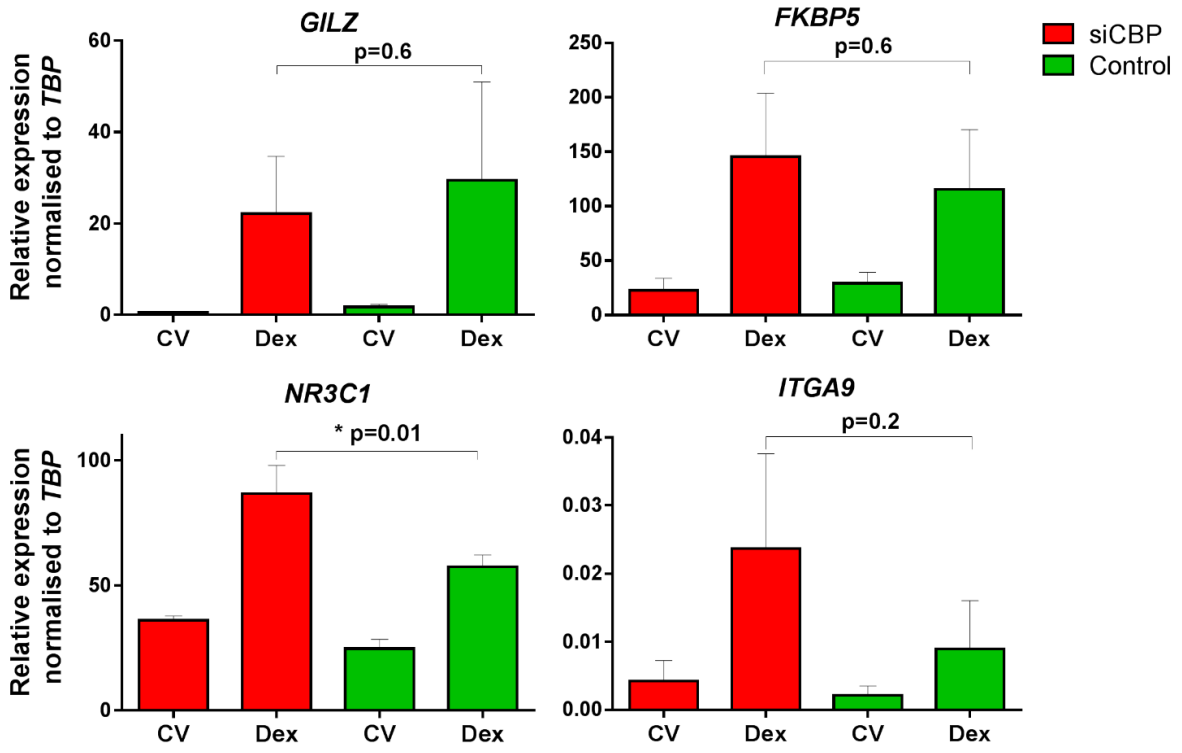

Figure 4.5. Effect of transient CREBBP knockdown in PreB 697 cells on GR target gene expression. PreB 697 siCBP and control cells were treated with either control vehicle (CV) or dexamethasone (Dex) for 24 hours before determining expression of GR target genes by QRT-PCR relative to endogenous *TBP* expression by the $\Delta\Delta C_T$ method. Histograms show mean ±SD (n=3).

4.2.4 Dexamethasone Sensitivity of PreB 697 Cells with Transient CREBBP Knockdown

Previously obtained data (MRes project) showed that stable knockdown of CREBBP in PreB 697 cells had no effect on sensitivity to dexamethasone (Section 3.2). To further validate this observation, siCBP and control cells were assessed for sensitivity to dexamethasone using alamar blue drug sensitivity assays (Section 2.6.2). Cells with transient CREBBP knockdown were no more resistant to dexamethasone than controls, but showed a small, statistically significant increase in sensitivity to dexamethasone (GI_{50} values, mean ±SD; siCBP 17nM ±1.6, control 34.7nM±2.7; p=0.0006) (Figure 4.6). Given the actual difference in GI_{50} values, this difference is likely too small to be biologically relevant.

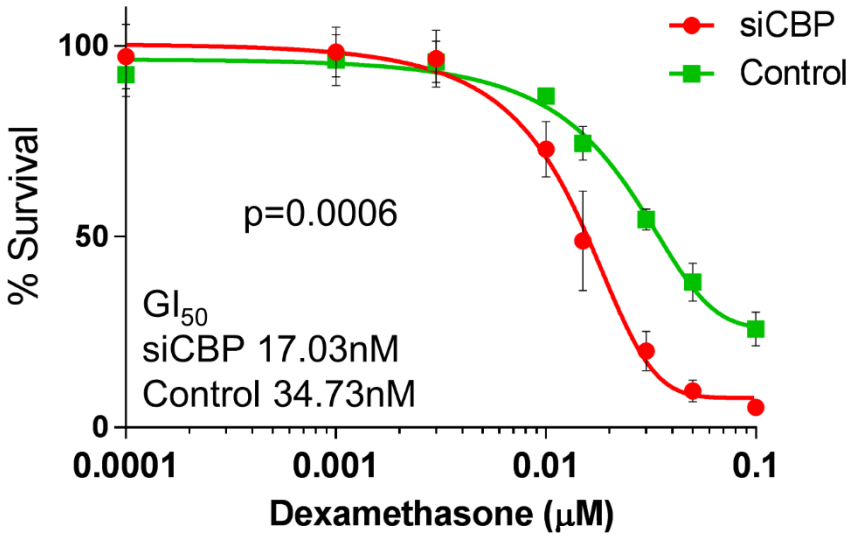

Figure 4.6 Dexamethasone sensitivity of PreB 697 cells with transient CREBBP knockdown. PreB 697 siCBP and control cells were treated with a range of dexamethasone concentrations or CV, 24 hours post-transfection and incubated for 96 hours. Alamar blue was used to determine cell survival as a % of CV treated cells. Values plotted represent the mean % survival ±SD (n=3).

4.2.5 Cell Proliferation in PreB 697 Cells with Transient CREBBP Knockdown

In Chapter 3, PreB 697 cells with stable CREBBP knockdown were shown to proliferate at the same rate as controls (Sections 3.2 and 3.5). To validate these data, PreB 697 cells with transient CREBBP knockdown were assessed for survival 96 hours post-transfection as described previously (Section 3.5). Fluorescent output readings from cells treated with CV only from dexamethasone sensitivity experiments were compared (Section 4.2.4). The average fluorescence output for PreB 697 siCBP cells compared to control was not significantly different (Mean fluorescent output ±SD; siCBP $1.22x10^5$ $\pm1.4x10^4$, control $1.21x10^5$ $\pm1.05x10^4$; p=0.8), suggesting that CREBBP knockdown did not influence cell proliferation over 96 hours (Figure 4.7).

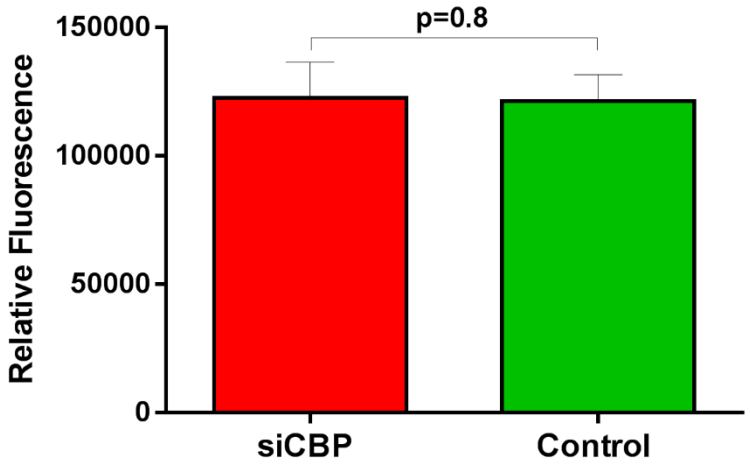

Figure 4.7. Transient CREBBP knockdown in PreB 697 cells and survival at 96 hours. The raw fluorescence output values from control treated cells used in dexamethasone sensitivity experiments were combined and compared. Graph shows average relative fluorescence ±SD (n=3).

4.2.6 Temozolomide Sensitivity of PreB 697 Cells with Transient CREBBP Knockdown

Stable knockdown of CREBBP in PreB 697 cells led to a significant increase in sensitivity to temozolomide, suggesting *CREBBP* mutation may impair direct DNA damage repair by MGMT (Section 3.8.3). Further study of these cells showed that MGMT was unaffected by stable CREBBP knockdown (Section 3.8.4). To explore these findings further, PreB 697 cells with transient CREBBP knockdown were assessed for sensitivity to temozolomide (Section 2.6.2). This showed that PreB 697 siCBP cells were not differentially sensitive to temozolomide compared to controls (GI_{50} values, mean ±SD; siCBP 225µM ±19.5, control 229µM ±14.8; p=0.8) (Figure 4.8). This would suggest that, contrary to results shown in stably knocked down cells, transient CREBBP knockdown does not lead to increased sensitivity to temozolomide. This may also explain the lack of MGMT deficiency seen in PreB 697 cells with stable CREBBP knockdown.

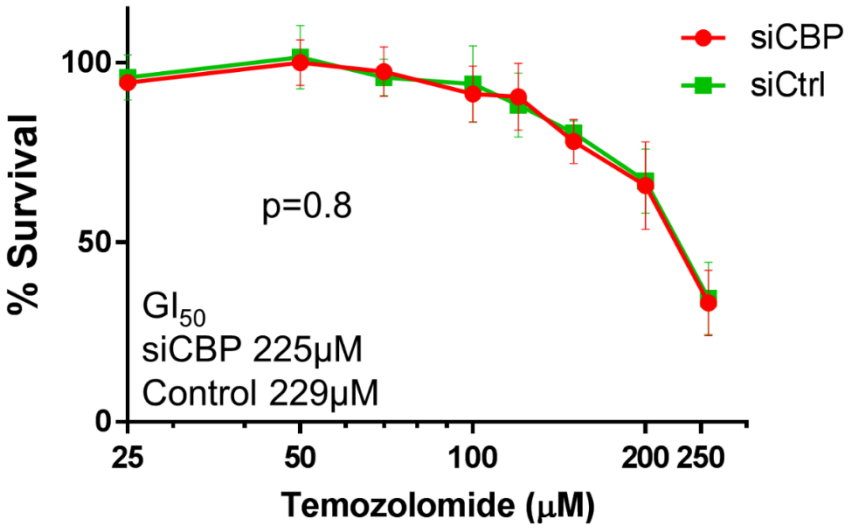

Figure 4.8. Effect of transient CREBBP knockdown in PreB 697 cells on sensitivity to temozolomide. Cells were treated with a range of temozolomide concentrations or CV, 24 hours post-transfection and incubated for 96 hours. Alamar blue was used to determine cell survival as a % of CV treated cells. Values plotted represent the mean % survival ±SD (n=3).

4.3 Transient CREBBP Knockdown in Hypodiploid MHH-CALL-2 Cells

Given that all observations on the effect of *CREBBP* haploinsufficiency had been made in the PreB 697 cell line, comparison with another cell line was sought. The MHH-CALL-2 cell line is a *CREBBP* wild type, BCP-ALL cell line and is near-haploid by cytogenetics (Aburawi *et al.*, 2011) (COSMIC database). This is of particular relevance as *CREBBP* mutations are enriched in this cytogenetic subgroup (Holmfeldt *et al.*, 2013).

4.3.1 Characterising the Effect of Transient CREBBP Knockdown in MHH-CALL-2 Cells

MHH-CALL-2 cells were transfected with an siRNA pool targeting *CREBBP* (Section 2.7.2). Again, given the transient nature of this procedure, knockdown was carried out before each individual experiment. CREBBP knockdown was confirmed at the mRNA and/or protein level. CREBBP knockdown by siRNA pool transfection in MHH-CALL-2 cells led to ~50% *CREBBP* mRNA reduction compared to control ($p=0.001$), similar to that achieved in PreB 697 cells with stable and transient knockdown (Sections 3.2 and 4.2.1) (Figure 4.9 A). CREBBP protein knockdown in MHH-CALL-2 cells was consistent with that shown in PreB 697 cells with stable and transient CREBBP knockdown, as well as patient derived material with mono-allelic *CREBBP* deletions (Sections 3.2 and 4.2.1) (Figure 4.9 B).

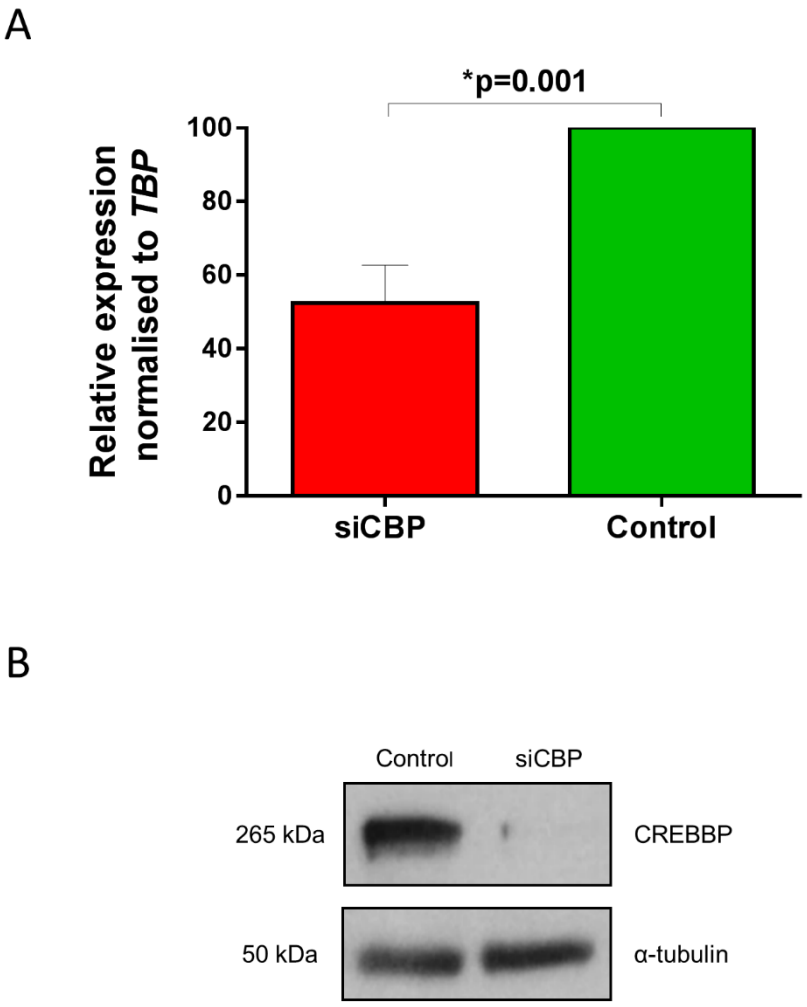

Figure 4.9. CREBBP mRNA and protein expression in MHH-CALL-2 cells with transient CREBBP knockdown. A. MHH-CALL-2 cells transfected with an siRNA pool targeting *CREBBP* (siCBP) and control cells were harvested 24 hours post-transfection and QRT-PCR was carried out for *CREBBP* expression. Expression levels were normalised to *TBP* by the $\Delta\Delta C_T$ method. Histogram represents mean ±SD of triplicate experiments. **B.** Whole cell lysates from MHH-CALL-2 siCBP or control cells were extracted 24 hours post-transfection and western blotting was carried out for CREBBP. Blot shown is representative of CREBBP protein expression following each siRNA transfection. Alpha tubulin was included as loading control.

The functional effect of CREBBP knockdown was assessed by western blotting for AcH3K18 and AcH3K27 (Section 2.5). Transient CREBBP knockdown in MHH-CALL-2 cells gave a consistent reduction of AcH3K18 and AcH3K27 levels, showing a clear functional impact of the knockdown (Figure 4.10). Cell growth was again analysed based on cell survival in CV treated cells from dexamethasone sensitivity experiments (Section 4.3.4). A trend towards reduced cell survival in MHH-CALL-2 siCBP cells compared to control was observed which was close to statistical significance (Mean fluorescent output ±SD; siCBP $2.7x10^4$ $\pm 8.94x10^3$, control $2.2x10^4$ $\pm 6.09x10^3$; p=0.06) (Figure 4.11), suggesting that CREBBP knockdown may influence cell proliferation in MHH-CALL-2 cells.

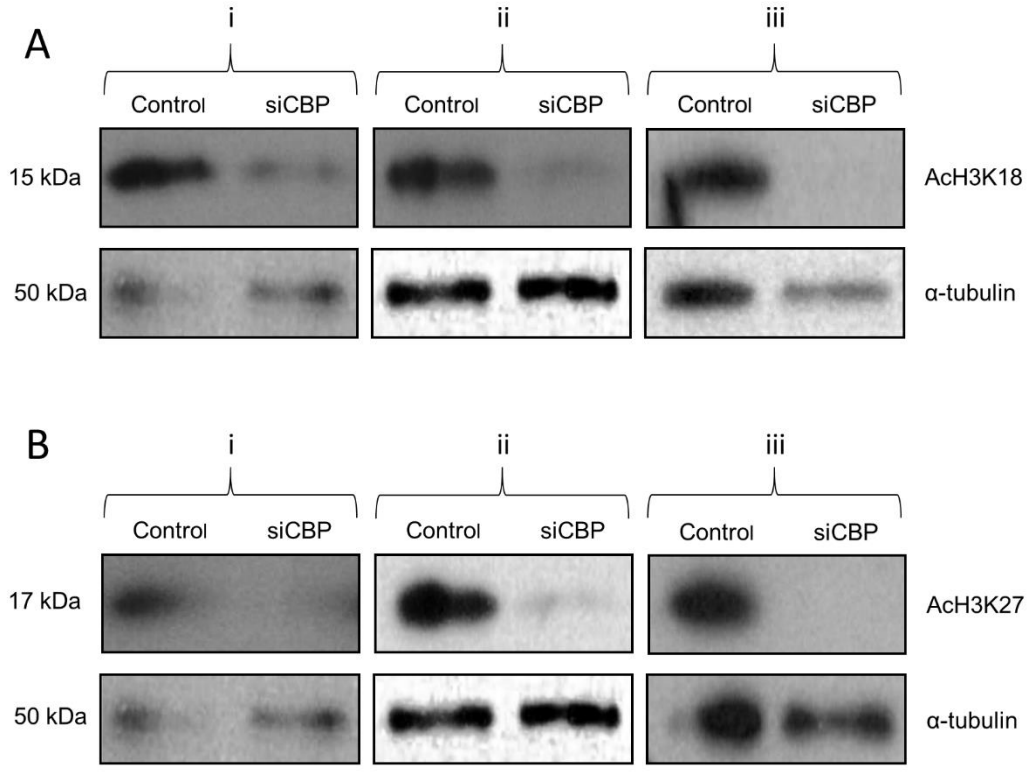

Figure 4.10. Expression of AcH3K18 and AcH3K27 in MHH-CALL-2 cells with transient CREBBP knockdown. MHH-CALL-2 cells were transfected with an siRNA pool targeting *CREBBP* (siCBP) or control on separate occasions and incubated for 48 hours before whole cell lysates were extracted and western blotting was carried out for AcH3K18 (**A**, i-iii) or AcH3K27 (**B**, i-iii). Alpha tubulin was included as loading control.

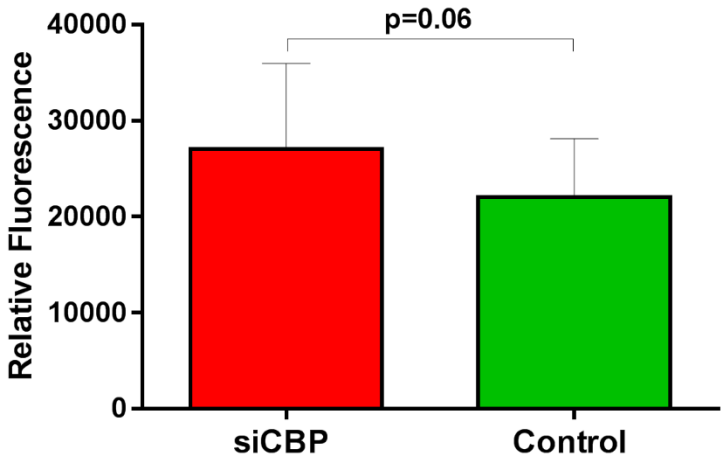

Figure 4.11. Transient CREBBP knockdown in MHH-CALL-2 cells and survival at 96 hours. The raw fluorescence output values from CV treated cells from MHH-CALL-2 siCBP dexamethasone sensitivity experiments were combined and compared. Histogram shows average relative fluorescence ±SD (n=3).

4.3.2 cAMP response in MHH-CALL-2 Cells with Transient CREBBP Knockdown

Both stable and transient knockdown of CREBBP in PreB 697 cells had no effect on cAMP-induced gene expression (Sections 3.3 and 4.2.3). To validate these data, induction of cAMP-dependent genes in response to cAMP stimulation was assessed in MHH-CALL-2 cells with transient CREBBP knockdown. Cells were treated with IBMX and forskolin to induce a maximal intracellular cAMP response or CV and QRT-PCR was carried out using probes specific to cAMP-dependent genes identified in PreB 697 cells in Chapter 3 (Sections 2.4.7 and 3.3). *CXCR4*, and *DUSP10* were significantly upregulated in both siCBP and control cells following cAMP stimulation (*CXCR4* ~4 fold upregulated; p values <0.01, *DUSP10* ~2 fold upregulated; p values <0.01). *RGS16* was shown to be significantly upregulated by cAMP in siCBP cells only, despite a trend towards cAMP induction being shown in control cells (siCBP; ~6 fold upregulation p=0.02, control; ~6 fold upregulation p=0.08). *MKNK2* was not significantly upregulated by cAMP in siCBP or control cells (p values >0.05) and basal expression of all genes was unaffected by CREBBP knockdown (p values >0.08). As shown in PreB 697 cells with both stable and transient CREBBP knockdown, transient CREBBP knockdown in MHH-CALL-2 cells had no effect on the level of cAMP-induced expression achieved for any cAMP-dependent gene assessed (p values >0.2) (Figure 4.12).

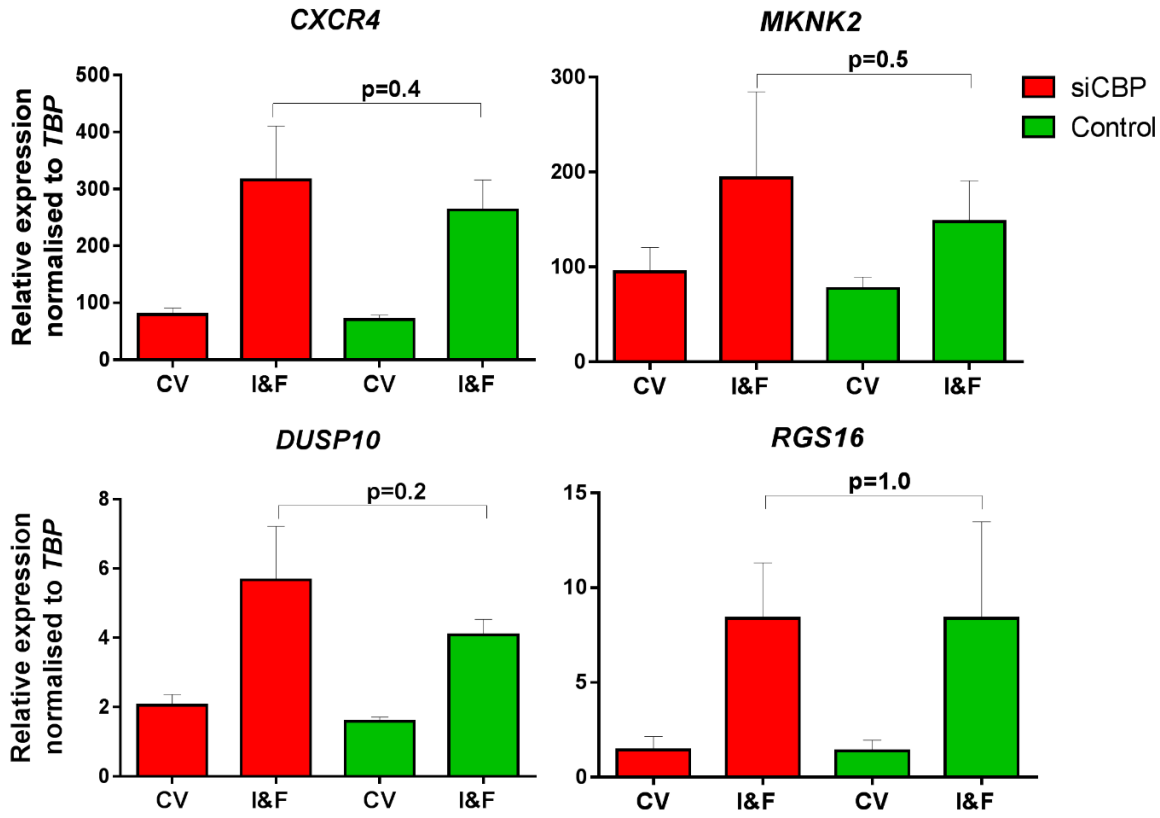

Figure 4.12. Effect of transient CREBBP knockdown in MHH-CALL-2 cells on cAMP-dependent gene expression. MHH-CALL-2 siCBP and control cells were treated with either control vehicle (CV) or IBMX and forskolin (I&F), before determining expression of cAMP-dependent genes by QRT-PCR relative to endogenous *TBP* expression by the $\Delta\Delta C_T$ method. Histograms show mean ±SD (n=3).

4.3.3 Induction of GR Transcriptional Targets in MHH-CALL-2 Cells with Transient CREBBP Knockdown

Knockdown of CREBBP in PreB 697 cells gave conflicting results on the induction of GR transcriptional targets, with stably knocked down cells showing impaired GC-induced expression of GR targets (Section 3.2), and transiently knocked down cells showing no such impairment (Section 4.2.3). To further study this effect, MHH-CALL-2 cells with transient CREBBP knockdown were assessed for GC-induced GR target expression (Section 2.4.7). Both *GILZ* and *FKBP5* showed significant induction in response to GC, in siCBP and control cells, unlike in PreB 697 siCBP cells (*GILZ*; ~50 fold increase, p values <0.02, *FKBP5*; ~10 fold increase, p values <0.02) (Section 4.2.3). *NR3C1* was only significantly induced by GC in MHH-CALL-2 control cells, but a trend towards induction was seen in siCBP cells (Control ~3 fold increase, p=0.04, siCBP ~2 fold increase, p=0.1). Unlike in PreB 697 cells, *ITGA9* was significantly induced by GC in both control and siCBP MHH-CALL-2 cells (~6 fold increase, p values <0.02). CREBBP knockdown had no significant effect on the basal expression of any gene assessed (p values >0.3). As in PreB 697 cells with transient CREBBP knockdown, the level of dexamethasone induced *GILZ* or *FKBP5* expression achieved was unaffected by CREBBP knockdown in MHH-CALL-2 cells (*GILZ*; p=0.9, *FKBP5*; p=0.7, *NR3C1*; p=0.9, *ITGA9*; p=1.0) (Figure 4.13).

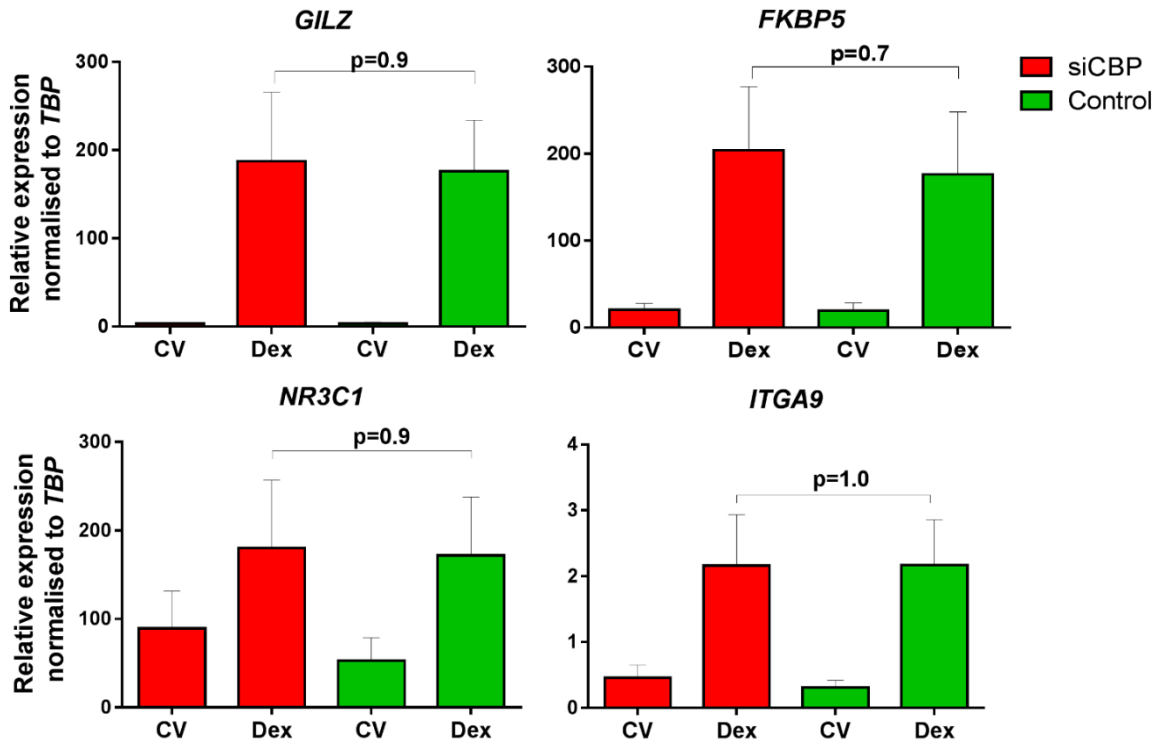

Figure 4.13. Effect of transient CREBBP knockdown in MHH-CALL-2 cells on GR target gene expression. MHH-CALL-2 siCBP and control cells were treated with either control vehicle (CV) or dexamethasone (Dex) for 24 hours before determining expression of GR target genes by QRT-PCR, relative to endogenous *TBP* expression, by the $\Delta\Delta C_T$ method. Histograms show mean ±SD (n=3).

4.3.4 Dexamethasone Sensitivity of MHH-CALL-2 Cells with Transient CREBBP Knockdown

Both stable and transient knockdown of CREBBP in PreB 697 cells did not lead to dexamethasone resistance (Sections 3.2 and 4.2.4). To further address this hypothesis, MHH-CALL-2 cells with transient CREBBP knockdown were assessed for sensitivity to dexamethasone (Section 2.6.2). CREBBP knockdown in these cells did not lead to dexamethasone resistance (GI_{50} values, mean ±SD; siCBP 2.8nM ±0.59, control 3.8nM ±SD 0.7; p=0.1), and no increase in dexamethasone sensitivity, as was seen in PreB 697 cells with transient CREBBP knockdown, was observed (Figure 4.14).

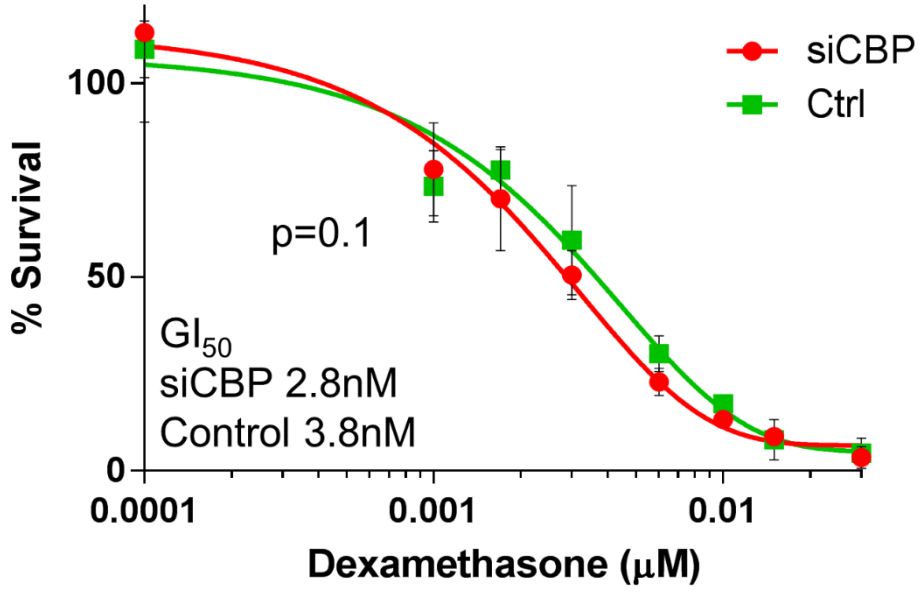

Figure 4.14. Dexamethasone sensitivity of MHH-CALL-2 cells with transient CREBBP knockdown. Cells were treated with a range of dexamethasone concentrations or CV, 24 hours post-transfection and incubated for 96 hours. Alamar blue was used to determine cell survival as a % of CV treated cells. Values plotted represent the mean % survival ±SD (n=3).

4.4 CREBBP Knockdown in Primagraft Cells

Cells lines are useful biological models of disease, they provide an unlimited supply of material, divide in culture (unlike primary leukaemia samples) and give a pure population of cells allowing reproducible results to be obtained (Kaur and Dufour, 2012). Cell lines are not perfect models however, they are genetically modified so their phenotype, native functions and response to stimuli may differ from that of primary samples in ways that are difficult to determine (Kaur and Dufour, 2012). In order to strengthen key findings in cell lines, it is important to carry out experiments using primary cells. To this end, a method for transient CREBBP knockdown was optimised and carried out in primagraft cells, primary patient cells implanted into mice to amplify their numbers. Three HHD primagraft samples were used for these experiments; L779, L829 relapse (L829R) and L914, all of which harboured RAS pathway mutations (Section 2.2.7).

HHD primagrafts were formed by intrafemoral injection into immunodeficient mice as described in section 2.2.7. Briefly, NSG mice were anaesthetised and $1x10^6$ patient cells were injected intrafemorally. Leukaemic engraftment was monitored in the peripheral blood using flow cytometry (Section 2.3.2). Mice were culled when peripheral blood leukaemia engraftment reached >30% and only spleens with leukaemia engraftment of >80% were used. Figure 4.15 shows a representative example of peripheral blood engraftment by flow cytometry, describing a peripheral blood engraftment of 88.6% for L914 cells 11 weeks after intrafemoral injection. Figure 4.16 shows the spleen engraftment of the same sample at the same time point (96.4% spleen engraftment).

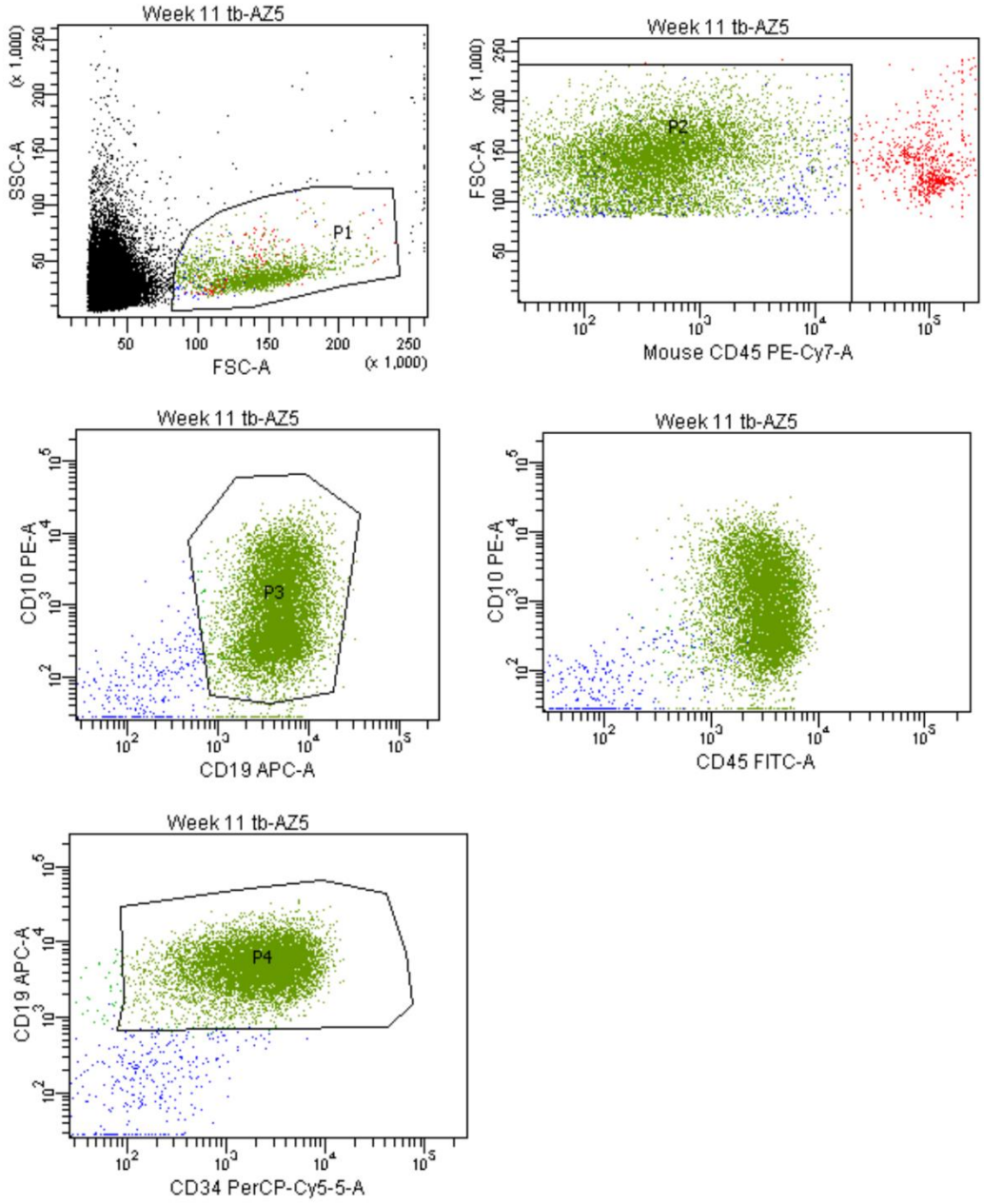

Figure 4.15. Monitoring peripheral blood leukaemia engraftment by flow cytometry. Peripheral blood taken from mice engrafted with leukaemia was stained with a panel of antibodies specific to human leukaemia and mouse blood cells. Living cells were gated based on forward and side scatter and human cells were gated based on low expression of mouse CD45.

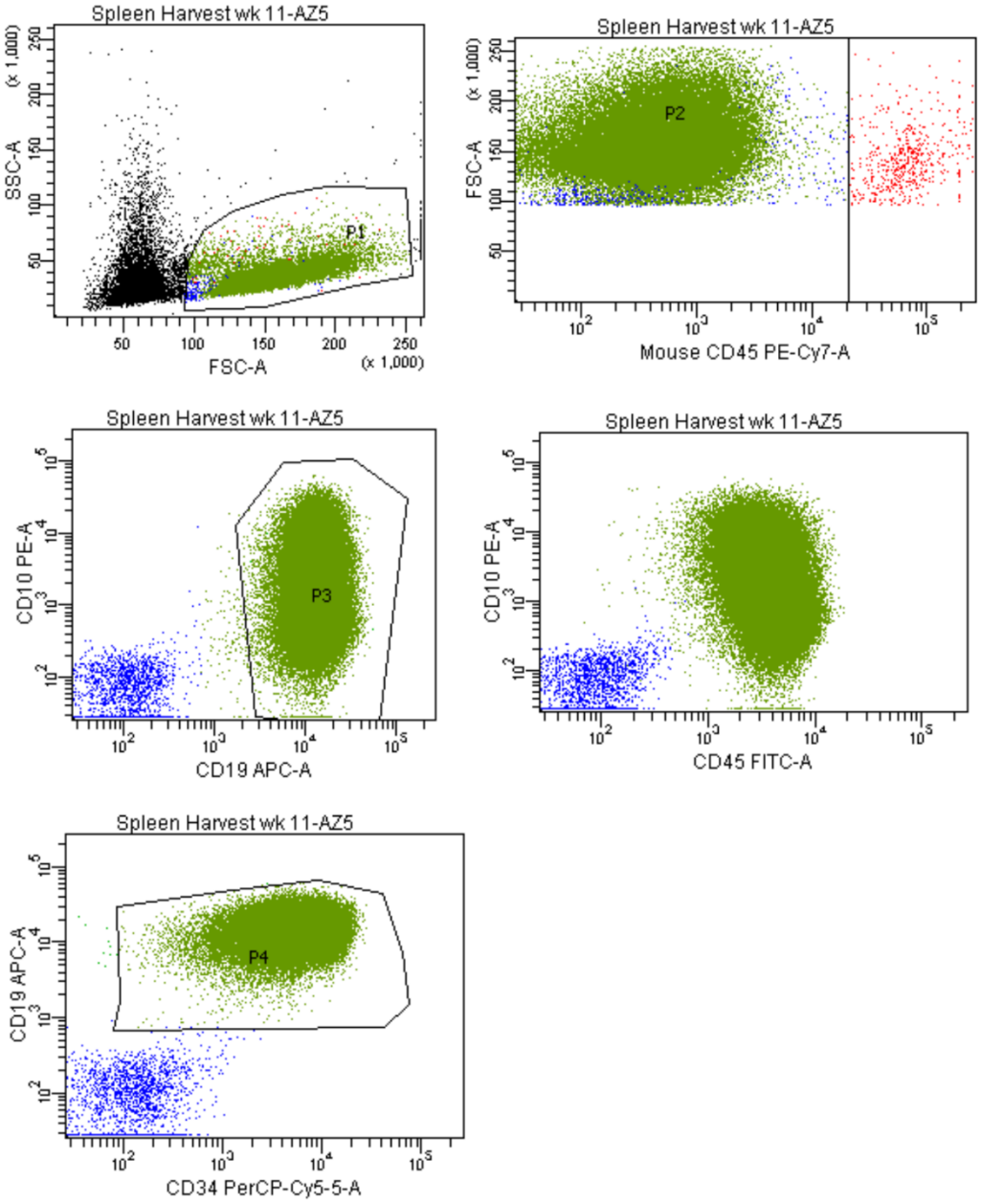

Figure 4.16. Assessment of leukaemia engraftment in mouse spleen by flow cytometry. Spleen cells were resuspended in growth media and stained with a panel of antibodies specific to human leukaemia and mouse blood cells. Living cells were gated based on forward and side scatter and human cells were gated based on low expression of mouse CD45.

4.4.1 Optimisation of an Electroporation Method for siRNA Delivery in Primagraft Cells

The transfection of primary cells with siRNA is known to be challenging. Electroporation is a highly effective method of siRNA delivery in suspension cell lines and has been shown to be effective in primary cells, though conditions differ between cell types and optimisation is required (Jordan *et al.*, 2008). To determine the effective concentration of CREBBP siRNA pool required to transduce primagraft cells, a dose titration was carried out. Cells were subjected to the same electroporation parameters as PreB 697 cells with between 250 and 750nM of siCBP pool, control siRNA or in the absence of siRNA (Section 2.7.2). Twenty four and forty eight hours post-transfection, western blotting was carried out to determine CREBBP protein expression (Section 2.5). A reduction in CREBBP protein expression was seen for all siRNA concentrations used at both 24 and 48 hours, with a greater degree of protein knockdown seen at 24 hours (Figure 4.17). For this reason, electroporation parameters used on cell lines and an siRNA concentration of 250nM was selected as optimal for knockdown of primagraft cells (Section 2.7.2). Twenty four hours was chosen as the optimal time point at which to assess protein knockdown in siRNA transfected primagraft cells.

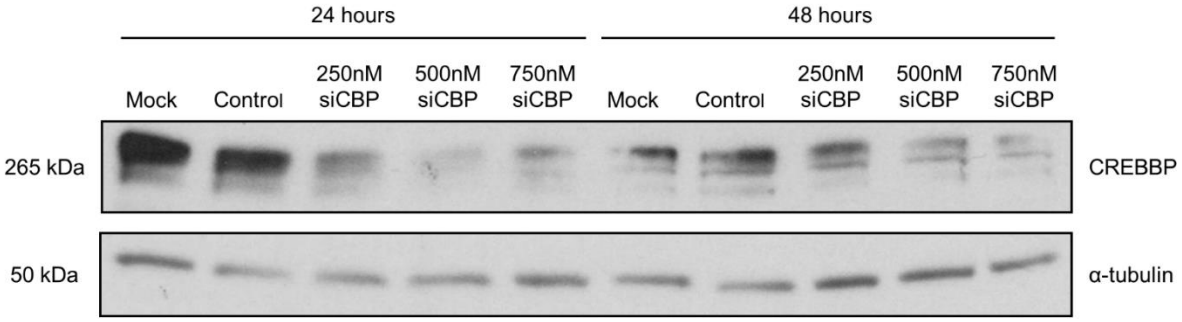

Figure 4.17. Optimisation of siRNA delivery by electroporation in primagraft cells. Primagraft cells were transfected with an siRNA pool targeting *CREBBP*, control siRNA or electroporated in the absence of siRNA (Mock) and incubated for 24 and 48 hours before whole cell lysates were extracted and western blotting was carried out for CREBBP. Alpha tubulin was included as loading control.

4.4.2 Characterising the Effect of Transient CREBBP Knockdown in Primagraft Samples

CREBBP mRNA and/or protein expression was assessed following each siRNA transfection to ensure CREBBP levels had been successfully reduced. To determine *CREBBP* mRNA expression, QRT-PCR was carried out probing for *CREBBP* (Section 2.4.7). Around 50% reduction of *CREBBP* mRNA expression was achieved in siCBP transfected primagraft cells, which is consistent with that shown in cell lines (Sections 3.2, 4.2.1 and 4.3.1) (Figure 4.18 A). Western blotting was used to determine CREBBP protein expression (Section 2.5). CREBBP knockdown by siRNA pool transfection in all primagraft samples led to a significant reduction in CREBBP protein expression that was in line with that seen in cell line models and in patient derived material with mono-allelic *CREBBP* deletion (Sections 3.2, 4.2.1 and 4.3.1) (Figure 4.18 B).

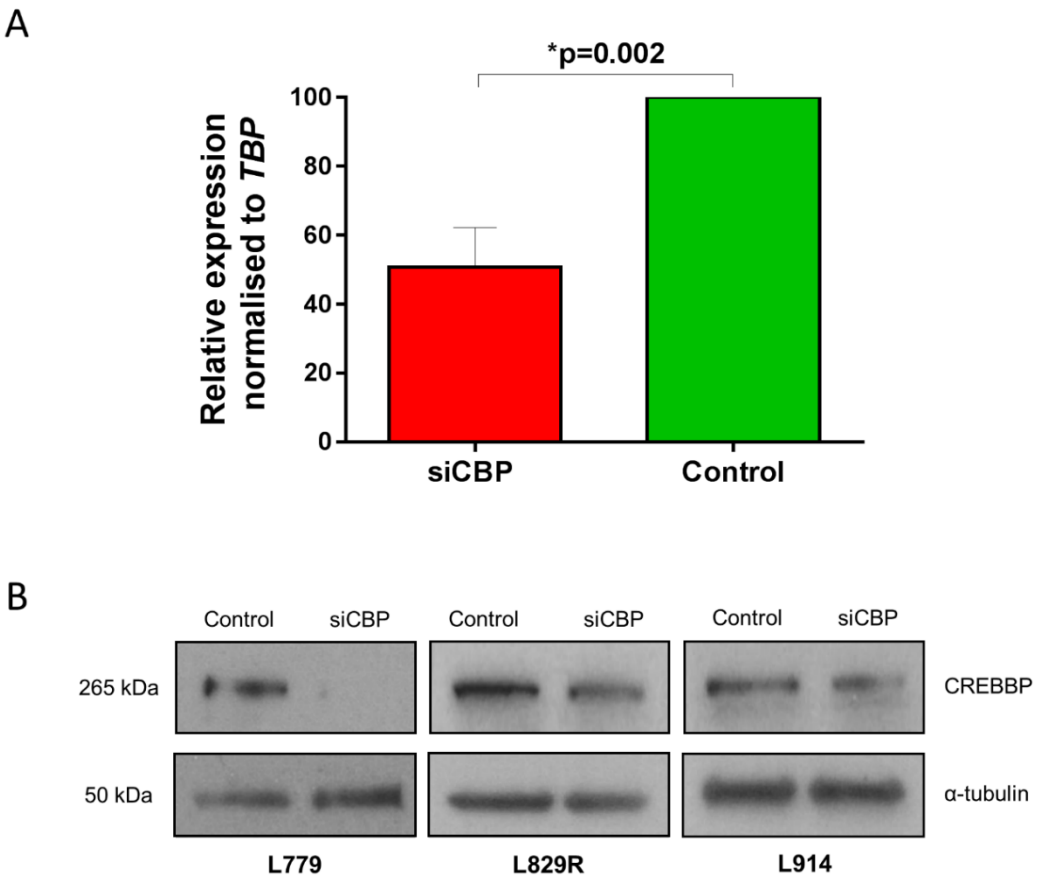

Figure 4.18 CREBBP mRNA and protein expression in primagraft cells with transient CREBBP knockdown. A. Cells transfected with an siRNA pool targeting *CREBBP* (siCBP) or control were harvested 24 hours post-transfection and QRT-PCR was carried out for *CREBBP* expression. Expression levels were normalised to *TBP* by the $\Delta\Delta C_T$ method. Histogram represents mean ±SD of triplicate experiments. **B.** Whole cell lysates from primagraft siCBP or control cells were extracted and western blotting was carried out for CREBBP. Blots shown are representative, α-tubulin was included as loading control.

To assess the functional impact of CREBBP knockdown, AcH3K18 expression was determined in each transfected primagraft sample by western blotting (Section 2.5). Knockdown of CREBBP led to reduced AcH3K18 expression in 2 of 3 primagraft samples (Figure 4.19). Cell survival was analysed, as described in section 3.5, based on fluorescence output readings from control treated cells in dexamethasone sensitivity alamar blue experiments (Section 4.4.5). As primagraft cells do not divide in culture, this assay was only able to assess the effect of CREBBP knockdown on the ability of cell to survive in culture. CREBBP knockdown in all primagraft cells had no effect on cell survival at 96 hours (Mean fluorescent output ±SD; siCBP $8.78x10^4$ $\pm3.73x10^4$, Control $7.43x10^4$ $\pm2.71x10^4$; p=0.3) (Figure 4.20).

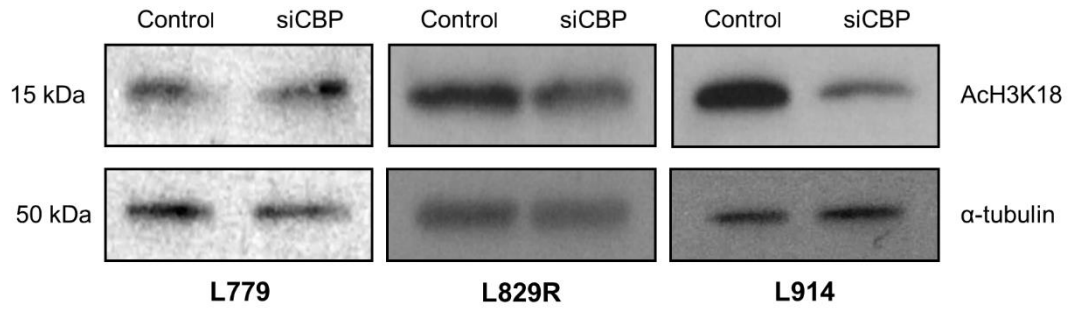

Figure 4.19. Expression of AcH3K18 in primagraft cells with transient CREBBP knockdown. Primagraft cells were transfected with an siRNA pool targeting *CREBBP* or control siRNA and incubated for 24 hours before whole cell lysates were extracted and western blotting was carried out for AcH3K18. Alpha tubulin was included as loading control.

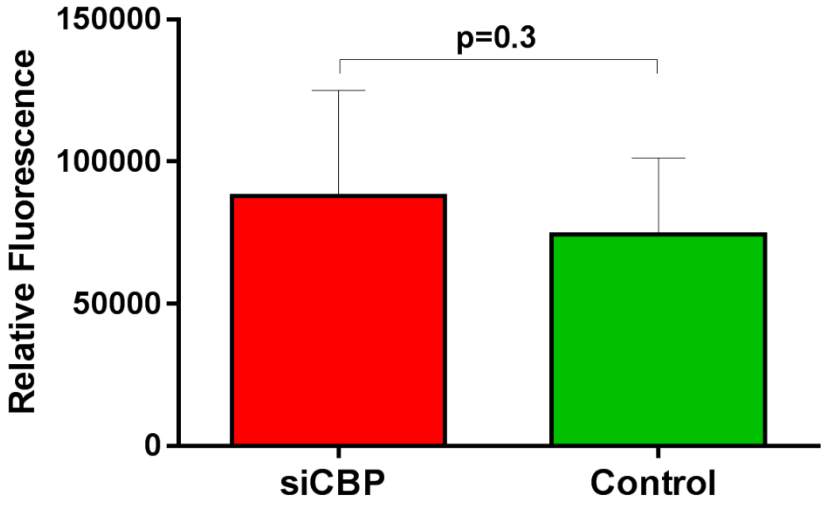

Figure 4.20. Transient CREBBP knockdown in HHD primagraft cells and survival at 96 hours. The raw fluorescence output values from CV treated cells from primagraft dexamethasone sensitivity experiments were combined and compared. Histogram shows average relative fluorescence ±SD (n=5).

4.4.3 cAMP response in HHD Primagraft Cells with Transient CREBBP Knockdown

CREBBP knockdown in cell lines was shown to have no effect on the expression of cAMP-dependent target genes (Sections 3.3, 4.2.2 and 4.3.2). HHD primagrafts were used to study this effect in a relevant cytogenetic context.

Transfected primagraft samples were treated with IBMX and forskolin to induce a maximal intracellular cAMP response, or CV and expression of the cAMP-dependent genes identified in Chapter 3 (Section 3.3) was assessed by QRT-PCR (Section 2.4.7). Primagraft sample L914 represents the most statistically powerful data as this sample was obtained from three separate mice, allowing triplicate experiments to be carried out. For L779 and L829R, only material from one mouse was available for each. In L914, all genes assessed were shown to be significantly upregulated by cAMP in both siCBP and control cells (*CXCR4* ~9 fold upregulated; p values <0.01, *MKNK2* ~5 fold upregulated; p values <0.006, *DUSP10* ~3 fold upregulated; p values <0.001, *RGS16* ~15 fold upregulated; p values <0.004). This differs from data collected in cells lines, where some of the assessed genes were not found to be significantly upregulated by cAMP (Sections 3.3, 4.2.3 and 4.3.3). In L914 primagraft cells, CREBBP knockdown had no effect on the basal expression of any cAMP-dependent gene assessed (p values >0.7). These data were recapitulated in both L779 and L829R primagraft cells, with all genes assessed shown to be significantly upregulated by cAMP stimulation, with comparable fold change (L779 fold upregulation; *CXCR4* ~6 fold, p values <0.0004, *MKNK2* ~5 fold, p values <0.0001, *DUSP10* ~3.5 fold, p values <0.002, *RGS16* ~3 fold, p values <0.0001, L829R fold upregulation; *CXCR4* ~6 fold, p values <0.0001, *MKNK2* ~5 fold, p values <0.0001, *DUSP10* ~3 fold, p values <0.001) with

the exception of *RGS16* in L829R cells which showed a much higher level of upregulation than in other primagraft cells (~43 fold upregulation, p values <0.0001). In L779, basal *DUSP10* expression was significantly reduced by CREBBP knockdown (p=0.01), with no effect being seen on basal expression of the other genes assessed (p values >0.08). In L829R cells basal expression of *CXCR4*, *MKNK2* and *DUSP10* was significantly impaired by CREBBP knockdown (p values <0.02) with no effect being seen on basal *RGS16* expression (p=0.6). Importantly, CREBBP knockdown did not lead to impaired cAMP-induced expression of the majority of genes assessed in primagraft samples (p values >0.06). However, a slight, statistically significant, reduction in *RGS16* expression was seen in L779 and L829 control transfected cells (p=0.002 and p=0.008 respectively), though this could be explained by the lack of biological replicates for these samples (Figure 4.21).

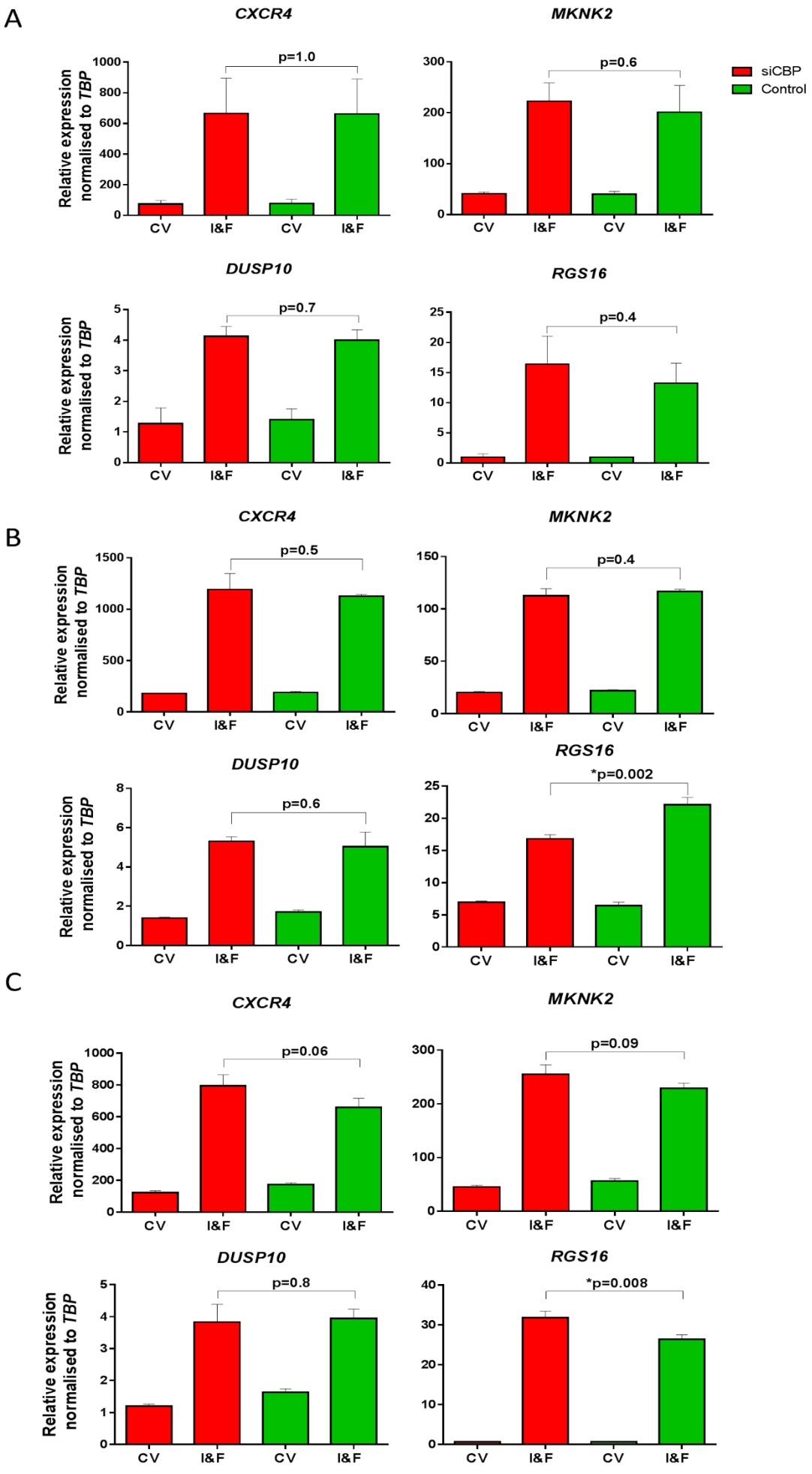
A
CXCR4
p=1.0
MKNK2
p=0.6
siCBP
Control
DUSP10
p=0.7
RGS16
p=0.4
B
CXCR4
p=0.5
MKNK2
p=0.4
DUSP10
p=0.6
RGS16
*p=0.002
C
CXCR4
p=0.06
MKNK2
p=0.09
DUSP10
p=0.8
RGS16
*p=0.008
Relative expression normalised to TBP
CV
I&F

Figure 4.21. Effect of transient CREBBP knockdown in primagraft cells on cAMP-dependent gene expression. SiCBP and control transfected primagraft cells **A.** L914, **B.** L779 and **C.** L829R, were treated with either control vehicle (CV) or IBMX and forskolin (I&F) before determining expression of cAMP-dependent genes by QRT-PCR relative to endogenous *TBP* expression by the $\Delta\Delta C_T$ method. Histograms show mean ±SD. Values plotted represent triplicate experiments for L914 and triplicate wells for L779 and L829R.

4.4.4 Induction of GR Transcriptional Targets in HHD Primagraft Cells with Transient CREBBP Knockdown

Cell line models with CREBBP knockdown showed a variable effect on the expression of GR targets in response to GC treatment, with the majority showing unaffected GR target expression (Sections 3.2, 4.2.3 and 4.3.3). To investigate this further, primagraft samples were assessed for GR target gene expression following stimulation with GC.

Transfected primagraft cells were treated with dexamethasone to induce GR target expression, or CV and expression of *GILZ* and *FKBP5* was assessed by QRT-PCR (Section 2.4.7). Both *GILZ* and *FKBP5* were significantly upregulated by dexamethasone exposure in L914 siCBP and control cells (*GILZ* ~8 fold, p values <0.02, *FKBP5* ~40 fold for siCBP and ~30 fold for control, p=<0.0001 for both) and basal expression was unaffected (p=0.2 and p=0.7 respectively). *GILZ* and *FKBP5* were significantly induced by dexamethasone in both L779 and L829R siCBP and control cells (L779 fold upregulation; *GILZ* ~19 fold, p values <0.0004, *FKBP5* ~23 fold, p values <0.0002, L829R fold upregulation; *GILZ* ~5 fold, p values <0.0002, *FKBP5* ~37 fold, p values <0.0001) and CREBBP knockdown had no effect on basal *GILZ* (L779; p=0.06 and L829R; p=0.2) or *FKBP5* expression in L892R cells (p=0.1), but led to a slight reduction in basal *FKBP5* expression in L779 cells (p=0.01).

The average fold induction of *GILZ* and *FKBP5* in response to dexamethasone varied across the three primagraft samples tested (*GILZ* 5-19 fold, *FKBP5* 23-40 fold) suggesting that the different patients have different transcriptional responses to dexamethasone. CREBBP knockdown had no effect on the GC-induced expression of *GILZ* in any primagraft sample (p values >0.05), but a slight, statistically significant increase in *FKBP5* expression was seen

in L914 (p=0.002), but not L779 or L829R cells (p values >0.5) (Figure 4.22). This recapitulates results from PreB 697 and MHH-CALL-2 cells with transient CREBBP knockdown, suggesting that CREBBP knockdown does not impair GR transcriptional response.

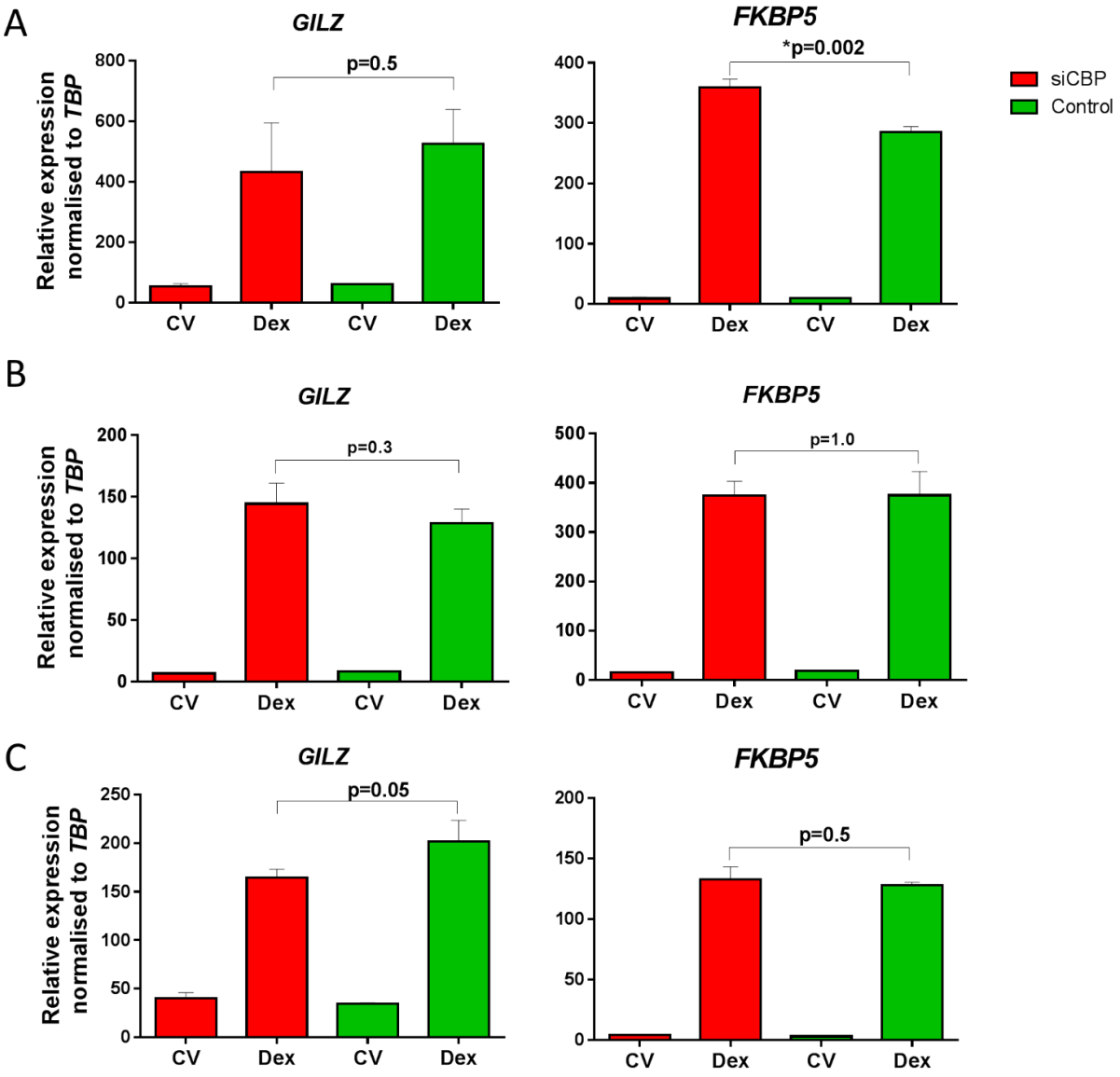

Figure 4.22. Effect of transient CREBBP knockdown in primagraft cells on GR target gene expression. SiCBP and control primagraft cells **A.** L914, **B.** L779 and **C.** L829R were treated with either CV or dexamethasone (Dex) for 24 hours before determining expression of GR target genes by QRT-PCR relative to endogenous *TBP* expression by the $\Delta\Delta C_T$ method. Histograms show mean ±SD. Values plotted represent triplicate experiments for L914 and triplicate wells for L779 and L829R.

4.4.5 Dexamethasone Sensitivity of Primagraft Cells with CREBBP Knockdown

Contrary to predictions, CREBBP knockdown in cell lines did not lead to dexamethasone resistance (Sections 3.2, 4.2.4 and 4.3.4). To further address this in a more biologically relevant context, primagraft samples with transient CREBBP knockdown were assessed for sensitivity to dexamethasone.

Transduced primagrafts were treated with a range of concentrations of dexamethasone or CV, and survival was assessed by alamar blue assay (Section 2.6.2). CREBBP knockdown had no effect on the dexamethasone sensitivity of any primagraft sample compared to control (GI_{50} values, mean ±SD; L914 siCBP 6.1nM ±2.2 versus control 5.6nM ±0.41; L779 siCBP 65.2nM ±38.3 versus control 90.8nM ±18.2; L829 >10µM for both) (Figure 4.23). These data are consistent with those in cells lines, and show that CREBBP knockdown has no effect on dexamethasone sensitivity in ALL cells.

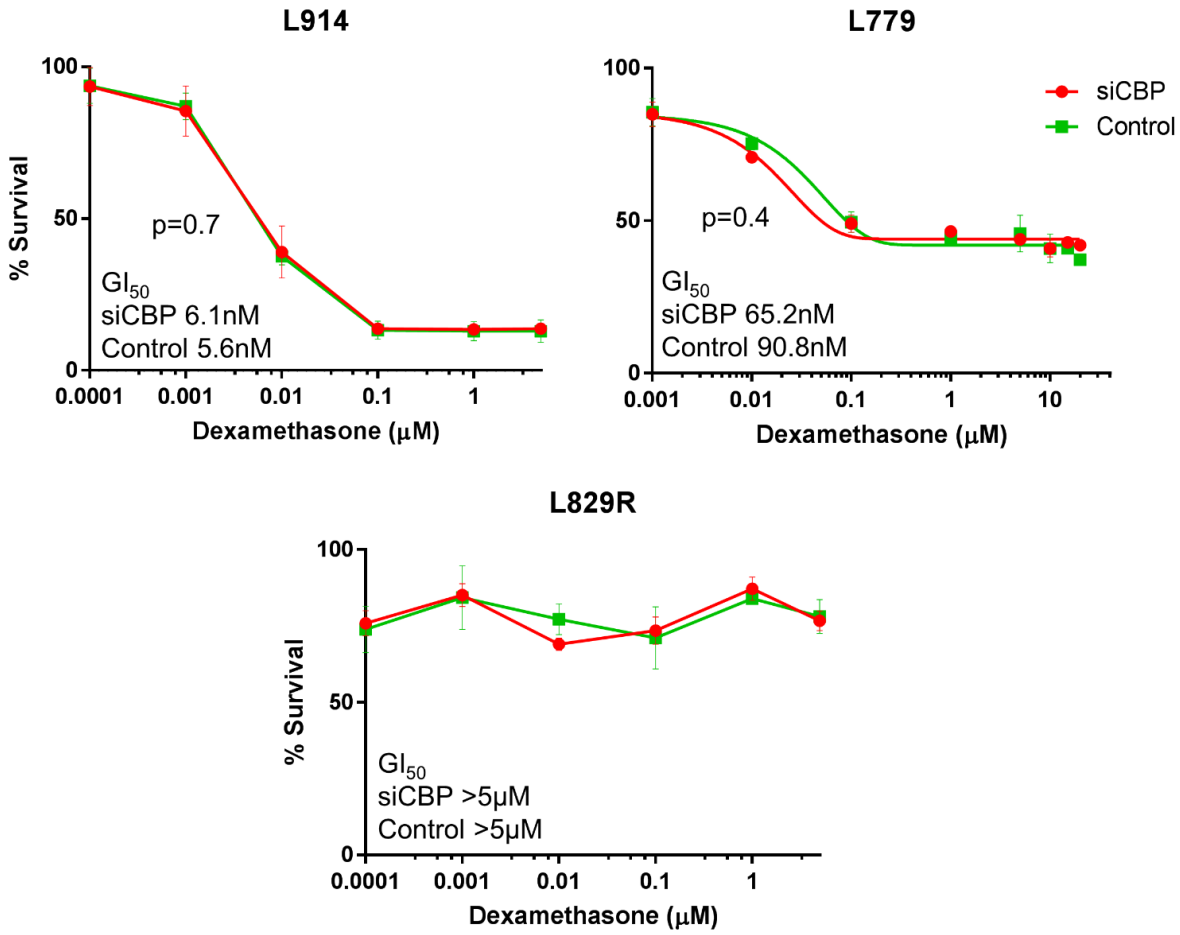

4.23. Dexamethasone sensitivity of primagraft cells with transient CREBBP knockdown. Cells were treated with a range of dexamethasone concentrations or CV, 24 hours post-transfection and incubated for 96 hours. Alamar blue was used to determine cell survival as a % of CV treated cells. Values plotted represent the mean % survival ±SD of triplicate experiments for L914 and triplicate wells for L779 and L829R.

4.4.6 Enhanced RAS Pathway Activation in RAS Mutant Primagraft Cells with Transient CREBBP Knockdown

In Chapter 3, it was shown that stable knockdown of CREBBP in the RAS pathway mutant cell line, PreB 697, led to enhanced RAS pathway activation, as assessed by p-ERK expression (Section 3.9). This is of particular importance as *CREBBP* mutations frequently co-exist with RAS pathway mutations (Malinowska-Ozdowy *et al.*, 2015). To further address this observation in a more biologically relevant context, transient CREBBP knockdown was carried out in primagraft samples with different RAS pathway mutations (L779; *NRAS*, L829R; *KRAS* and L914; *CBL/FLT3* deletion) then each was assessed for RAS pathway activation, determined by ERK phosphorylation.

Twenty four hours post-transfection whole cell lysates were harvested from RAS pathway mutant primagraft samples, and western blotting was carried out for p-ERK and ERK with α-tubulin serving as loading control (Section 2.5). CREBBP knockdown in L914 and L829R cells led to increased expression of p-ERK compared to control, but had no effect on p-ERK expression in *NRAS* mutant L779 cells (Figure 4.24). ERK expression was consistent between L914 siCBP and control cells and slightly decreased in L829R siCBP compared to control cells, so reduced p-ERK expression in these cells cannot be explained by reduced basal ERK levels. These data, along with those observed in PreB 697 cells with CREBBP knockdown, suggest that CREBBP knockdown leads to increased RAS pathway activation in RAS pathway mutant cells.

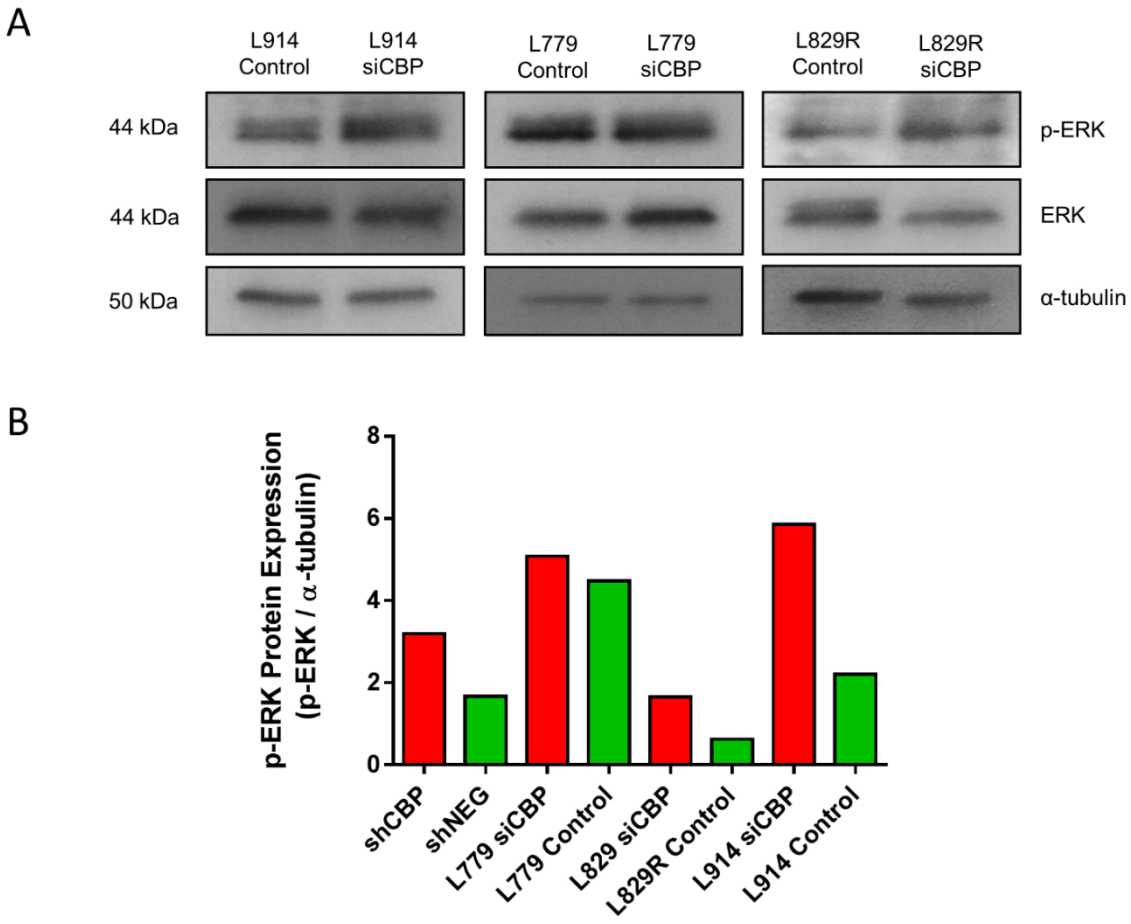

Figure 4.24. Transient CREBBP knockdown in RAS mutant primagraft cells and p-ERK expression. A. Primagraft cells were transfected with an siRNA pool targeting *CREBBP* or control siRNA and incubated for 24 hours before whole cell lysates were extracted and western blotting was carried out for ERK and p-ERK. Alpha tubulin was included as loading control. **B.** Histogram of the relative expression of p-ERK in PreB 697 (shCBP and shNEG) and CREBBP knockdown primagraft samples normalised to ERK after densitometric analyses.

4.5 Discussion

The aim of this Chapter was to validate data gathered from the study of PreB 697 cells with stable CREBBP knockdown described in Chapter 3, using cell lines and primary derived samples with relevant cytogenetic context (i.e. High hyperdiploid or hypodiploid), as well as addressing the importance of the *in vivo* growth environment.

The use of siRNA pool transfection to knockdown CREBBP in PreB 697 and MHH-CALL-2 cells confirmed a high level of comparability with the shRNA method used in Chapter 3. Reductions of *CREBBP* at the mRNA and protein level were similar to those shown in cells with stable CREBBP knockdown, and in patient samples with *CREBBP* deletions. CREBBP knockdown had no effect on cell proliferation in PreB 697 cells, but MHH-CALL-2 cells with CREBBP knockdown showed slightly more cell growth at 96 hours, approaching statistical significance ($p=0.06$). This suggests that *CREBBP* mutations may influence cell cycle control in ALL.

Whilst both stable and transient CREBBP knockdown in PreB 697 cells showed no significant effect on cAMP-induced expression of cAMP-dependent target genes, the fold induction of *CXCR4* and *MKNK2* differed between the two knockdown models (*CXCR4* shRNA ~14 fold induction vs siRNA ~11 fold induction, *MKNK2* shRNA ~6 fold induction vs siRNA ~3 fold induction), and in transiently transfected cells *DUSP10* and *RGS16* were not found to be significantly induced by cAMP. Basal expression of all cAMP-dependent genes assessed was unaffected by transient knockdown of CREBBP, whereas basal *MKNK2* and *RGS16* expression was altered in cells with stable CREBBP knockdown. In MHH-CALL-2 cells, CREBBP knockdown similarly had no effect on cAMP-induced gene expression,

though the fold induction of targets differed in this cell line compared to PreB 697 cells (E.g. PreB 697 *CXCR4* ~14 fold induction vs MHH-CALL-2 ~4 fold induction). These data suggest that CREBBP knockdown in BCP-ALL cell lines is not sufficient to significantly alter cAMP-dependent gene expression.

Transient knockdown of CREBBP in PreB 697 cells did not lead to impaired GC-induced expression of the GR targets, *GILZ*, *FKBP5* and *NR3C1* as it did in stably knocked down cells, but showed greater induction in response to the same dexamethasone concentration (*GILZ* shRNA ~20 fold induction vs siRNA ~40 fold induction, *FKBP5* shRNA ~3 fold inductions vs siRNA ~6 fold induction, *NR3C1* shRNA ~1.5 fold induction vs siRNA ~2.4 fold induction). As in PreB 697 cells with stable CREBBP knockdown, basal *GILZ* expression was shown to be slightly reduced in PreB 697 cells with CREBBP knockdown. A slight, statistically significant increase in basal *NR3C1* expression was seen in PreB 697 siCBP cells but no effect on basal *FKBP5* or *ITGA9* expression was seen. Similar results were shown in MHH-CALL-2 cells with transient CREBBP knockdown, again with different fold changes in induced expression achieved (*GILZ* PreB 697 ~40 fold induction vs MHH-CALL-2 ~ 50 fold induction, *FKBP5* PreB 697 ~6 fold induction vs MHH-CALL-2 ~10 fold). Importantly, neither cell line showed any significant reduction in sensitivity to dexamethasone when CREBBP was transiently knocked down compared to control, with a small, statistically significant increase in dexamethasone sensitivity seen in PreB 697 cells (siCBP 17nM vs control 34.7nM). However, given the size of this increase, it is unlikely to be biologically relevant. These data validate those collected in PreB 697 cells with stable CREBBP knockdown, further suggesting that *CREBBP* haploinsufficiency does not lead to GC resistance in ALL.

One possible explanation for the discrepancies in GR target expression between PreB 697 cells with stable knockdown and PreB 697 and MHH-CALL-2 cells with transient CREBBP knockdown is the use of different RNAi methods. It could be argued that transient knockdown may not be maintained for a sufficient period of time to see an effect on GR target expression or GC sensitivity. However, transient CREBBP knockdown was shown to be maintained at the protein level for at least 96 hours and the level of knockdown achieved at the mRNA and protein levels and effect on markers of CREBBP activity such as acetylation of H3K18, were found to be consistent between stable and transient knockdown models. This suggests that transient knockdown of CREBBP in cell lines is a relevant model of *CREBBP* haploinsufficiency in ALL.

To overcome the limitations associated with the use of cell line models, a method of siRNA knockdown in primagraft samples was optimised and used to knockdown CREBBP in 3 individual HHD primagraft samples. One of these samples, L914, was amplified in 3 separate mice, giving access to 3 biological repeats. CREBBP mRNA and protein reduction were consistent with that achieved in cell lines and patients with *CREBBP* deletions. All cAMP-dependent targets assayed in primagrafts samples were significantly induced by cAMP stimulation, and showed a high degree of similarity in terms of fold induction achieved (E.g. *MKNK2* ~5 fold induction in L914, L779 and L829R) except for *RGS16*, in which fold induction varied between primagraft samples (L914 ~15 fold, L779 ~3 fold, L829R ~43 fold). CREBBP knockdown only had a significant effect on the cAMP-induced expression of *RGS16* in L914 cells, where it led to an increase in expression compared to control cells. The effect of CREBBP knockdown on basal expression of cAMP-dependent genes differed between primagraft samples, with L914 showing similar results to PreB 697

and MHH-CALL-2, with no altered basal expression for any genes tested, whereas L779 showed altered basal *DUSP10* expression and L829R showed altered basal *CXCR4, MKNK2* and *DUSP10* expression. These data support those from cell line studies, suggesting that *CREBBP* knockdown does not affect cAMP-dependent gene transcription in ALL, with remnant CREBBP expression sufficient to compensate.

Fold induction of the GR target, *GILZ*, in response to GC in primagraft cells was much lower in all primagraft samples compared to cell lines (E.g. MHH-CALL-2 ~50 fold induction vs L914 ~8 fold induction) with the fold induction of *FKBP5* being higher in primagraft samples than cell lines (E.g. MHH-CALL-2 ~10 fold induction vs L914 ~40 fold induction). Basal expression of *GILZ* and *FKBP5* was unaffected by CREBBP knockdown in all primagrafts except L779, which showed a small reduction in basal *FKBP5* expression. Importantly, CREBBP knockdown had no effect on sensitivity to dexamethasone in any of the primagraft samples tested, recapitulating the observations from cell line studies. Taken together these data validate those collected in BCP-ALL cell lines, with a high level of biological and cytogenetic relevance. They suggest that CREBBP knockdown in BCP-ALL cell lines is a relevant model of *CREBBP* haploinsufficiency in ALL and provide a robust data set for the understanding of the mechanisms of this mutation in relapsed disease. Overall, these data do not support a role for *CREBBP* haploinsufficiency in resistance to GC.

Whilst a trend towards reduced acetylation of H3K18 and/or H3K27 was seen for all cells with CREBBP knockdown, thus indicating a functional effect of CREBBP knockdown, the level of reduction, and residue which was reduced, differed greatly between cell lines and primagraft samples. CREBBP and its paralog EP300 are known to have different specificities for histone lysine acetylation, specificities which change based on amount of

H3 or acetyl-CoA availability (Henry *et al.*, 2013). The varying effect of CREBBP knockdown between cell lines and between primagraft cells could be explained by the observation that specificities for H3 acetylation vary in a complex way and that there is overlap of H3 acetylation sites between EP300 and CREBBP, so EP300 or residual CREBBP expression could compensate when CREBBP is knocked down (Henry *et al.*, 2013).

As discussed in Chapter 1, RAS pathway mutations are common in relapsed childhood ALL, led to enhanced signalling down the RAS/RAF/MEK/ERK pathway and are associated with high risk features and poor prognosis (Case *et al.*, 2008; Irving *et al.*, 2014; Irving *et al.*, 2016). Further to this, as discussed in Chapter 3, *CREBBP* mutations frequently co-occur with RAS pathway activating mutations, including *KRAS*, *NRAS*, *PTPN11* and *FLT3* (Malinowska-Ozdowy *et al.*, 2015). Two of three RAS pathway mutant primagraft samples (L829R; *KRAS* G13D and L914; *CBL/FLT3* large del/Δ836) showed increased p-ERK expression when CREBBP was transiently knocked down. This shows that CREBBP knockdown is able to enhance oncogenic RAS signalling in cells with RAS pathway mutations. Taken together with data from Chapter 3, these data further support the hypothesis that *CREBBP* haploinsufficiency enhances signalling of the RAS/RAF/MEK/ERK pathway in RAS pathway mutated ALL cells.

In summary, the results presented in this chapter validate those collected in Chapter 3, with observations made in primary derived cell models with relevant cytogenetic context. Data collected in this chapter do not support a role for *CREBBP* haploinsufficiency in

resistance to GC but further support the hypothesis that *CREBBP* haploinsufficiency in ALL cells harbouring RAS pathway mutation leads to increased RAS/RAF/MEK/ERK signalling.

Chapter 5 (Results 3) – Stable CREBBP Knockdown in Diffuse Large B-Cell Lymphoma

CREBBP Knockdown in Diffuse Large B-Cell Lymphoma

5.1 Introduction

CREBBP mutation is a frequent event in DLBCL, with 39% of cases identified as *CREBBP* mutant (Pasqualucci *et al.*, 2011). As in relapsed ALL, mutations commonly affect one allele of *CREBBP*, with the intact allele conferring expression of wild type *CREBBP*, indicating that haploinsufficiency is important (Pasqualucci *et al.*, 2011). Given that these mutations are more frequently seen at diagnosis, it is clear that *CREBBP* haploinsufficiency contributes to DLBCL pathogenesis in a different way to ALL, where mutations are more commonly associated with relapse (Pasqualucci *et al.*, 2011). *CREBBP* mutations lead to defects in p53 activation and BCL6 inactivation, which have important implications in lymphomagenesis and drug sensitivity (Pasqualucci *et al.*, 2011). Understanding the mechanisms of *CREBBP* mutation in DLBCL is important as it may pave the way for novel therapy that is clearly needed, and also facilitate the understanding of *CREBBP* mutation in other tumour types, such as relapsed childhood ALL and FL. In order to study *CREBBP* haploinsufficiency in DLBCL, cell lines with stable CREBBP knockdown and isogenic control were created and characterised.

5.2 Creation of a DLBCL Cell Line with Stable CREBBP Knockdown

Lentiviral transduction of shRNA was used to create a DLBCL cell line with stable CREBBP knockdown (Section 2.7.1). SU-DHL-4 was selected as a suitable cell line as it had been previously shown to express wild type *CREBBP* (Epstein and Kaplan, 1979; Pasqualucci *et al.*, 2011). Following puromycin selection, cells with stable CREBBP knockdown

(SUDshCBP) and control cells (SUDshNEG) were assessed for CREBBP expression by QRT-PCR and western blotting (Sections 2.4.7 and 2.5). Around 30% reduction in *CREBBP* mRNA expression was achieved, which is slightly lower than that seen in CREBBP knockdown models of ALL (40-50% reduction in PreB 697, MHH-CALL-2 and primagraft cells) (Sections 3.2, 4.2.1, 4.3.1 and 4.4.2) (Figure 5.1A). Despite this, a clear reduction in CREBBP protein expression was seen in SU-DHL-4 cells with CREBBP knockdown (SUDshCBP) compared to control (SUDshNEG), comparable to that achieved in ALL cells and ALL patient samples with *CREBBP* deletions (Sections 3.2, 4.2.1, 4.3.1 and 4.4.2) (Figure 5.1 B).

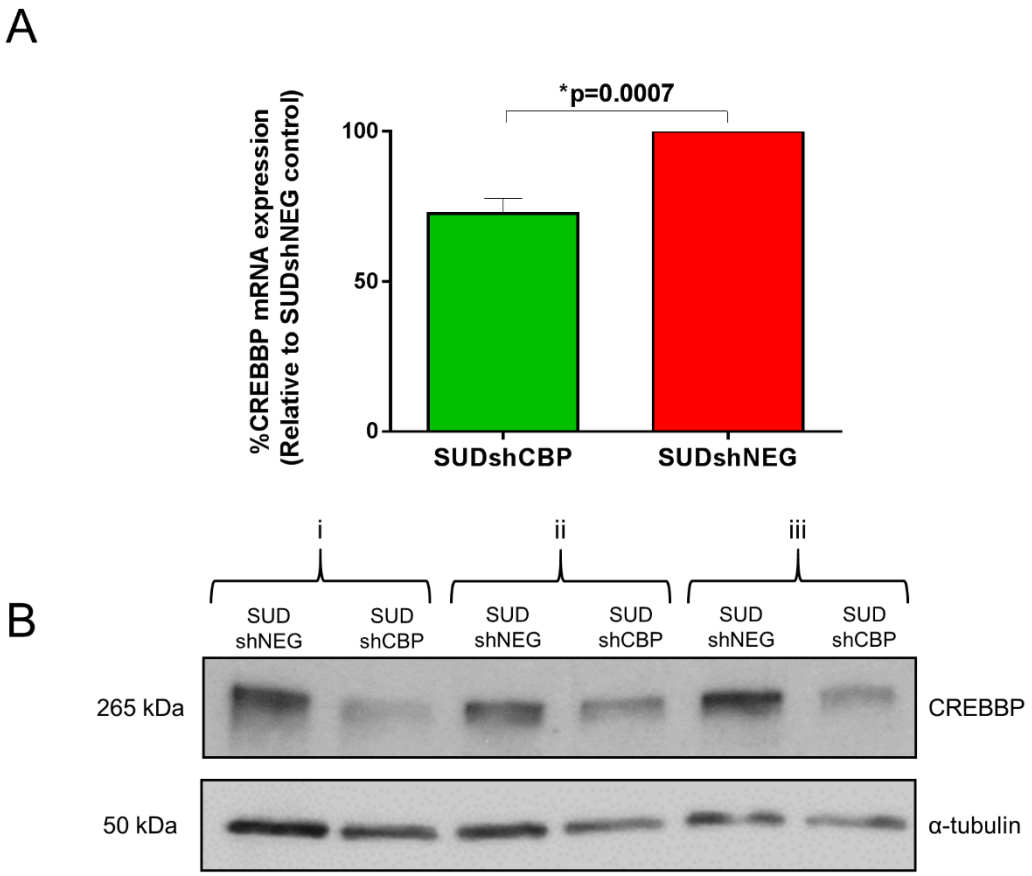

Figure 5.1. CREBBP mRNA and protein expression in SU-DHL-4 cells with stable CREBBP knockdown. Cells were transduced with shRNA targeting *CREBBP* (SUDshCBP) or a non-silencing control (SUDshNEG). **A.** Following puromycin selection cells were harvested in exponential growth phase on three separate occasions and QRT-PCR was carried out for *CREBBP* expression. Expression levels were normalised to *TBP* by the $\Delta\Delta C_T$ method. Histogram represents mean ±SD of triplicate experiments. **B.** Whole cell lysates from transduced cells in exponential growth phase were extracted on three separate occasions (i-iii) and western blotting was carried out for CREBBP. Alpha tubulin was included as loading control.

To assess the functional effect of the knockdown, western blotting was carried out for AcH3K18 and AcH3K27 (Section 2.5). The effect of CREBBP knockdown in SU-DHL-4 cells was variable, with a lack of consistency seen between replicates for either residue (Figure 5.2 A, i-iv & B, i-iii). AcH3K18 levels were unaffected by CREBBP knockdown, whereas AcH3K27 levels were reduced by CREBBP knockdown in one of the three replicates and slightly increased in another.

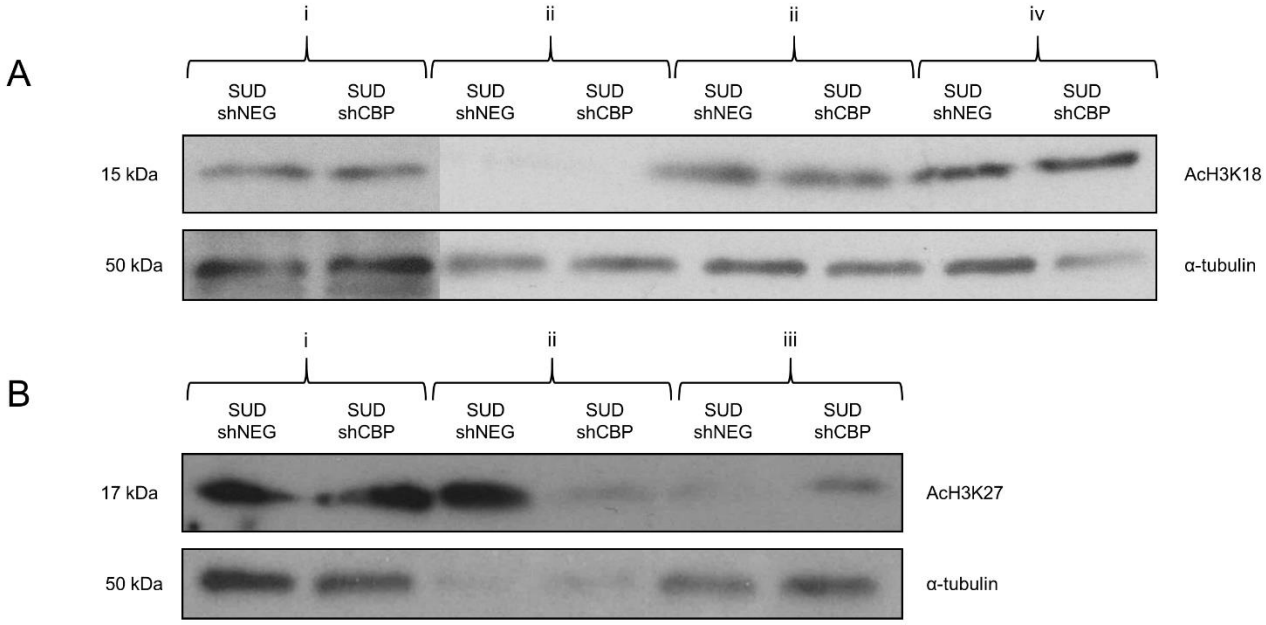

Figure 5.2. Expression of AcH3K18 and AcH3K27 in SU-DHL-4 cells with stable CREBBP knockdown. Whole cell lysates were extracted from SUDshCBP and SUDshNEG cells and western blotting was carried out for AcH3K18 (**A**, i-iv) or AcH3K27 (**B**, i-iii). Alpha tubulin was included as loading control. Brackets represent individual biological repeats.

The effect of CREBBP knockdown in SU-DHL-4 on cells growth was assessed by seeding cells at 3 different densities and counting every 24 hours for 120 hours by trypan blue staining, using a haemocytometer (Section 2.6.1). This showed that CREBBP knockdown had no effect on cell proliferation, with no significant difference in average doubling time seen between SUDshCBP and SUDshNEG cells at any of the seeding densities (Average doubling time ±SD; SUDshCBP 38.2 ±10.8 vs SUDshNEG 38.4 hours ±11.6; p=1.0) (Figure 5.3). The effect of CREBBP knockdown on cell proliferation in these cells was further assessed by comparing the fluorescence output readings from control treated groups from drug sensitivity experiments conducted using SUDshCBP and SUDshNEG cells (Section 5.4). These are in keeping with those collected in ALL cell models of CREBBP knockdown and confirmed no effect on cell proliferation (Mean fluorescent output ±SD; SUDshCBP 7.69x104 ±1.17x10^4, SUDshNEG 7.64x10^4 ±1.22x10^4; p=0.8) (Figure 5.4).

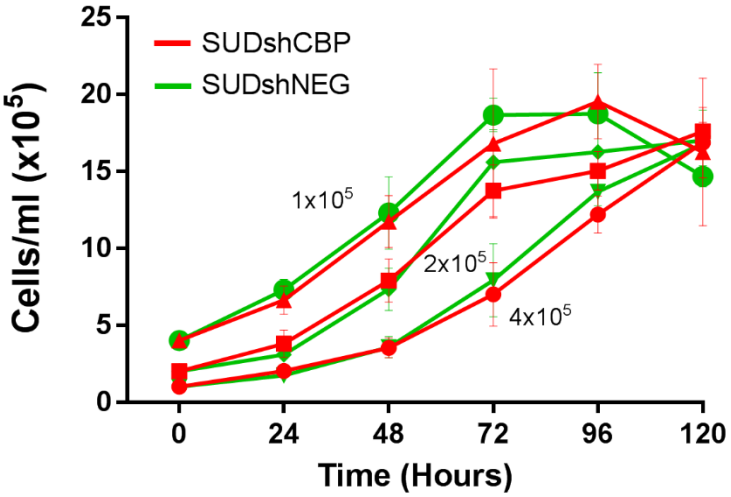

Figure 5.3. Stable CREBBP knockdown in SU-DHL-4 cells and cell proliferation. SUDshCBP and SUDshNEG cells were seeded at $1x10^5$ cells/ml, $2x10^5$ cells/ml and $4x10^5$ cells/ml and counted every 24 hours for 120 hours by trypan blue staining and a haemocytometer. Values plotted represent mean cell count (cells/ml) at each given time point ±SD (n=3).

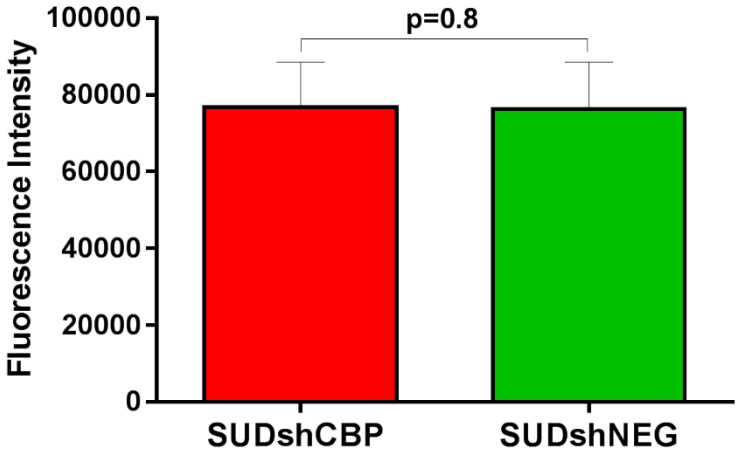

Figure 5.4. Stable CREBBP knockdown in SU-DHL-4 cells and survival at 96 hours. The raw fluorescence output values from CV treated cells from drug sensitivity experiments were combined and compared. Graph shows average relative fluorescence ±SD (n=17).

5.3 cAMP response in SU-DHL-4 Cells with Stable CREBBP Knockdown

As described in Chapter 3 (Section 3.3), CREBBP is involved in cAMP-dependent signalling, a ubiquitous process which modulates transcription of a large number of genes. In Chapters 3 and 4, it was shown that CREBBP knockdown had no significant effect on cAMP-induced gene expression in ALL cell lines and primagraft cells. To study this effect of DLBCL, SU-DHL-4 cells with a stable CREBBP knockdown were assessed for cAMP-induced gene expression.

Firstly, to determine relevant cAMP-dependent targets in SU-DHL-4 cells, gene expression profiling was carried out using the Affymetrix U133 Plus 2.0 platform. As described previously for ALL cells (Section 3.3), SUDshNEG cells were treated with IBMX and forskolin or CV for 90 minutes, RNA was then extracted and sent to Source Bioscience for gene expression analysis (Section 2.4.8). To select the most significant cAMP-dependent genes in SU-DHL-4, genes which were upregulated in the IBMX and forskolin treated group were ordered by greatest increase in expression. The two genes at the top of this list, *RGS1* and *DUSP5* were selected as representative cAMP-dependent genes in SU-DHL-4 cells (Table 5.1). Genes identified as cAMP-dependent in ALL cells (Section 3.3) were also included as they appeared on this list (*CXCR4*), and QRT-PCR probes were available.

Feature	Gene	Log2FC
216834_at	*RGS1*	3.72
209457_at	*DUSP5*	2.92
204912_at	*IL10RA*	2.52
228846_at	*MXD1*	2.38
231124_x_at	*LY9*	2.32
235444_at	*FOXP1*	2.24
225191_at	*CIRBP*	2.20
211962_s_at	*ZFP36L1*	2.16
209201_x_at	***CXCR4***	2.15
1564970_at	*SETDB2*	2.13
230142_s_at	*CIRBP*	2.08
211919_s_at	***CXCR4***	2.07
221986_s_at	*KLHL24*	2.07
236293_at	*RHOH*	2.03
211965_at	*ZFP36L1*	2.02
201739_at	*SGK1*	1.97
228426_at	*CLEC2D*	1.90
221985_at	*KLHL24*	1.89
217028_at	***CXCR4***	1.89
242814_at	*SERPINB9*	1.85
201041_s_at	*DUSP1*	1.83
1568751_at	*RGS13*	1.80
201925_s_at	*CD55*	1.76
213593_s_at	*TRA2A*	1.75
233463_at	*RASSF6*	1.74
208763_s_at	*TSC22D3*	1.73
202388_at	*RGS2*	1.71
1555858_at	*THUMPD3-AS1*	1.70
227223_at	*RBM39*	1.70
215012_at	*ZNF451*	1.69
1555827_at	*CCNL1*	1.69
217591_at	*SKIL*	1.66
201926_s_at	*CD55*	1.63
213575_at	*TRA2A*	1.63
225867_at	*VASN*	1.62
222542_x_at	*ADCK3*	1.62
202861_at	*PER1*	1.60
204951_at	*RHOH*	1.58

1555950_a_at	*CD55*	1.57
208536_s_at	*BCL2L11*	1.56
210322_x_at	*UTY*	1.55
226541_at	*FBXO30*	1.55
220035_at	*NUP210*	1.54
209102_s_at	*HBP1*	1.53
226404_at	*RBM39*	1.50
214802_at	*EXOC7*	1.48
228030_at	*RBM6*	1.48
1560172_at	*INTS10*	1.46
1552542_s_at	*TAGAP*	1.42
202340_x_at	*NR4A1*	1.42

Table 5.1. Genes upregulated by cAMP in SU-DHL-4 cells. List shows the top 50 most upregulated genes in SUDshNEG cells treated with IBMX and forskolin compared to cells treated with CV. *RGS1* and *DUSP5* were selected as representative cAMP-dependent genes in SU-DHL-4. Genes identified as cAMP-dependent in ALL cells were also upregulated upon cAMP stimulation in these cells (List of genes with Log2FC ≥1 available in appendix) (n=1).

SUDshCBP and SUDshNEG cells were treated with IBMX and forskolin for 90 minutes to induce a maximal intracellular cAMP response, or CV and QRT-PCR was carried out using probes specific to cAMP-dependent targets identified above (Section 2.4.7). Only the genes identified by GEP, *RGS1* and *DUSP5*, were found to be significantly upregulated by cAMP-stimulation in both SUDshCBP and SUDshNEG cells (Fold upregulation; *RGS1* ~36 fold; p values <0.003, *DUSP5* ~7 fold for SUDshCBP and ~9 fold for SUDshNEG; p values <0.003) (Figure 5.5). *CXCR4* was only significantly induced by cAMP stimulation in SUDshNEG cells (~4 fold induction, p=0.001) and other genes assessed did not show significantly increased expression in either cell line (p values >0.3) (Figure 5.5). The cAMP-induced expression of *DUSP5* was significantly impaired in cells with CREBBP knockdown compared to control (*DUSP5* ~7 fold for SUDshCBP and ~9 fold for SUDshNEG; p=0.047) (Figure 5.5). *RGS1* expression also appeared reduced in SUDshCBP cells compared to SUDshNEG, but this was not statistically significant (p=0.1). CREBBP knockdown had no effect on basal expression of any of the genes assessed (p values >0.2). These data suggest that, as in BCP-ALL models, CREBBP knockdown does not have a significant effect on cAMP-dependent signalling in SU-DHL-4 cells.

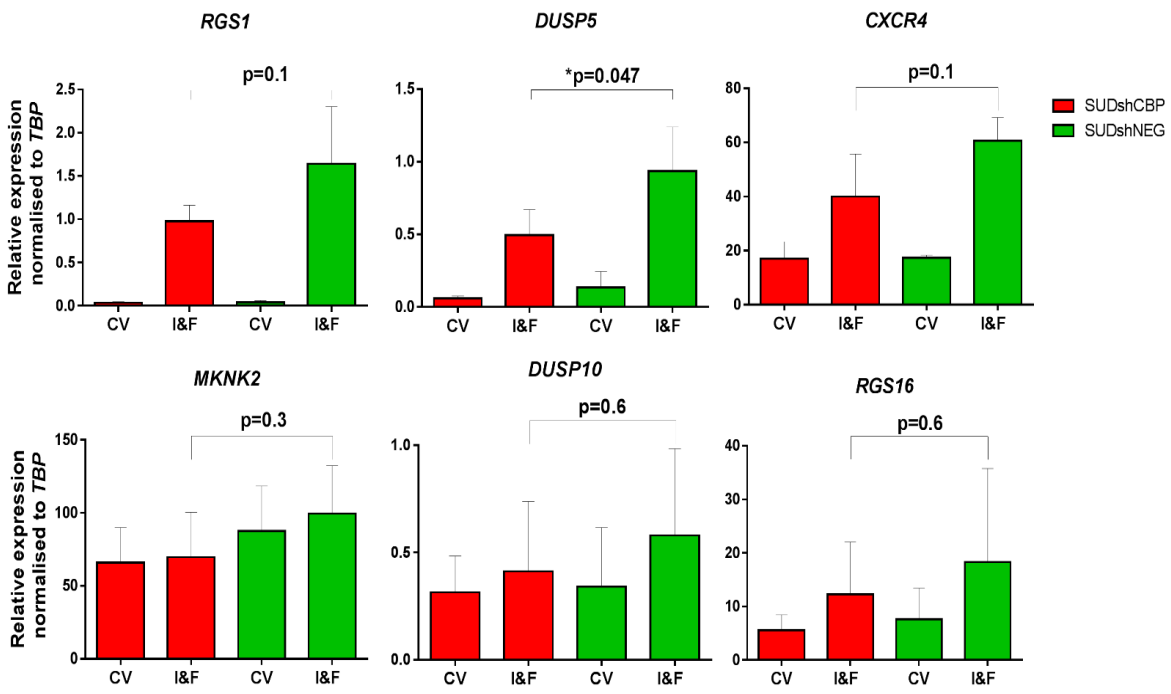

Figure 5.5. Effect of transient CREBBP knockdown in SU-DHL-4 cells on cAMP-dependent gene expression. SUDshCBP and SUDshNEG cells were treated with either control vehicle (CV) or IBMX and forskolin (I&F) before determining expression of cAMP-dependent genes by QRT-PCR relative to endogenous *TBP* expression by the $\Delta\Delta C_T$ method. Histograms show mean ±SD (n=3).

5.4 Chemosensitivity of SU-DHL-4 Cells with Stable CREBBP Knockdown

To elucidate the effect of CREBBP knockdown on drug response in DLBCL, SU-DHL-4 cells with stable CREBBP knockdown were tested for sensitivity to a range of chemotherapeutics used in the treatment of lymphoma.

As discussed in previous chapters, *CREBBP* haploinsufficiency has been implicated in resistance to GC therapy (Mullighan *et al.*, 2011). SUDshCBP and SUDshNEG cells were therefore assessed for sensitivity to the GC, dexamethasone by alamar blue drug sensitivity assay (Section 2.6.2). Unfortunately, both SUDshCBP and SUDshNEG cells were found to be resistant to dexamethasone, making these cells a poor model for assessment of response to GC (GI_{50} values >100µM) (Figure 5.6). CREBBP plays a role in global acetylation, small changes in which have been shown to give significant biological consequences, through altering a wide range of cellular functions (Legube and Trouche, 2003). Treatment with HDACi could be used as a novel therapeutic strategy, in an attempt to rebalance levels of acetylation in *CREBBP*-mutated cells. To test this hypothesis, SUDshCBP and SUDshNEG cells were assessed for sensitivity to vorinostat using an alamar blue drug sensitivity assay (Section 2.6.2). This showed that CREBBP knockdown in SU-DHL-4 cells had no effect on sensitivity to HDACi (GI_{50} values, mean ±SD; SUDshCBP 1.9µM ±0.21 versus SUDshNEG 1.9µM ±0.43; p=1.0) (Figure 5.6).

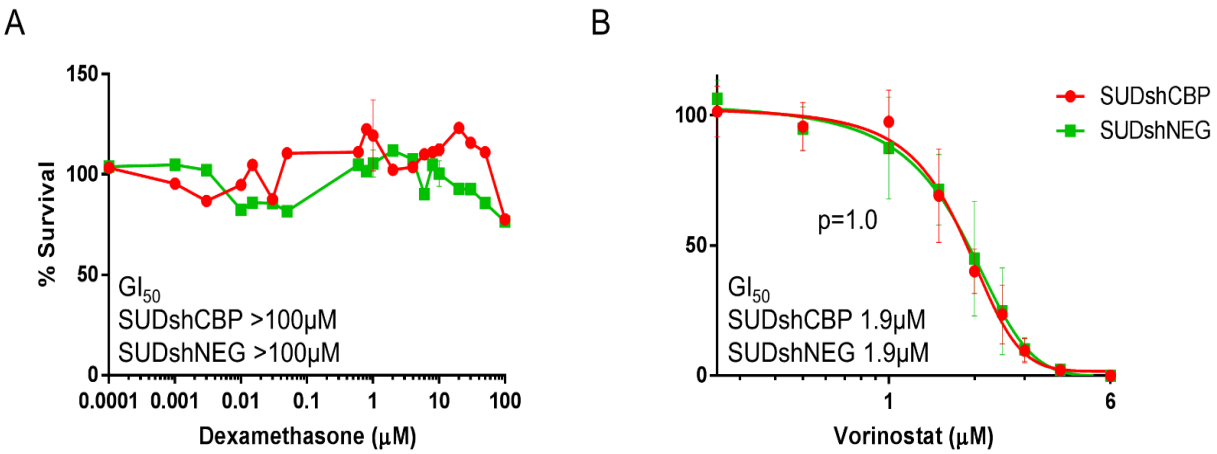

Figure 5.6. Dexamethasone and vorinostat sensitivity of SU-DHL-4 cells with stable CREBBP knockdown. SUDshCBP and SUDshNEG cells were assessed for sensitivity to **A.** dexamethasone and **B.** vorinostat by alamar blue drug sensitivity assay over 96 hours. Histograms show mean survival ±SD (n=3).

Given that CREBBP knockdown had no effect on sensitivity to GC or HDACi treatment, SUDshCBP and SUDshNEG cells were assessed for sensitivity to a panel of chemotherapeutics used to treat lymphoid malignancies (Section 2.6.2). CREBBP knockdown had no effect on sensitivity to daunorubicin or 6-thioguanine (GI_{50} values, mean ±SD; daunorubicin SUDshCBP 42.5nM ±7.6 versus SUDshNEG 76.9nM ±23.1; p=0.07, 6-thioguanine SUDshCBP 12.8µM ±5.7 versus SUDshNEG 13.1µM ±8.1; p=1.0), but gave a statistically significant reduction in sensitivity to vincristine (GI_{50} values, mean ±SD; SUDshCBP 2.6nM ±0.12 versus SUDshNEG 3.1nM ±0.11; p=0.009) (Figure 5.7). Given the size of the difference in GI_{50} values however (2.6nM vs 3.1nM) this difference is unlikely to be biologically relevant. Taken together these data support those found in ALL cell lines and primagrafts, suggesting that *CREBBP* haploinsufficiency does not lead to chemoresistance in DLBCL.

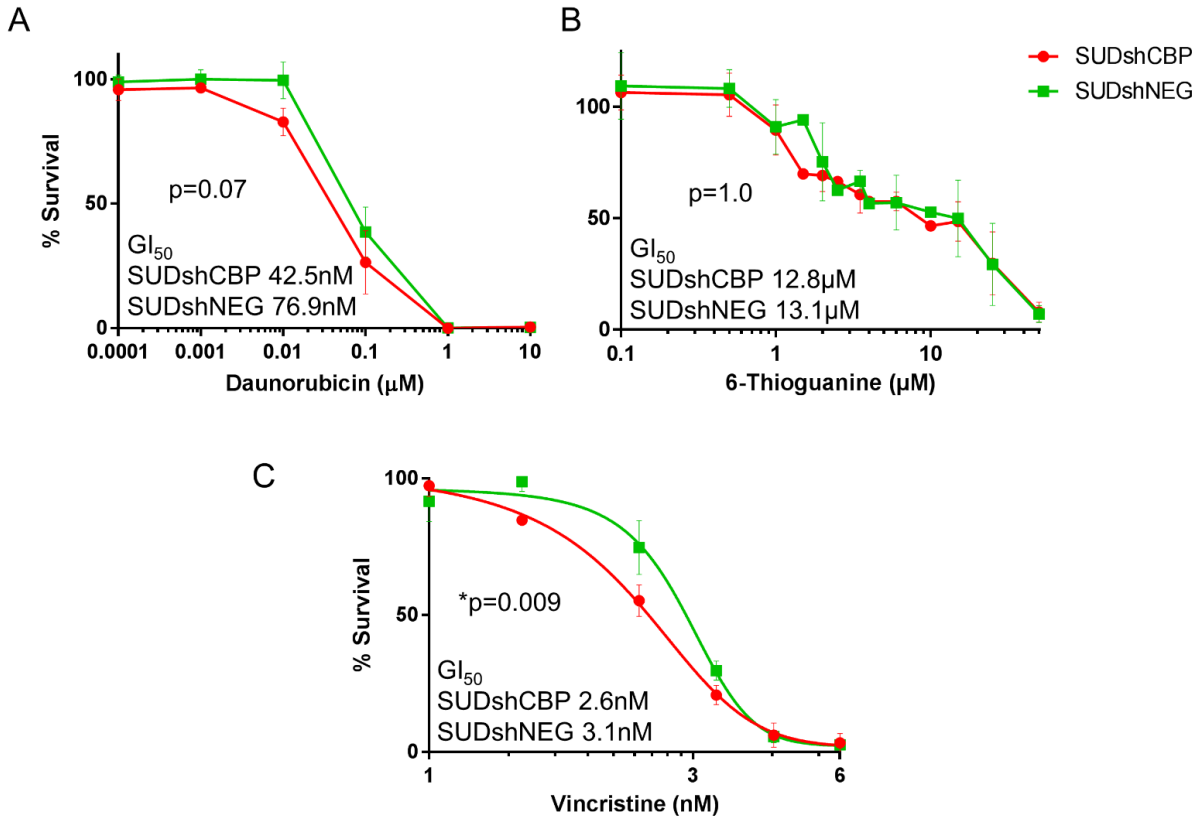

Figure 5.7. Effect of stable CREBBP knockdown in SU-DHL-4 cells on sensitivity to chemotherapeutics used to treat lymphoid malignancies. SUDshCBP and SUDshNEG cells were assessed for sensitivity to **A.** daunorubicin, **B.** 6-thioguanine and **C.** vincristine by alamar blue drug sensitivity assay over 96 hours. Histograms show mean survival ±SD (n=3).

5.5 DNA Damage Repair in SU-DHL-4 Cells with Stable CREBBP Knockdown

As discussed in Chapter 1, CREBBP plays a role in multiple DNA repair pathways. Of particular note is the discovery that mice heterozygous for *CREBBP*, are hypersensitivity to gamma radiation (Zimmer *et al.*, 2012). Experiments carried out in PreB 697 cells in suggest that CREBBP deficiency does not significantly influence DNA damage response in ALL (Section 3.8). To understand the effect of *CREBBP* haploinsufficiency on DNA damage response in the context of DLBCL however, these experiments were carried out in SU-DHL-4 cells with stable CREBBP knockdown.

5.5.1 CREBBP Knockdown and PARP Expression

As discussed in Chapter 3, CREBBP is known to acetylate PARP allowing its interaction with p50 and synergistic co-activation of NF-κB by p300 (Hassa *et al.*, 2005). Knockdown of CREBBP in PreB 697 cells had no effect on PARP-1 protein expression however (Section 3.8.2). To study the effect of CREBBP knockdown on PARP-1 expression in SU-DHL-4 cells, western blotting was carried out (Section 2.5). This showed that, like in the PreB 697 model, CREBBP knockdown had no effect on PARP-1 protein expression (Figure 5.8). In the third replicate experiment there was some evidence of increased cleaved PARP-1 expression, however this was not consistent.

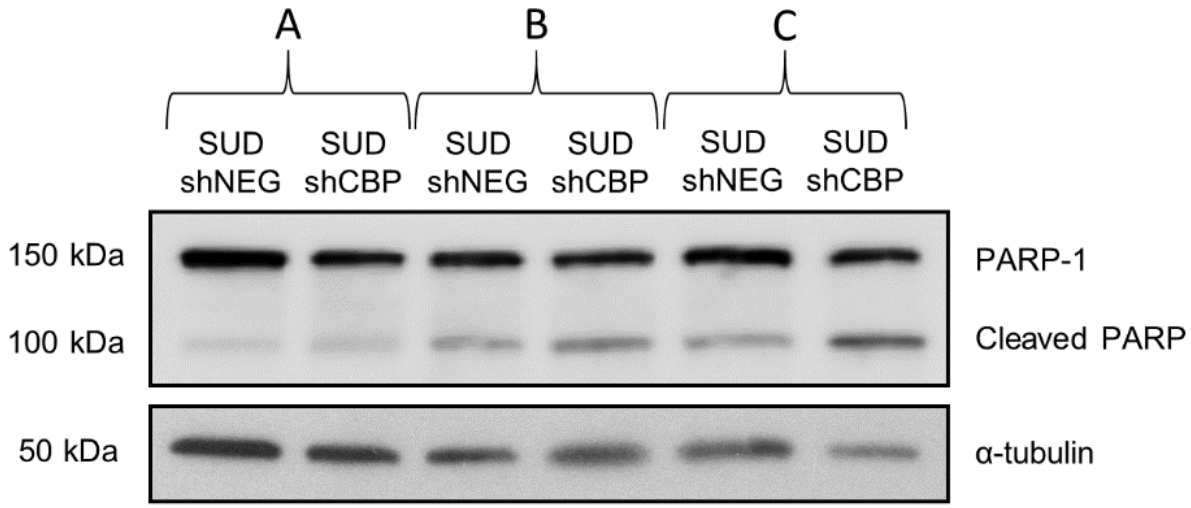

Figure 5.8. PARP-1 expression in SU-DHL-4 cells with stable CREBBP knockdown. Whole cell lysates from SUDshCBP and SUDshNEG were collected on three separate occasions (A-C) and western blotting for PARP-1 expression was carried out. A band for cleaved PARP was also detected by the antibody and can be seen at around 100kDa. Alpha tubulin was included as loading control.

5.5.2 CREBBP Knockdown and Temozolomide Sensitivity

As discussed previously, temozolomide is an alkylating agent which can add methyl adducts to N^7 guanine, O^6 guanine and N^3 adenine (Horspool *et al.*, 1990; Cheng *et al.*, 2005). This makes it a useful tool for studying DNA damage repair. CREBBP knockdown in PreB 697 ALL cells gave inconsistent results, with shRNA transduced cells showing an increased sensitivity to temozolomide and siRNA transfected cells showing no differential sensitivity (Sections 3.8.3 and 4.2.6). To test this in the context of DLBCL, SUDshCBP and SUDshNEG cells were treated with temozolomide and cell viability was assessed after 96 hours by alamar blue assay (Section 2.6.2). Both cell lines were found to be completely resistant to temozolomide with a GI_{50} concentration not being reached at up to 257µM temozolomide treatment (Figure 5.9). Given that these cells were resistant to temozolomide, it is clear that they are not an informative model for the study of CREBBP knockdown on response to damage induced by alkylating agents in DLBCL.

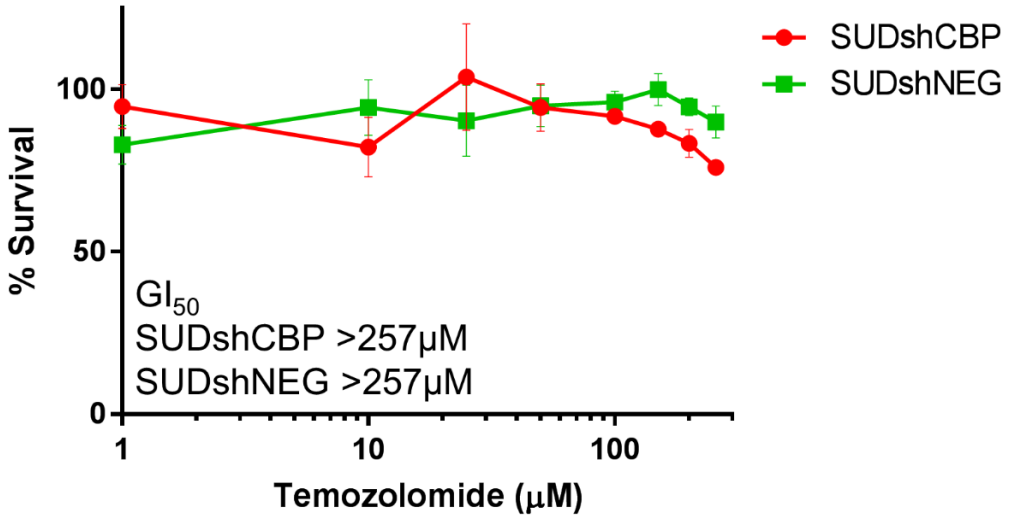

Figure 5.9. Effect of transient CREBBP knockdown in SU-DHL-4 cells on sensitivity to temozolomide. SUDshCBP and SUDshNEG cells were assessed for sensitivity to temozolomide by alamar blue drug sensitivity assay over 96 hours. Histogram shows mean survival ±SD (n=1).

5.5.3 CREBBP Knockdown and MGMT Expression

Given that SU-DHL-4 cells were found to be resistant to temozolomide, other means were sought to study the effect of CREBBP knockdown on direct DNA damage response. In Chapter 3 PreB ALL cells with CREBBP knockdown were shown to have no effect on the expression of direct DNA damage repair protein MGMT (Section 3.8.4). To assess this in DLBCL, western blotting for MGMT was carried out using whole cell lysates from SUDshCBP and SUDshNEG cells (Section 2.5). MGMT is predicted to separate at 25kDa on a western blot but the antibody used showed bands at 37kDa and 20kDa as well as a band at 25kDa. This suggests that other isoforms or modified versions of MGMT could be present in the cell line, or that the antibody is prone to non-specific binding. Attempts were made to establish western blotting with an alternative anti-MGMT antibody (Santa Cruz N-16) but were not successful. Regardless of antibody complications, there is no consistent evidence in the band pattern to suggest that MGMT protein expression is altered in CREBBP knockdown cells compared to controls (Figure 5.10).

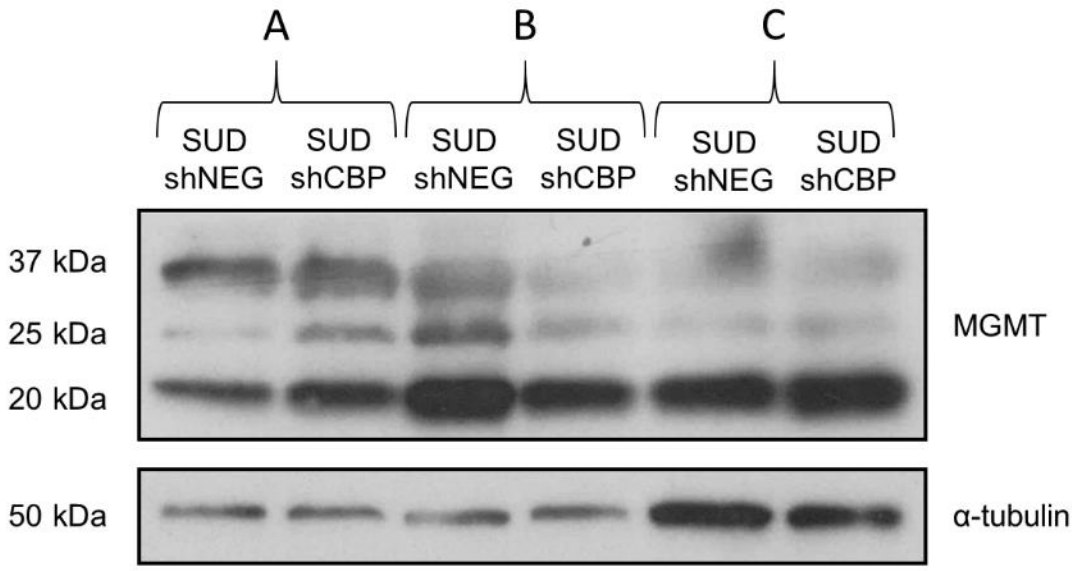

Figure 5.10. MGMT expression in SU-DHL-4 cells with stable CREBBP Knockdown. Whole cell lysates from SUDshCBP and SUDshNEG were collected on three separate occasions (A-C) and western blotting for MGMT expression was carried out. Alpha tubulin was included as loading control.

5.5.4 CREBBP Knockdown and Ionising Radiation Sensitivity

To study the effect of CREBBP knockdown on response to ionising radiation in DLBCL, SUDshCBP and SUDshNEG cells were assessed for sensitivity to ionising radiation. Cells were exposed to 0.3-8.8 Gy radiation and their viability was assessed by alamar blue assay following 96 hours incubation (Section 2.6.2). SU-DHL-4 cells were found to be highly resistant to ionising radiation, with a GI_{50} concentration not being reached (>8Gy) (Figure 5.8). This makes them a poor model for studying the effects of CREBBP knockdown in lymphoma on sensitivity to ionising radiation, and indeed no differential sensitivity was seen between SUDshCBP and SUDshNEG cells.

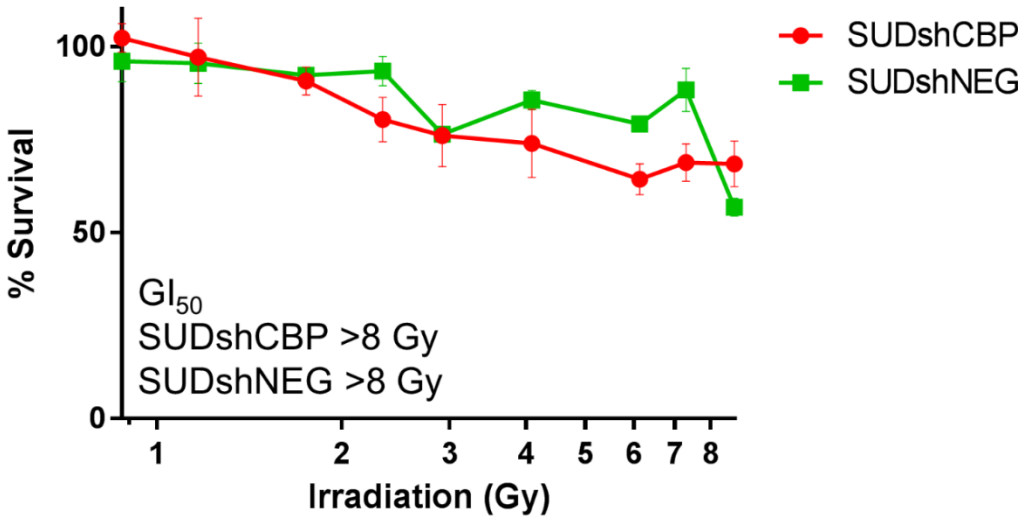

Figure 5.11. Effect of stable CREBBP knockdown in SU-DHL-4 cells on sensitivity to ionising radiation. SUDshCBP and SUDshNEG cells were assessed for sensitivity to ionising radiation by alamar blue drug sensitivity assay over 96 hours. Histogram shows mean survival ±SD (n=1).

5.6 Assessment of MHC Class II Surface Expression on SU-DHL-4 and PreB 697 Cells with Stable CREBBP Knockdown

Studies in FL have identified that *CREBBP* mutations are associated with a signature of decreased antigen presentation, with reduction in the abundance of MHC class II on tumour B cells, hypothesised to contribute to immune evasion by the tumour (Green *et al.*, 2015). To assess this in DLBCL, SU-DHL-4 cells with CREBBP knockdown were assessed for cell surface expression of the MHC class II protein, HLA-DR, by flow cytometry. Though antigen presentation by ALL cells is known to be weak, PreB 697 cells with stable CREBBP knockdown were also assessed for HLA-DR surface expression to assess this hypothesis in the context of ALL (Todisco *et al.*, 2002).

Cells were stained with an antibody targeting HLA-DR and assessed by flow cytometry (Section 2.3.3). A trend towards reduced HLA-DR expression was seen in SU-DHL-4 cells with CREBBP knockdown, with ~1.2 fold reduction compared to control, much less than the ~8 fold reduction seen in FL cells with *CREBBP* mutation (Figure 5.12) (Green *et al.*, 2015). As expected, cell surface expression of HLA-DR was lower in SU-DHL-4 cells compared to PreB 697 cells, with around ~5 fold lower expression observed (Figure 5.12). Interestingly, PreB 697 cells with stable CREBBP knockdown had ~1.3 fold greater expression of HLA-DR compared to control (Figure 5.12). These data suggest that *CREBBP* haploinsufficiency may play a role in suppression of antigen presentation as in FL, though may have the opposite effect in BCP-ALL cells.

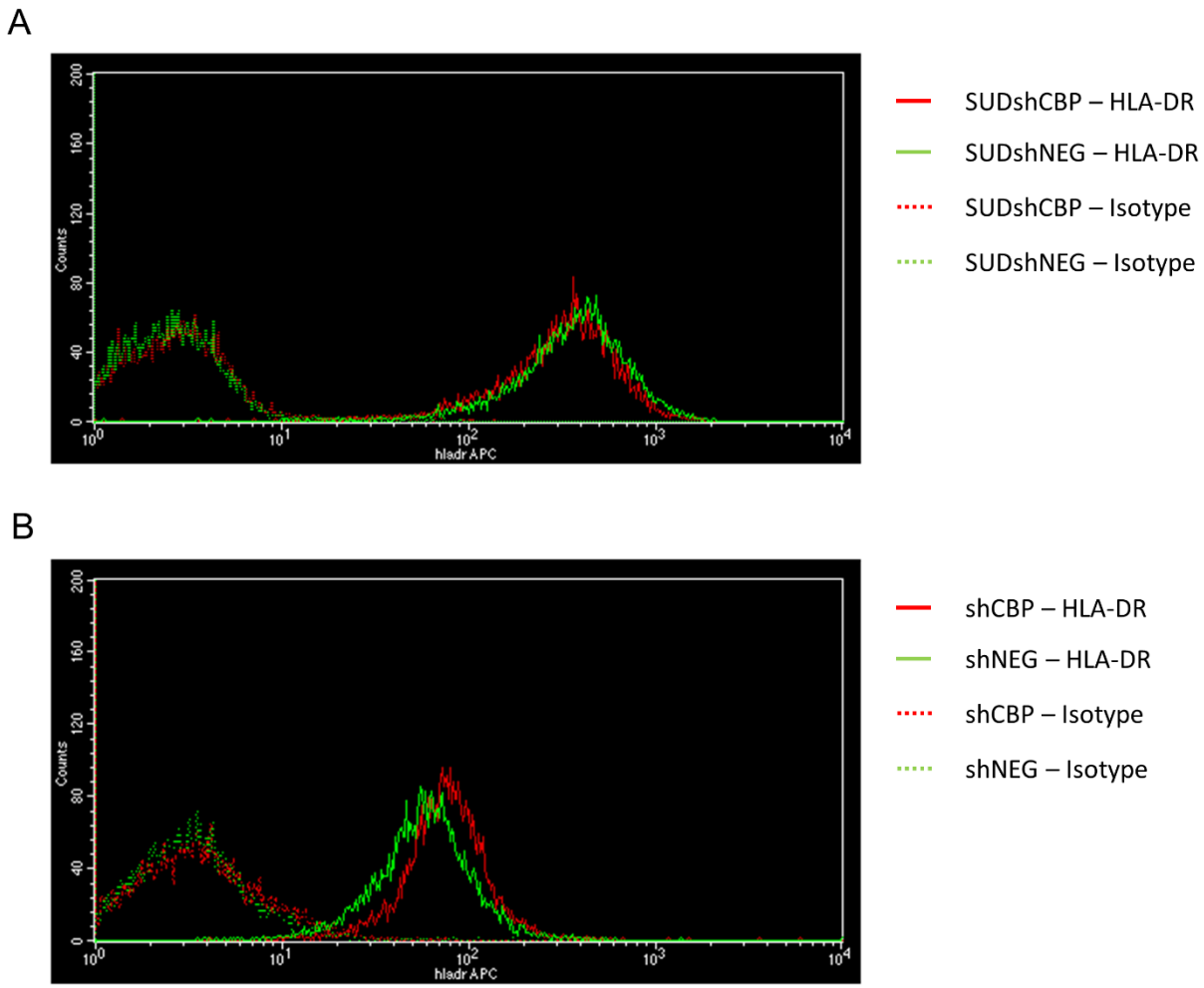

Figure 5.12. Effect of stable CREBBP knockdown in SU-DHL-4 and PreB 697 cells on HLA-DR expression. A. SU-DHL-4 and **B.** PreB 697 cells in exponential growth phase were assessed for cell surface expression of the MHC class II protein HLA-DR by flow cytometry using a HLA-DR APC antibody and isotype control.

5.7 Discussion

The aim of this chapter was to investigate the molecular pathology of *CREBBP* mutations in DLBCL through the creation and characterisation of an isogenic cell line with stable CREBBP knockdown and to compare data with those gathered in ALL cells. This chapter has addressed the effects of CREBBP knockdown in DLBCL on cell proliferation, cAMP-dependent gene expression, drug sensitivity, DNA damage repair and antigen presentation.

Stable knockdown of CREBBP in SU-DHL-4 produced a model of *CREBBP* haploinsufficiency in DLBCL with CREBBP protein expression that closely matched that seen in DLBCL cell lines with *CREBBP* mutation and patients with mono-allelic *CREBBP* deletions (Pasqualucci *et al.*, 2011). Whilst reduction in *CREBBP* mRNA expression was slightly lower in SU-DHL-4 cells with CREBBP knockdown than was shown in BCP-ALL cell lines, protein knockdown was comparable. In keeping with data collected in BCP-ALL cell lines and primagraft samples, CREBBP knockdown in SU-DHL-4 cells showed no effect on cell proliferation, further suggesting that *CREBBP* haploinsuffiency does not contribute to relapse/tumour progression by disrupting cell cycle control. CREBBP knockdown in SU-DHL-4 cells had an inconsistent effect on acetylation of H3K18 and H3K27, which differs from studies in BCP-ALL cells and primagrafts in which acetylation of at least one of these residues was reduced by CREBBP knockdown. This is however, in keeping with previous evidence which shows that different *CREBBP* mutations lead to varying levels of AcH3K18 impairment (Pasqualucci *et al.*, 2011).

The cAMP-dependency of genes differed in SU-DHL-4 cells compared to BCP-ALL cells, with *RGS1* and *DUSP5* identified as most cAMP-dependent by GEP (3.7 and 2.9 Log2 fold change compared to untreated, respectively) and none of the genes identified as cAMP-dependent in BCP-ALL showing significant upregulation in response to cAMP stimulation. Importantly however, CREBBP knockdown only led to impaired cAMP-induced expression of *DUSP5* that just reached statistical significance (p=0.047) and had no significant effect on *RGS1*, suggesting that, like in ALL *CREBBP* haploinsufficiency does not significantly impair cAMP-dependent gene expression and that residual CREBBP expression is able to compensate.

Previous studies have shown that HDACi can lead to apoptosis in GC-resistant cells, that *CREBBP*/EP300 mutation in DLBCL may lead to increased sensitivity to HDACi and that histone acetylation deficits in RSTS cell lines can be reversed using HDACi (Tsapis *et al.*, 2007; Mullighan *et al.*, 2011; Andersen *et al.*, 2012; Lopez-Atalaya *et al.*, 2012). Despite this and as shown in BCP-ALL models of CREBBP knockdown, SU-DHL-4 cells with CREBBP knockdown were not shown to be differentially sensitivity to vorinostat compared to control. This suggests that, in both BCP-ALL and DLBCL, rebalancing HDAC levels alone is not sufficient to cause cell death in *CREBBP* haploinsufficient cells.

In FL, *CREBBP* haploinsufficiency has been linked to immune evasion. *CREBBP* mutation was shown to cause an 8.1 fold reduction in expression of the MHC class II protein HLA-DR on the surface of *CREBBP* mutant tumour B cells compared to those with wild type *CREBBP* expression (Green *et al.*, 2015). Similar to FL, expression of HLA-DR was lower in SU-DHL-4 cells with stable CREBBP knockdown compared to control cells, though the fold difference was much more modest (~1.2 fold SU-DHL-4). This suggests that, as in FL,

CREBBP haploinsufficiency in DLBCL may contribute to tumour progression and drug resistance through immune evasion, though to a lesser extent. As expected, given that PreB cells are poor antigen presenting cells (Todisco *et al.*, 2002), PreB 697 cells had lower expression of HLA-DR but surprisingly, cells with stable CREBBP knockdown showed ~1.3 fold increase in HLA-DR expression compared to control cells. This suggest that *CREBBP* haploinsufficiency may not contribute to immune evasion in ALL but may actually serve to increase antigen presentation.

Unfortunately, SU-DHL-4 cells proved to be a poor model for the study of many molecular mechanisms in which CREBBP is involved. For example, SU-DHL-4 cells were shown to be dexamethasone resistant, precluding any studies into the effects of CREBBP knockdown on GC induced GR target expression and GC sensitivity. Further to this cells were found to be p53 mutant and resistant to ionising radiation and temozolomide, so studying the effects of CREBBP knockdown on p53 acetylation and DNA damage response in DLBCL was not possible using this cell line. SU-DHL-4 cells do not harbour a RAS pathway mutation and though important, RAS pathway mutations are rare in DLBCL so studies into the effect of *CREBBP* haploinsufficiency on enhancement of oncogenic RAS pathway activation were not carried out using this cell line (Lohr *et al.*, 2012).

Given the drawbacks of using the SU-DHL-4 cell line and that many B-NHL cell lines with *CREBBP* wild type status are GC resistant and/or p53 mutant, the use of *in vivo* models may be more effective for future studies (Chang *et al.*, 1995; Amini *et al.*, 2002; Warris *et al.*, 2015). Patient lymphoma cells are amenable to engraftment in immunodeficient mice, as was shown using patient ALL samples in Chapter 4 (Donnou *et al.*, 2012). Again, the tumour microenvironment is a vital and complicated part of tumour growth and

development, which is not present *in vitro*. The use of *in vivo* models for future studies is further supported by data collected in Chapter 4, which suggest that CREBBP knockdown alters cell line growth *in vivo*. A study looking at *NF1* mutations cooperating with *SUZ12* mutations in cancer showed consistency between shRNA knockdown in cell lines, patient samples and *in vivo* models of NF1 and SUZ12 deficiency (De Raedt *et al.*, 2014). This shows that use of shRNA and *in vitro* models can successfully model patient disease. On the other hand inconsistency between *in vitro* and *in vivo* data often occurs. For example, resveratrol was shown to cause cell death in the mouse myeloid leukaemia cell line 32Dp210, but only a very weak anti-leukaemic effect was seen when administered to mice injected with leukaemia cells (Gao *et al.*, 2002). Further to this, inconsistencies between *in vitro*, *ex vivo* and *in vivo* models have been shown in a study of stress hormones on the cell cytotoxicity of natural killer cells, with *in vitro* models overestimating the suppressive effects of stress hormones and *ex vivo* models potentially exaggerating suppression by GC (Gotlieb *et al.*, 2015).

In summary, data collected in SU-DHL-4 cells with stable CREBBP knockdown show many similarities with those collected in ALL cell lines and primagraft samples. Expression of MHC class II surface protein HLA-DR was reduced in SU-DHL-4 cells with CREBBP knockdown suggesting that *CREBBP* haploinsufficiency in DLBCL, like FL, may lead to immune evasion by reduced antigen presentation to some extent. The opposite effect was seen in PreB 697 cells with stable CREBBP knockdown suggesting that this immune evasion phenotype may not exist in ALL. Whilst DLBCL cells clearly have different specificities for acetylation of H3 lysines and cAMP-dependent targets, CREBBP

knockdown only had a minor effect on cAMP-dependent target expression. Similarly, CREBBP knockdown does not appear to induce chemoresistance in DLBCL or impact on DNA damage response. Unfortunately, the use of a cell line based approach did not allow for assessment of GC response or p53/BCL6 activity and so future studies *in vivo* are required to address the effect of *CREBBP* haploinsufficiency in DLBCL on these processes. Further to this, a similar approach should be carried out in FL to address to address the role of *CREBBP* haploinsufficiency in this form of B-NHL.

Chapter 6 – Overall Summary and Future Directions

6.1 Overall Summary and Future Directions

Childhood relapsed ALL, DLBCL and FL represent a group of malignancies which have a poor prognosis and for which there is a clear need for development of novel therapies. All three of these malignancies show frequent heterozygous inactivating mutations in the epigenetic modifier *CREBBP* (Mullighan et al., 2011, Pasqualucci et al., 2011). The molecular mechanisms behind the pathogenesis of *CREBBP* haploinsufficiency in these diseases remains poorly understood, with few functional studies carried out to date. A previous study in T-ALL and MEF cell lines suggested that *CREBBP* haploinsufficiency alters GC response and with GC comprising a pivotal treatment for lymphoid malignancies, could explain the frequency of *CREBBP* mutation in these diseases (Mullighan et al., 2011). Understanding the role of *CREBBP* haploinsufficiency in lymphoid malignancies is of key importance and could allow the development of novel therapies which are so crucially needed.

The aim of the study described in this thesis was to investigate the molecular pathology of *CREBBP* haploinsufficiency in relapsed ALL and B-NHL, addressing the hypothesis that *CREBBP* haploinsufficiency leads to drug resistance and that targeting it may allow resensitisation to therapy in childhood relapsed ALL, DLBCL and FL.

As the majority of *CREBBP* mutations found in ALL and DLBCL lead to mono-allelic HAT inactivation, recapitulation of this was sought in model systems (Mullighan et al., 2011, Pasqualucci et al., 2011). Initially, an isogenic BCP-ALL cell line with stable CREBBP knockdown (established as part of MRes project) was characterised. This PreB 697 cell line was shown to have around 40% reduction of *CREBBP* mRNA expression and a protein reduction similar to that observed in primary ALL samples with monoallelic *CREBBP*

deletions. Transient CREBBP knockdown was also carried out in PreB 697 cells, hypodiploid MHH-CALL-2 cells and a method of transient knockdown of CREBBP in primagraft cells was optimised and carried out in 3 individual primagraft samples to validate data collected in PreB 697 cells with stable CREBBP knockdown. This allowed the study of *CREBBP* haploinsufficiency in relevant cytogenetic contexts and in patient derived ALL. Reduction in mRNA and protein expression was found to be similar across all of these models and protein reduction was in line with that seen in patient derived material. Using the same shRNA construct, stable CREBBP knockdown was carried out in the DLBCL cell line SU-DHL-4, in order to study the effects of *CREBBP* haploinsufficiency in the context of DLBCL. CREBBP mRNA and protein reduction were in line with those seen in ALL CREBBP knockdown models and also DLBCL cell lines with *CREBBP* mutation (Pasqualucci et al., 2011). Two key CREBBP target residues include H3K18 and H3K27 and these were used to assess the functional effect of CREBBP knockdown in cell lines and primagraft samples. In the majority of cases acetylation at one of these residues was reduced when CREBBP was knocked down. This was not true in all cases, for example L779 primagraft cells and SU-DHL-4 cells showed no consistent effect of CREBBP knockdown on acetylation of these residues. This could be explained by compensation from EP300, or different specificities for acetylation of these residues between cell types (Henry et al., 2013).

New, more specific techniques for modelling heterozygous mutations now exist, such as the clustered regularly interspaced short palindromic repeats (CRISPR)/Cas9 system. CRISPR/Cas9 is a genome editing technique in which cells are transfected with the Cas9 endonuclease along with specifically designed RNA guides which direct the induction of double strand DNA breaks through hybridisation. This system can be used to specifically

induce mono-allelic sequence changes (Paquet et al., 2016). Using this system in ALL and DLBCL cell lines and primagraft samples would allow modelling of patient specific mono-allelic *CREBBP* mutations, better representing patient disease and allowing more precise study and comparison of specific individual *CREBBP* mutations.

CREBBP plays an important role in cAMP-dependent signalling, a ubiquitous signalling pathway which regulates genes involved in metabolism, signalling, proliferation, differentiation and survival, through CREB activation (Mayr and Montminy, 2001). This pathway is critically involved in lymphocyte development and is known to interplay with the GC-induced apoptotic response in lymphoma cells (Rickles et al., 2010). De-regulation of cAMP signalling is found in a number of cancers, including AML, with CREB playing a role in myelopoiesis and CREB knockdown shown to reduce proliferation of myeloid cells (Sakamoto and Frank, 2009). Lymphocytes at different stages of differentiation are highly susceptible to cAMP/PDE-induced apoptosis, a susceptibility which has also been shown in murine lymphoma models and T-ALL cell lines (Daniel et al., 1973, Coffino et al., 1975, Ogawa et al., 2002, Smith et al., 2005). Crucially, this signalling pathway can be enhanced by using cAMP agonists, or by inhibiting PDEs, an approach which has proved successful in overcoming CREBBP functional deficiency in a mouse mode of RSTS (Bourtchouladze et al., 2003). The cAMP-induced expression of cAMP transcriptional targets was unaffected by CREBBP knockdown in the majority of ALL models and similarly, most targets were unaffected in SU-DHL-4 cells. These data suggest that *CREBBP* haploinsufficiency does not interfere with cAMP-dependent gene expression in ALL and DLBCL and preclude the use of PDEi to enhance cAMP signalling in *CREBBP* haploinsufficient disease.

CREBBP plays a body-wide role in transcription and cell cycle control, interacting with the TATA-box binding protein (TBP) and transcription factor II B (TFIIB), both of which are involved in the formation of the RNA polymerase pre-initiation complex, as well as the APC/C which is involved in cell cycle progression (Yuan et al., 1996, Kwok et al., 1994, Turnell et al., 2005). Further to this, CREBBP has been shown to play a role in cell fate decisions, influencing the timing and level of pre-mRNA processing in genes involved in HSC regulation (Lemieux et al., 2011). Although stable CREBBP knockdown in PreB 697, or transient knockdown in any cell line or primagraft sample, had no significant impact on cell proliferation *in vitro*, the *in vivo* growth of stably transduced PreB 697 cells was markedly different. Cells with stable CREBBP knockdown maintained this knockdown when engrafted into mice, as assessed by GFP expression of spleen cells. Mice engrafted with these CREBBP knockdown cells lived longer and had larger spleens and livers than mice engrafted with control cells. The actions of CREBBP are known to be highly context dependent, so it is possible that growth *in vivo* offers a better insight into the behaviour of cells with *CREBBP* haploinsufficiency (Giordano and Avantaggiati, 1999, Goodman and Smolik, 2000). Given the role of CREBBP in HSC regulation, it is possible that CREBBP knockdown alters *in vivo* cell growth through the production of a sub-set of cells with a stem-cell-like profile. In AML, stem cell gene expression signatures have been linked to inferior outcomes (Eppert et al., 2011). Cell cycle studies should be carried out to determine any differences between CREBBP knockdown and control cells grown *in vivo* and future experiments should utilise *in vivo* models of *CREBBP* haploinsufficiency, so as not to miss any important microenvironment-mediated effects.

Glucocorticoids are a mainstay treatment for lymphoid malignancies, so resistance to these therapeutic agents could contribute to refractory disease or establishment of relapse. In childhood ALL, GC sensitivity is a significant prognostic indicator, with patients who respond well shown to have a better outcome than poor responders (Riehm et al., 1987, Reiter et al., 1994, Schrappe et al., 2000). Further to this, the *in vitro* sensitivity of cells from patients with relapsed ALL is reduced up to 300 fold compared to cells taken at diagnosis (Klumper et al., 1995, Kaspers et al., 2005). Stable CREBBP knockdown in PreB 697 cells showed impaired induction of *GILZ*, *FKBP5* and *NR3C1* following GC stimulation and microarray data predicted impaired GR transcription. This was not recapitulated in transiently knocked down cell lines and primagraft samples, all of which showed normal GC-induced GR target expression for the majority of genes assayed. This could be explained by differences between stable and transient knockdown of CREBBP, though protein and mRNA knockdown were consistent between these RNAi methods. Crucially CREBBP knockdown did not lead to GC resistance in any cell line or primagraft sample assayed, suggesting that *CREBBP* haploinsufficiency in ALL does not contribute to relapse through GC resistance. Taken together, these data suggest that *CREBBP* haploinsufficiency in ALL does not impair GC response and that residual wild type CREBBP expression is clearly sufficient to compensate for this haploinsufficient loss of expression. This hypothesis was not addressed in SU-DHL-4 cells as they were found to be inherently GC resistant.

Though CREBBP knockdown did not lead to GC resistance in any ALL cell model assessed, it was hypothesised that it may play a role in drug resistance, explaining the frequency of *CREBBP* mutations at relapse. Heterozygous loss of the methyltransferase *SETD2* in

leukaemia has been shown to cause resistance to the ALL chemotherapeutics, 6-thioguanine and cytarabine (Mar et al., 2015). PreB 697 cells with stable CREBBP knockdown were assessed for sensitivity to a panel of common ALL chemotherapeutics and it was found that CREBBP knockdown had no effect on sensitivity to these agents. Similarly stable CREBBP knockdown in SU-DHL-4 cells had no effect on sensitivity to daunorubicin or 6-thioguanine. These cells did however, show a slight significant increase in sensitivity to the tubulin binding drug vincristine, though given that this difference was in the nm range (GI_{50} values, mean ±SD; SUDshCBP 2.6nM ±0.12 versus SUDshNEG 3.1nM ±0.11; p=0.009), it is unlikely to be biologically relevant. Taken together with dexamethasone sensitivity data, these data suggests that *CREBBP* haploinsufficiency does not induce a drug resistance phenotype *in vitro* in ALL and DLBCL.

Previous studies have shown that HDACi can lead to apoptosis in GC-resistant cells, that *CREBBP*/*EP300* mutation in DLBCL may lead to increased sensitivity to HDACi and that histone acetylation deficits in RSTS cell lines can be reversed using HDACi (Mullighan et al., 2011, Tsapis et al., 2007, Andersen et al., 2012, Lopez-Atalaya et al., 2012). Haematological malignancies seem to be particularly sensitive to HDACi and this type of therapy is generally well tolerated in patients, with two HDACi drugs being approved for the treatment of cutaneous T-cell lymphoma (Stimson et al., 2009, Thurn et al., 2011, Mann et al., 2007). Dexamethasone sensitivity data precluded the hypothesis that the use of HDACi could resensitise to GC treatment by rebalancing acetylation levels in *CREBBP* haploinsufficient cells and indeed, PreB 697 and SU-DHL-4 cells with stable CREBBP knockdown were no more sensitive to HDACi alone or in combination with GC treatment.

CREBBP mutations frequently co-occur with RAS pathway mutations, including *KRAS*, *NRAS*, *PTPN11* and *FLT3* (Malinowska-Ozdowy et al., 2015). Further to this, CREBBP can directly acetylate KRAS (manuscript submitted), a secondary modification shown to have a negative regulatory effect on RAS activity by altering conformational stability of the Switch II domain and thus interaction with guanine nucleotide exchange factors (Yang et al., 2012). This prompted investigation into the effects of *CREBBP* mutation on RAS signalling. Both cell lines and primagraft cells with different RAS pathway mutations, showed consistently increased levels of p-ERK, suggesting that CREBBP inactivation enhances the oncogenic action of RAS pathway activation. Epigenetic modifiers have previously been shown to enhance the oncogenic action of RAS pathway mutations, with homozygous inactivation of the polycomb repressive complex 2 (PRC2) methyltransferase *EZH2* shown to cooperate with *NRAS* (Q16K) mutation in a model of early T-cell precursor (ETP) ALL (Danis et al., 2016). Inactivation of the methyltransferase, EZH2 was shown to cooperate with mutant RAS to induce hyperactive cytokine signalling, principally through STAT3 and was associated with a reduced sensitivity to JAK inhibitors (Danis et al., 2016). Another member of the PRC2, *SUZ12*, has also been shown to cooperate with RAS mutation in a number of solid tumours (De Raedt et al., 2014). Aside from direct interaction with KRAS, another possible candidate to mediate interaction between CREBBP and the RAS pathway is *WNT3*, which was found to be significantly upregulated in CREBBP knockdown cells and which has been shown to activate MAPK signalling in other cell types through a non-canonical pathway (Anne et al., 2013). Notably, increased RAS pathway activation was associated with retention of MEKi sensitivity, which may have important clinical implications. Our group has recently reported on the preclinical evaluation of the MEKi, selumetinib, and demonstrated significant differential sensitivity

in RAS pathway-mutated ALL compared to ALL without RAS mutations, both *in vitro* and in an orthotopic xenograft model engrafted with primary ALL cells (Irving et al., 2014). We recently showed the same response in iAMP21-ALL patients with RAS pathway mutations (Ryan et al., 2016). These robust data have prompted clinical trials of selumetinib for multiple relapsed RAS pathway mutated ALL. As our data show that CREBBP deficient, RAS mutated cells retain sensitivity to MEKi, patients with co-occurring *CREBBP* and RAS mutations are clearly candidates for MEKi therapy. Future studies should concentrate on determining the nature of the interaction between CREBBP and the RAS pathway, particularly KRAS, at relapse in ALL, addressing the potential for targeting CREBBP alongside RAS pathway components as a novel therapeutic approach in *CREBBP*-mutated cancer.

TP53, the gene which encodes p53, is the most commonly mutated gene in cancer (Kandoth et al., 2013). Expression of p53 is also altered by epigenetic regulation, with methylation of the p53 promotor region seen in ~50% of epithelial ovarian cancer specimens (Chmelarova et al., 2013). BCL6 is a transcriptional repressor which provides an environment tolerant of DNA breaks important in the development of germinal centre B-cells and is able to supress apoptosis by directly inhibiting p53 (Basso and Dalla-Favera, 2012, Phan and Dalla-Favera, 2004). Acetylation by CREBBP is vital for the activity of p53, influencing its stability, DNA binding and recruitment of co-activators (Brooks and Gu, 2003, Tang et al., 2008). CREBBP mediated acetylation is also important in the inactivation of BCL6 by disrupting interaction with HDACs and reducing the ability to repress transcription of anti-apoptotic genes, including p53 (Bereshchenko et al., 2002). *CREBBP* mutation has been shown to cause reduced acetylation of p53 and BCL6 *in vitro* and has

also been associated with impaired BCL6 activity (Green et al., 2013, Pasqualucci et al., 2011). The consequence of losing this regulation in lymphoid malignancies would be an environment with increased tolerance for DNA damage with reduced control of cell cycle arrest and apoptosis. Stable CREBBP knockdown in PreB 697 cells had a variable effect on the acetylation of p53, but crucially showed no effect on its basal expression or the expression of downstream p21, suggesting an intact p53 response. Similarly, CREBBP knockdown did not alter basal BCL6 expression. This was not addressed in SU-DHL-4 cells as they were found to be inherently p53 mutant. Taken together these data suggest that *CREBBP* haploinsufficiency does not lead to imbalance of p53/BCL6 activity in ALL. Further experimentation is required to understand the role of *CREBBP* haploinsufficiency in regulation of this tumour suppressor/oncogene pair in B-NHL and solid tumours.

CREBBP has functions within a number of DNA damage response pathways, so abrogation of DNA damage repair represents a potential mechanism of relapse establishment/development in *CREBBP* haploinsufficient malignancies. Indeed, hypermutable genotypes at relapse in ALL have been identified by whole exome sequencing (Ma et al., 2015). A study of *CREBBP* heterozygous mice showed hypersensitivity to gamma radiation, with reduced expression of BER components and reduced PARP activity (Zimmer et al., 2012). This was not recapitulated in PreB 697 cells with stable CREBBP knockdown, suggesting intact BER in these cells. CREBBP plays a role in regulation of the direct DNA damage repair protein MGMT (Bhakat and Mitra, 2000, Teo et al., 2001). MGMT deficiency is known to cause hypersensitivity to chemotherapeutic methylating agents such as temozolomide (Glassner et al., 1999). Interestingly, PreB 697 cells with stable CREBBP knockdown were hypersensitive to

temozolomide, though this was not explained by impairment in MGMT protein expression. Data were not consistent in PreB 697 cells with transient CREBBP knockdown however, where cells were equally sensitive to temozolomide as controls. This difference may be due to the transient nature of siRNA knockdown, however this is unlikely as temozolomide and its derivative 5-(3-methyltriazen-1-yl)imidazole-4-carboxamide (MTIC), have a half-life of around 2 hours and CREBBP protein knockdown was shown to be sustained for at least 96 hours (Kim et al., 1997). SU-DHL-4 cells were found to be resistant to temozolomide and ionising radiation so could not be used for assessment of these DNA damage repair pathways. These observations suggest that *CREBBP* haploinsufficiency in ALL does not alter BER or direct DNA damage repair, though further studies are required to understand if these pathways are abrogated in B-NHL with *CREBBP* mutation.

CREBBP mutations in FL have been associated with reduced antigen presentation, which may allow *CREBBP* mutated cells to evade the immune system (Green et al., 2015). Immune evasion represents a method by which cancer cells can thrive, preventing recognition and destruction by the immune system. As seen in FL cells with *CREBBP* mutation, DLBCL cells with stable CREBBP knockdown showed reduced expression of the MHC class II protein HLA-DR, though the level of reduction was much less profound (~1.2 fold in SU-DHL-4 compared to ~8 fold in FL derived B-cells) (Green et al., 2015). Antigen presentation by ALL cells has been shown to be weak and indeed PreB 697 cells were shown to express lower levels of HLA-DR than SU-DHL-4 cells (Todisco et al., 2002). Interestingly, CREBBP knockdown in PreB 697 cells led to an increase in expression of HLA-DR. These data suggest that *CREBBP* haploinsufficiency may contribute to reduced antigen

presentation in DLBCL, much like FL, but not in ALL, where it appears to enhance antigen presentation. Future studies should investigate this further, looking at a range of MHC class II components and using primary derived samples.

Mutations in epigenetic regulators represents a mechanism by which cancer cells can drastically alter gene expression and cellular functions. Global alterations in the epigenetic landscape are a hallmark of cancer and can result in inhibition or activation of various signalling pathways which lead to cancer (Sharma et al., 2010). A wide range of epigenetic regulators have been identified as frequently mutated in cancer, but the exact functional impact of these mutations is poorly understood because of their complex and often context-dependent roles. For example, a number of epigenetic regulators are frequently mutated in AML, including *DNMT3A* and *TET2*, both of which are associated with adverse outcome (Abdel-Wahab and Levine, 2013, Chou et al., 2011). *CREBBP* mutations have been identified as a frequent event in a large number of solid tumours including; transitional cell carcinoma of the bladder, medulloblastoma, small cell lung cancer, adenoid cystic carcinoma, oesophageal squamous cell cancer, glioblastoma, squamous cell carcinoma and breast cancer (Gui et al., 2011, Robinson et al., 2012, Huether et al., 2014, Peifer et al., 2012, Gao et al., 2014a, Han et al., 2014, Ho et al., 2013, Song et al., 2014, Gao et al., 2014b, Mukasa et al., 2014, Watt et al., 2016, Jansen et al., 2016). Given that CREBBP appears to be acting as an enhancer of oncogenic signalling in relapsed ALL, this suggests that it may carry out a similar role in solid tumours. Further to this, mutations in other epigenetic regulators found in cancer may play a similar role. Screening for genes which are synthetically lethal when knocked out in *CREBBP* mutant cells could unearth therapeutic targets for these *CREBBP* mutant tumours. This also could allow the

development of a novel therapeutic targeting method in which both oncogene and respective epigenetic enhancer are targeted in order to achieve better treatment efficacy.

6.2 Overview

This study has shown some of the first mechanistic insights into *CREBBP* haploinsufficiency in childhood relapsed ALL and DLBCL, using cell lines and primary derived cells. The data collected in this study do not support a role for *CREBBP* mutation in resistance to chemotherapy, but have identified its role in enhancing oncogenic RAS signalling in ALL. This function may be relevant in a wide range of cancers, with targeting of *CREBBP* mutation in combination with cancer-specific oncogenes representing a potential novel therapeutic approach.

Appendices

Appendix 1 – Gene expression microarray data

Differential Gene Expression in PreB 697 Cells Treated with IBMX and Forskolin

ID	symbol	log2FC	AveExpr	P.Value
217028_at	CXCR4	3.964	10.779	7.896E-08
218205_s_at	MKNK2	2.544	10.695	2.126E-09
202431_s_at	MYC	-5.790	10.323	5.765E-08
209486_at	UTP3	-1.783	9.042	1.590E-09
215111_s_at	TSC22D1	2.151	9.002	1.068E-08
209201_x_at	CXCR4	4.618	8.848	1.938E-09
203752_s_at	JUND	2.139	8.837	5.571E-08
202284_s_at	CDKN1A	1.260	8.406	4.629E-08
211919_s_at	CXCR4	4.697	8.163	6.295E-09
201751_at	JOSD1	1.927	8.152	4.067E-08
208622_s_at	EZR	2.343	8.117	6.804E-08
201368_at	ZFP36L2	3.152	7.895	5.680E-09
212430_at	RBM38	2.511	7.439	1.058E-07
223199_at	MKNK2	2.736	7.426	4.413E-08
227846_at	GPR176	1.734	7.424	3.331E-08
209324_s_at	RGS16	4.134	7.118	2.218E-08
201473_at	JUNB	3.488	7.076	2.146E-10
239427_at	SLAMF1	-1.610	6.983	4.900E-08
201531_at	ZFP36	2.975	6.723	3.457E-08
243174_at	NA	-3.080	6.613	3.467E-08
202499_s_at	SLC2A3	4.614	6.176	2.055E-08
226924_at	LINC00909	-2.144	6.029	4.134E-08
205289_at	BMP2	4.636	5.992	3.463E-09
227410_at	FAM43A	4.165	5.698	5.124E-09
202815_s_at	HEXIM1	2.343	5.561	9.961E-08
41577_at	PPP1R16B	2.960	5.436	1.450E-08
203910_at	ARHGAP29	5.476	5.421	3.930E-08
207630_s_at	CREM	4.677	5.327	3.560E-09
1553099_at	TIGD1	-2.468	4.891	8.901E-08
201236_s_at	BTG2	4.681	4.624	2.678E-08
208763_s_at	TSC22D3	5.218	4.599	1.821E-10
202340_x_at	NR4A1	3.749	4.432	4.547E-08
216236_s_at	NA	3.165	4.374	5.753E-10
204491_at	PDE4D	4.680	4.244	4.040E-09
214508_x_at	CREM	5.503	4.231	3.122E-10
217875_s_at	PMEPA1	3.738	4.147	5.145E-08
209967_s_at	CREM	4.776	4.094	7.059E-09
205463_s_at	PDGFA	4.373	4.082	2.710E-11

221563_at	DUSP10	1.475	4.040	3.286E-08
216268_s_at	JAG1	2.661	4.007	2.022E-08
214873_at	LRP5L	1.481	3.837	5.431E-08
222088_s_at	NA	4.718	3.761	2.727E-08
209189_at	FOS	5.394	3.756	3.202E-08
202497_x_at	SLC2A3	4.615	3.713	1.253E-10
209305_s_at	GADD45B	3.376	3.507	7.289E-08
209099_x_at	JAG1	3.574	3.365	1.887E-09
230233_at	NA	3.181	3.292	3.351E-11
229072_at	RAB30	3.367	3.229	5.222E-08
223217_s_at	NFKBIZ	2.235	2.962	6.877E-10
223887_at	GPR132	2.057	2.896	2.594E-08
201883_s_at	B4GALT1	2.685	7.103	1.150E-07
224797_at	ARRDC3	2.521	6.437	1.153E-07
202498_s_at	SLC2A3	3.375	3.926	1.174E-07
238039_at	LOC728769	-1.699	5.326	1.175E-07
200605_s_at	PRKAR1A	1.399	9.717	1.325E-07
226767_s_at	FAHD1	-1.354	5.693	1.342E-07
223218_s_at	NFKBIZ	3.467	3.300	1.421E-07
219522_at	FJX1	-2.820	7.427	1.451E-07
227558_at	CBX4	3.113	9.107	1.488E-07
202388_at	RGS2	5.405	7.243	1.559E-07
209304_x_at	GADD45B	3.397	6.011	1.609E-07
201369_s_at	ZFP36L2	2.560	5.154	1.711E-07
204602_at	DKK1	-4.014	5.168	1.743E-07
225606_at	BCL2L11	2.604	8.398	1.778E-07
204908_s_at	BCL3	2.296	3.881	1.882E-07
200921_s_at	BTG1	3.034	9.400	1.920E-07
222449_at	PMEPA1	3.868	3.807	2.076E-07
225224_at	C20orf112	1.712	5.261	2.151E-07
203708_at	PDE4B	4.283	3.421	2.821E-07
200920_s_at	BTG1	3.242	8.676	2.894E-07
228498_at	B4GALT1	3.078	5.993	2.894E-07
201739_at	SGK1	3.055	4.453	3.009E-07
201170_s_at	BHLHE40	3.875	3.624	3.406E-07
205562_at	RPP38	-1.941	5.736	3.897E-07
212558_at	SPRY1	4.361	4.694	4.289E-07
229817_at	ZNF608	-1.517	7.625	4.536E-07
212750_at	PPP1R16B	2.799	4.832	4.590E-07
202241_at	TRIB1	-1.314	5.707	4.727E-07
209325_s_at	RGS16	3.736	6.443	4.769E-07
210260_s_at	TNFAIP8	-1.277	9.464	5.377E-07
201631_s_at	IER3	2.179	4.741	5.475E-07
201416_at	SOX4	1.429	10.364	5.482E-07

229943_at	TRIM13	-1.821	7.898	5.625E-07
205290_s_at	BMP2	5.636	4.800	5.935E-07
209034_at	PNRC1	1.198	7.768	6.034E-07
206724_at	CBX4	3.083	3.368	6.083E-07
208078_s_at	NA	5.494	5.076	6.304E-07
204015_s_at	DUSP4	3.499	8.014	6.638E-07
225954_s_at	MIDN	1.142	7.122	6.666E-07
225227_at	SKIL	4.563	4.847	7.224E-07
228098_s_at	MYLIP	2.211	5.610	7.318E-07
223130_s_at	MYLIP	1.616	5.735	7.386E-07
204014_at	DUSP4	3.485	8.347	7.907E-07
212642_s_at	HIVEP2	1.137	7.805	8.700E-07
222450_at	PMEPA1	3.437	3.754	8.841E-07
1555372_at	BCL2L11	2.295	3.502	8.856E-07
202644_s_at	TNFAIP3	3.556	8.071	9.461E-07
204523_at	ZNF140	-1.282	7.949	9.788E-07
209567_at	RRS1	-1.204	9.806	1.020E-06

Genes were sorted by highest average expression then sorted by most significant P value. Top 100 most significant are displayed above. See section 3.3.

Differential Gene Expression in SU-DHL-4 Cells Treated with IBMX and Forskolin

ID	symbol	log2FC
216834_at	RGS1	3.725
209457_at	DUSP5	2.922
204912_at	IL10RA	2.525
228846_at	MXD1	2.379
231124_x_at	LY9	2.318
235444_at	FOXP1	2.241
225191_at	CIRBP	2.205
211962_s_at	ZFP36L1	2.155
209201_x_at	CXCR4	2.147
1564970_at	SETDB2	2.127
230142_s_at	CIRBP	2.083
211919_s_at	CXCR4	2.070
221986_s_at	KLHL24	2.068
236293_at	RHOH	2.028
211965_at	ZFP36L1	2.019
201739_at	SGK1	1.969
228426_at	CLEC2D	1.898
221985_at	KLHL24	1.894
217028_at	CXCR4	1.893
242814_at	SERPINB9	1.849
201041_s_at	DUSP1	1.830
1568751_at	RGS13	1.802
201925_s_at	CD55	1.760
213593_s_at	TRA2A	1.745
233463_at	RASSF6	1.741
208763_s_at	TSC22D3	1.728
202388_at	RGS2	1.714
1555858_at	THUMPD3-AS1	1.703
227223_at	RBM39	1.696
215012_at	ZNF451	1.693
1555827_at	CCNL1	1.692
217591_at	SKIL	1.656
201926_s_at	CD55	1.633
213575_at	TRA2A	1.632
225867_at	VASN	1.623
222542_x_at	ADCK3	1.621
202861_at	PER1	1.605
204951_at	RHOH	1.585
1555950_a_at	CD55	1.565
208536_s_at	BCL2L11	1.556
210322_x_at	UTY	1.548

226541_at	FBXO30	1.548
220035_at	NUP210	1.539
209102_s_at	HBP1	1.526
226404_at	RBM39	1.496
214802_at	EXOC7	1.480
228030_at	RBM6	1.477
1560172_at	INTS10	1.465
1552542_s_at	TAGAP	1.424
202340_x_at	NR4A1	1.420
229574_at	TRA2A	1.410
209750_at	NR1D2	1.399
227231_at	KIAA1211	1.399
235287_at	CDK6	1.396
235167_at	LOC100190986	1.386
225957_at	CREBRF	1.378
210001_s_at	SOCS1	1.377
226318_at	TBRG1	1.373
213359_at	HNRNPD	1.369
225606_at	BCL2L11	1.357
209034_at	PNRC1	1.342
207001_x_at	TSC22D3	1.341
1553785_at	RASGEF1B	1.337
205115_s_at	RBM19	1.313
230060_at	CDCA7	1.313
223494_at	MGEA5	1.310
224797_at	ARRDC3	1.308
1556088_at	RPAIN	1.308
222863_at	ZBTB10	1.301
214508_x_at	CREM	1.284
232431_at	NR3C1	1.274
206530_at	RAB30	1.265
233819_s_at	LTN1	1.263
232421_at	SCARB1	1.241
1553703_at	ZNF791	1.232
228723_at	NPTN-IT1	1.228
229072_at	RAB30	1.225
226158_at	KLHL24	1.218
1565681_s_at	DIP2C	1.216
207980_s_at	CITED2	1.208
206126_at	CXCR5	1.182
221768_at	SFPQ	1.158
207339_s_at	LTB	1.158
204286_s_at	PMAIP1	1.151
1553096_s_at	BCL2L11	1.151

216734_s_at	CXCR5	1.147
219312_s_at	ZBTB10	1.135
81737_at	LOC100505915	1.123
209606_at	CYTIP	1.123
228793_at	JMJD1C	1.123
1558143_a_at	BCL2L11	1.122
236402_at	BRAF	1.120
209357_at	CITED2	1.119
215933_s_at	HHEX	1.113
228390_at	RAB30	1.107
230083_at	USP53	1.107
211584_s_at	NPAT	1.088
237625_s_at	IGKC	1.083
1555878_at	RPS24	1.079
200920_s_at	BTG1	1.066
210077_s_at	SRSF5	1.064
235638_at	RASSF6	1.061
1553704_x_at	ZNF791	1.061
217173_s_at	LDLR	1.060
1556318_s_at	CAND1	1.060
212400_at	FAM102A	1.058
204269_at	PIM2	1.045
229723_at	TAGAP	1.043
238787_at	DENND1B	1.039
213450_s_at	ICOSLG	1.038
219889_at	FRAT1	1.036
201295_s_at	WSB1	1.034
222343_at	BCL2L11	1.032
237504_at	INTS10	1.030
219841_at	AICDA	1.029
217921_at	MAN1A2	1.022
1556183_at	ANKRD36BP2	1.021
236613_at	RBM25	1.018
224499_s_at	AICDA	1.018
1557081_at	RBM25	1.013
232330_at	COA1	1.003
202842_s_at	DNAJB9	1.003

Genes were sorted by greatest Log2 fold change (Log2FC). Shown above are all genes with a Log2FC of ≥1 in IBMX and forskolin treated cells compared to controls. See section 5.3.

Appendix 2 – Presentations

'Targeted therapy for *CREBBP*-mutated lymphoid disease' **Oral Presentation, Childhood Leukaemia Research UK Annual Meeting**, September 2015, The Royal Marsden Education and Conference Centre, London

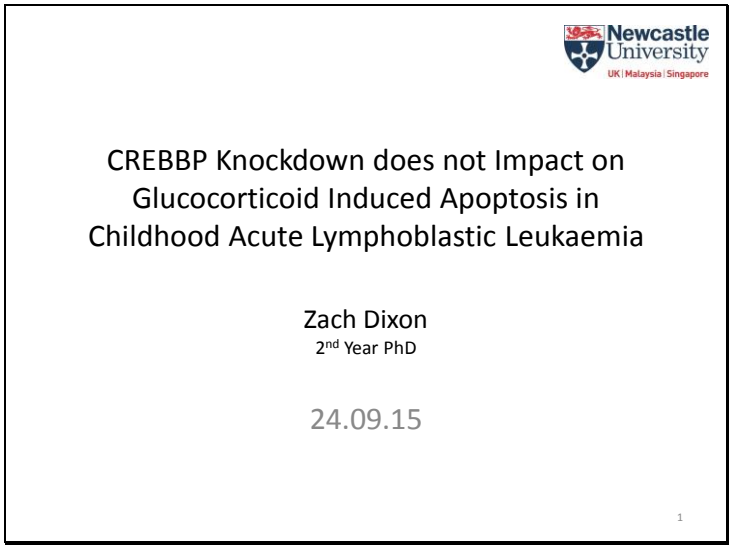

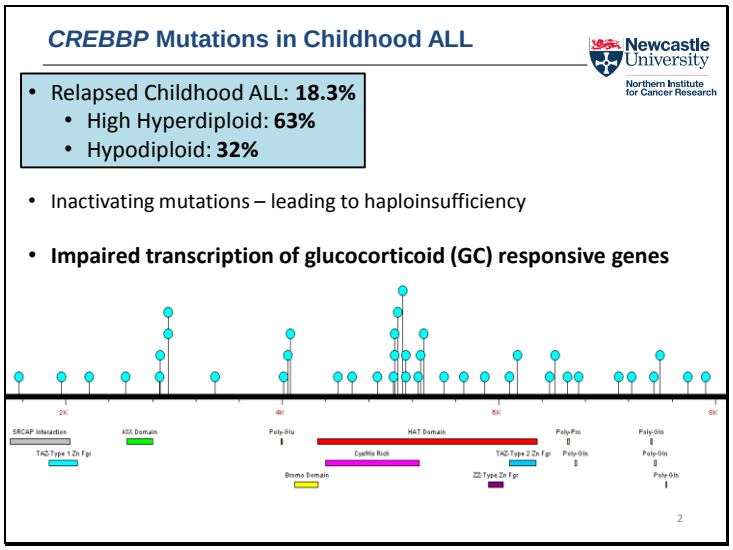

CREBBP

Newcastle University
Northern Institute for Cancer Research

- Cyclic adenosine monophosphate (cAMP) response element binding protein (CREB), binding protein (**CREBBP**)
- Multiple functions carried out by numerous discrete functional domains

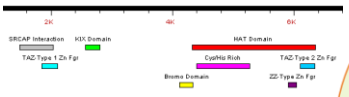

- Cotranscription factor for CREB
  - cAMP Dependent Signalling

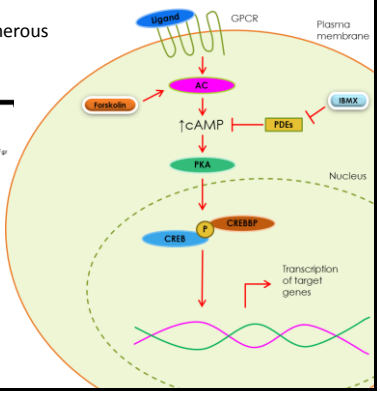

CREBBP

Newcastle University
Northern Institute for Cancer Research

- Acetylation of histone tails
  - H3K18
  - H3K27
- Acetylation mediated activation and inactivation of non-histone proteins
  - **p53**
  - **BCL6**
- Association with DNA damage repair
  - BER (Radiation, alkylating agents)
  - Direct
- Inherited haploinsufficiency = Rubinstein-Taybi Syndrome

4

Aims

Newcastle University
Northern Institute for Cancer Research

- To assess CREBBP as a novel target for therapy in relapsed childhood ALL
  - Study the effect of CREBBP knockdown on glucocorticoid sensitivity

5

CREBBP Knockdown PreB ALL Cell Line

Newcastle University
Northern Institute for Cancer Research

- PreB 697 cells are *CREBBP* wild type
- Lentiviral transduction of shRNA used

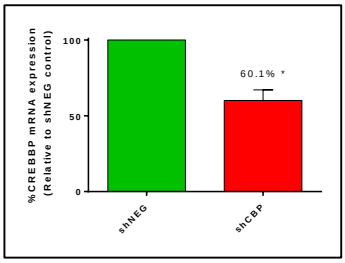

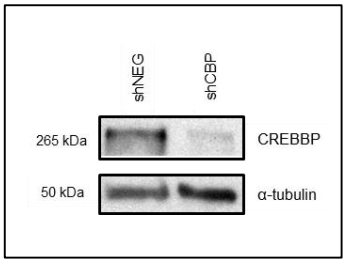

6

CREBBP Knockdown Does Not Influence Induction of cAMP-dependent Genes

Newcastle University
Northern Institute for Cancer Research

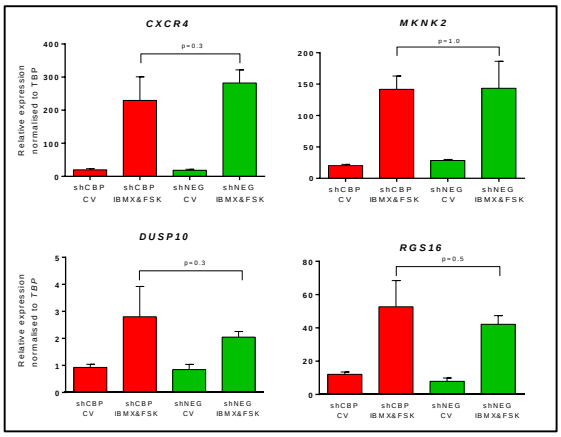

8

CREBBP Knockdown in PreB 697 shCBP Cells is Functionally Relevant

Newcastle University
Northern Institute for Cancer Research

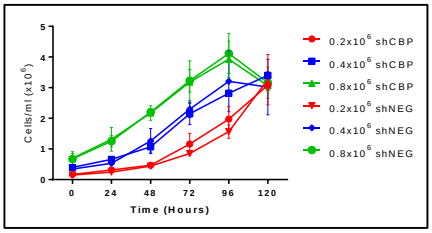

- Average doubling times
  - 32.4 hours shCBP
  - 30.7 hours shNEG
    - p=0.7

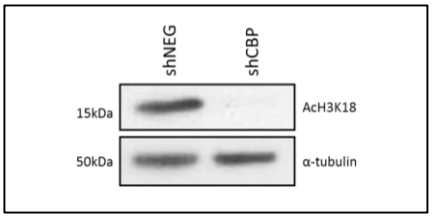

7

CREBBP Knockdown Leads to Impaired Induction of Glucocorticoid Receptor (GR) Targets

Newcastle University
Northern Institute for Cancer Research

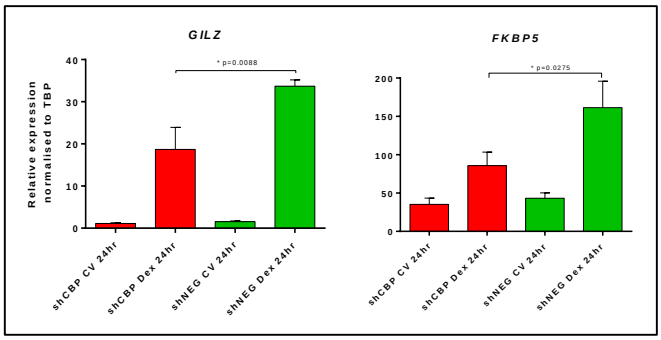

- As seen in Dexamethasone resistant sublines

9

Ingenuity Pathway Analysis Predicts Altered Glucocorticoid Receptor Transcription in PreB 697 shCBP Cells

Newcastle University
Northern Institute for Cancer Research

Symbol	Name	log2FC
SCG2	secretogranin II	2.811834464
THSD7B	thrombospondin, type I, domain containing 7B	2.639797207
OAT	ornithine aminotransferase	2.589780949
DNAJC15	DnaJ (Hsp40) homolog, subfamily C, member 15	-2.498590624
PTGER4	prostaglandin E receptor 4 (subtype EP4)	-2.482098654
FAM198B	family with sequence similarity 198, member B	-2.264160273
SLC22A16	solute carrier family 22 (organic cation/carnitine transporter), member 16	-1.703688787
CASP1	caspase 1, apoptosis-related cysteine peptidase	-1.614572454
SLC16A14	solute carrier family 16, member 14	-1.6082457
ARL10	ADP-ribosylation factor-like 10	-1.563078133
PDIA5	protein disulfide isomerase family A, member 5	-1.500770057
RRAS2	related RAS viral (r-ras) oncogene homolog 2	-1.377499619
SAMHD1	SAM domain and HD domain 1	1.369527899
SMARCAD1	SWI/SNF-related, matrix-associated actin-dependent regulator of chromatin, subfamily a, containing DEAD/H box 1	-1.330626813
CASP2	caspase 2, apoptosis-related cysteine peptidase	-1.283517323
FAM169A	family with sequence similarity 169, member A	1.226601308
ADCY3	adenylate cyclase 3	-1.187742915
PTPRF	protein tyrosine phosphatase, receptor type, F	-1.174186892
NA	NA	-1.173135969
FSCN1	fascin homolog 1, actin-bundling protein (Strongylocentrotus purpuratus)	1.168795854
PHACTR2	phosphatase and actin regulator 2	1.161687475
CASP1	caspase 1, apoptosis-related cysteine peptidase	-1.156531947
TPST1	tyrosylprotein sulfotransferase 1	-1.145784216
PMS2P1	postmeiotic segregation increased 2 pseudogene 1	-1.131322987
PHF20	PHD finger protein 20	-1.126434047
WNT3	wingless-type MMTV integration site family, member 3	1.114859575
LGR6	leucine-rich repeat containing G protein-coupled receptor 6	1.053475268
KIAA1462	KIAA1462	-1.01380384

10

CREBBP Knockdown Has No Effect on Sensitivity to Dexamethasone

Newcastle University
Northern Institute for Cancer Research

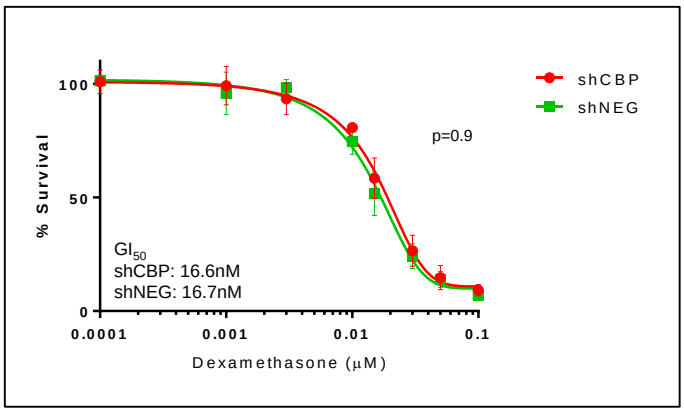

11

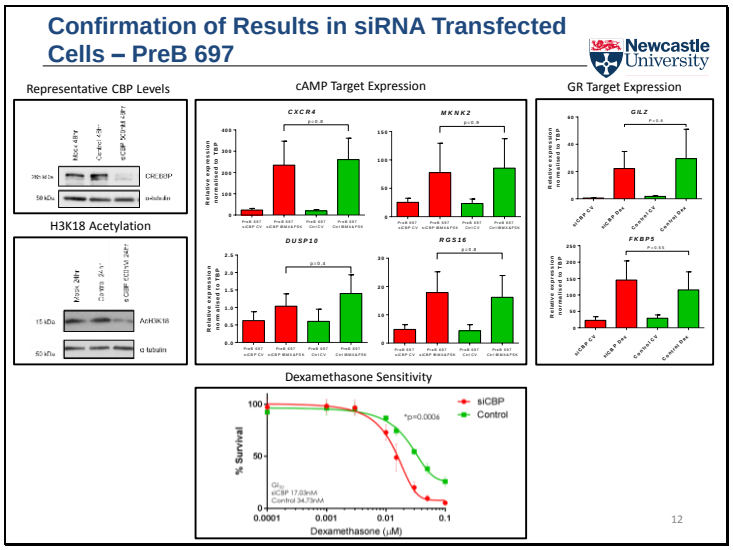
Confirmation of Results in siRNA Transfected Cells – PreB 697
Newcastle University
Representative CBP Levels
cAMP Target Expression
GR Target Expression
H3K18 Acetylation
Dexamethasone Sensitivity
siCBP
Control
% Survival
Dexamethasone (μM)
12

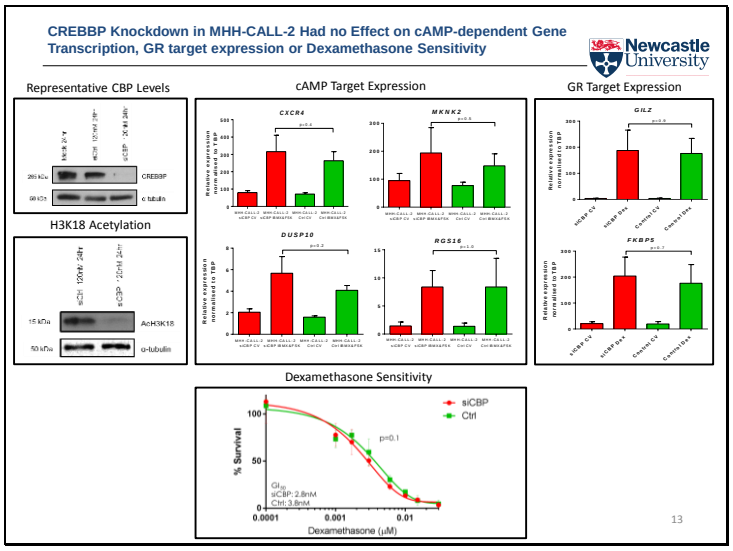
CREBBP Knockdown in MHH-CALL-2 Had no Effect on cAMP-dependent Gene Transcription, GR target expression or Dexamethasone Sensitivity
Newcastle University
Representative CBP Levels
cAMP Target Expression
GR Target Expression
H3K18 Acetylation
Dexamethasone Sensitivity
siCBP
Ctrl
% Survival
Dexamethasone (μM)
13

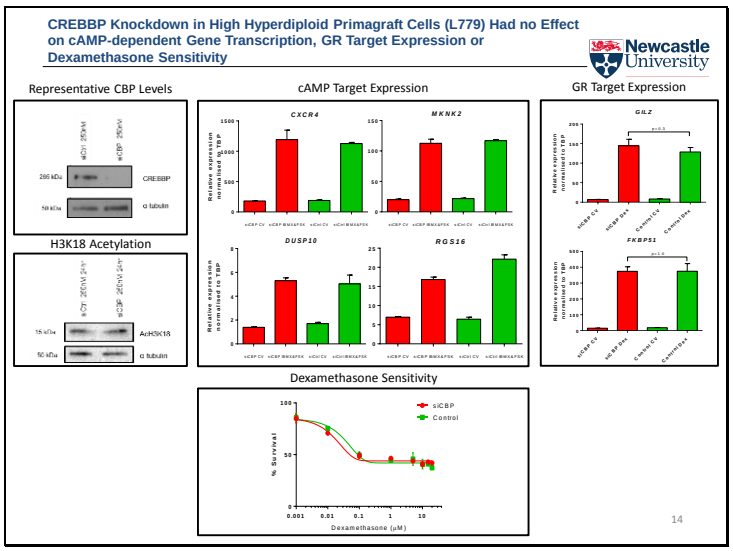
CREBBP Knockdown in High Hyperdiploid Primagraft Cells (L779) Had no Effect on cAMP-dependent Gene Transcription, GR Target Expression or Dexamethasone Sensitivity
Newcastle University
Representative CBP Levels
cAMP Target Expression
GR Target Expression
H3K18 Acetylation
Dexamethasone Sensitivity
siCBP
Control
% Survival
Dexamethasone (μM)
14

Conclusion

Newcastle University
Northern Institute for Cancer Research

- CREBBP Knockdown in ALL cell lines and high hyperdiploid primagraft cells
  - No significant effect on induction of cAMP dependent genes
  - Variable effect on glucocorticoid receptor target induction
  - **No reduction in GC sensitivity**
- CREBBP mutation at relapse in childhood ALL may be exerting its effect through other mechanisms
  - DNA damage repair?
  - p53/BCL6 balance?
  - Interaction with RAS pathway mutations?

15

Future Work

Newcastle University
Northern Institute for Cancer Research

- Carry out CREBBP knockdown on more high hyperdiploid primagraft samples
- CREBBP Knockdown in Lymphoma Cell lines
- Synthetic lethality screen in CREBBP knockdown clones

16

Acknowledgements

Newcastle University
Northern Institute for Cancer Research

- Supervisors
  - Julie Irving
  - Lindsay Nicholson
- Leukaemia & Lymphoma Research Group
  - Marian Case
  - Liz Matheson
  - Lynne Minto
  - Rosie Jackson
  - Ali Alhammer
- Funding

CANCER RESEARCH UK

17

American Society for Hematology Annual Meeting 2015, Orlando Convention Center, Florida

1429 Crebbp Knockdown Does Not Impact on Glucocorticoid Induced Apoptosis in Childhood Acute Lymphoblastic Leukemia

Acute Lymphoblastic Leukemia: Biology, Cytogenetics and Molecular Markers in Diagnosis and Prognosis

Program: Oral and Poster Abstracts

Session: 618. Acute Lymphoblastic Leukemia: Biology, Cytogenetics and Molecular Markers in Diagnosis and Prognosis: Poster I

Saturday, December 5, 2015, 5:30 PM-7:30 PM

Hall A, Level 2 (Orange County Convention Center)

Zach Dixon, BSc Hons, MRes[1]*, Julie A.E. Irving, PhD1 and Lindsay Nicholson, PhD[2]*

[1]Northern Institute for Cancer Research, Newcastle University, Newcastle upon Tyne, United Kingdom

[2]Haematological Sciences, Newcastle University, Newcastle upon Tyne, United Kingdom

Childhood acute lymphoblastic leukemia (ALL) is the most common childhood cancer and, despite a cure rate approaching 90%, relapse is a significant cause of death in young people. Recently it has been shown that inactivating mutations in the histone acetyltransferase, CREB binding protein (CREBBP or CBP) are frequently seen at relapse in childhood ALL, with enrichment in high hyperdiploid and hypodiploid cases. Mutations

are usually heterozygous, suggesting haploinsufficiency, and are often acquired at relapse, implying a role in drug resistance. Since glucocorticoid (GC) response genes are known targets of CREBBP and, given the pivotal role of GCs in ALL therapy, it has been postulated that CREBBP mutations confer GC chemoresistance.

CREBBP is a multifunctional protein, playing a role in cAMP dependent signalling, acetylation mediated activation of p53 and inactivation of BCL6 and a range of DNA damage repair pathways including base excision repair (BER) and direct DNA damage repair. To assess the role of CREBBP haploinsufficiency in ALL, RNAi techniques were used to create isogenic CREBBP knockdown models of ALL. CREBBP knockdown was carried out using small hairpin RNA (shRNA) transduction (termed shCBP cells) or small interfering RNA (siRNA) transfection (termed siCBP cells) in the PreB 697 B-cell precursor cell line (t(1;19)) and the hypodiploid MHH-CALL-2 cell line, as well as high hyperdiploid primagraft ALL cells. Knockdown of at least 50% of control was confirmed at both mRNA and protein level. The functional impact of CREBBP knockdown in cells was determined by analysis of known CREBBP target residues; acetyl H3K18 and H3K27, and transcription of cAMP dependent genes (CXCR4, MKNK2, DUSP5, DUSP10 and RGS16). To assess the impact of CREBBP knockdown on response to GCs, cells were treated with dexamethasone and expression of the classic glucocorticoid receptor (GR) targets; GILZ and FKBP51, was assessed by quantitative reverse transcriptase PCR (QRT-PCR). Alamar blue cell viability assays were used to determine the sensitivity of each CREBBP knockdown model to dexamethasone compared to isogenic controls.

Three out of four cell models displayed a reduction in H3K18 or H3K27 acetylation compared to isogenic control, indicating a relevant functional impact of CREBBP knockdown. Cell lines showed a trend towards reduced induction of some of the selected cAMP dependent targets but statistical significance was not achieved (p values >0.2). Gene expression profiling and Ingenuity Pathway Analysis of PreB 697 shCBP cells compared to isogenic control predicted that upstream transcription of NR3C1, the gene encoding the GR, would be affected in CREBBP knockdown cells. However, while induction of GILZ and FKBP51 in PreB 697 shCBP cells in response to GC was significantly impaired in knockdown compared to control cells (GILZ p=0.009, FKBP51 p=0.03), they were no more resistant to dexamethasone (p=0.9). This was mirrored in siCBP cell lines and primagraft cells, where a significant impairment in basal expression of GILZ and/or FKBP51 was seen in some lines (GILZ reduction; p=0.03 PreB 697 shCBP, p=0.02 PreB 697 siCBP, FKBP51 reduction; p=0.01 primagraft siCBP cells) but no significant impairment in the transcriptional induction of these genes in response to GC compared to isogenic control was observed (p values >0.5). Importantly, no decreased sensitivity to dexamethasone was seen in any model after CREBBP knockdown (p values >0.1).

CREBBP knockdown in ALL cells had no significant effect on the induction of cAMP dependent genes, had a variable effect on GR target expression, but consistently showed no impact on GC sensitivity, regardless of cytogenetic context. These data show that the acquisition of CREBBP mutations at relapse in childhood ALL is not mediated through GC resistance and suggest that other CREBBP associated mechanisms, such as DNA damage repair, may influence drug response. Understanding the role of CREBBP in carcinogenesis

and drug resistance is crucial as it is implicated as a tumour suppressor in a growing number of cancers, making it a potential multi-tumour target for novel therapies.

CREBBP Knockdown Does Not Impact on Glucocorticoid Induced Apoptosis in Childhood Acute Lymphoblastic Leukemia

Newcastle University

Zach Dixon BSc, MRes, Dr. Lindsay Nicholson and Dr. Julie Irving

Northern Institute for Cancer Research, Paul O'Gorman Building, Medical School, Newcastle University, Newcastle upon Tyne, NE2 4HH.

The authors declare no conflict of interest.

References

1) Mullighan *et al.* Nature (2011)

2) Inthal *et al.* Leukemia (2012)

Introduction

- *CREBBP* is frequently mutated in relapsed childhood acute lymphoblastic leukemia (ALL) (1)
  - And is enriched in the high hyperdiploid (HHD) subgroup (2)
- Glucocorticoid (GC) therapy is pivotal in the treatment of childhood ALL
  - *CREBBP* mutation has been associated with reduced expression of glucocorticoid receptor (GR) target genes
- ***CREBBP* mutation may lead to GC resistance and propagation of relapse in childhood ALL**

Aim

- **To assess the effect of CREBBP deficiency on response to GC therapy in models of childhood ALL**

Conclusions

- **CREBBP haploinsufficiency is unlikely to affect clinical response to glucocorticoid therapy**
- **The oncogenic mechanisms of CREBBP haploinsufficiency may reside within its many other associated functions, such as p53 and BCL6 regulation or DNA damage repair**
- **Understanding the oncogenic mechanisms of CREBBP is paramount as it may serve as a therapeutic target across multi-tumour types**

Methods

- Small hairpin RNA (shRNA) or a small interfering RNA (siRNA) pool was used to knock down the expression of CREBBP in the following cell models;
  - PreB 697 & MHH-CALL-2 B-ALL cell lines
  - Three high hyperdiploid primagraft samples
- These models were characterised for CREBBP expression by quantitative reverse-transcriptase PCR (QRT-PCR) and western blotting
- Expression of cAMP-dependent targets and glucocorticoid receptor (GR) targets was assessed by QRT-PCR following treatment with IBMX and forskolin or dexamethasone respectively
- Sensitivity to dexamethasone was determined using an alamar blue drug sensitivity assay over 96 hours

CANCER RESEARCH UK

BACR

Bloodwise

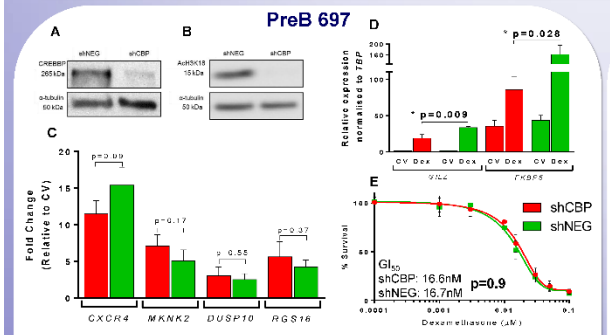

Figure 1. Creation and characterisation of a Pre B leukemia cell line with stable CREBBP knockdown. CREBBP knockdown was assessed by western blotting (**A**) with a functional impact being observed by way of reduced acetyl histone 3 lysine 18 (AcH3K18) (**B**) (blots representative of N=3). CREBBP knockdown by shRNA in PreB 697 cells had no significant impact on the transcription of cAMP-dependent targets following cAMP stimulation by IBMX and forskolin treatment (p values >0.09), as assessed by QRT-PCR (N=3) (**C**). Transcription of the GR targets; *GILZ* and *FKBP5* in response to dexamethasone (Dex) treatment (GI_{50} concentration of 17nM) was found to be significantly impaired in CREBBP knockdown cells compared to controls (p=0.009 and p=0.028 respectively), as assessed by QRT-PCR (N=3) (**D**). CREBBP knockdown in PreB 697 cells had no significant impact on sensitivity to dexamethasone compared to controls (p=0.9), as assessed by alamar blue drug sensitivity assay (N=3) (**E**). Values plotted in C, D & E are mean ± SEM.

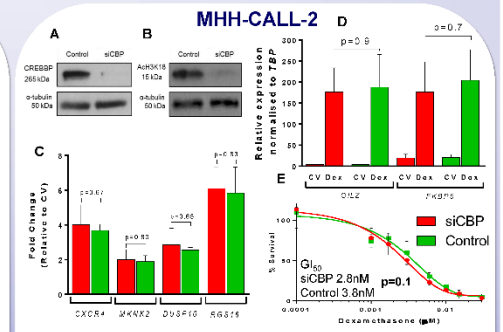

Figure 2. CREBBP knockdown by siRNA in hypodiploid B-ALL cell line, MHH-CALL-2. Knockdown was assessed by western blotting (**A**), with a functional impact being observed by way of reduced AcH3K18 (**B**) (blots representative of N=3). CREBBP knockdown in MHH-CALL-2 cells had no significant impact on the induction of cAMP-dependent targets following cAMP stimulation by IBMX and forskolin (p values >0.67), as assessed by QRT-PCR (N=3) (**C**). Induction of GR targets; *GILZ* and *FKBP5* in response to dexamethasone (Dex) however, was not affected by CREBBP knockdown (p values >0.7), as assessed by QRT-PCR (N=3) (**D**). MHH-CALL-2 cells with CREBBP knockdown were equally sensitivity to dexamethasone as controls, as assessed by alamar blue drug sensitivity assay (**E**) (N=3). Values plotted in C, D & E are mean ± SEM.

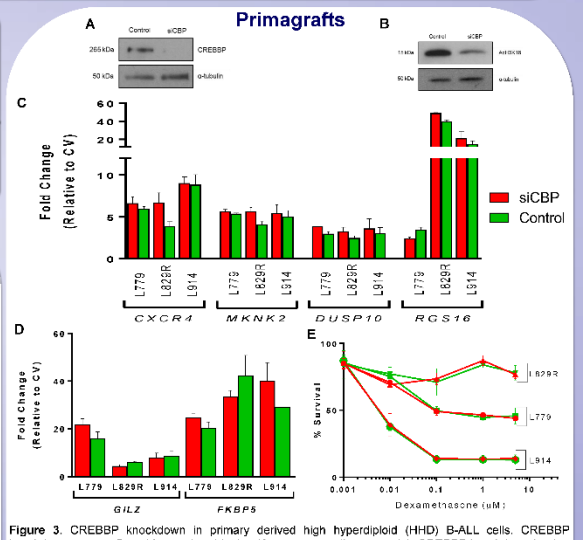

Figure 3. CREBBP knockdown in primary derived high hyperdiploid (HHD) B-ALL cells. CREBBP knockdown was confirmed by western blotting (**A** = representative example). CREBBP knockdown lead to reduced AcH3K18 levels in 2 of 3 HHD primagraft samples (**B** = representative example). Consistent with results in PreB 697 and MHH-CALL-2 cells. CREBBP knockdown did not significantly impair transcription of cAMP-dependent target genes in response to cAMP stimulation by IBMX and forskolin, as assessed by QRT-PCR (L779 & L829R N=1, L914 N=3) (p values >0.06) (**C**). CREBBP knockdown in HHD primagraft cells did not significantly impair induction of the GR targets; *GILZ* (p values >0.05) and *FKBP5* (p values >0.5) following dexamethasone treatment (1μM) compared to controls (**D**). CREBBP knockdown in HHD primagraft cells had no significant impact on sensitivity to dexamethasone, as assessed by alamar blue drug sensitivity assay (L779 & L829R N=1, L914 N=3) (p values >0.3) (**E**). Values plotted in C, D & E are (intra-assay for L779 & L829R and inter-assay for L914) mean ± SEM.

Appendix 3 – Publications

1. Dixon, Z., Nicholson, L., Zeppetzauer, M., Matheson, E., Sinclair, P., Harrison, C. J., and Irving, J. A. E. (2016) CREBBP knockdown enhances RAS/RAF/MEK/ERK signalling in Ras pathway mutated acute lymphoblastic leukaemia but does not modulate chemotherapeutic response [Resubmitted to Haematologica following revisions] (**Impact factor 6.671**)

References

References

ABDEL-WAHAB, O. & LEVINE, R. L. 2013. Mutations in epigenetic modifiers in the pathogenesis and therapy of acute myeloid leukemia. *Blood,* 121**,** 3563-72.

ABURAWI, H. E., BILOGLAV, A., JOHANSSON, B. & PAULSSON, K. 2011. Cytogenetic and molecular genetic characterization of the 'high hyperdiploid' B-cell precursor acute lymphoblastic leukaemia cell line MHH-CALL-2 reveals a near-haploid origin. *Br J Haematol,* 154**,** 275-7.

ACKERMANN, M., LIEBHABER, S., KLUSMANN, J. H. & LACHMANN, N. 2015. Lost in translation: pluripotent stem cell-derived hematopoiesis. *EMBO Mol Med*.

ADVANI, R., ROSENBERG, S. A. & HORNING, S. J. 2004. Stage I and II follicular non-Hodgkin's lymphoma: long-term follow-up of no initial therapy. *J Clin Oncol,* 22**,** 1454-9.

AGLIANO, A., MARTIN-PADURA, I., MANCUSO, P., MARIGHETTI, P., RABASCIO, C., PRUNERI, G., SHULTZ, L. D. & BERTOLINI, F. 2008. Human acute leukemia cells injected in NOD/LtSz-scid/IL-2Rgamma null mice generate a faster and more efficient disease compared to other NOD/scid-related strains. *Int J Cancer,* 123**,** 2222-7.

AKASAKA, T., LOSSOS, I. S. & LEVY, R. 2003. BCL6 gene translocation in follicular lymphoma: a harbinger of eventual transformation to diffuse aggressive lymphoma. *Blood,* 102**,** 1443-8.

ALARCON, J. M., MALLERET, G., TOUZANI, K., VRONSKAYA, S., ISHII, S., KANDEL, E. R. & BARCO, A. 2004. Chromatin acetylation, memory, and LTP are impaired in CBP+/- mice: a model for the cognitive deficit in Rubinstein-Taybi syndrome and its amelioration. *Neuron,* 42**,** 947-59.

ALIZADEH, A. A., EISEN, M. B., DAVIS, R. E., MA, C., LOSSOS, I. S., ROSENWALD, A., BOLDRICK, J. C., SABET, H., TRAN, T., YU, X., POWELL, J. I., YANG, L., MARTI, G. E., MOORE, T., HUDSON, J., JR., LU, L., LEWIS, D. B., TIBSHIRANI, R., SHERLOCK, G., CHAN, W. C., GREINER, T. C., WEISENBURGER, D. D., ARMITAGE, J. O., WARNKE, R., LEVY, R., WILSON, W., GREVER, M. R., BYRD, J. C., BOTSTEIN, D., BROWN, P. O. & STAUDT, L. M. 2000. Distinct types of diffuse large B-cell lymphoma identified by gene expression profiling. *Nature,* 403**,** 503-11.

ALNEMRI, E. S., FERNANDES, T. F., HALDAR, S., CROCE, C. M. & LITWACK, G. 1992. Involvement of BCL-2 in glucocorticoid-induced apoptosis of human pre-B-leukemias. *Cancer Res,* 52**,** 491-5.

AMINI, R. M., BERGLUND, M., ROSENQUIST, R., VON HEIDEMAN, A., LAGERCRANTZ, S., THUNBERG, U., BERGH, J., SUNDSTROM, C., GLIMELIUS, B. & ENBLAD, G. 2002. A novel B-cell line (U-2932) established from a patient with diffuse large B-cell lymphoma following Hodgkin lymphoma. *Leuk Lymphoma,* 43**,** 2179-89.

ANDERSEN, C. L., ASMAR, F., KLAUSEN, T., HASSELBALCH, H. & GRONBAEK, K. 2012. Somatic mutations of the CREBBP and EP300 genes affect response to histone deacetylase inhibition in malignant DLBCL clones. *Leuk Res Rep,* 2**,** 1-3.

ANNE, S. L., GOVEK, E. E., AYRAULT, O., KIM, J. H., ZHU, X., MURPHY, D. A., VAN AELST, L., ROUSSEL, M. F. & HATTEN, M. E. 2013. WNT3 inhibits cerebellar granule neuron progenitor proliferation and medulloblastoma formation via MAPK activation. *PLoS One,* 8**,** e81769.

ANSELL, S. M., MAURER, M. J., ZIESMER, S. C., SLAGER, S. L., HABERMANN, T. M., LINK, B. K., WITZIG, T. E., MACON, W. R., DOGAN, A., CERHAN, J. R. & NOVAK, A. J. 2012. Elevated pretreatment serum levels of interferon-inducible protein-10 (CXCL10) predict disease relapse and prognosis in diffuse large B-cell lymphoma patients. *Am J Hematol,* 87**,** 865-9.

AQUILINA, G., BIONDO, R., DOGLIOTTI, E., MEUTH, M. & BIGNAMI, M. 1992. Expression of the endogenous O6-methylguanine-DNA-methyltransferase protects Chinese hamster ovary cells from spontaneous G:C to A:T transitions. *Cancer Res,* 52**,** 6471-5.

ARICO, M., SCHRAPPE, M., HUNGER, S. P., CARROLL, W. L., CONTER, V., GALIMBERTI, S., MANABE, A., SAHA, V., BARUCHEL, A., VETTENRANTA, K., HORIBE, K., BENOIT, Y., PIETERS, R.,

ESCHERICH, G., SILVERMAN, L. B., PUI, C. H. & VALSECCHI, M. G. 2010. Clinical outcome of children with newly diagnosed Philadelphia chromosome-positive acute lymphoblastic leukemia treated between 1995 and 2005. *J Clin Oncol,* 28**,** 4755-61.

ARMITAGE, J. O. & WEISENBURGER, D. D. 1998. New approach to classifying non-Hodgkin's lymphomas: clinical features of the major histologic subtypes. Non-Hodgkin's Lymphoma Classification Project. *J Clin Oncol,* 16**,** 2780-95.

AUKEMA, S. M., SIEBERT, R., SCHUURING, E., VAN IMHOFF, G. W., KLUIN-NELEMANS, H. C., BOERMA, E. J. & KLUIN, P. M. 2011. Double-hit B-cell lymphomas. *Blood,* 117**,** 2319-31.

AUR, R. J., SIMONE, J., HUSTU, H. O., WALTERS, T., BORELLA, L., PRATT, C. & PINKEL, D. 1971. Central nervous system therapy and combination chemotherapy of childhood lymphocytic leukemia. *Blood,* 37**,** 272-81.

BANNISTER, A. J. & KOUZARIDES, T. 1996. The CBP co-activator is a histone acetyltransferase. *Nature,* 384**,** 641-3.

BARRANS, S., CROUCH, S., SMITH, A., TURNER, K., OWEN, R., PATMORE, R., ROMAN, E. & JACK, A. 2010. Rearrangement of MYC is associated with poor prognosis in patients with diffuse large B-cell lymphoma treated in the era of rituximab. *J Clin Oncol,* 28**,** 3360-5.

BASSO, K. & DALLA-FAVERA, R. 2012. Roles of BCL6 in normal and transformed germinal center B cells. *Immunol Rev,* 247**,** 172-83.

BAUDINO, T. A. 2015. Targeted Cancer Therapy: The Next Generation of Cancer Treatment. *Curr Drug Discov Technol,* 12**,** 3-20.

BEDFORD, D. C., KASPER, L. H., FUKUYAMA, T. & BRINDLE, P. K. 2010. Target gene context influences the transcriptional requirement for the KAT3 family of CBP and p300 histone acetyltransferases. *Epigenetics,* 5**,** 9-15.

BELTRAN, B. E., QUINONES, P., MORALES, D., REVILLA, J. C., ALVA, J. C. & CASTILLO, J. J. 2012. Diffuse large B-cell lymphoma in human T-lymphotropic virus type 1 carriers. *Leuk Res Treatment,* 2012**,** 262363.

BERESHCHENKO, O. R., GU, W. & DALLA-FAVERA, R. 2002. Acetylation inactivates the transcriptional repressor BCL6. *Nat Genet,* 32**,** 606-13.

BHAKAT, K. K. & MITRA, S. 2000. Regulation of the human O(6)-methylguanine-DNA methyltransferase gene by transcriptional coactivators cAMP response element-binding protein-binding protein and p300. *J Biol Chem,* 275**,** 34197-204.

BHOJWANI, D. & PUI, C. H. 2013. Relapsed childhood acute lymphoblastic leukaemia. *Lancet Oncol,* 14**,** e205-17.

BILALOVIC, N., BLYSTAD, A. K., GOLOUH, R., NESLAND, J. M., SELAK, I., TRINH, D. & TORLAKOVIC, E. 2004. Expression of bcl-6 and CD10 protein is associated with longer overall survival and time to treatment failure in follicular lymphoma. *Am J Clin Pathol,* 121**,** 34-42.

BIONDI, A., SCHRAPPE, M., DE LORENZO, P., CASTOR, A., LUCCHINI, G., GANDEMER, V., PIETERS, R., STARY, J., ESCHERICH, G., CAMPBELL, M., LI, C. K., VORA, A., ARICO, M., ROTTGERS, S., SAHA, V. & VALSECCHI, M. G. 2012. Imatinib after induction for treatment of children and adolescents with Philadelphia-chromosome-positive acute lymphoblastic leukaemia (EsPhALL): a randomised, open-label, intergroup study. *Lancet Oncol,* 13**,** 936-45.

BITTENBRING, J. T., NEUMANN, F., ALTMANN, B., ACHENBACH, M., REICHRATH, J., ZIEPERT, M., GEISEL, J., REGITZ, E., HELD, G. & PFREUNDSCHUH, M. 2014. Vitamin D deficiency impairs rituximab-mediated cellular cytotoxicity and outcome of patients with diffuse large B-cell lymphoma treated with but not without rituximab. *J Clin Oncol,* 32**,** 3242-8.

BLOBEL, G. A. 2000. CREB-binding protein and p300: molecular integrators of hematopoietic transcription. *Blood,* 95**,** 745-55.

BLOBEL, G. A., NAKAJIMA, T., ECKNER, R., MONTMINY, M. & ORKIN, S. H. 1998. CREB-binding protein cooperates with transcription factor GATA-1 and is required for erythroid differentiation. *Proc Natl Acad Sci U S A,* 95**,** 2061-6.

BLOOD 1997. A clinical evaluation of the International Lymphoma Study Group classification of non-Hodgkin's lymphoma. The Non-Hodgkin's Lymphoma Classification Project. *Blood,* 89**,** 3909-18.

BODOR, C., GROSSMANN, V., POPOV, N., OKOSUN, J., O'RIAIN, C., TAN, K., MARZEC, J., ARAF, S., WANG, J., LEE, A. M., CLEAR, A., MONTOTO, S., MATTHEWS, J., IQBAL, S., RAJNAI, H., ROSENWALD, A., OTT, G., CAMPO, E., RIMSZA, L. M., SMELAND, E. B., CHAN, W. C., BRAZIEL, R. M., STAUDT, L. M., WRIGHT, G., LISTER, T. A., ELEMENTO, O., HILLS, R., GRIBBEN, J. G., CHELALA, C., MATOLCSY, A., KOHLMANN, A., HAFERLACH, T., GASCOYNE, R. D. & FITZGIBBON, J. 2013. EZH2 mutations are frequent and represent an early event in follicular lymphoma. *Blood,* 122**,** 3165-8.

BOROWITZ, M. J., DEVIDAS, M., HUNGER, S. P., BOWMAN, W. P., CARROLL, A. J., CARROLL, W. L., LINDA, S., MARTIN, P. L., PULLEN, D. J., VISWANATHA, D., WILLMAN, C. L., WINICK, N. & CAMITTA, B. M. 2008. Clinical significance of minimal residual disease in childhood acute lymphoblastic leukemia and its relationship to other prognostic factors: a Children's Oncology Group study. *Blood,* 111**,** 5477-85.

BORROW, J., STANTON, V. P., JR., ANDRESEN, J. M., BECHER, R., BEHM, F. G., CHAGANTI, R. S., CIVIN, C. I., DISTECHE, C., DUBE, I., FRISCHAUF, A. M., HORSMAN, D., MITELMAN, F., VOLINIA, S., WATMORE, A. E. & HOUSMAN, D. E. 1996. The translocation t(8;16)(p11;p13) of acute myeloid leukaemia fuses a putative acetyltransferase to the CREB-binding protein. *Nat Genet,* 14**,** 33-41.

BOURTCHOULADZE, R., LIDGE, R., CATAPANO, R., STANLEY, J., GOSSWEILER, S., ROMASHKO, D., SCOTT, R. & TULLY, T. 2003. A mouse model of Rubinstein-Taybi syndrome: defective long-term memory is ameliorated by inhibitors of phosphodiesterase 4. *Proc Natl Acad Sci U S A,* 100**,** 10518-22.

BOUSKA, A., ZHANG, W., GONG, Q., IQBAL, J., SCUTO, A., VOSE, J., LUDVIGSEN, M., FU, K., WEISENBURGER, D. D., GREINER, T. C., GASCOYNE, R. D., ROSENWALD, A., OTT, G., CAMPO, E., RIMSZA, L. M., DELABIE, J., JAFFE, E. S., BRAZIEL, R. M., CONNORS, J. M., WU, C. I., STAUDT, L. M., D'AMORE, F., MCKEITHAN, T. W. & CHAN, W. C. 2016. Combined copy number and mutation analysis identifies oncogenic pathways associated with transformation of follicular lymphoma. *Leukemia*.

BRANCH, P., HAMPSON, R. & KARRAN, P. 1995. DNA mismatch binding defects, DNA damage tolerance, and mutator phenotypes in human colorectal carcinoma cell lines. *Cancer Res,* 55**,** 2304-9.

BROOKS, C. L. & GU, W. 2003. Ubiquitination, phosphorylation and acetylation: the molecular basis for p53 regulation. *Curr Opin Cell Biol,* 15**,** 164-71.

BUCHMANN, I., REINHARDT, M., ELSNER, K., BUNJES, D., ALTEHOEFER, C., FINKE, J., MOSER, E., GLATTING, G., KOTZERKE, J., GUHLMANN, C. A., SCHIRRMEISTER, H. & RESKE, S. N. 2001. 2-(fluorine-18)fluoro-2-deoxy-D-glucose positron emission tomography in the detection and staging of malignant lymphoma. A bicenter trial. *Cancer,* 91**,** 889-99.

CAMPANA, D. 2012. Minimal residual disease monitoring in childhood acute lymphoblastic leukemia. *Curr Opin Hematol,* 19**,** 313-8.

CAMPO, E., SWERDLOW, S. H., HARRIS, N. L., PILERI, S., STEIN, H. & JAFFE, E. S. 2011. The 2008 WHO classification of lymphoid neoplasms and beyond: evolving concepts and practical applications. *Blood,* 117**,** 5019-32.

CANCER RESEARCH UK. 2010. *Non-Hodgkin lymphoma incidence statistics* [Online]. Available: http://www.cancerresearchuk.org/cancer-info/cancerstats/types/nhl/incidence/ [Accessed 2014].

CARDULLO, R. A., AGRAWAL, S., FLORES, C., ZAMECNIK, P. C. & WOLF, D. E. 1988. Detection of nucleic acid hybridization by nonradiative fluorescence resonance energy transfer. *Proc Natl Acad Sci U S A,* 85**,** 8790-4.

CASE, M., MATHESON, E., MINTO, L., HASSAN, R., HARRISON, C. J., BOWN, N., BAILEY, S., VORMOOR, J., HALL, A. G. & IRVING, J. A. 2008. Mutation of genes affecting the RAS pathway is common in childhood acute lymphoblastic leukemia. *Cancer Res,* 68**,** 6803-9.

CHANG, H., BLONDAL, J. A., BENCHIMOL, S., MINDEN, M. D. & MESSNER, H. A. 1995. p53 mutations, c-myc and bcl-2 rearrangements in human non-Hodgkin's lymphoma cell lines. *Leuk Lymphoma,* 19**,** 165-71.

CHEN, Y., CHENG, G. & MAHATO, R. I. 2008. RNAi for treating hepatitis B viral infection. *Pharm Res,* 25**,** 72-86.

CHENG, C. L., JOHNSON, S. P., KEIR, S. T., QUINN, J. A., ALI-OSMAN, F., SZABO, C., LI, H., SALZMAN, A. L., DOLAN, M. E., MODRICH, P., BIGNER, D. D. & FRIEDMAN, H. S. 2005. Poly(ADP-ribose) polymerase-1 inhibition reverses temozolomide resistance in a DNA mismatch repair-deficient malignant glioma xenograft. *Mol Cancer Ther,* 4**,** 1364-8.

CHEUNG, K. J., SHAH, S. P., STEIDL, C., JOHNSON, N., RELANDER, T., TELENIUS, A., LAI, B., MURPHY, K. P., LAM, W., AL-TOURAH, A. J., CONNORS, J. M., NG, R. T., GASCOYNE, R. D. & HORSMAN, D. E. 2009. Genome-wide profiling of follicular lymphoma by array comparative genomic hybridization reveals prognostically significant DNA copy number imbalances. *Blood,* 113**,** 137-48.

CHIAPPELLA, A., TUCCI, A., CASTELLINO, A., PAVONE, V., BALDI, I., CARELLA, A. M., ORSUCCI, L., ZANNI, M., SALVI, F., LIBERATI, A. M., GAIDANO, G., BOTTELLI, C., ROSSINI, B., PERTICONE, S., DE MASI, P., LADETTO, M., CICCONE, G., PALUMBO, A., ROSSI, G. & VITOLO, U. 2013. Lenalidomide plus cyclophosphamide, doxorubicin, vincristine, prednisone and rituximab is safe and effective in untreated, elderly patients with diffuse large B-cell lymphoma: a phase I study by the Fondazione Italiana Linfomi. *Haematologica,* 98**,** 1732-8.

CHIARETTI, S., ZINI, G. & BASSAN, R. 2014. Diagnosis and subclassification of acute lymphoblastic leukemia. *Mediterr J Hematol Infect Dis,* 6**,** e2014073.

CHMELAROVA, M., KREPINSKA, E., SPACEK, J., LACO, J., BERANEK, M. & PALICKA, V. 2013. Methylation in the p53 promoter in epithelial ovarian cancer. *Clin Transl Oncol,* 15**,** 160-3.

CHOU, W. C., CHOU, S. C., LIU, C. Y., CHEN, C. Y., HOU, H. A., KUO, Y. Y., LEE, M. C., KO, B. S., TANG, J. L., YAO, M., TSAY, W., WU, S. J., HUANG, S. Y., HSU, S. C., CHEN, Y. C., CHANG, Y. C., KUO, Y. Y., KUO, K. T., LEE, F. Y., LIU, M. C., LIU, C. W., TSENG, M. H., HUANG, C. F. & TIEN, H. F. 2011. TET2 mutation is an unfavorable prognostic factor in acute myeloid leukemia patients with intermediate-risk cytogenetics. *Blood,* 118**,** 3803-10.

CHRIVIA, J. C., KWOK, R. P., LAMB, N., HAGIWARA, M., MONTMINY, M. R. & GOODMAN, R. H. 1993. Phosphorylated CREB binds specifically to the nuclear protein CBP. *Nature,* 365**,** 855-9.

COFFINO, P., BOURNE, H. R. & TOMKINS, G. M. 1975. Mechanism of lymphoma cell death induced by cyclic AMP. *Am J Pathol,* 81**,** 199-204.

COIFFIER, B., LEPAGE, E., BRIERE, J., HERBRECHT, R., TILLY, H., BOUABDALLAH, R., MOREL, P., VAN DEN NESTE, E., SALLES, G., GAULARD, P., REYES, F., LEDERLIN, P. & GISSELBRECHT, C. 2002. CHOP chemotherapy plus rituximab compared with CHOP alone in elderly patients with diffuse large-B-cell lymphoma. *N Engl J Med,* 346**,** 235-42.

COMPAGNO, M., LIM, W. K., GRUNN, A., NANDULA, S. V., BRAHMACHARY, M., SHEN, Q., BERTONI, F., PONZONI, M., SCANDURRA, M., CALIFANO, A., BHAGAT, G., CHADBURN, A., DALLA-FAVERA, R. & PASQUALUCCI, L. 2009. Mutations of multiple genes cause deregulation of NF-kappaB in diffuse large B-cell lymphoma. *Nature,* 459**,** 717-21.

CONTER, V., BARTRAM, C. R., VALSECCHI, M. G., SCHRAUDER, A., PANZER-GRUMAYER, R., MORICKE, A., ARICO, M., ZIMMERMANN, M., MANN, G., DE ROSSI, G., STANULLA, M., LOCATELLI, F., BASSO, G., NIGGLI, F., BARISONE, E., HENZE, G., LUDWIG, W. D., HAAS, O. A., CAZZANIGA, G., KOEHLER, R., SILVESTRI, D., BRADTKE, J., PARASOLE, R., BEIER, R., VAN DONGEN, J. J., BIONDI, A. & SCHRAPPE, M. 2010. Molecular response to treatment

redefines all prognostic factors in children and adolescents with B-cell precursor acute lymphoblastic leukemia: results in 3184 patients of the AIEOP-BFM ALL 2000 study. *Blood,* 115**,** 3206-14.

COUSTAN-SMITH, E., MULLIGHAN, C. G., ONCIU, M., BEHM, F. G., RAIMONDI, S. C., PEI, D., CHENG, C., SU, X., RUBNITZ, J. E., BASSO, G., BIONDI, A., PUI, C. H., DOWNING, J. R. & CAMPANA, D. 2009. Early T-cell precursor leukaemia: a subtype of very high-risk acute lymphoblastic leukaemia. *Lancet Oncol,* 10**,** 147-56.

COUSTAN-SMITH, E., SANCHO, J., HANCOCK, M. L., BOYETT, J. M., BEHM, F. G., RAIMONDI, S. C., SANDLUND, J. T., RIVERA, G. K., RUBNITZ, J. E., RIBEIRO, R. C., PUI, C. H. & CAMPANA, D. 2000. Clinical importance of minimal residual disease in childhood acute lymphoblastic leukemia. *Blood,* 96**,** 2691-6.

CURTIN, N. J. 2012. DNA repair dysregulation from cancer driver to therapeutic target. *Nat Rev Cancer,* 12**,** 801-17.

DANIEL, V., LITWACK, G. & TOMKINS, G. M. 1973. Induction of cytolysis of cultured lymphoma cells by adenosine 3':5'-cyclic monophosphate and the isolation of resistant variants. *Proc Natl Acad Sci U S A,* 70**,** 76-9.

DANIS, E., YAMAUCHI, T., ECHANIQUE, K., ZHANG, X., HALADYNA, J. N., RIEDEL, S. S., ZHU, N., XIE, H., ORKIN, S. H., ARMSTRONG, S. A., BERNT, K. M. & NEFF, T. 2016. Ezh2 Controls an Early Hematopoietic Program and Growth and Survival Signaling in Early T Cell Precursor Acute Lymphoblastic Leukemia. *Cell Rep,* 14**,** 1953-65.

DAVIS, R. E., BROWN, K. D., SIEBENLIST, U. & STAUDT, L. M. 2001. Constitutive nuclear factor kappaB activity is required for survival of activated B cell-like diffuse large B cell lymphoma cells. *J Exp Med,* 194**,** 1861-74.

DAVIS, R. E., NGO, V. N., LENZ, G., TOLAR, P., YOUNG, R. M., ROMESSER, P. B., KOHLHAMMER, H., LAMY, L., ZHAO, H., YANG, Y., XU, W., SHAFFER, A. L., WRIGHT, G., XIAO, W., POWELL, J., JIANG, J. K., THOMAS, C. J., ROSENWALD, A., OTT, G., MULLER-HERMELINK, H. K., GASCOYNE, R. D., CONNORS, J. M., JOHNSON, N. A., RIMSZA, L. M., CAMPO, E., JAFFE, E. S., WILSON, W. H., DELABIE, J., SMELAND, E. B., FISHER, R. I., BRAZIEL, R. M., TUBBS, R. R., COOK, J. R., WEISENBURGER, D. D., CHAN, W. C., PIERCE, S. K. & STAUDT, L. M. 2010. Chronic active B-cell-receptor signalling in diffuse large B-cell lymphoma. *Nature,* 463**,** 88-92.

DE GUZMAN, R. N., LIU, H. Y., MARTINEZ-YAMOUT, M., DYSON, H. J. & WRIGHT, P. E. 2000. Solution structure of the TAZ2 (CH3) domain of the transcriptional adaptor protein CBP. *J Mol Biol,* 303**,** 243-53.

DE GUZMAN, R. N., MARTINEZ-YAMOUT, M. A., DYSON, H. J. & WRIGHT, P. E. 2004. Interaction of the TAZ1 domain of the CREB-binding protein with the activation domain of CITED2: regulation by competition between intrinsically unstructured ligands for non-identical binding sites. *J Biol Chem,* 279**,** 3042-9.

DE RAEDT, T., BEERT, E., PASMANT, E., LUSCAN, A., BREMS, H., ORTONNE, N., HELIN, K., HORNICK, J. L., MAUTNER, V., KEHRER-SAWATZKI, H., CLAPP, W., BRADNER, J., VIDAUD, M., UPADHYAYA, M., LEGIUS, E. & CICHOWSKI, K. 2014. PRC2 loss amplifies Ras-driven transcription and confers sensitivity to BRD4-based therapies. *Nature,* 514**,** 247-51.

DEN BOER, M. L., VAN SLEGTENHORST, M., DE MENEZES, R. X., CHEOK, M. H., BUIJS-GLADDINES, J. G., PETERS, S. T., VAN ZUTVEN, L. J., BEVERLOO, H. B., VAN DER SPEK, P. J., ESCHERICH, G., HORSTMANN, M. A., JANKA-SCHAUB, G. E., KAMPS, W. A., EVANS, W. E. & PIETERS, R. 2009. A subtype of childhood acute lymphoblastic leukaemia with poor treatment outcome: a genome-wide classification study. *Lancet Oncol,* 10**,** 125-34.

DOMENECH, C., SUCIU, S., DE MOERLOOSE, B., MAZINGUE, F., PLAT, G., FERSTER, A., UYTTEBROECK, A., SIRVENT, N., LUTZ, P., YAKOUBEN, K., MUNZER, M., ROHRLICH, P., PLANTAZ, D., MILLOT, F., PHILIPPET, P., DASTUGUE, N., GIRARD, S., CAVE, H., BENOIT, Y. & BERTRANDFOR, Y. 2014. Dexamethasone (6 mg/m2/day) and prednisolone (60

mg/m2/day) were equally effective as induction therapy for childhood acute lymphoblastic leukemia in the EORTC CLG 58951 randomized trial. *Haematologica,* 99**,** 1220-7.

DONNOU, S., GALAND, C., TOUITOU, V., XE, RIE, SAUT, XE, S-FRIDMAN, C., FABRY, Z. & FISSON, S. 2012. *Murine Models of B-Cell Lymphomas: Promising Tools for Designing Cancer Therapies*.

DORDELMANN, M., REITER, A., BORKHARDT, A., LUDWIG, W. D., GOTZ, N., VIEHMANN, S., GADNER, H., RIEHM, H. & SCHRAPPE, M. 1999. Prednisone response is the strongest predictor of treatment outcome in infant acute lymphoblastic leukemia. *Blood,* 94**,** 1209-17.

DREXLER, H. G. & UPHOFF, C. C. 2002. Mycoplasma contamination of cell cultures: Incidence, sources, effects, detection, elimination, prevention. *Cytotechnology,* 39**,** 75-90.

DUNCIA, J. V., SANTELLA, J. B., 3RD, HIGLEY, C. A., PITTS, W. J., WITYAK, J., FRIETZE, W. E., RANKIN, F. W., SUN, J. H., EARL, R. A., TABAKA, A. C., TELEHA, C. A., BLOM, K. F., FAVATA, M. F., MANOS, E. J., DAULERIO, A. J., STRADLEY, D. A., HORIUCHI, K., COPELAND, R. A., SCHERLE, P. A., TRZASKOS, J. M., MAGOLDA, R. L., TRAINOR, G. L., WEXLER, R. R., HOBBS, F. W. & OLSON, R. E. 1998. MEK inhibitors: the chemistry and biological activity of U0126, its analogs, and cyclization products. *Bioorg Med Chem Lett,* 8**,** 2839-44.

DUPUIS, J., ITTI, E., RAHMOUNI, A., HEMERY, F., GISSELBRECHT, C., LIN, C., COPIE-BERGMAN, C., BELHADJ, K., EL GNAOUI, T., GAILLARD, I., KUHNOWSKI, F., MEIGNAN, M. & HAIOUN, C. 2009. Response assessment after an inductive CHOP or CHOP-like regimen with or without rituximab in 103 patients with diffuse large B-cell lymphoma: integrating 18fluorodeoxyglucose positron emission tomography to the International Workshop Criteria. *Ann Oncol,* 20**,** 503-7.

EL-DEIRY, W. S., HARPER, J. W., O'CONNOR, P. M., VELCULESCU, V. E., CANMAN, C. E., JACKMAN, J., PIETENPOL, J. A., BURRELL, M., HILL, D. E., WANG, Y. & ET AL. 1994. WAF1/CIP1 is induced in p53-mediated G1 arrest and apoptosis. *Cancer Res,* 54**,** 1169-74.

ENNISHI, D., YOKOYAMA, M., TERUI, Y., ASAI, H., SAKAJIRI, S., MISHIMA, Y., TAKAHASHI, S., KOMATSU, H., IKEDA, K., TAKEUCHI, K., TANIMOTO, M. & HATAKE, K. 2009. Soluble interleukin-2 receptor retains prognostic value in patients with diffuse large B-cell lymphoma receiving rituximab plus CHOP (RCHOP) therapy. *Ann Oncol,* 20**,** 526-33.

EPPERT, K., TAKENAKA, K., LECHMAN, E. R., WALDRON, L., NILSSON, B., VAN GALEN, P., METZELER, K. H., POEPPL, A., LING, V., BEYENE, J., CANTY, A. J., DANSKA, J. S., BOHLANDER, S. K., BUSKE, C., MINDEN, M. D., GOLUB, T. R., JURISICA, I., EBERT, B. L. & DICK, J. E. 2011. Stem cell gene expression programs influence clinical outcome in human leukemia. *Nat Med,* 17**,** 1086-93.

EPSTEIN, A. L. & KAPLAN, H. S. 1979. Feeder layer and nutritional requirements for the establishment and cloning of human malignant lymphoma cell lines. *Cancer Res,* 39**,** 1748-59.

FEDERICO, M., BELLEI, M., MARCHESELLI, L., LUMINARI, S., LOPEZ-GUILLERMO, A., VITOLO, U., PRO, B., PILERI, S., PULSONI, A., SOUBEYRAN, P., CORTELAZZO, S., MARTINELLI, G., MARTELLI, M., RIGACCI, L., ARCAINI, L., DI RAIMONDO, F., MERLI, F., SABATTINI, E., MCLAUGHLIN, P. & SOLAL-CELIGNY, P. 2009. Follicular lymphoma international prognostic index 2: a new prognostic index for follicular lymphoma developed by the international follicular lymphoma prognostic factor project. *J Clin Oncol,* 27**,** 4555-62.

FINDLEY, H. W., JR., COOPER, M. D., KIM, T. H., ALVARADO, C. & RAGAB, A. H. 1982. Two new acute lymphoblastic leukemia cell lines with early B-cell phenotypes. *Blood,* 60**,** 1305-9.

FISCHER, M., SCHWIEGER, M., HORN, S., NIEBUHR, B., FORD, A., ROSCHER, S., BERGHOLZ, U., GREAVES, M., LOHLER, J. & STOCKING, C. 2005. Defining the oncogenic function of the TEL/AML1 (ETV6/RUNX1) fusion protein in a mouse model. *Oncogene,* 24**,** 7579-91.

FISCHER, U., FORSTER, M., RINALDI, A., RISCH, T., SUNGALEE, S., WARNATZ, H. J., BORNHAUSER, B., GOMBERT, M., KRATSCH, C., STUTZ, A. M., SULTAN, M., TCHINDA, J., WORTH, C. L., AMSTISLAVSKIY, V., BADARINARAYAN, N., BARUCHEL, A., BARTRAM, T., BASSO, G., CANPOLAT, C., CARIO, G., CAVE, H., DAKAJ, D., DELORENZI, M., DOBAY, M. P., ECKERT, C., ELLINGHAUS, E., EUGSTER, S., FRISMANTAS, V., GINZEL, S., HAAS, O. A., HEIDENREICH, O., HEMMRICH-STANISAK, G., HEZAVEH, K., HOLL, J. I., HORNHARDT, S., HUSEMANN, P., KACHROO, P., KRATZ, C. P., KRONNIE, G. T., MAROVCA, B., NIGGLI, F., MCHARDY, A. C., MOORMAN, A. V., PANZER-GRUMAYER, R., PETERSEN, B. S., RAEDER, B., RALSER, M., ROSENSTIEL, P., SCHAFER, D., SCHRAPPE, M., SCHREIBER, S., SCHUTTE, M., STADE, B., THIELE, R., WEID, N., VORA, A., ZALIOVA, M., ZHANG, L., ZICHNER, T., ZIMMERMANN, M., LEHRACH, H., BORKHARDT, A., BOURQUIN, J. P., FRANKE, A., KORBEL, J. O., STANULLA, M. & YASPO, M. L. 2015. Genomics and drug profiling of fatal TCF3-HLF-positive acute lymphoblastic leukemia identifies recurrent mutation patterns and therapeutic options. *Nat Genet,* 47**,** 1020-9.

FISHER, R. I., GAYNOR, E. R., DAHLBERG, S., OKEN, M. M., GROGAN, T. M., MIZE, E. M., GLICK, J. H., COLTMAN, C. A., JR. & MILLER, T. P. 1993. Comparison of a standard regimen (CHOP) with three intensive chemotherapy regimens for advanced non-Hodgkin's lymphoma. *N Engl J Med,* 328**,** 1002-6.

FREEDMAN, A. 2014. Follicular lymphoma: 2014 update on diagnosis and management. *Am J Hematol,* 89**,** 429-36.

FRIEDBERG, J. W., BYRTEK, M., LINK, B. K., FLOWERS, C., TAYLOR, M., HAINSWORTH, J., CERHAN, J. R., ZELENETZ, A. D., HIRATA, J. & MILLER, T. P. 2012. Effectiveness of first-line management strategies for stage I follicular lymphoma: analysis of the National LymphoCare Study. *J Clin Oncol,* 30**,** 3368-75.

GAO, X., XU, Y. X., DIVINE, G., JANAKIRAMAN, N., CHAPMAN, R. A. & GAUTAM, S. C. 2002. Disparate in vitro and in vivo antileukemic effects of resveratrol, a natural polyphenolic compound found in grapes. *J Nutr,* 132**,** 2076-81.

GAO, Y., GENG, J., HONG, X., QI, J., TENG, Y., YANG, Y., QU, D. & CHEN, G. 2014a. Expression of p300 and CBP is associated with poor prognosis in small cell lung cancer. *Int J Clin Exp Pathol,* 7**,** 760-7.

GAO, Y. B., CHEN, Z. L., LI, J. G., HU, X. D., SHI, X. J., SUN, Z. M., ZHANG, F., ZHAO, Z. R., LI, Z. T., LIU, Z. Y., ZHAO, Y. D., SUN, J., ZHOU, C. C., YAO, R., WANG, S. Y., WANG, P., SUN, N., ZHANG, B. H., DONG, J. S., YU, Y., LUO, M., FENG, X. L., SHI, S. S., ZHOU, F., TAN, F. W., QIU, B., LI, N., SHAO, K., ZHANG, L. J., ZHANG, L. J., XUE, Q., GAO, S. G. & HE, J. 2014b. Genetic landscape of esophageal squamous cell carcinoma. *Nat Genet*.

GASCOYNE, R. D., ADOMAT, S. A., KRAJEWSKI, S., KRAJEWSKA, M., HORSMAN, D. E., TOLCHER, A. W., O'REILLY, S. E., HOSKINS, P., COLDMAN, A. J., REED, J. C. & CONNORS, J. M. 1997. Prognostic significance of Bcl-2 protein expression and Bcl-2 gene rearrangement in diffuse aggressive non-Hodgkin's lymphoma. *Blood,* 90**,** 244-51.

GEORGE, P., HERNANDEZ, K., HUSTU, O., BORELLA, L., HOLTON, C. & PINKEL, D. 1968. A study of "total therapy" of acute lymphocytic leukemia in children. *J Pediatr,* 72**,** 399-408.

GHOSH, S., TAYLOR, A., CHIN, M., HUANG, H. R., CONERY, A. R., MERTZ, J. A., SALMERON, A., DAKLE, P. J., MELE, D., COTE, A., JAYARAM, H., SETSER, J. W., POY, F., HATZIVASSILIOU, G., DEALMEIDA-NAGATA, D., SANDY, P., HATTON, C., ROMERO, F. A., CHIANG, E., REIMER, T., CRAWFORD, T., PARDO, E., WATSON, V. G., TSUI, V., COCHRAN, A. G., ZAWADZKE, L., HARMANGE, J. C., AUDIA, J. E., BRYANT, B. M., CUMMINGS, R. T., MAGNUSON, S. R., GROGAN, J. L., BELLON, S. F., ALBRECHT, B. K., SIMS, R. J., 3RD & LORA, J. M. 2016. Regulatory T Cell Modulation by CBP/EP300 Bromodomain Inhibition. *J Biol Chem*.

GILES, R. H., PETRIJ, F., DAUWERSE, H. G., DEN HOLLANDER, A. I., LUSHNIKOVA, T., VAN OMMEN, G. J., GOODMAN, R. H., DEAVEN, L. L., DOGGETT, N. A., PETERS, D. J. & BREUNING, M. H. 1997. Construction of a 1.2-Mb contig surrounding, and molecular analysis of, the human

CREB-binding protein (CBP/CREBBP) gene on chromosome 16p13.3. *Genomics,* 42**,** 96-114.

GIORDANO, A. & AVANTAGGIATI, M. L. 1999. p300 and CBP: partners for life and death. *J Cell Physiol,* 181**,** 218-30.

GLASSNER, B. J., WEEDA, G., ALLAN, J. M., BROEKHOF, J. L., CARLS, N. H., DONKER, I., ENGELWARD, B. P., HAMPSON, R. J., HERSMUS, R., HICKMAN, M. J., ROTH, R. B., WARREN, H. B., WU, M. M., HOEIJMAKERS, J. H. & SAMSON, L. D. 1999. DNA repair methyltransferase (Mgmt) knockout mice are sensitive to the lethal effects of chemotherapeutic alkylating agents. *Mutagenesis,* 14**,** 339-47.

GOODMAN, R. H. & SMOLIK, S. 2000. CBP/p300 in cell growth, transformation, and development. *Genes Dev,* 14**,** 1553-77.

GOPAL, A. K., KAHL, B. S., DE VOS, S., WAGNER-JOHNSTON, N. D., SCHUSTER, S. J., JURCZAK, W. J., FLINN, I. W., FLOWERS, C. R., MARTIN, P., VIARDOT, A., BLUM, K. A., GOY, A. H., DAVIES, A. J., ZINZANI, P. L., DREYLING, M., JOHNSON, D., MILLER, L. L., HOLES, L., LI, D., DANSEY, R. D., GODFREY, W. R. & SALLES, G. A. 2014. PI3Kdelta inhibition by idelalisib in patients with relapsed indolent lymphoma. *N Engl J Med,* 370**,** 1008-18.

GOTLIEB, N., ROSENNE, E., MATZNER, P., SHAASHUA, L., SORSKI, L. & BEN-ELIYAHU, S. 2015. The misleading nature of in vitro and ex vivo findings in studying the impact of stress hormones on NK cell cytotoxicity. *Brain Behav Immun,* 45**,** 277-86.

GREAVES, M. 2006. Infection, immune responses and the aetiology of childhood leukaemia. *Nat Rev Cancer,* 6**,** 193-203.

GREAVES, M. F., MAIA, A. T., WIEMELS, J. L. & FORD, A. M. 2003. Leukemia in twins: lessons in natural history. *Blood,* 102**,** 2321-33.

GREEN, M. R., GENTLES, A. J., NAIR, R. V., IRISH, J. M., KIHIRA, S., LIU, C. L., KELA, I., HOPMANS, E. S., MYKLEBUST, J. H., JI, H., PLEVRITIS, S. K., LEVY, R. & ALIZADEH, A. A. 2013. Hierarchy in somatic mutations arising during genomic evolution and progression of follicular lymphoma. *Blood,* 121**,** 1604-11.

GREEN, M. R., KIHIRA, S., LIU, C. L., NAIR, R. V., SALARI, R., GENTLES, A. J., IRISH, J., STEHR, H., VICENTE-DUENAS, C., ROMERO-CAMARERO, I., SANCHEZ-GARCIA, I., PLEVRITIS, S. K., ARBER, D. A., BATZOGLOU, S., LEVY, R. & ALIZADEH, A. A. 2015. Mutations in early follicular lymphoma progenitors are associated with suppressed antigen presentation. *Proc Natl Acad Sci U S A,* 112**,** E1116-25.

GUI, Y., GUO, G., HUANG, Y., HU, X., TANG, A., GAO, S., WU, R., CHEN, C., LI, X., ZHOU, L., HE, M., LI, Z., SUN, X., JIA, W., CHEN, J., YANG, S., ZHOU, F., ZHAO, X., WAN, S., YE, R., LIANG, C., LIU, Z., HUANG, P., LIU, C., JIANG, H., WANG, Y., ZHENG, H., SUN, L., LIU, X., JIANG, Z., FENG, D., CHEN, J., WU, S., ZOU, J., ZHANG, Z., YANG, R., ZHAO, J., XU, C., YIN, W., GUAN, Z., YE, J., ZHANG, H., LI, J., KRISTIANSEN, K., NICKERSON, M. L., THEODORESCU, D., LI, Y., ZHANG, X., LI, S., WANG, J., YANG, H., WANG, J. & CAI, Z. 2011. Frequent mutations of chromatin remodeling genes in transitional cell carcinoma of the bladder. *Nat Genet,* 43**,** 875-8.

HABERMANN, T. M., WELLER, E. A., MORRISON, V. A., GASCOYNE, R. D., CASSILETH, P. A., COHN, J. B., DAKHIL, S. R., WODA, B., FISHER, R. I., PETERSON, B. A. & HORNING, S. J. 2006. Rituximab-CHOP versus CHOP alone or with maintenance rituximab in older patients with diffuse large B-cell lymphoma. *J Clin Oncol,* 24**,** 3121-7.

HAN, J. Y., LEE, Y. S., KIM, B. C., LEE, G. K., LEE, S., KIM, E. H., KIM, H. M. & BHAK, J. 2014. Whole-genome analysis of a patient with early-stage small-cell lung cancer. *Pharmacogenomics J*.

HARRIS, N. L., JAFFE, E. S., DIEBOLD, J., FLANDRIN, G., MULLER-HERMELINK, H. K., VARDIMAN, J., LISTER, T. A. & BLOOMFIELD, C. D. 1999. World Health Organization classification of neoplastic diseases of the hematopoietic and lymphoid tissues: report of the Clinical

Advisory Committee meeting-Airlie House, Virginia, November 1997. *J Clin Oncol,* 17**,** 3835-49.

HARRISON, C. J., MOORMAN, A. V., SCHWAB, C., CARROLL, A. J., RAETZ, E. A., DEVIDAS, M., STREHL, S., NEBRAL, K., HARBOTT, J., TEIGLER-SCHLEGEL, A., ZIMMERMAN, M., DASTUGE, N., BARUCHEL, A., SOULIER, J., AUCLERC, M. F., ATTARBASCHI, A., MANN, G., STARK, B., CAZZANIGA, G., CHILTON, L., VANDENBERGHE, P., FORESTIER, E., HALTRICH, I., RAIMONDI, S. C., PARIHAR, M., BOURQUIN, J. P., TCHINDA, J., HAFERLACH, C., VORA, A., HUNGER, S. P., HEEREMA, N. A. & HAAS, O. A. 2014. An international study of intrachromosomal amplification of chromosome 21 (iAMP21): cytogenetic characterization and outcome. *Leukemia,* 28**,** 1015-21.

HARTAGE, P., WANG, S. S., BRACCI, P. M., DEVESA, S. S. & HOLLY, E. A. 2006. *Non-Hodgkin lymphoma,* New York, Oxford University Press.

HARVEY, R. C., MULLIGHAN, C. G., CHEN, I. M., WHARTON, W., MIKHAIL, F. M., CARROLL, A. J., KANG, H., LIU, W., DOBBIN, K. K., SMITH, M. A., CARROLL, W. L., DEVIDAS, M., BOWMAN, W. P., CAMITTA, B. M., REAMAN, G. H., HUNGER, S. P., DOWNING, J. R. & WILLMAN, C. L. 2010. Rearrangement of CRLF2 is associated with mutation of JAK kinases, alteration of IKZF1, Hispanic/Latino ethnicity, and a poor outcome in pediatric B-progenitor acute lymphoblastic leukemia. *Blood,* 115**,** 5312-21.

HASSA, P. O., HAENNI, S. S., BUERKI, C., MEIER, N. I., LANE, W. S., OWEN, H., GERSBACH, M., IMHOF, R. & HOTTIGER, M. O. 2005. Acetylation of poly(ADP-ribose) polymerase-1 by p300/CREB-binding protein regulates coactivation of NF-kappaB-dependent transcription. *J Biol Chem,* 280**,** 40450-64.

HE, L., THOMSON, J. M., HEMANN, M. T., HERNANDO-MONGE, E., MU, D., GOODSON, S., POWERS, S., CORDON-CARDO, C., LOWE, S. W., HANNON, G. J. & HAMMOND, S. M. 2005. A microRNA polycistron as a potential human oncogene. *Nature,* 435**,** 828-33.

HENEL, G. & SCHMITZ, J. L. 2007. Basic Theory and Clinical Applications of Flow Cytometry. *Laboratory Medicine,* 38**,** 428-436.

HENRY, R. A., KUO, Y. M. & ANDREWS, A. J. 2013. Differences in specificity and selectivity between CBP and p300 acetylation of histone H3 and H3/H4. *Biochemistry,* 52**,** 5746-59.

HERMINE, O., HAIOUN, C., LEPAGE, E., D'AGAY, M. F., BRIERE, J., LAVIGNAC, C., FILLET, G., SALLES, G., MAROLLEAU, J. P., DIEBOLD, J., REYAS, F. & GAULARD, P. 1996. Prognostic significance of bcl-2 protein expression in aggressive non-Hodgkin's lymphoma. Groupe d'Etude des Lymphomes de l'Adulte (GELA). *Blood,* 87**,** 265-72.

HERRIOTT, A., TUDHOPE, S. J., JUNGE, G., RODRIGUES, N., PATTERSON, M. J., WOODHOUSE, L., LUNEC, J., HUNTER, J. E., MULLIGAN, E. A., COLE, M., ALLINSON, L. M., WALLIS, J. P., MARSHALL, S., WANG, E., CURTIN, N. J. & WILLMORE, E. 2015. PARP1 expression, activity and ex vivo sensitivity to the PARP inhibitor, talazoparib (BMN 673), in chronic lymphocytic leukaemia. *Oncotarget,* 6**,** 43978-91.

HILL, M. E., MACLENNAN, K. A., CUNNINGHAM, D. C., VAUGHAN HUDSON, B., BURKE, M., CLARKE, P., DI STEFANO, F., ANDERSON, L., VAUGHAN HUDSON, G., MASON, D., SELBY, P. & LINCH, D. C. 1996. Prognostic significance of BCL-2 expression and bcl-2 major breakpoint region rearrangement in diffuse large cell non-Hodgkin's lymphoma: a British National Lymphoma Investigation Study. *Blood,* 88**,** 1046-51.

HO, A. S., KANNAN, K., ROY, D. M., MORRIS, L. G., GANLY, I., KATABI, N., RAMASWAMI, D., WALSH, L. A., ENG, S., HUSE, J. T., ZHANG, J., DOLGALEV, I., HUBERMAN, K., HEGUY, A., VIALE, A., DROBNJAK, M., LEVERSHA, M. A., RICE, C. E., SINGH, B., IYER, N. G., LEEMANS, C. R., BLOEMENA, E., FERRIS, R. L., SEETHALA, R. R., GROSS, B. E., LIANG, Y., SINHA, R., PENG, L., RAPHAEL, B. J., TURCAN, S., GONG, Y., SCHULTZ, N., KIM, S., CHIOSEA, S., SHAH, J. P., SANDER, C., LEE, W. & CHAN, T. A. 2013. The mutational landscape of adenoid cystic carcinoma. *Nat Genet,* 45**,** 791-8.

HOF, J., KRENTZ, S., VAN SCHEWICK, C., KORNER, G., SHALAPOUR, S., RHEIN, P., KARAWAJEW, L., LUDWIG, W. D., SEEGER, K., HENZE, G., VON STACKELBERG, A., HAGEMEIER, C., ECKERT, C. & KIRSCHNER-SCHWABE, R. 2011. Mutations and deletions of the TP53 gene predict nonresponse to treatment and poor outcome in first relapse of childhood acute lymphoblastic leukemia. *J Clin Oncol,* 29**,** 3185-93.

HOLMFELDT, L., WEI, L., DIAZ-FLORES, E., WALSH, M., ZHANG, J., DING, L., PAYNE-TURNER, D., CHURCHMAN, M., ANDERSSON, A., CHEN, S. C., MCCASTLAIN, K., BECKSFORT, J., MA, J., WU, G., PATEL, S. N., HEATLEY, S. L., PHILLIPS, L. A., SONG, G., EASTON, J., PARKER, M., CHEN, X., RUSCH, M., BOGGS, K., VADODARIA, B., HEDLUND, E., DRENBERG, C., BAKER, S., PEI, D., CHENG, C., HUETHER, R., LU, C., FULTON, R. S., FULTON, L. L., TABIB, Y., DOOLING, D. J., OCHOA, K., MINDEN, M., LEWIS, I. D., TO, L. B., MARLTON, P., ROBERTS, A. W., RACA, G., STOCK, W., NEALE, G., DREXLER, H. G., DICKINS, R. A., ELLISON, D. W., SHURTLEFF, S. A., PUI, C. H., RIBEIRO, R. C., DEVIDAS, M., CARROLL, A. J., HEEREMA, N. A., WOOD, B., BOROWITZ, M. J., GASTIER-FOSTER, J. M., RAIMONDI, S. C., MARDIS, E. R., WILSON, R. K., DOWNING, J. R., HUNGER, S. P., LOH, M. L. & MULLIGHAN, C. G. 2013. The genomic landscape of hypodiploid acute lymphoblastic leukemia. *Nat Genet,* 45**,** 242-52.

HORN, H., ZIEPERT, M., BECHER, C., BARTH, T. F., BERND, H. W., FELLER, A. C., KLAPPER, W., HUMMEL, M., STEIN, H., HANSMANN, M. L., SCHMELTER, C., MOLLER, P., COGLIATTI, S., PFREUNDSCHUH, M., SCHMITZ, N., TRUMPER, L., SIEBERT, R., LOEFFLER, M., ROSENWALD, A. & OTT, G. 2013. MYC status in concert with BCL2 and BCL6 expression predicts outcome in diffuse large B-cell lymphoma. *Blood,* 121**,** 2253-63.

HORSPOOL, K. R., STEVENS, M. F., NEWTON, C. G., LUNT, E., WALSH, R. J., PEDGRIFT, B. L., BAIG, G. U., LAVELLE, F. & FIZAMES, C. 1990. Antitumor imidazotetrazines. 20. Preparation of the 8-acid derivative of mitozolomide and its utility in the preparation of active antitumor agents. *J Med Chem,* 33**,** 1393-9.

HUETHER, R., DONG, L., CHEN, X., WU, G., PARKER, M., WEI, L., MA, J., EDMONSON, M. N., HEDLUND, E. K., RUSCH, M. C., SHURTLEFF, S. A., MULDER, H. L., BOGGS, K., VADORDARIA, B., CHENG, J., YERGEAU, D., SONG, G., BECKSFORT, J., LEMMON, G., WEBER, C., CAI, Z., DANG, J., WALSH, M., GEDMAN, A. L., FABER, Z., EASTON, J., GRUBER, T., KRIWACKI, R. W., PARTRIDGE, J. F., DING, L., WILSON, R. K., MARDIS, E. R., MULLIGHAN, C. G., GILBERTSON, R. J., BAKER, S. J., ZAMBETTI, G., ELLISON, D. W., ZHANG, J. & DOWNING, J. R. 2014. The landscape of somatic mutations in epigenetic regulators across 1,000 paediatric cancer genomes. *Nat Commun,* 5**,** 3630.

HUNGER, S. P. 1996. Chromosomal translocations involving the E2A gene in acute lymphoblastic leukemia: clinical features and molecular pathogenesis. *Blood,* 87**,** 1211-24.

HUNGER, S. P., LU, X., DEVIDAS, M., CAMITTA, B. M., GAYNON, P. S., WINICK, N. J., REAMAN, G. H. & CARROLL, W. L. 2012. Improved Survival for Children and Adolescents With Acute Lymphoblastic Leukemia Between 1990 and 2005: A Report From the Children's Oncology Group. *Journal of Clinical Oncology,* 30**,** 1663-1669.

HUNGER, S. P. & MULLIGHAN, C. G. 2015. Acute Lymphoblastic Leukemia in Children. *New England Journal of Medicine,* 373**,** 1541-1552.

INABA, H., GREAVES, M. & MULLIGHAN, C. G. 2013. Acute lymphoblastic leukaemia. *Lancet,* 381**,** 1943-55.

INAGAKI, Y., SHIRAKI, K., SUGIMOTO, K., YADA, T., TAMEDA, M., OGURA, S., YAMAMOTO, N., TAKEI, Y. & ITO, M. 2016. Epigenetic regulation of proliferation and invasion in hepatocellular carcinoma cells by CBP/p300 histone acetyltransferase activity. *Int J Oncol,* 48**,** 533-40.

INTHAL, A., ZEITLHOFER, P., ZEGINIGG, M., MORAK, M., GRAUSENBURGER, R., FRONKOVA, E., FAHRNER, B., MANN, G., HAAS, O. A. & PANZER-GRUMAYER, R. 2012. CREBBP HAT domain mutations prevail in relapse cases of high hyperdiploid childhood acute lymphoblastic leukemia. *Leukemia,* 26**,** 1797-803.

IQBAL, J., SANGER, W. G., HORSMAN, D. E., ROSENWALD, A., PICKERING, D. L., DAVE, B., DAVE, S., XIAO, L., CAO, K., ZHU, Q., SHERMAN, S., HANS, C. P., WEISENBURGER, D. D., GREINER, T. C., GASCOYNE, R. D., OTT, G., MULLER-HERMELINK, H. K., DELABIE, J., BRAZIEL, R. M., JAFFE, E. S., CAMPO, E., LYNCH, J. C., CONNORS, J. M., VOSE, J. M., ARMITAGE, J. O., GROGAN, T. M., STAUDT, L. M. & CHAN, W. C. 2004. BCL2 translocation defines a unique tumor subset within the germinal center B-cell-like diffuse large B-cell lymphoma. *Am J Pathol,* 165**,** 159-66.

IRVING, J., MATHESON, E., MINTO, L., BLAIR, H., CASE, M., HALSEY, C., SWIDENBANK, I., PONTHAN, F., KIRSCHNER-SCHWABE, R., GROENEVELD-KRENTZ, S., HOF, J., ALLAN, J., HARRISON, C., VORMOOR, J., VON STACKELBERG, A. & ECKERT, C. 2014. Ras pathway mutations are prevalent in relapsed childhood acute lymphoblastic leukemia and confer sensitivity to MEK inhibition. *Blood,* 124**,** 3420-30.

IRVING, J. A., ENSHAEI, A., PARKER, C. A., SUTTON, R., KUIPER, R. P., ERHORN, A., MINTO, L., VENN, N. C., LAW, T., YU, J., SCHWAB, C., DAVIES, R., MATHESON, E., DAVIES, A., SONNEVELD, E., DEN BOER, M. L., LOVE, S. B., HARRISON, C. J., HOOGERBRUGGE, P. M., REVESZ, T., SAHA, V. & MOORMAN, A. V. 2016. Integration of genetic and clinical risk factors improves prognostication in relapsed childhood B-cell precursor acute lymphoblastic leukaemia. *Blood*.

ISHIBASHI, T., YAGUCHI, A., TERADA, K., UENO-YOKOHATA, H., TOMITA, O., IIJIMA, K., KOBAYASHI, K., OKITA, H., FUJIMURA, J., OHKI, K., SHIMIZU, T. & KIYOKAWA, N. 2016. Ph-like ALL-related novel fusion kinase ATF7IP-PDGFRB exhibits high sensitivity to tyrosine kinase inhibitors in murine cells. *Exp Hematol,* 44**,** 177-88.e5.

IWASAKI, H., SOMOZA, C., SHIGEMATSU, H., DUPREZ, E. A., IWASAKI-ARAI, J., MIZUNO, S., ARINOBU, Y., GEARY, K., ZHANG, P., DAYARAM, T., FENYUS, M. L., ELF, S., CHAN, S., KASTNER, P., HUETTNER, C. S., MURRAY, R., TENEN, D. G. & AKASHI, K. 2005. Distinctive and indispensable roles of PU.1 in maintenance of hematopoietic stem cells and their differentiation. *Blood,* 106**,** 1590-600.

JANSEN, M. P., MARTENS, J. W., HELMIJR, J. C., BEAUFORT, C. M., VAN MARION, R., KROL, N. M., MONKHORST, K., TRAPMAN-JANSEN, A. M., MEIJER-VAN GELDER, M. E., WEERTS, M. J., RAMIREZ-ARDILA, D. E., DUBBINK, H. J., FOEKENS, J. A., SLEIJFER, S. & BERNS, E. M. 2016. Cell-free DNA mutations as biomarkers in breast cancer patients receiving tamoxifen. *Oncotarget*.

JERUSALEM, G., BEGUIN, Y., FASSOTTE, M. F., NAJJAR, F., PAULUS, P., RIGO, P. & FILLET, G. 1999. Whole-body positron emission tomography using 18F-fluorodeoxyglucose for posttreatment evaluation in Hodgkin's disease and non-Hodgkin's lymphoma has higher diagnostic and prognostic value than classical computed tomography scan imaging. *Blood,* 94**,** 429-33.

JIN, Q., YU, L. R., WANG, L., ZHANG, Z., KASPER, L. H., LEE, J. E., WANG, C., BRINDLE, P. K., DENT, S. Y. & GE, K. 2011. Distinct roles of GCN5/PCAF-mediated H3K9ac and CBP/p300-mediated H3K18/27ac in nuclear receptor transactivation. *Embo j,* 30**,** 249-62.

JOHNSTON, H., KNEER, J., CHACKALAPARAMPIL, I., YACIUK, P. & CHRIVIA, J. 1999. Identification of a novel SNF2/SWI2 protein family member, SRCAP, which interacts with CREB-binding protein. *J Biol Chem,* 274**,** 16370-6.

JORDAN, E. T., COLLINS, M., TEREFE, J., UGOZZOLI, L. & RUBIO, T. 2008. Optimizing Electroporation Conditions in Primary and Other Difficult-to-Transfect Cells. *J Biomol Tech,* 19**,** 328-34.

KAHL, B. S., BARTLETT, N. L., LEONARD, J. P., CHEN, L., GANJOO, K., WILLIAMS, M. E., CZUCZMAN, M. S., ROBINSON, K. S., JOYCE, R., VAN DER JAGT, R. H. & CHESON, B. D. 2010. Bendamustine is effective therapy in patients with rituximab-refractory, indolent B-cell non-Hodgkin lymphoma: results from a Multicenter Study. *Cancer,* 116**,** 106-14.

KAHL, B. S. & YANG, D. T. 2016. Follicular lymphoma: evolving therapeutic strategies. *Blood,* 127**,** 2055-63.

KALKHOVEN, E. 2004. CBP and p300: HATs for different occasions. *Biochem Pharmacol,* 68**,** 1145-55.

KAMPS, M. P. 1997. E2A-Pbx1 induces growth, blocks differentiation, and interacts with other homeodomain proteins regulating normal differentiation. *Curr Top Microbiol Immunol,* 220**,** 25-43.

KANDOTH, C., MCLELLAN, M. D., VANDIN, F., YE, K., NIU, B., LU, C., XIE, M., ZHANG, Q., MCMICHAEL, J. F., WYCZALKOWSKI, M. A., LEISERSON, M. D. M., MILLER, C. A., WELCH, J. S., WALTER, M. J., WENDL, M. C., LEY, T. J., WILSON, R. K., RAPHAEL, B. J. & DING, L. 2013. Mutational landscape and significance across 12 major cancer types. *Nature,* 502**,** 333-339.

KASPER, L. H., LERACH, S., WANG, J., WU, S., JEEVAN, T. & BRINDLE, P. K. 2010. CBP/p300 double null cells reveal effect of coactivator level and diversity on CREB transactivation. *EMBO J,* 29**,** 3660-72.

KASPERS, G. J., WIJNANDS, J. J., HARTMANN, R., HUISMANS, L., LOONEN, A. H., STACKELBERG, A., HENZE, G., PIETERS, R., HAHLEN, K., VAN WERING, E. R. & VEERMAN, A. J. 2005. Immunophenotypic cell lineage and in vitro cellular drug resistance in childhood relapsed acute lymphoblastic leukaemia. *Eur J Cancer,* 41**,** 1300-3.

KAUR, G. & DUFOUR, J. M. 2012. Cell lines: Valuable tools or useless artifacts. *Spermatogenesis,* 2**,** 1-5.

KELLY, G., BELL, A. & RICKINSON, A. 2002. Epstein-Barr virus-associated Burkitt lymphomagenesis selects for downregulation of the nuclear antigen EBNA2. *Nat Med,* 8**,** 1098-104.

KHAN, N. I., BRADSTOCK, K. F. & BENDALL, L. J. 2007. Activation of Wnt/beta-catenin pathway mediates growth and survival in B-cell progenitor acute lymphoblastic leukaemia. *Br J Haematol,* 138**,** 338-48.

KIM, D. H., BAEK, J. H., CHAE, Y. S., KIM, Y. K., KIM, H. J., PARK, Y. H., SONG, H. S., CHUNG, J. S., HYUN, M. S. & SOHN, S. K. 2007. Absolute lymphocyte counts predicts response to chemotherapy and survival in diffuse large B-cell lymphoma. *Leukemia,* 21**,** 2227-30.

KIM, H. K., LIN, C. C., PARKER, D., VEALS, J., LIM, J., LIKHARI, P., STATKEVICH, P., MARCO, A. & NOMEIR, A. A. 1997. High-performance liquid chromatographic determination and stability of 5-(3-methyltriazen-1-yl)-imidazo-4-carboximide, the biologically active product of the antitumor agent temozolomide, in human plasma. *J Chromatogr B Biomed Sci Appl,* 703**,** 225-33.

KINLEN, L. 2004. Infections and immune factors in cancer: the role of epidemiology. *Oncogene,* 23**,** 6341-8.

KINO, T., NORDEEN, S. K. & CHROUSOS, G. P. 1999. Conditional modulation of glucocorticoid receptor activities by CREB-binding protein (CBP) and p300. *J Steroid Biochem Mol Biol,* 70**,** 15-25.

KLAPPER, W., STOECKLEIN, H., ZEYNALOVA, S., OTT, G., KOSARI, F., ROSENWALD, A., LOEFFLER, M., TRUMPER, L., PFREUNDSCHUH, M. & SIEBERT, R. 2008. Structural aberrations affecting the MYC locus indicate a poor prognosis independent of clinical risk factors in diffuse large B-cell lymphomas treated within randomized trials of the German High-Grade Non-Hodgkin's Lymphoma Study Group (DSHNHL). *Leukemia,* 22**,** 2226-9.

KLUMPER, E., PIETERS, R., VEERMAN, A. J., HUISMANS, D. R., LOONEN, A. H., HAHLEN, K., KASPERS, G. J., VAN WERING, E. R., HARTMANN, R. & HENZE, G. 1995. In vitro cellular drug resistance in children with relapsed/refractory acute lymphoblastic leukemia. *Blood,* 86**,** 3861-8.

KORZUS, E., ROSENFELD, M. G. & MAYFORD, M. 2004. CBP histone acetyltransferase activity is a critical component of memory consolidation. *Neuron,* 42**,** 961-72.

KOSTAKOGLU, L., LEONARD, J. P., COLEMAN, M. & GOLDSMITH, S. J. 2004. The role of FDG-PET imaging in the management of lymphoma. *Clin Adv Hematol Oncol,* 2**,** 115-21.

KOVACS, K. A., STEINMANN, M., MAGISTRETTI, P. J., HALFON, O. & CARDINAUX, J. R. 2003. CCAAT/enhancer-binding protein family members recruit the coactivator CREB-binding protein and trigger its phosphorylation. *J Biol Chem,* 278**,** 36959-65.

KRAMER, M. H., HERMANS, J., WIJBURG, E., PHILIPPO, K., GEELEN, E., VAN KRIEKEN, J. H., DE JONG, D., MAARTENSE, E., SCHUURING, E. & KLUIN, P. M. 1998. Clinical relevance of BCL2, BCL6, and MYC rearrangements in diffuse large B-cell lymphoma. *Blood,* 92**,** 3152-62.

KUIPER, R. P., WAANDERS, E., VAN DER VELDEN, V. H., VAN REIJMERSDAL, S. V., VENKATACHALAM, R., SCHEIJEN, B., SONNEVELD, E., VAN DONGEN, J. J., VEERMAN, A. J., VAN LEEUWEN, F. N., VAN KESSEL, A. G. & HOOGERBRUGGE, P. M. 2010. IKZF1 deletions predict relapse in uniformly treated pediatric precursor B-ALL. *Leukemia,* 24**,** 1258-64.

KUMAGAI, M., MANABE, A., PUI, C. H., BEHM, F. G., RAIMONDI, S. C., HANCOCK, M. L., MAHMOUD, H., CRIST, W. M. & CAMPANA, D. 1996. Stroma-supported culture in childhood B-lineage acute lymphoblastic leukemia cells predicts treatment outcome. *J Clin Invest,* 97**,** 755-60.

KUNG, A. L., REBEL, V. I., BRONSON, R. T., CH'NG, L. E., SIEFF, C. A., LIVINGSTON, D. M. & YAO, T. P. 2000. Gene dose-dependent control of hematopoiesis and hematologic tumor suppression by CBP. *Genes Dev,* 14**,** 272-7.

KUZE, T., NAKAMURA, N., HASHIMOTO, Y., SASAKI, Y. & ABE, M. 2000. The characteristics of Epstein-Barr virus (EBV)-positive diffuse large B-cell lymphoma: comparison between EBV(+) and EBV(-) cases in Japanese population. *Jpn J Cancer Res,* 91**,** 1233-40.

KWOK, R. P., LUNDBLAD, J. R., CHRIVIA, J. C., RICHARDS, J. P., BACHINGER, H. P., BRENNAN, R. G., ROBERTS, S. G., GREEN, M. R. & GOODMAN, R. H. 1994. Nuclear protein CBP is a coactivator for the transcription factor CREB. *Nature,* 370**,** 223-6.

LADETTO, M., DRANDI, D., COMPAGNO, M., ASTOLFI, M., VOLPATO, F., VOENA, C., NOVARINO, A., POLLIO, B., ADDEO, A., RICCA, I., FALCO, P., CAVALLO, F., VALLET, S., CORRADINI, P., PILERI, A., TAMPONI, G., PALUMBO, A., BERTETTO, O., BOCCADORO, M. & TARELLA, C. 2003. PCR-detectable nonneoplastic Bcl-2/IgH rearrangements are common in normal subjects and cancer patients at diagnosis but rare in subjects treated with chemotherapy. *J Clin Oncol,* 21**,** 1398-403.

LEGER, H., SMET-NOCCA, C., ATTMANE-ELAKEB, A., MORLEY-FLETCHER, S., BENECKE, A. G. & EILEBRECHT, S. 2014. A TDG/CBP/RARalpha ternary complex mediates the retinoic acid-dependent expression of DNA methylation-sensitive genes. *Genomics Proteomics Bioinformatics,* 12**,** 8-18.

LEGUBE, G. & TROUCHE, D. 2003. Regulating histone acetyltransferases and deacetylases. *EMBO Rep,* 4**,** 944-7.

LEMIEUX, M. E., CHENG, Z., ZHOU, Q., WHITE, R., CORNELL, J., KUNG, A. L. & REBEL, V. I. 2011. Inactivation of a single copy of Crebbp selectively alters pre-mRNA processing in mouse hematopoietic stem cells. *PLoS One,* 6**,** e24153.

LENZ, G., DAVIS, R. E., NGO, V. N., LAM, L., GEORGE, T. C., WRIGHT, G. W., DAVE, S. S., ZHAO, H., XU, W., ROSENWALD, A., OTT, G., MULLER-HERMELINK, H. K., GASCOYNE, R. D., CONNORS, J. M., RIMSZA, L. M., CAMPO, E., JAFFE, E. S., DELABIE, J., SMELAND, E. B., FISHER, R. I., CHAN, W. C. & STAUDT, L. M. 2008a. Oncogenic CARD11 mutations in human diffuse large B cell lymphoma. *Science,* 319**,** 1676-9.

LENZ, G., NAGEL, I., SIEBERT, R., ROSCHKE, A. V., SANGER, W., WRIGHT, G. W., DAVE, S. S., TAN, B., ZHAO, H., ROSENWALD, A., MULLER-HERMELINK, H. K., GASCOYNE, R. D., CAMPO, E., JAFFE, E. S., SMELAND, E. B., FISHER, R. I., KUEHL, W. M., CHAN, W. C. & STAUDT, L. M. 2007. Aberrant immunoglobulin class switch recombination and switch translocations in activated B cell-like diffuse large B cell lymphoma. *J Exp Med,* 204**,** 633-43.

LENZ, G., WRIGHT, G. W., EMRE, N. C., KOHLHAMMER, H., DAVE, S. S., DAVIS, R. E., CARTY, S., LAM, L. T., SHAFFER, A. L., XIAO, W., POWELL, J., ROSENWALD, A., OTT, G., MULLER-HERMELINK, H. K., GASCOYNE, R. D., CONNORS, J. M., CAMPO, E., JAFFE, E. S., DELABIE, J., SMELAND,

E. B., RIMSZA, L. M., FISHER, R. I., WEISENBURGER, D. D., CHAN, W. C. & STAUDT, L. M. 2008b. Molecular subtypes of diffuse large B-cell lymphoma arise by distinct genetic pathways. *Proc Natl Acad Sci U S A,* 105**,** 13520-5.

LI, Y., SCHWAB, C., RYAN, S. L., PAPAEMMANUIL, E., ROBINSON, H. M., JACOBS, P., MOORMAN, A. V., DYER, S., BORROW, J., GRIFFITHS, M., HEEREMA, N. A., CARROLL, A. J., TALLEY, P., BOWN, N., TELFORD, N., ROSS, F. M., GAUNT, L., MCNALLY, R. J., YOUNG, B. D., SINCLAIR, P., RAND, V., TEIXEIRA, M. R., JOSEPH, O., ROBINSON, B., MADDISON, M., DASTUGUE, N., VANDENBERGHE, P., HAFERLACH, C., STEPHENS, P. J., CHENG, J., VAN LOO, P., STRATTON, M. R., CAMPBELL, P. J. & HARRISON, C. J. 2014. Constitutional and somatic rearrangement of chromosome 21 in acute lymphoblastic leukaemia. *Nature,* 508**,** 98-102.

LIN, C., SMITH, E. R., TAKAHASHI, H., LAI, K. C., MARTIN-BROWN, S., FLORENS, L., WASHBURN, M. P., CONAWAY, J. W., CONAWAY, R. C. & SHILATIFARD, A. 2010. AFF4, a component of the ELL/P-TEFb elongation complex and a shared subunit of MLL chimeras, can link transcription elongation to leukemia. *Mol Cell,* 37**,** 429-37.

LO COCO, F., GAIDANO, G., LOUIE, D. C., OFFIT, K., CHAGANTI, R. S. & DALLA-FAVERA, R. 1993. p53 mutations are associated with histologic transformation of follicular lymphoma. *Blood,* 82**,** 2289-95.

LOEB, L. A. 2001. A mutator phenotype in cancer. *Cancer Res,* 61**,** 3230-9.

LOHR, J. G., STOJANOV, P., LAWRENCE, M. S., AUCLAIR, D., CHAPUY, B., SOUGNEZ, C., CRUZ-GORDILLO, P., KNOECHEL, B., ASMANN, Y. W., SLAGER, S. L., NOVAK, A. J., DOGAN, A., ANSELL, S. M., LINK, B. K., ZOU, L., GOULD, J., SAKSENA, G., STRANSKY, N., RANGEL-ESCARENO, C., FERNANDEZ-LOPEZ, J. C., HIDALGO-MIRANDA, A., MELENDEZ-ZAJGLA, J., HERNANDEZ-LEMUS, E., SCHWARZ-CRUZ Y CELIS, A., IMAZ-ROSSHANDLER, I., OJESINA, A. I., JUNG, J., PEDAMALLU, C. S., LANDER, E. S., HABERMANN, T. M., CERHAN, J. R., SHIPP, M. A., GETZ, G. & GOLUB, T. R. 2012. Discovery and prioritization of somatic mutations in diffuse large B-cell lymphoma (DLBCL) by whole-exome sequencing. *Proc Natl Acad Sci U S A,* 109**,** 3879-84.

LOPEZ-ATALAYA, J. P., GERVASINI, C., MOTTADELLI, F., SPENA, S., PICCIONE, M., SCARANO, G., SELICORNI, A., BARCO, A. & LARIZZA, L. 2012. Histone acetylation deficits in lymphoblastoid cell lines from patients with Rubinstein-Taybi syndrome. *J Med Genet,* 49**,** 66-74.

LOSSOS, I. S., ALIZADEH, A. A., DIEHN, M., WARNKE, R., THORSTENSON, Y., OEFNER, P. J., BROWN, P. O., BOTSTEIN, D. & LEVY, R. 2002. Transformation of follicular lymphoma to diffuse large-cell lymphoma: alternative patterns with increased or decreased expression of c-myc and its regulated genes. *Proc Natl Acad Sci U S A,* 99**,** 8886-91.

LOSSOS, I. S., ALIZADEH, A. A., EISEN, M. B., CHAN, W. C., BROWN, P. O., BOTSTEIN, D., STAUDT, L. M. & LEVY, R. 2000. Ongoing immunoglobulin somatic mutation in germinal center B cell-like but not in activated B cell-like diffuse large cell lymphomas. *Proc Natl Acad Sci U S A,* 97**,** 10209-13.

LOYOLA, A. & ALMOUZNI, G. 2004. Bromodomains in living cells participate in deciphering the histone code. *Trends Cell Biol,* 14**,** 279-81.

MA, S. 2012. Risk Factors of Follicular Lymphoma. *Expert Opin Med Diagn,* 6**,** 323-333.

MA, X., EDMONSON, M., YERGEAU, D., MUZNY, D. M., HAMPTON, O. A., RUSCH, M., SONG, G., EASTON, J., HARVEY, R. C., WHEELER, D. A., MA, J., DODDAPANENI, H., VADODARIA, B., WU, G., NAGAHAWATTE, P., CARROLL, W. L., CHEN, I. M., GASTIER-FOSTER, J. M., RELLING, M. V., SMITH, M. A., DEVIDAS, M., GUIDRY AUVIL, J. M., DOWNING, J. R., LOH, M. L., WILLMAN, C. L., GERHARD, D. S., MULLIGHAN, C. G., HUNGER, S. P. & ZHANG, J. 2015. Rise and fall of subclones from diagnosis to relapse in pediatric B-acute lymphoblastic leukaemia. *Nat Commun,* 6**,** 6604.

MALHOTRA, S. & KINCADE, P. W. 2009. Wnt-related molecules and signaling pathway equilibrium in hematopoiesis. *Cell Stem Cell,* 4**,** 27-36.

MALINOWSKA-OZDOWY, K., FRECH, C., SCHONEGGER, A., ECKERT, C., CAZZANIGA, G., STANULLA, M., ZUR STADT, U., MECKLENBRAUKER, A., SCHUSTER, M., KNEIDINGER, D., VON STACKELBERG, A., LOCATELLI, F., SCHRAPPE, M., HORSTMANN, M. A., ATTARBASCHI, A. & BOCK, C. 2015. KRAS and CREBBP mutations: a relapse-linked malicious liaison in childhood high hyperdiploid acute lymphoblastic leukemia. 29**,** 1656-67.

MANABE, A., COUSTAN-SMITH, E., BEHM, F. G., RAIMONDI, S. C. & CAMPANA, D. 1992. Bone marrow-derived stromal cells prevent apoptotic cell death in B-lineage acute lymphoblastic leukemia. *Blood,* 79**,** 2370-7.

MANN, B. S., JOHNSON, J. R., COHEN, M. H., JUSTICE, R. & PAZDUR, R. 2007. FDA approval summary: vorinostat for treatment of advanced primary cutaneous T-cell lymphoma. *Oncologist,* 12**,** 1247-52.

MAR, B. G., KAHN, J., ZON, R. L., GRAUMAN, P. V., BOETTGER, K., CHU, S. H., ARMSTRONG, S. A. & EBERT, B. L. 2015. *SETD2* Heterozygous Loss in Leukemia Leads to Chemotherapy Resistance through Attenuation of the DNA Damage Response. *Blood [Abstract],* 126**,** 2626.

MARTINEZ-BALBAS, M. A., BAUER, U. M., NIELSEN, S. J., BREHM, A. & KOUZARIDES, T. 2000. Regulation of E2F1 activity by acetylation. *Embo j,* 19**,** 662-71.

MARTINEZ-CLIMENT, J. A., ALIZADEH, A. A., SEGRAVES, R., BLESA, D., RUBIO-MOSCARDO, F., ALBERTSON, D. G., GARCIA-CONDE, J., DYER, M. J., LEVY, R., PINKEL, D. & LOSSOS, I. S. 2003. Transformation of follicular lymphoma to diffuse large cell lymphoma is associated with a heterogeneous set of DNA copy number and gene expression alterations. *Blood,* 101**,** 3109-17.

MARZIO, G., WAGENER, C., GUTIERREZ, M. I., CARTWRIGHT, P., HELIN, K. & GIACCA, M. 2000. E2F family members are differentially regulated by reversible acetylation. *J Biol Chem,* 275**,** 10887-92.

MAURER, M. J., MICALLEF, I. N., CERHAN, J. R., KATZMANN, J. A., LINK, B. K., COLGAN, J. P., HABERMANN, T. M., INWARDS, D. J., MARKOVIC, S. N., ANSELL, S. M., PORRATA, L. F., JOHNSTON, P. B., NOWAKOWSKI, G. S., THOMPSON, C. A., GUPTA, M., SYRBU, S. I., KURTIN, P. J., MACON, W. R., NIKCEVICH, D. A. & WITZIG, T. E. 2011. Elevated serum free light chains are associated with event-free and overall survival in two independent cohorts of patients with diffuse large B-cell lymphoma. *J Clin Oncol,* 29**,** 1620-6.

MAYR, B. & MONTMINY, M. 2001. Transcriptional regulation by the phosphorylation-dependent factor CREB. *Nat Rev Mol Cell Biol,* 2**,** 599-609.

MEYER, J. A., WANG, J., HOGAN, L. E., YANG, J. J., DANDEKAR, S., PATEL, J. P., TANG, Z., ZUMBO, P., LI, S., ZAVADIL, J., LEVINE, R. L., CARDOZO, T., HUNGER, S. P., RAETZ, E. A., EVANS, W. E., MORRISON, D. J., MASON, C. E. & CARROLL, W. L. 2013. Relapse-specific mutations in NT5C2 in childhood acute lymphoblastic leukemia. *Nat Genet,* 45**,** 290-4.

MICALLEF, I. N., MAURER, M. J., WISEMAN, G. A., NIKCEVICH, D. A., KURTIN, P. J., CANNON, M. W., PEREZ, D. G., SOORI, G. S., LINK, B. K., HABERMANN, T. M. & WITZIG, T. E. 2011. Epratuzumab with rituximab, cyclophosphamide, doxorubicin, vincristine, and prednisone chemotherapy in patients with previously untreated diffuse large B-cell lymphoma. *Blood,* 118**,** 4053-61.

MIKHAEEL, N. G., TIMOTHY, A. R., O'DOHERTY, M. J., HAIN, S. & MAISEY, M. N. 2000. 18-FDG-PET as a prognostic indicator in the treatment of aggressive Non-Hodgkin's Lymphoma-comparison with CT. *Leuk Lymphoma,* 39**,** 543-53.

MILLER, R. W. & RUBINSTEIN, J. H. 1995. Tumors in Rubinstein-Taybi syndrome. *Am J Med Genet,* 56**,** 112-5.

MONTOTO, S. & FITZGIBBON, J. 2011. Transformation of indolent B-cell lymphomas. *J Clin Oncol,* 29**,** 1827-34.

MOORMAN, A. V., ENSOR, H. M., RICHARDS, S. M., CHILTON, L., SCHWAB, C., KINSEY, S. E., VORA, A., MITCHELL, C. D. & HARRISON, C. J. 2010. Prognostic effect of chromosomal

abnormalities in childhood B-cell precursor acute lymphoblastic leukaemia: results from the UK Medical Research Council ALL97/99 randomised trial. *Lancet Oncol,* 11**,** 429-38.

MOORMAN, A. V., RICHARDS, S. M., ROBINSON, H. M., STREFFORD, J. C., GIBSON, B. E., KINSEY, S. E., EDEN, T. O., VORA, A. J., MITCHELL, C. D. & HARRISON, C. J. 2007. Prognosis of children with acute lymphoblastic leukemia (ALL) and intrachromosomal amplification of chromosome 21 (iAMP21). *Blood,* 109**,** 2327-30.

MOORMAN, A. V., ROBINSON, H., SCHWAB, C., RICHARDS, S. M., HANCOCK, J., MITCHELL, C. D., GOULDEN, N., VORA, A. & HARRISON, C. J. 2013. Risk-directed treatment intensification significantly reduces the risk of relapse among children and adolescents with acute lymphoblastic leukemia and intrachromosomal amplification of chromosome 21: a comparison of the MRC ALL97/99 and UKALL2003 trials. *J Clin Oncol,* 31**,** 3389-96.

MORALES, D., BELTRAN, B., DE MENDOZA, F. H., RIVA, L., YABAR, A., QUINONES, P., BUTERA, J. N. & CASTILLO, J. 2010. Epstein-Barr virus as a prognostic factor in de novo nodal diffuse large B-cell lymphoma. *Leuk Lymphoma,* 51**,** 66-72.

MORALES, J., LI, L., FATTAH, F. J., DONG, Y., BEY, E. A., PATEL, M., GAO, J. & BOOTHMAN, D. A. 2014. Review of poly (ADP-ribose) polymerase (PARP) mechanisms of action and rationale for targeting in cancer and other diseases. *Crit Rev Eukaryot Gene Expr,* 24**,** 15-28.

MORI, H., COLMAN, S. M., XIAO, Z., FORD, A. M., HEALY, L. E., DONALDSON, C., HOWS, J. M., NAVARRETE, C. & GREAVES, M. 2002. Chromosome translocations and covert leukemic clones are generated during normal fetal development. *Proc Natl Acad Sci U S A,* 99**,** 8242-7.

MORIN, R. D., JOHNSON, N. A., SEVERSON, T. M., MUNGALL, A. J., AN, J., GOYA, R., PAUL, J. E., BOYLE, M., WOOLCOCK, B. W., KUCHENBAUER, F., YAP, D., HUMPHRIES, R. K., GRIFFITH, O. L., SHAH, S., ZHU, H., KIMBARA, M., SHASHKIN, P., CHARLOT, J. F., TCHERPAKOV, M., CORBETT, R., TAM, A., VARHOL, R., SMAILUS, D., MOKSA, M., ZHAO, Y., DELANEY, A., QIAN, H., BIROL, I., SCHEIN, J., MOORE, R., HOLT, R., HORSMAN, D. E., CONNORS, J. M., JONES, S., APARICIO, S., HIRST, M., GASCOYNE, R. D. & MARRA, M. A. 2010. Somatic mutations altering EZH2 (Tyr641) in follicular and diffuse large B-cell lymphomas of germinal-center origin. *Nat Genet,* 42**,** 181-5.

MORIN, R. D., MENDEZ-LAGO, M., MUNGALL, A. J., GOYA, R., MUNGALL, K. L., CORBETT, R. D., JOHNSON, N. A., SEVERSON, T. M., CHIU, R., FIELD, M., JACKMAN, S., KRZYWINSKI, M., SCOTT, D. W., TRINH, D. L., TAMURA-WELLS, J., LI, S., FIRME, M. R., ROGIC, S., GRIFFITH, M., CHAN, S., YAKOVENKO, O., MEYER, I. M., ZHAO, E. Y., SMAILUS, D., MOKSA, M., CHITTARANJAN, S., RIMSZA, L., BROOKS-WILSON, A., SPINELLI, J. J., BEN-NERIAH, S., MEISSNER, B., WOOLCOCK, B., BOYLE, M., MCDONALD, H., TAM, A., ZHAO, Y., DELANEY, A., ZENG, T., TSE, K., BUTTERFIELD, Y., BIROL, I., HOLT, R., SCHEIN, J., HORSMAN, D. E., MOORE, R., JONES, S. J., CONNORS, J. M., HIRST, M., GASCOYNE, R. D. & MARRA, M. A. 2011. Frequent mutation of histone-modifying genes in non-Hodgkin lymphoma. *Nature,* 476**,** 298-303.

MORROW, M., HORTON, S., KIOUSSIS, D., BRADY, H. J. & WILLIAMS, O. 2004. TEL-AML1 promotes development of specific hematopoietic lineages consistent with preleukemic activity. *Blood,* 103**,** 3890-6.

MOUNIER, N., BRIERE, J., GISSELBRECHT, C., EMILE, J. F., LEDERLIN, P., SEBBAN, C., BERGER, F., BOSLY, A., MOREL, P., TILLY, H., BOUABDALLAH, R., REYES, F., GAULARD, P. & COIFFIER, B. 2003. Rituximab plus CHOP (R-CHOP) overcomes bcl-2--associated resistance to chemotherapy in elderly patients with diffuse large B-cell lymphoma (DLBCL). *Blood,* 101**,** 4279-84.

MUDRY, R. E., FORTNEY, J. E., YORK, T., HALL, B. M. & GIBSON, L. F. 2000. Stromal cells regulate survival of B-lineage leukemic cells during chemotherapy. *Blood,* 96**,** 1926-32.

MUELLER, D., BACH, C., ZEISIG, D., GARCIA-CUELLAR, M. P., MONROE, S., SREEKUMAR, A., ZHOU, R., NESVIZHSKII, A., CHINNAIYAN, A., HESS, J. L. & SLANY, R. K. 2007. A role for the MLL

fusion partner ENL in transcriptional elongation and chromatin modification. *Blood,* 110**,** 4445-54.

MUELLER, D., GARCIA-CUELLAR, M. P., BACH, C., BUHL, S., MAETHNER, E. & SLANY, R. K. 2009. Misguided transcriptional elongation causes mixed lineage leukemia. *PLoS Biol,* 7**,** e1000249.

MUKASA, A., AIHARA, K., GOTOH, K., SAITO, K., NAGAE, G., TSUJI, S., TATUNO, K., YAMAMOTO, S., TAKAYANAGI, S., NARITA, Y., SHIBUI, S., ABURATANI, H. & SAITO, N. 2014. Frequent h3f3a k27m mutations in thalamic gliomas from young adult patients. *Neuro Oncol,* 16 Suppl 3**,** iii9-iii10.

MULLIGHAN, C. G. 2012. The molecular genetic makeup of acute lymphoblastic leukemia. *Hematology Am Soc Hematol Educ Program,* 2012**,** 389-96.

MULLIGHAN, C. G., GOORHA, S., RADTKE, I., MILLER, C. B., COUSTAN-SMITH, E., DALTON, J. D., GIRTMAN, K., MATHEW, S., MA, J., POUNDS, S. B., SU, X., PUI, C. H., RELLING, M. V., EVANS, W. E., SHURTLEFF, S. A. & DOWNING, J. R. 2007. Genome-wide analysis of genetic alterations in acute lymphoblastic leukaemia. *Nature,* 446**,** 758-64.

MULLIGHAN, C. G., MILLER, C. B., RADTKE, I., PHILLIPS, L. A., DALTON, J., MA, J., WHITE, D., HUGHES, T. P., LE BEAU, M. M., PUI, C. H., RELLING, M. V., SHURTLEFF, S. A. & DOWNING, J. R. 2008. BCR-ABL1 lymphoblastic leukaemia is characterized by the deletion of Ikaros. *Nature,* 453**,** 110-4.

MULLIGHAN, C. G., SU, X., ZHANG, J., RADTKE, I., PHILLIPS, L. A., MILLER, C. B., MA, J., LIU, W., CHENG, C., SCHULMAN, B. A., HARVEY, R. C., CHEN, I. M., CLIFFORD, R. J., CARROLL, W. L., REAMAN, G., BOWMAN, W. P., DEVIDAS, M., GERHARD, D. S., YANG, W., RELLING, M. V., SHURTLEFF, S. A., CAMPANA, D., BOROWITZ, M. J., PUI, C. H., SMITH, M., HUNGER, S. P., WILLMAN, C. L. & DOWNING, J. R. 2009. Deletion of IKZF1 and prognosis in acute lymphoblastic leukemia. *N Engl J Med,* 360**,** 470-80.

MULLIGHAN, C. G., ZHANG, J., KASPER, L. H., LERACH, S., PAYNE-TURNER, D., PHILLIPS, L. A., HEATLEY, S. L., HOLMFELDT, L., COLLINS-UNDERWOOD, J. R., MA, J., BUETOW, K. H., PUI, C. H., BAKER, S. D., BRINDLE, P. K. & DOWNING, J. R. 2011. CREBBP mutations in relapsed acute lymphoblastic leukaemia. *Nature,* 471**,** 235-9.

NACHMAN, J. B., HEEREMA, N. A., SATHER, H., CAMITTA, B., FORESTIER, E., HARRISON, C. J., DASTUGUE, N., SCHRAPPE, M., PUI, C. H., BASSO, G., SILVERMAN, L. B. & JANKA-SCHAUB, G. E. 2007. Outcome of treatment in children with hypodiploid acute lymphoblastic leukemia. *Blood,* 110**,** 1112-5.

NAKAMURA, S., JAFFE, E. & SWERDLOW, S. 2008. "EBV positive diffuse large b-cell of the elderly" in WHO Classification of Tumours of Haematopoietic and Lymphoid. *IARC Press***,** 243-244.

NEMEC, A. A., WALLACE, S. S. & SWEASY, J. B. 2010. Variant base excision repair proteins: contributors to genomic instability. *Semin Cancer Biol,* 20**,** 320-8.

NEUMANN, E., SCHAEFER-RIDDER, M., WANG, Y. & HOFSCHNEIDER, P. H. 1982. Gene transfer into mouse lyoma cells by electroporation in high electric fields. *Embo j,* 1**,** 841-5.

NGO, V. N., YOUNG, R. M., SCHMITZ, R., JHAVAR, S., XIAO, W., LIM, K. H., KOHLHAMMER, H., XU, W., YANG, Y., ZHAO, H., SHAFFER, A. L., ROMESSER, P., WRIGHT, G., POWELL, J., ROSENWALD, A., MULLER-HERMELINK, H. K., OTT, G., GASCOYNE, R. D., CONNORS, J. M., RIMSZA, L. M., CAMPO, E., JAFFE, E. S., DELABIE, J., SMELAND, E. B., FISHER, R. I., BRAZIEL, R. M., TUBBS, R. R., COOK, J. R., WEISENBURGER, D. D., CHAN, W. C. & STAUDT, L. M. 2011. Oncogenically active MYD88 mutations in human lymphoma. *Nature,* 470**,** 115-9.

NGUYEN, K., DEVIDAS, M., CHENG, S. C., LA, M., RAETZ, E. A., CARROLL, W. L., WINICK, N. J., HUNGER, S. P., GAYNON, P. S. & LOH, M. L. 2008. Factors influencing survival after relapse from acute lymphoblastic leukemia: a Children's Oncology Group study. *Leukemia,* 22**,** 2142-50.

NOGAI, H., DORKEN, B. & LENZ, G. 2011. Pathogenesis of non-Hodgkin's lymphoma. *J Clin Oncol,* 29**,** 1803-11.

NOWAKOWSKI, G. S., LAPLANT, B., HABERMANN, T. M., RIVERA, C. E., MACON, W. R., INWARDS, D. J., MICALLEF, I. N., JOHNSTON, P. B., PORRATA, L. F., ANSELL, S. M., KLEBIG, R. R., REEDER, C. B. & WITZIG, T. E. 2011. Lenalidomide can be safely combined with R-CHOP (R2CHOP) in the initial chemotherapy for aggressive B-cell lymphomas: phase I study. *Leukemia,* 25**,** 1877-81.

O'SHEA, D., O'RIAIN, C., GUPTA, M., WATERS, R., YANG, Y., WRENCH, D., GRIBBEN, J., ROSENWALD, A., OTT, G., RIMSZA, L. M., HOLTE, H., CAZIER, J. B., JOHNSON, N. A., CAMPO, E., CHAN, W. C., GASCOYNE, R. D., YOUNG, B. D., STAUDT, L. M., LISTER, T. A. & FITZGIBBON, J. 2009. Regions of acquired uniparental disomy at diagnosis of follicular lymphoma are associated with both overall survival and risk of transformation. *Blood,* 113**,** 2298-301.

OCHS, K. & KAINA, B. 2000. Apoptosis induced by DNA damage O6-methylguanine is Bcl-2 and caspase-9/3 regulated and Fas/caspase-8 independent. *Cancer Res,* 60**,** 5815-24.

OGAWA, R., STREIFF, M. B., BUGAYENKO, A. & KATO, G. J. 2002. Inhibition of PDE4 phosphodiesterase activity induces growth suppression, apoptosis, glucocorticoid sensitivity, p53, and p21(WAF1/CIP1) proteins in human acute lymphoblastic leukemia cells. *Blood,* 99**,** 3390-7.

OGIWARA, H., SASAKI, M., MITACHI, T., OIKE, T., HIGUCHI, S., TOMINAGA, Y. & KOHNO, T. 2015. Targeting p300 addiction in CBP-deficient cancers causes synthetic lethality via apoptotic cell death due to abrogation of MYC expression. *Cancer Discov*.

OGRYZKO, V. V., SCHILTZ, R. L., RUSSANOVA, V., HOWARD, B. H. & NAKATANI, Y. 1996. The transcriptional coactivators p300 and CBP are histone acetyltransferases. *Cell,* 87**,** 953-9.

OKI, Y., YAMAMOTO, K., KATO, H., KUWATSUKA, Y., TAJI, H., KAGAMI, Y. & MORISHIMA, Y. 2008. Low absolute lymphocyte count is a poor prognostic marker in patients with diffuse large B-cell lymphoma and suggests patients' survival benefit from rituximab. *Eur J Haematol,* 81**,** 448-53.

ONCIU, M. 2009. Acute lymphoblastic leukemia. *Hematol Oncol Clin North Am,* 23**,** 655-74.

OTA, A., TAGAWA, H., KARNAN, S., TSUZUKI, S., KARPAS, A., KIRA, S., YOSHIDA, Y. & SETO, M. 2004. Identification and characterization of a novel gene, C13orf25, as a target for 13q31-q32 amplification in malignant lymphoma. *Cancer Res,* 64**,** 3087-95.

OYAMA, T., YAMAMOTO, K., ASANO, N., OSHIRO, A., SUZUKI, R., KAGAMI, Y., MORISHIMA, Y., TAKEUCHI, K., IZUMO, T., MORI, S., OHSHIMA, K., SUZUMIYA, J., NAKAMURA, N., ABE, M., ICHIMURA, K., SATO, Y., YOSHINO, T., NAOE, T., SHIMOYAMA, Y., KAMIYA, Y., KINOSHITA, T. & NAKAMURA, S. 2007. Age-related EBV-associated B-cell lymphoproliferative disorders constitute a distinct clinicopathologic group: a study of 96 patients. *Clin Cancer Res,* 13**,** 5124-32.

PAO, G. M., JANKNECHT, R., RUFFNER, H., HUNTER, T. & VERMA, I. M. 2000. CBP/p300 interact with and function as transcriptional coactivators of BRCA1. *Proc Natl Acad Sci U S A,* 97**,** 1020-5.

PAQUET, D., KWART, D., CHEN, A., SPROUL, A., JACOB, S., TEO, S., OLSEN, K. M., GREGG, A., NOGGLE, S. & TESSIER-LAVIGNE, M. 2016. Efficient introduction of specific homozygous and heterozygous mutations using CRISPR/Cas9. *Nature,* 533**,** 125-9.

PASINI, D., MALATESTA, M., JUNG, H. R., WALFRIDSSON, J., WILLER, A., OLSSON, L., SKOTTE, J., WUTZ, A., PORSE, B., JENSEN, O. N. & HELIN, K. 2010. Characterization of an antagonistic switch between histone H3 lysine 27 methylation and acetylation in the transcriptional regulation of Polycomb group target genes. *Nucleic Acids Res,* 38**,** 4958-69.

PASQUALUCCI, L., COMPAGNO, M., HOULDSWORTH, J., MONTI, S., GRUNN, A., NANDULA, S. V., ASTER, J. C., MURTY, V. V., SHIPP, M. A. & DALLA-FAVERA, R. 2006. Inactivation of the PRDM1/BLIMP1 gene in diffuse large B cell lymphoma. *J Exp Med,* 203**,** 311-7.

PASQUALUCCI, L. & DALLA-FAVERA, R. 2014. SnapShot: diffuse large B cell lymphoma. *Cancer Cell,* 25**,** 132-132 e1.

PASQUALUCCI, L., DOMINGUEZ-SOLA, D., CHIARENZA, A., FABBRI, G., GRUNN, A., TRIFONOV, V., KASPER, L. H., LERACH, S., TANG, H., MA, J., ROSSI, D., CHADBURN, A., MURTY, V. V., MULLIGHAN, C. G., GAIDANO, G., RABADAN, R., BRINDLE, P. K. & DALLA-FAVERA, R. 2011a. Inactivating mutations of acetyltransferase genes in B-cell lymphoma. *Nature,* 471**,** 189-95.

PASQUALUCCI, L., KHIABANIAN, H., FANGAZIO, M., VASISHTHA, M., MESSINA, M., HOLMES, A. B., OUILLETTE, P., TRIFONOV, V., ROSSI, D., TABBO, F., PONZONI, M., CHADBURN, A., MURTY, V. V., BHAGAT, G., GAIDANO, G., INGHIRAMI, G., MALEK, S. N., RABADAN, R. & DALLA-FAVERA, R. 2014. Genetics of follicular lymphoma transformation. *Cell Rep,* 6**,** 130-40.

PASQUALUCCI, L., MIGLIAZZA, A., BASSO, K., HOULDSWORTH, J., CHAGANTI, R. S. & DALLA-FAVERA, R. 2003. Mutations of the BCL6 proto-oncogene disrupt its negative autoregulation in diffuse large B-cell lymphoma. *Blood,* 101**,** 2914-23.

PASQUALUCCI, L., TRIFONOV, V., FABBRI, G., MA, J., ROSSI, D., CHIARENZA, A., WELLS, V. A., GRUNN, A., MESSINA, M., ELLIOT, O., CHAN, J., BHAGAT, G., CHADBURN, A., GAIDANO, G., MULLIGHAN, C. G., RABADAN, R. & DALLA-FAVERA, R. 2011b. Analysis of the coding genome of diffuse large B-cell lymphoma. *Nat Genet,* 43**,** 830-7.

PASTORE, A., JURINOVIC, V., KRIDEL, R., HOSTER, E., STAIGER, A. M., SZCZEPANOWSKI, M., POTT, C., KOPP, N., MURAKAMI, M., HORN, H., LEICH, E., MOCCIA, A. A., MOTTOK, A., SUNKAVALLI, A., VAN HUMMELEN, P., DUCAR, M., ENNISHI, D., SHULHA, H. P., HOTHER, C., CONNORS, J. M., SEHN, L. H., DREYLING, M., NEUBERG, D., MOLLER, P., FELLER, A. C., HANSMANN, M. L., STEIN, H., ROSENWALD, A., OTT, G., KLAPPER, W., UNTERHALT, M., HIDDEMANN, W., GASCOYNE, R. D., WEINSTOCK, D. M. & WEIGERT, O. 2015. Integration of gene mutations in risk prognostication for patients receiving first-line immunochemotherapy for follicular lymphoma: a retrospective analysis of a prospective clinical trial and validation in a population-based registry. *Lancet Oncol*.

PAULSSON, K., LILLJEBJORN, H., BILOGLAV, A., OLSSON, L., RISSLER, M., CASTOR, A., BARBANY, G., FOGELSTRAND, L., NORDGREN, A., SJOGREN, H., FIORETOS, T. & JOHANSSON, B. 2015. The genomic landscape of high hyperdiploid childhood acute lymphoblastic leukemia. *Nat Genet,* 47**,** 672-6.

PEIFER, M., FERNANDEZ-CUESTA, L., SOS, M. L., GEORGE, J., SEIDEL, D., KASPER, L. H., PLENKER, D., LEENDERS, F., SUN, R., ZANDER, T., MENON, R., KOKER, M., DAHMEN, I., MULLER, C., DI CERBO, V., SCHILDHAUS, H. U., ALTMULLER, J., BAESSMANN, I., BECKER, C., DE WILDE, B., VANDESOMPELE, J., BOHM, D., ANSEN, S., GABLER, F., WILKENING, I., HEYNCK, S., HEUCKMANN, J. M., LU, X., CARTER, S. L., CIBULSKIS, K., BANERJI, S., GETZ, G., PARK, K. S., RAUH, D., GRUTTER, C., FISCHER, M., PASQUALUCCI, L., WRIGHT, G., WAINER, Z., RUSSELL, P., PETERSEN, I., CHEN, Y., STOELBEN, E., LUDWIG, C., SCHNABEL, P., HOFFMANN, H., MULEY, T., BROCKMANN, M., ENGEL-RIEDEL, W., MUSCARELLA, L. A., FAZIO, V. M., GROEN, H., TIMENS, W., SIETSMA, H., THUNNISSEN, E., SMIT, E., HEIDEMAN, D. A., SNIJDERS, P. J., CAPPUZZO, F., LIGORIO, C., DAMIANI, S., FIELD, J., SOLBERG, S., BRUSTUGUN, O. T., LUND-IVERSEN, M., SANGER, J., CLEMENT, J. H., SOLTERMANN, A., MOCH, H., WEDER, W., SOLOMON, B., SORIA, J. C., VALIDIRE, P., BESSE, B., BRAMBILLA, E., BRAMBILLA, C., LANTUEJOUL, S., LORIMIER, P., SCHNEIDER, P. M., HALLEK, M., PAO, W., MEYERSON, M., SAGE, J., SHENDURE, J., SCHNEIDER, R., BUTTNER, R., WOLF, J., NURNBERG, P., PERNER, S., HEUKAMP, L. C., BRINDLE, P. K., HAAS, S. & THOMAS, R. K. 2012. Integrative genome analyses identify key somatic driver mutations of small-cell lung cancer. *Nat Genet,* 44**,** 1104-10.

PFREUNDSCHUH, M., SCHUBERT, J., ZIEPERT, M., SCHMITS, R., MOHREN, M., LENGFELDER, E., REISER, M., NICKENIG, C., CLEMENS, M., PETER, N., BOKEMEYER, C., EIMERMACHER, H., HO, A., HOFFMANN, M., MERTELSMANN, R., TRUMPER, L., BALLEISEN, L., LIERSCH, R., METZNER, B., HARTMANN, F., GLASS, B., POESCHEL, V., SCHMITZ, N., RUEBE, C., FELLER, A. C. & LOEFFLER, M. 2008. Six versus eight cycles of bi-weekly CHOP-14 with or without

rituximab in elderly patients with aggressive CD20+ B-cell lymphomas: a randomised controlled trial (RICOVER-60). *Lancet Oncol,* 9**,** 105-16.

PFREUNDSCHUH, M., TRUMPER, L., OSTERBORG, A., PETTENGELL, R., TRNENY, M., IMRIE, K., MA, D., GILL, D., WALEWSKI, J., ZINZANI, P. L., STAHEL, R., KVALOY, S., SHPILBERG, O., JAEGER, U., HANSEN, M., LEHTINEN, T., LOPEZ-GUILLERMO, A., CORRADO, C., SCHELIGA, A., MILPIED, N., MENDILA, M., RASHFORD, M., KUHNT, E. & LOEFFLER, M. 2006. CHOP-like chemotherapy plus rituximab versus CHOP-like chemotherapy alone in young patients with good-prognosis diffuse large-B-cell lymphoma: a randomised controlled trial by the MabThera International Trial (MInT) Group. *Lancet Oncol,* 7**,** 379-91.

PHAN, R. T. & DALLA-FAVERA, R. 2004. The BCL6 proto-oncogene suppresses p53 expression in germinal-centre B cells. *Nature,* 432**,** 635-9.

PIETERS, R., DEN BOER, M. L., DURIAN, M., JANKA, G., SCHMIEGELOW, K., KASPERS, G. J., VAN WERING, E. R. & VEERMAN, A. J. 1998. Relation between age, immunophenotype and in vitro drug resistance in 395 children with acute lymphoblastic leukemia--implications for treatment of infants. *Leukemia,* 12**,** 1344-8.

PINYOL, M., COBO, F., BEA, S., JARES, P., NAYACH, I., FERNANDEZ, P. L., MONTSERRAT, E., CARDESA, A. & CAMPO, E. 1998. p16(INK4a) gene inactivation by deletions, mutations, and hypermethylation is associated with transformed and aggressive variants of non-Hodgkin's lymphomas. *Blood,* 91**,** 2977-84.

PLUMMER, E. R., MIDDLETON, M. R., JONES, C., OLSEN, A., HICKSON, I., MCHUGH, P., MARGISON, G. P., MCGOWN, G., THORNCROFT, M., WATSON, A. J., BODDY, A. V., CALVERT, A. H., HARRIS, A. L., NEWELL, D. R. & CURTIN, N. J. 2005. Temozolomide pharmacodynamics in patients with metastatic melanoma: dna damage and activity of repair enzymes O6-alkylguanine alkyltransferase and poly(ADP-ribose) polymerase-1. *Clin Cancer Res,* 11**,** 3402-9.

PORRATA, L. F., RISTOW, K., HABERMANN, T. M., OZSAN, N., DOGAN, A., MACON, W., COLGAN, J. P., WITZIG, T. E., INWARDS, D. J., ANSELL, S. M., MICALLEF, I. N., JOHNSTON, P. B., NOWAKOWSKI, G. S., THOMPSON, C. & MARKOVIC, S. N. 2012. Absolute monocyte/lymphocyte count prognostic score is independent of immunohistochemically determined cell of origin in predicting survival in diffuse large B-cell lymphoma. *Leuk Lymphoma,* 53**,** 2159-65.

PUI, C.-H., ROBISON, L. L. & LOOK, A. T. 2008. Acute lymphoblastic leukaemia. *The Lancet,* 371**,** 1030-1043.

PUI, C. H., CAMPANA, D., PEI, D., BOWMAN, W. P., SANDLUND, J. T., KASTE, S. C., RIBEIRO, R. C., RUBNITZ, J. E., RAIMONDI, S. C., ONCIU, M., COUSTAN-SMITH, E., KUN, L. E., JEHA, S., CHENG, C., HOWARD, S. C., SIMMONS, V., BAYLES, A., METZGER, M. L., BOYETT, J. M., LEUNG, W., HANDGRETINGER, R., DOWNING, J. R., EVANS, W. E. & RELLING, M. V. 2009. Treating childhood acute lymphoblastic leukemia without cranial irradiation. *N Engl J Med,* 360**,** 2730-41.

PUI, C. H., PEI, D., COUSTAN-SMITH, E., JEHA, S., CHENG, C., BOWMAN, W. P., SANDLUND, J. T., RIBEIRO, R. C., RUBNITZ, J. E., INABA, H., BHOJWANI, D., GRUBER, T. A., LEUNG, W. H., DOWNING, J. R., EVANS, W. E., RELLING, M. V. & CAMPANA, D. 2015. Clinical utility of sequential minimal residual disease measurements in the context of risk-based therapy in childhood acute lymphoblastic leukaemia: a prospective study. *Lancet Oncol,* 16**,** 465-74.

PUI, C. H., RELLING, M. V. & DOWNING, J. R. 2004. Acute lymphoblastic leukemia. *N Engl J Med,* 350**,** 1535-48.

PUI, C. H., SANDLUND, J. T., PEI, D., RIVERA, G. K., HOWARD, S. C., RIBEIRO, R. C., RUBNITZ, J. E., RAZZOUK, B. I., HUDSON, M. M., CHENG, C., RAIMONDI, S. C., BEHM, F. G., DOWNING, J. R., RELLING, M. V. & EVANS, W. E. 2003. Results of therapy for acute lymphoblastic leukemia in black and white children. *Jama,* 290**,** 2001-7.

RADHAKRISHNAN, I., PEREZ-ALVARADO, G. C., PARKER, D., DYSON, H. J., MONTMINY, M. R. & WRIGHT, P. E. 1997. Solution structure of the KIX domain of CBP bound to the transactivation domain of CREB: a model for activator:coactivator interactions. *Cell,* 91**,** 741-52.

RAMOS, Y. F., HESTAND, M. S., VERLAAN, M., KRABBENDAM, E., ARIYUREK, Y., VAN GALEN, M., VAN DAM, H., VAN OMMEN, G. J., DEN DUNNEN, J. T., ZANTEMA, A. & T HOEN, P. A. 2010. Genome-wide assessment of differential roles for p300 and CBP in transcription regulation. *Nucleic Acids Res,* 38**,** 5396-408.

RAO, P. H., HOULDSWORTH, J., DYOMINA, K., PARSA, N. Z., CIGUDOSA, J. C., LOUIE, D. C., POPPLEWELL, L., OFFIT, K., JHANWAR, S. C. & CHAGANTI, R. S. 1998. Chromosomal and gene amplification in diffuse large B-cell lymphoma. *Blood,* 92**,** 234-40.

REBEL, V. I., KUNG, A. L., TANNER, E. A., YANG, H., BRONSON, R. T. & LIVINGSTON, D. M. 2002. Distinct roles for CREB-binding protein and p300 in hematopoietic stem cell self-renewal. *Proc Natl Acad Sci U S A,* 99**,** 14789-94.

REITER, A., SCHRAPPE, M., LUDWIG, W. D., HIDDEMANN, W., SAUTER, S., HENZE, G., ZIMMERMANN, M., LAMPERT, F., HAVERS, W., NIETHAMMER, D. & ET AL. 1994. Chemotherapy in 998 unselected childhood acute lymphoblastic leukemia patients. Results and conclusions of the multicenter trial ALL-BFM 86. *Blood,* 84**,** 3122-33.

RELANDER, T., JOHNSON, N. A., FARINHA, P., CONNORS, J. M., SEHN, L. H. & GASCOYNE, R. D. 2010. Prognostic factors in follicular lymphoma. *J Clin Oncol,* 28**,** 2902-13.

REN, R. 2005. Mechanisms of BCR-ABL in the pathogenesis of chronic myelogenous leukaemia. *Nat Rev Cancer,* 5**,** 172-83.

RICKLES, R. J., PIERCE, L. T., GIORDANO, T. P., 3RD, TAM, W. F., MCMILLIN, D. W., DELMORE, J., LAUBACH, J. P., BORISY, A. A., RICHARDSON, P. G. & LEE, M. S. 2010. Adenosine A2A receptor agonists and PDE inhibitors: a synergistic multitarget mechanism discovered through systematic combination screening in B-cell malignancies. *Blood,* 116**,** 593-602.

RIEHM, H., GADNER, H., HENZE, G., LANGERMANN, H.-J. & ODENWALD, E. 1980. The Berlin Childhood Acute Lymphoblastic Leukemia Therapy Study, 1970-1976. *Journal of Pediatric Hematology/Oncology,* 2**,** 299-306.

RIEHM, H., REITER, A., SCHRAPPE, M., BERTHOLD, F., DOPFER, R., GEREIN, V., LUDWIG, R., RITTER, J., STOLLMANN, B. & HENZE, G. 1987. [Corticosteroid-dependent reduction of leukocyte count in blood as a prognostic factor in acute lymphoblastic leukemia in childhood (therapy study ALL-BFM 83)]. *Klin Padiatr,* 199**,** 151-60.

ROBERTS, K. G., LI, Y., PAYNE-TURNER, D., HARVEY, R. C., YANG, Y. L., PEI, D., MCCASTLAIN, K., DING, L., LU, C., SONG, G., MA, J., BECKSFORT, J., RUSCH, M., CHEN, S. C., EASTON, J., CHENG, J., BOGGS, K., SANTIAGO-MORALES, N., IACOBUCCI, I., FULTON, R. S., WEN, J., VALENTINE, M., CHENG, C., PAUGH, S. W., DEVIDAS, M., CHEN, I. M., RESHMI, S., SMITH, A., HEDLUND, E., GUPTA, P., NAGAHAWATTE, P., WU, G., CHEN, X., YERGEAU, D., VADODARIA, B., MULDER, H., WINICK, N. J., LARSEN, E. C., CARROLL, W. L., HEEREMA, N. A., CARROLL, A. J., GRAYSON, G., TASIAN, S. K., MOORE, A. S., KELLER, F., FREI-JONES, M., WHITLOCK, J. A., RAETZ, E. A., WHITE, D. L., HUGHES, T. P., GUIDRY AUVIL, J. M., SMITH, M. A., MARCUCCI, G., BLOOMFIELD, C. D., MROZEK, K., KOHLSCHMIDT, J., STOCK, W., KORNBLAU, S. M., KONOPLEVA, M., PAIETTA, E., PUI, C. H., JEHA, S., RELLING, M. V., EVANS, W. E., GERHARD, D. S., GASTIER-FOSTER, J. M., MARDIS, E., WILSON, R. K., LOH, M. L., DOWNING, J. R., HUNGER, S. P., WILLMAN, C. L., ZHANG, J. & MULLIGHAN, C. G. 2014. Targetable kinase-activating lesions in Ph-like acute lymphoblastic leukemia. *N Engl J Med,* 371**,** 1005-15.

ROBINSON, G., PARKER, M., KRANENBURG, T. A., LU, C., CHEN, X., DING, L., PHOENIX, T. N., HEDLUND, E., WEI, L., ZHU, X., CHALHOUB, N., BAKER, S. J., HUETHER, R., KRIWACKI, R., CURLEY, N., THIRUVENKATAM, R., WANG, J., WU, G., RUSCH, M., HONG, X., BECKSFORT, J., GUPTA, P., MA, J., EASTON, J., VADODARIA, B., ONAR-THOMAS, A., LIN, T., LI, S.,

POUNDS, S., PAUGH, S., ZHAO, D., KAWAUCHI, D., ROUSSEL, M. F., FINKELSTEIN, D., ELLISON, D. W., LAU, C. C., BOUFFET, E., HASSALL, T., GURURANGAN, S., COHN, R., FULTON, R. S., FULTON, L. L., DOOLING, D. J., OCHOA, K., GAJJAR, A., MARDIS, E. R., WILSON, R. K., DOWNING, J. R., ZHANG, J. & GILBERTSON, R. J. 2012. Novel mutations target distinct subgroups of medulloblastoma. *Nature,* 488**,** 43-8.

ROELFSEMA, J. H. & PETERS, D. J. 2007. Rubinstein-Taybi syndrome: clinical and molecular overview. *Expert Rev Mol Med,* 9**,** 1-16.

ROSENWALD, A., WRIGHT, G., CHAN, W. C., CONNORS, J. M., CAMPO, E., FISHER, R. I., GASCOYNE, R. D., MULLER-HERMELINK, H. K., SMELAND, E. B., GILTNANE, J. M., HURT, E. M., ZHAO, H., AVERETT, L., YANG, L., WILSON, W. H., JAFFE, E. S., SIMON, R., KLAUSNER, R. D., POWELL, J., DUFFEY, P. L., LONGO, D. L., GREINER, T. C., WEISENBURGER, D. D., SANGER, W. G., DAVE, B. J., LYNCH, J. C., VOSE, J., ARMITAGE, J. O., MONTSERRAT, E., LOPEZ-GUILLERMO, A., GROGAN, T. M., MILLER, T. P., LEBLANC, M., OTT, G., KVALOY, S., DELABIE, J., HOLTE, H., KRAJCI, P., STOKKE, T. & STAUDT, L. M. 2002. The use of molecular profiling to predict survival after chemotherapy for diffuse large-B-cell lymphoma. *N Engl J Med,* 346**,** 1937-47.

ROSENWALD, A., WRIGHT, G., LEROY, K., YU, X., GAULARD, P., GASCOYNE, R. D., CHAN, W. C., ZHAO, T., HAIOUN, C., GREINER, T. C., WEISENBURGER, D. D., LYNCH, J. C., VOSE, J., ARMITAGE, J. O., SMELAND, E. B., KVALOY, S., HOLTE, H., DELABIE, J., CAMPO, E., MONTSERRAT, E., LOPEZ-GUILLERMO, A., OTT, G., MULLER-HERMELINK, H. K., CONNORS, J. M., BRAZIEL, R., GROGAN, T. M., FISHER, R. I., MILLER, T. P., LEBLANC, M., CHIORAZZI, M., ZHAO, H., YANG, L., POWELL, J., WILSON, W. H., JAFFE, E. S., SIMON, R., KLAUSNER, R. D. & STAUDT, L. M. 2003. Molecular diagnosis of primary mediastinal B cell lymphoma identifies a clinically favorable subgroup of diffuse large B cell lymphoma related to Hodgkin lymphoma. *J Exp Med,* 198**,** 851-62.

RUAN, J., MARTIN, P., FURMAN, R. R., LEE, S. M., CHEUNG, K., VOSE, J. M., LACASCE, A., MORRISON, J., ELSTROM, R., ELY, S., CHADBURN, A., CESARMAN, E., COLEMAN, M. & LEONARD, J. P. 2011. Bortezomib plus CHOP-rituximab for previously untreated diffuse large B-cell lymphoma and mantle cell lymphoma. *J Clin Oncol,* 29**,** 690-7.

RUSSELL, L. J., CAPASSO, M., VATER, I., AKASAKA, T., BERNARD, O. A., CALASANZ, M. J., CHANDRASEKARAN, T., CHAPIRO, E., GESK, S., GRIFFITHS, M., GUTTERY, D. S., HAFERLACH, C., HARDER, L., HEIDENREICH, O., IRVING, J., KEARNEY, L., NGUYEN-KHAC, F., MACHADO, L., MINTO, L., MAJID, A., MOORMAN, A. V., MORRISON, H., RAND, V., STREFFORD, J. C., SCHWAB, C., TONNIES, H., DYER, M. J., SIEBERT, R. & HARRISON, C. J. 2009. Deregulated expression of cytokine receptor gene, CRLF2, is involved in lymphoid transformation in B-cell precursor acute lymphoblastic leukemia. *Blood,* 114**,** 2688-98.

RYAN, S. L., MATHESON, E., GROSSMANN, V., SINCLAIR, P., BASHTON, M., SCHWAB, C., TOWERS, W., PARTINGTON, M., ELLIOTT, A., MINTO, L., RICHARDSON, S., RAHMAN, T., KEAVNEY, B., SKINNER, R., BOWN, N., HAFERLACH, T., VANDENBERGHE, P., HAFERLACH, C., SANTIBANEZ-KOREF, M., MOORMAN, A. V., KOHLMANN, A., IRVING, J. A. E. & HARRISON, C. J. 2016. The role of the RAS pathway in iAMP21-ALL. *Leukemia (in press)*.

SAFFHILL, R., MARGISON, G. P. & O'CONNOR, P. J. 1985. Mechanisms of carcinogenesis induced by alkylating agents. *Biochim Biophys Acta,* 823**,** 111-45.

SAKAMOTO, K. M. & FRANK, D. A. 2009. CREB in the pathophysiology of cancer: implications for targeting transcription factors for cancer therapy. *Clin Cancer Res,* 15**,** 2583-7.

SANDER, C. A., YANO, T., CLARK, H. M., HARRIS, C., LONGO, D. L., JAFFE, E. S. & RAFFELD, M. 1993. p53 mutation is associated with progression in follicular lymphomas. *Blood,* 82**,** 1994-2004.

SANGER, F., NICKLEN, S. & COULSON, A. R. 1977. DNA sequencing with chain-terminating inhibitors. *Proc Natl Acad Sci U S A,* 74**,** 5463-7.

SASAKI, M., KUWABARA, Y., KOGA, H., NAKAGAWA, M., CHEN, T., KANEKO, K., HAYASHI, K., NAKAMURA, K. & MASUDA, K. 2002. Clinical impact of whole body FDG-PET on the staging and therapeutic decision making for malignant lymphoma. *Ann Nucl Med,* 16**,** 337-45.

SAVAGE, K. J., JOHNSON, N. A., BEN-NERIAH, S., CONNORS, J. M., SEHN, L. H., FARINHA, P., HORSMAN, D. E. & GASCOYNE, R. D. 2009. MYC gene rearrangements are associated with a poor prognosis in diffuse large B-cell lymphoma patients treated with R-CHOP chemotherapy. *Blood,* 114**,** 3533-7.

SCHMIEGELOW, K., FORESTIER, E., HELLEBOSTAD, M., HEYMAN, M., KRISTINSSON, J., SODERHALL, S. & TASKINEN, M. 2010. Long-term results of NOPHO ALL-92 and ALL-2000 studies of childhood acute lymphoblastic leukemia. *Leukemia,* 24**,** 345-54.

SCHMITTGEN, T. D. & LIVAK, K. J. 2008. Analyzing real-time PCR data by the comparative C(T) method. *Nat Protoc,* 3**,** 1101-8.

SCHODER, H., META, J., YAP, C., ARIANNEJAD, M., RAO, J., PHELPS, M. E., VALK, P. E., SAYRE, J. & CZERNIN, J. 2001. Effect of whole-body (18)F-FDG PET imaging on clinical staging and management of patients with malignant lymphoma. *J Nucl Med,* 42**,** 1139-43.

SCHRAPPE, M., REITER, A., ZIMMERMANN, M., HARBOTT, J., LUDWIG, W. D., HENZE, G., GADNER, H., ODENWALD, E. & RIEHM, H. 2000. Long-term results of four consecutive trials in childhood ALL performed by the ALL-BFM study group from 1981 to 1995. Berlin-Frankfurt-Munster. *Leukemia,* 14**,** 2205-22.

SCHRAPPE, M., VALSECCHI, M. G., BARTRAM, C. R., SCHRAUDER, A., PANZER-GRUMAYER, R., MORICKE, A., PARASOLE, R., ZIMMERMANN, M., DWORZAK, M., BULDINI, B., REITER, A., BASSO, G., KLINGEBIEL, T., MESSINA, C., RATEI, R., CAZZANIGA, G., KOEHLER, R., LOCATELLI, F., SCHAFER, B. W., ARICO, M., WELTE, K., VAN DONGEN, J. J., GADNER, H., BIONDI, A. & CONTER, V. 2011. Late MRD response determines relapse risk overall and in subsets of childhood T-cell ALL: results of the AIEOP-BFM-ALL 2000 study. *Blood,* 118**,** 2077-84.

SCHUETZ, J. M., JOHNSON, N. A., MORIN, R. D., SCOTT, D. W., TAN, K., BEN-NIERAH, S., BOYLE, M., SLACK, G. W., MARRA, M. A., CONNORS, J. M., BROOKS-WILSON, A. R. & GASCOYNE, R. D. 2012. BCL2 mutations in diffuse large B-cell lymphoma. *Leukemia,* 26**,** 1383-90.

SCHULTZ, K. R., BOWMAN, W. P., ALEDO, A., SLAYTON, W. B., SATHER, H., DEVIDAS, M., WANG, C., DAVIES, S. M., GAYNON, P. S., TRIGG, M., RUTLEDGE, R., BURDEN, L., JORSTAD, D., CARROLL, A., HEEREMA, N. A., WINICK, N., BOROWITZ, M. J., HUNGER, S. P., CARROLL, W. L. & CAMITTA, B. 2009. Improved early event-free survival with imatinib in Philadelphia chromosome-positive acute lymphoblastic leukemia: a children's oncology group study. *J Clin Oncol,* 27**,** 5175-81.

SCHULTZ, K. R., CARROLL, A., HEEREMA, N. A., BOWMAN, W. P., ALEDO, A., SLAYTON, W. B., SATHER, H., DEVIDAS, M., ZHENG, H. W., DAVIES, S. M., GAYNON, P. S., TRIGG, M., RUTLEDGE, R., JORSTAD, D., WINICK, N., BOROWITZ, M. J., HUNGER, S. P., CARROLL, W. L. & CAMITTA, B. 2014. Long-term follow-up of imatinib in pediatric Philadelphia chromosome-positive acute lymphoblastic leukemia: Children's Oncology Group study AALL0031. *Leukemia,* 28**,** 1467-71.

SCHWAENEN, C., VIARDOT, A., BERGER, H., BARTH, T. F., BENTINK, S., DOHNER, H., ENZ, M., FELLER, A. C., HANSMANN, M. L., HUMMEL, M., KESTLER, H. A., KLAPPER, W., KREUZ, M., LENZE, D., LOEFFLER, M., MOLLER, P., MULLER-HERMELINK, H. K., OTT, G., ROSOLOWSKI, M., ROSENWALD, A., RUF, S., SIEBERT, R., SPANG, R., STEIN, H., TRUEMPER, L., LICHTER, P., BENTZ, M. & WESSENDORF, S. 2009. Microarray-based genomic profiling reveals novel genomic aberrations in follicular lymphoma which associate with patient survival and gene expression status. *Genes Chromosomes Cancer,* 48**,** 39-54.

SEAM, P., JUWEID, M. E. & CHESON, B. D. 2007. The role of FDG-PET scans in patients with lymphoma. *Blood,* 110**,** 3507-16.

SHAFFER, A. L., 3RD, YOUNG, R. M. & STAUDT, L. M. 2012. Pathogenesis of human B cell lymphomas. *Annu Rev Immunol,* 30**,** 565-610.

SHAH, K. M. & YOUNG, L. S. 2009. Epstein-Barr virus and carcinogenesis: beyond Burkitt's lymphoma. *Clin Microbiol Infect,* 15**,** 982-8.

SHARMA, S., KELLY, T. K. & JONES, P. A. 2010. Epigenetics in cancer. *Carcinogenesis,* 31**,** 27-36.

SHI, D., POP, M. S., KULIKOV, R., LOVE, I. M., KUNG, A. L. & GROSSMAN, S. R. 2009. CBP and p300 are cytoplasmic E4 polyubiquitin ligases for p53. *Proc Natl Acad Sci U S A,* 106**,** 16275-80.

SHIPP 1993. A predictive model for aggressive non-Hodgkin's lymphoma. The International Non-Hodgkin's Lymphoma Prognostic Factors Project. *N Engl J Med,* 329**,** 987-94.

SHULTZ, L. D., ISHIKAWA, F. & GREINER, D. L. 2007. Humanized mice in translational biomedical research. *Nat Rev Immunol,* 7**,** 118-30.

SHULTZ, L. D., LYONS, B. L., BURZENSKI, L. M., GOTT, B., CHEN, X., CHALEFF, S., KOTB, M., GILLIES, S. D., KING, M., MANGADA, J., GREINER, D. L. & HANDGRETINGER, R. 2005. Human lymphoid and myeloid cell development in NOD/LtSz-scid IL2R gamma null mice engrafted with mobilized human hemopoietic stem cells. *J Immunol,* 174**,** 6477-89.

SISON, E. A. & BROWN, P. 2011. The bone marrow microenvironment and leukemia: biology and therapeutic targeting. *Expert Rev Hematol,* 4**,** 271-83.

SMITH, M., ARTHUR, D., CAMITTA, B., CARROLL, A. J., CRIST, W., GAYNON, P., GELBER, R., HEEREMA, N., KORN, E. L., LINK, M., MURPHY, S., PUI, C. H., PULLEN, J., REAMON, G., SALLAN, S. E., SATHER, H., SHUSTER, J., SIMON, R., TRIGG, M., TUBERGEN, D., UCKUN, F. & UNGERLEIDER, R. 1996. Uniform approach to risk classification and treatment assignment for children with acute lymphoblastic leukemia. *J Clin Oncol,* 14**,** 18-24.

SMITH, P. G., WANG, F., WILKINSON, K. N., SAVAGE, K. J., KLEIN, U., NEUBERG, D. S., BOLLAG, G., SHIPP, M. A. & AGUIAR, R. C. 2005. The phosphodiesterase PDE4B limits cAMP-associated PI3K/AKT-dependent apoptosis in diffuse large B-cell lymphoma. *Blood,* 105**,** 308-16.

SOLAL-CELIGNY, P., ROY, P., COLOMBAT, P., WHITE, J., ARMITAGE, J. O., ARRANZ-SAEZ, R., AU, W. Y., BELLEI, M., BRICE, P., CABALLERO, D., COIFFIER, B., CONDE-GARCIA, E., DOYEN, C., FEDERICO, M., FISHER, R. I., GARCIA-CONDE, J. F., GUGLIELMI, C., HAGENBEEK, A., HAIOUN, C., LEBLANC, M., LISTER, A. T., LOPEZ-GUILLERMO, A., MCLAUGHLIN, P., MILPIED, N., MOREL, P., MOUNIER, N., PROCTOR, S. J., ROHATINER, A., SMITH, P., SOUBEYRAN, P., TILLY, H., VITOLO, U., ZINZANI, P. L., ZUCCA, E. & MONTSERRAT, E. 2004. Follicular lymphoma international prognostic index. *Blood,* 104**,** 1258-65.

SONG, M. K., CHUNG, J. S., SEOL, Y. M., KIM, S. G., SHIN, H. J., CHOI, Y. J., CHO, G. J. & SHIN, D. H. 2010. Influence of low absolute lymphocyte count of patients with nongerminal center type diffuse large B-cell lymphoma with R-CHOP therapy. *Ann Oncol,* 21**,** 140-4.

SONG, Y., LI, L., OU, Y., GAO, Z., LI, E., LI, X., ZHANG, W., WANG, J., XU, L., ZHOU, Y., MA, X., LIU, L., ZHAO, Z., HUANG, X., FAN, J., DONG, L., CHEN, G., MA, L., YANG, J., CHEN, L., HE, M., LI, M., ZHUANG, X., HUANG, K., QIU, K., YIN, G., GUO, G., FENG, Q., CHEN, P., WU, Z., WU, J., MA, L., ZHAO, J., LUO, L., FU, M., XU, B., CHEN, B., LI, Y., TONG, T., WANG, M., LIU, Z., LIN, D., ZHANG, X., YANG, H., WANG, J. & ZHAN, Q. 2014. Identification of genomic alterations in oesophageal squamous cell cancer. *Nature,* 509**,** 91-5.

SPAEPEN, K., STROOBANTS, S., DUPONT, P., VAN STEENWEGHEN, S., THOMAS, J., VANDENBERGHE, P., VANUYTSEL, L., BORMANS, G., BALZARINI, J., DE WOLF-PEETERS, C., MORTELMANS, L. & VERHOEF, G. 2001. Prognostic value of positron emission tomography (PET) with fluorine-18 fluorodeoxyglucose ([18F]FDG) after first-line chemotherapy in non-Hodgkin's lymphoma: is [18F]FDG-PET a valid alternative to conventional diagnostic methods? *J Clin Oncol,* 19**,** 414-9.

STEAD, L. F., SUTTON, K. M., TAYLOR, G. R., QUIRKE, P. & RABBITTS, P. 2013. Accurately identifying low-allelic fraction variants in single samples with next-generation sequencing: applications in tumor subclone resolution. *Hum Mutat,* 34**,** 1432-8.

STIMSON, L., WOOD, V., KHAN, O., FOTHERINGHAM, S. & LA THANGUE, N. B. 2009. HDAC inhibitor-based therapies and haematological malignancy. *Ann Oncol,* 20**,** 1293-302.

SU, G. H., CHEN, H. M., MUTHUSAMY, N., GARRETT-SINHA, L. A., BAUNOCH, D., TENEN, D. G. & SIMON, M. C. 1997. Defective B cell receptor-mediated responses in mice lacking the Ets protein, Spi-B. *EMBO J,* 16**,** 7118-29.

SUBRAMANIAN, A., TAMAYO, P., MOOTHA, V. K., MUKHERJEE, S., EBERT, B. L., GILLETTE, M. A., PAULOVICH, A., POMEROY, S. L., GOLUB, T. R., LANDER, E. S. & MESIROV, J. P. 2005. Gene set enrichment analysis: a knowledge-based approach for interpreting genome-wide expression profiles. *Proc Natl Acad Sci U S A,* 102**,** 15545-50.

SUGAR, I. P. & NEUMANN, E. 1984. Stochastic model for electric field-induced membrane pores. Electroporation. *Biophys Chem,* 19**,** 211-25.

SWINNEN, L. J. 1999. Overview of posttransplant B-cell lymphoproliferative disorders. *Semin Oncol,* 26**,** 21-5.

SZCZEPANSKI, T. 2007. Why and how to quantify minimal residual disease in acute lymphoblastic leukemia? *Leukemia,* 21**,** 622-6.

TAKAWA, M., MASUDA, K., KUNIZAKI, M., DAIGO, Y., TAKAGI, K., IWAI, Y., CHO, H. S., TOYOKAWA, G., YAMANE, Y., MAEJIMA, K., FIELD, H. I., KOBAYASHI, T., AKASU, T., SUGIYAMA, M., TSUCHIYA, E., ATOMI, Y., PONDER, B. A., NAKAMURA, Y. & HAMAMOTO, R. 2011. Validation of the histone methyltransferase EZH2 as a therapeutic target for various types of human cancer and as a prognostic marker. *Cancer Sci,* 102**,** 1298-305.

TAN, S. C. & YIAP, B. C. 2009. DNA, RNA, and protein extraction: the past and the present. *J Biomed Biotechnol,* 2009**,** 574398.

TANG, Y., ZHAO, W., CHEN, Y., ZHAO, Y. & GU, W. 2008. Acetylation is indispensable for p53 activation. *Cell,* 133**,** 612-26.

TEO, A. K., OH, H. K., ALI, R. B. & LI, B. F. 2001. The modified human DNA repair enzyme O(6)-methylguanine-DNA methyltransferase is a negative regulator of estrogen receptor-mediated transcription upon alkylation DNA damage. *Mol Cell Biol,* 21**,** 7105-14.

THORLEY-LAWSON, D. A. & GROSS, A. 2004. Persistence of the Epstein-Barr virus and the origins of associated lymphomas. *N Engl J Med,* 350**,** 1328-37.

THURN, K. T., THOMAS, S., MOORE, A. & MUNSTER, P. N. 2011. Rational therapeutic combinations with histone deacetylase inhibitors for the treatment of cancer. *Future Oncol,* 7**,** 263-83.

TINI, M., BENECKE, A., UM, S. J., TORCHIA, J., EVANS, R. M. & CHAMBON, P. 2002. Association of CBP/p300 acetylase and thymine DNA glycosylase links DNA repair and transcription. *Mol Cell,* 9**,** 265-77.

TODISCO, E., GAIPA, G., BIAGI, E., BONAMINO, M., GRAMIGNA, R., INTRONA, M. & BIONDI, A. 2002. CD40 ligand-stimulated B cell precursor leukemic cells elicit interferon-gamma production by autologous bone marrow T cells in childhood acute lymphoblastic leukemia. *Leukemia,* 16**,** 2046-54.

TOMECZKOWSKI, J., YAKISAN, E., WIELAND, B., REITER, A., WELTE, K. & SYKORA, K. W. 1995. Absence of G-CSF receptors and absent response to G-CSF in childhood Burkitt's lymphoma and B-ALL cells. *Br J Haematol,* 89**,** 771-9.

TSAPIS, M., LIEB, M., MANZO, F., SHANKARANARAYANAN, P., HERBRECHT, R., LUTZ, P. & GRONEMEYER, H. 2007. HDAC inhibitors induce apoptosis in glucocorticoid-resistant acute lymphatic leukemia cells despite a switch from the extrinsic to the intrinsic death pathway. *Int J Biochem Cell Biol,* 39**,** 1500-9.

TSUZUKI, S., SETO, M., GREAVES, M. & ENVER, T. 2004. Modeling first-hit functions of the t(12;21) TEL-AML1 translocation in mice. *Proc Natl Acad Sci U S A,* 101**,** 8443-8.

TUBBS, J. L., PEGG, A. E. & TAINER, J. A. 2007. DNA binding, nucleotide flipping, and the helix-turn-helix motif in base repair by O6-alkylguanine-DNA alkyltransferase and its implications for cancer chemotherapy. *DNA Repair (Amst),* 6**,** 1100-15.

TURNELL, A. S., STEWART, G. S., GRAND, R. J., ROOKES, S. M., MARTIN, A., YAMANO, H., ELLEDGE, S. J. & GALLIMORE, P. H. 2005. The APC/C and CBP/p300 cooperate to regulate transcription and cell-cycle progression. *Nature,* 438**,** 690-5.

VAIDYA, R. & WITZIG, T. E. 2014. Prognostic factors for diffuse large B-cell lymphoma in the R(X)CHOP era. *Ann Oncol,* 25**,** 2124-33.

VECSEY, C. G., HAWK, J. D., LATTAL, K. M., STEIN, J. M., FABIAN, S. A., ATTNER, M. A., CABRERA, S. M., MCDONOUGH, C. B., BRINDLE, P. K., ABEL, T. & WOOD, M. A. 2007. Histone deacetylase inhibitors enhance memory and synaptic plasticity via CREB:CBP-dependent transcriptional activation. *J Neurosci,* 27**,** 6128-40.

VEERMAN, A. J., KAMPS, W. A., VAN DEN BERG, H., VAN DEN BERG, E., BOKKERINK, J. P., BRUIN, M. C., VAN DEN HEUVEL-EIBRINK, M. M., KORBIJN, C. M., KORTHOF, E. T., VAN DER PAL, K., STIJNEN, T., VAN WEEL SIPMAN, M. H., VAN WEERDEN, J. F., VAN WERING, E. R. & VAN DER DOES-VAN DEN BERG, A. 2009. Dexamethasone-based therapy for childhood acute lymphoblastic leukaemia: results of the prospective Dutch Childhood Oncology Group (DCOG) protocol ALL-9 (1997-2004). *Lancet Oncol,* 10**,** 957-66.

VIARDOT, A., MOLLER, P., HOGEL, J., WERNER, K., MECHTERSHEIMER, G., HO, A. D., OTT, G., BARTH, T. F., SIEBERT, R., GESK, S., SCHLEGELBERGER, B., DOHNER, H. & BENTZ, M. 2002. Clinicopathologic correlations of genomic gains and losses in follicular lymphoma. *J Clin Oncol,* 20**,** 4523-30.

VIRE, E., BRENNER, C., DEPLUS, R., BLANCHON, L., FRAGA, M., DIDELOT, C., MOREY, L., VAN EYNDE, A., BERNARD, D., VANDERWINDEN, J. M., BOLLEN, M., ESTELLER, M., DI CROCE, L., DE LAUNOIT, Y. & FUKS, F. 2006. The Polycomb group protein EZH2 directly controls DNA methylation. *Nature,* 439**,** 871-4.

VORA, A., GOULDEN, N., MITCHELL, C., HANCOCK, J., HOUGH, R., ROWNTREE, C., MOORMAN, A. V. & WADE, R. 2014. Augmented post-remission therapy for a minimal residual disease-defined high-risk subgroup of children and young people with clinical standard-risk and intermediate-risk acute lymphoblastic leukaemia (UKALL 2003): a randomised controlled trial. *Lancet Oncol,* 15**,** 809-18.

VORA, A., GOULDEN, N., WADE, R., MITCHELL, C., HANCOCK, J., HOUGH, R., ROWNTREE, C. & RICHARDS, S. 2013. Treatment reduction for children and young adults with low-risk acute lymphoblastic leukaemia defined by minimal residual disease (UKALL 2003): a randomised controlled trial. *Lancet Oncol,* 14**,** 199-209.

VROOMAN, L. M., STEVENSON, K. E., SUPKO, J. G., O'BRIEN, J., DAHLBERG, S. E., ASSELIN, B. L., ATHALE, U. H., CLAVELL, L. A., KELLY, K. M., KUTOK, J. L., LAVERDIERE, C., LIPSHULTZ, S. E., MICHON, B., SCHORIN, M., RELLING, M. V., COHEN, H. J., NEUBERG, D. S., SALLAN, S. E. & SILVERMAN, L. B. 2013. Postinduction dexamethasone and individualized dosing of Escherichia Coli L-asparaginase each improve outcome of children and adolescents with newly diagnosed acute lymphoblastic leukemia: results from a randomized study--Dana-Farber Cancer Institute ALL Consortium Protocol 00-01. *J Clin Oncol,* 31**,** 1202-10.

WARRIS, L. T., VAN DEN HEUVEL-EIBRINK, M. M., ARIES, I. M., PIETERS, R., VAN DEN AKKER, E. L. & DEN BOER, M. L. 2015. Hydrocortisone does not influence glucocorticoid sensitivity of acute lymphoblastic leukemia cells. *Haematologica,* 100**,** e137-9.

WATT, S. A., PURDIE, K. J., DEN BREEMS, N. Y., DIMON, M., TUCKER, S., ARRON, S. T., MCHUGH, A., XUE, D. J., DAYAL, J. H., HARWOOD, C. A., LEIGH, I. M., PROBY, C. M. & SOUTH, A. P. 2016. CREBBP mutation in human cutaneous squamous cell carcinoma. *Exp Dermatol*.

WEIGERT, O., KOPP, N., LANE, A. A., YODA, A., DAHLBERG, S. E., NEUBERG, D., BAHAR, A. Y., CHAPUY, B., KUTOK, J. L., LONGTINE, J. A., KUO, F. C., HALEY, T., SALOIS, M., SULLIVAN, T. J., FISHER, D. C., FOX, E. A., RODIG, S. J., ANTIN, J. H. & WEINSTOCK, D. M. 2012. Molecular ontogeny of donor-derived follicular lymphomas occurring after hematopoietic cell transplantation. *Cancer Discov,* 2**,** 47-55.

WEISS, L. M., WARNKE, R. A., SKLAR, J. & CLEARY, M. L. 1987. Molecular analysis of the t(14;18) chromosomal translocation in malignant lymphomas. *N Engl J Med,* 317**,** 1185-9.

WILCOX, R. A., RISTOW, K., HABERMANN, T. M., INWARDS, D. J., MICALLEF, I. N., JOHNSTON, P. B., COLGAN, J. P., NOWAKOWSKI, G. S., ANSELL, S. M., WITZIG, T. E., MARKOVIC, S. N. & PORRATA, L. 2011. The absolute monocyte and lymphocyte prognostic score predicts survival and identifies high-risk patients in diffuse large-B-cell lymphoma. *Leukemia,* 25**,** 1502-9.

WILDER, R. B., JONES, D., TUCKER, S. L., FULLER, L. M., HA, C. S., MCLAUGHLIN, P., HESS, M. A., CABANILLAS, F. & COX, J. D. 2001. Long-term results with radiotherapy for Stage I-II follicular lymphomas. *Int J Radiat Oncol Biol Phys,* 51**,** 1219-27.

WILLIS, T. G. & DYER, M. J. 2000. The role of immunoglobulin translocations in the pathogenesis of B-cell malignancies. *Blood,* 96**,** 808-22.

WILSON, R. C. & DOUDNA, J. A. 2013. Molecular mechanisms of RNA interference. *Annu Rev Biophys,* 42**,** 217-39.

WOITERSKI, J., EBINGER, M., WITTE, K. E., GOECKE, B., HEININGER, V., PHILIPPEK, M., BONIN, M., SCHRAUDER, A., ROTTGERS, S., HERR, W., LANG, P., HANDGRETINGER, R., HARTWIG, U. F. & ANDRE, M. C. 2013. Engraftment of low numbers of pediatric acute lymphoid and myeloid leukemias into NOD/SCID/IL2Rcgammanull mice reflects individual leukemogenecity and highly correlates with clinical outcome. *Int J Cancer,* 133**,** 1547-56.

YAMAMOTO, H., KIHARA-NEGISHI, F., YAMADA, T., HASHIMOTO, Y. & OIKAWA, T. 1999. Physical and functional interactions between the transcription factor PU.1 and the coactivator CBP. *Oncogene,* 18**,** 1495-501.

YANG, M. H., NICKERSON, S., KIM, E. T., LIOT, C., LAURENT, G., SPANG, R., PHILIPS, M. R., SHAN, Y., SHAW, D. E., BAR-SAGI, D., HAIGIS, M. C. & HAIGIS, K. M. 2012. Regulation of RAS oncogenicity by acetylation. *Proc Natl Acad Sci U S A,* 109**,** 10843-8.

YOKOYAMA, A., LIN, M., NARESH, A., KITABAYASHI, I. & CLEARY, M. L. 2010. A higher-order complex containing AF4 and ENL family proteins with P-TEFb facilitates oncogenic and physiologic MLL-dependent transcription. *Cancer Cell,* 17**,** 198-212.

YU, J., WAANDERS, E., VAN REIJMERSDAL, S. V., SONNEVELD, E., VAN LEEUWEN, F. N., PIETERS, R., GEURTS VAN KESSEL, A., HOOGERBRUGGE, P. M. & KUIPER, R. P. 2015. Genetic Architecture of Relapsed Pediatric B Cell Precursor Acute Lymphoblastic Leukemia Are Related to the Intensity of Upfront Therapy. *Blood,* 126**,** 247-247.

YUAN, W., CONDORELLI, G., CARUSO, M., FELSANI, A. & GIORDANO, A. 1996. Human p300 protein is a coactivator for the transcription factor MyoD. *J Biol Chem,* 271**,** 9009-13.

ZELENETZ, A. D., CHU, G., GALILI, N., BANGS, C. D., HORNING, S. J., DONLON, T. A., CLEARY, M. L. & LEVY, R. 1991. Enhanced detection of the t(14;18) translocation in malignant lymphoma using pulsed-field gel electrophoresis. *Blood,* 78**,** 1552-60.

ZENG, L. & ZHOU, M. M. 2002. Bromodomain: an acetyl-lysine binding domain. *FEBS Lett,* 513**,** 124-8.

ZHANG, J., GRUBOR, V., LOVE, C. L., BANERJEE, A., RICHARDS, K. L., MIECZKOWSKI, P. A., DUNPHY, C., CHOI, W., AU, W. Y., SRIVASTAVA, G., LUGAR, P. L., RIZZIERI, D. A., LAGOO, A. S., BERNAL-MIZRACHI, L., MANN, K. P., FLOWERS, C., NARESH, K., EVENS, A., GORDON, L. I., CZADER, M., GILL, J. I., HSI, E. D., LIU, Q., FAN, A., WALSH, K., JIMA, D., SMITH, L. L., JOHNSON, A. J., BYRD, J. C., LUFTIG, M. A., NI, T., ZHU, J., CHADBURN, A., LEVY, S., DUNSON, D. & DAVE, S. S. 2013. Genetic heterogeneity of diffuse large B-cell lymphoma. *Proc Natl Acad Sci U S A,* 110**,** 1398-403.

ZHANG, J., MULLIGHAN, C. G., HARVEY, R. C., WU, G., CHEN, X., EDMONSON, M., BUETOW, K. H., CARROLL, W. L., CHEN, I. M., DEVIDAS, M., GERHARD, D. S., LOH, M. L., REAMAN, G. H., RELLING, M. V., CAMITTA, B. M., BOWMAN, W. P., SMITH, M. A., WILLMAN, C. L., DOWNING, J. R. & HUNGER, S. P. 2011. Key pathways are frequently mutated in high-risk

childhood acute lymphoblastic leukemia: a report from the Children's Oncology Group. *Blood,* 118**,** 3080-7.

ZHANG, X., ODOM, D. T., KOO, S. H., CONKRIGHT, M. D., CANETTIERI, G., BEST, J., CHEN, H., JENNER, R., HERBOLSHEIMER, E., JACOBSEN, E., KADAM, S., ECKER, J. R., EMERSON, B., HOGENESCH, J. B., UNTERMAN, T., YOUNG, R. A. & MONTMINY, M. 2005. Genome-wide analysis of cAMP-response element binding protein occupancy, phosphorylation, and target gene activation in human tissues. *Proc Natl Acad Sci U S A,* 102**,** 4459-64.

ZIMMER, S. N., LEMIEUX, M. E., KARIA, B. P., DAY, C., ZHOU, T., ZHOU, Q., KUNG, A. L., SURESH, U., CHEN, Y., KINNEY, M. C., BISHOP, A. J. & REBEL, V. I. 2012. Mice heterozygous for CREB binding protein are hypersensitive to gamma-radiation and invariably develop myelodysplastic/myeloproliferative neoplasm. *Exp Hematol,* 40**,** 295-306 e5.

ZIMMER, S. N., ZHOU, Q., ZHOU, T., CHENG, Z., ABBOUD-WERNER, S. L., HORN, D., LECOCKE, M., WHITE, R., KRIVTSOV, A. V., ARMSTRONG, S. A., KUNG, A. L., LIVINGSTON, D. M. & REBEL, V. I. 2011. Crebbp haploinsufficiency in mice alters the bone marrow microenvironment, leading to loss of stem cells and excessive myelopoiesis. *Blood,* 118**,** 69-79.